



# Orodispersible Tablets Containing Taste-Masked Lipid Pellets with Metformin Hydrochloride for Use by Elderly Patients

Inaugural-Dissertation

zur Erlangung des Doktorgrades  
der Mathematisch-Naturwissenschaftlichen Fakultät  
der Heinrich-Heine-Universität Düsseldorf

vorgelegt von

**M.Sc. Gustavo Freire Petrovick**  
aus Münster

Düsseldorf, May 2015

aus dem Institut für  
Pharmazeutische Technologie und Biopharmazie  
der Heinrich-Heine Universität Düsseldorf

Gedruckt mit der Genehmigung der  
Mathematisch-Naturwissenschaftlichen Fakultät der  
Heinrich-Heine-Universität Düsseldorf

Referent: Prof. Dr. Jörg Breitzkreutz

Korreferent: Prof. Dr. Dr. h.c. Peter Kleinebudde

Tag der mündlichen Prüfung: 08.06.2015

“It is better to conquer yourself than to win a thousand battles.  
Then the victory is yours. It cannot be taken from you, not by angels  
or by demons, heaven or hell”

Buddha

*In memoriam*

Für meinen Großvater

Prof. Emer. Dr. Joao Ruy Jardim Freire



---

# Table of Content

Abbreviations .....	v
1. Introduction.....	1
2. General Part.....	5
2.1. Type 2 Diabetes <i>Mellitus</i> .....	5
2.2. Metformin .....	7
2.3. Taste Issues with Metformin HCl Formulations and Patient Compliance.....	8
2.4. Taste-Masking of Solid Dosage Forms.....	10
2.5. Lipids in Solid Oral Dosage Forms .....	13
2.6. Extrusion and Spheronization.....	16
2.6.1. Solid Lipid Cold Extrusion.....	16
2.6.2. Solid Lipid Spheronization .....	19
2.7. Orodispersible Tablets .....	23
3. Aim of the Study .....	27
4. Results and Discussion .....	29
4.1. Material Characterization.....	29
4.1.1. Introduction.....	29
4.1.2. Particle Shape and Size Characterization .....	29
4.1.3. Powder Properties .....	33
4.1.4. Thermal Properties.....	34
4.1.5. Crystallographic Properties.....	36
4.1.6. Conclusions.....	37
4.2. Pre-Formulation Studies for the Extrudates Development .....	37
4.2.1. Introduction.....	37
4.2.2. Thermal Properties.....	38
4.2.3. Crystallographic Properties.....	41
4.2.4. Conclusions.....	43
4.3. Solid Lipid Cold Extrusion .....	44
4.3.1. Introduction.....	44
4.3.2. Preparation of Lipid Extrudates .....	45

4.3.3. Morphological Characterization of Extrudates .....	47
4.3.4. Thermal properties.....	48
4.3.5. Crystallographic properties .....	50
4.3.6. Drug content of Extrudates .....	52
4.3.7. Dissolution Studies.....	53
4.3.8. Conclusions.....	56
4.4. Lipid Spheronization.....	57
4.4.1. Introduction .....	57
4.4.2. Investigation of the Spheronization Process.....	57
4.4.2.1. Influence of Spheronization Parameters on Material Temperature and Process Time .....	57
4.4.2.2. Influence of Friction Plate Temperature on Material Temperature..	64
4.4.2.3. Improved Equipment Setup.....	69
4.4.3. Particle Size Distribution, Shape Characterization, and Flow Properties of Lipid Pellets.....	72
4.4.4. Shape Formation Mechanism.....	75
4.4.5. Thermal and Crystallographic Properties.....	78
4.4.6. Drug Content of Lipid Micropellets.....	80
4.4.7. Drug Dissolution Studies of Lipid Micropellets.....	81
4.4.8. Electronic Tongue Investigations .....	87
4.4.8.1. Electronic Tongue Calibration.....	87
4.4.8.2. Electronic Tongue Investigation of Lipid Based Micropellets .....	90
4.4.8.3. Euclidean Distances.....	94
4.4.9. Preparation and characterization of Lipid Micropellets for ODT Development .....	95
4.4.10. Conclusions.....	97
4.5. Orodispersible Tablets Development .....	97
4.5.1. Introduction .....	97
4.5.2. Design of Experiments (DoE) .....	98
4.5.2.1. Factors.....	98
4.5.2.2. Quality of the Model .....	99
4.5.2.3. Results .....	101
4.5.3. ODT with Ludiflash® .....	104

---

4.5.3.1. Morphological Characterization of the ODTs.....	104
4.5.3.2. Uniformity of Dose of the ODTs .....	106
4.5.3.3. Loss on Drying, Water absorption and Wetting Test of the ODTs	106
4.5.3.4. Drug Release of the ODTs.....	108
4.5.3.5. Electronic Tongue Investigations.....	110
4.5.4. Conclusions.....	113
5. Summary .....	115
6. Zusammenfassung.....	117
7. Material and Methods .....	119
7.1. Materials .....	119
7.2. Preparative Methods.....	120
7.2.1. Pre-Formulation Studies of Solid Mixtures for the Preparation of Lipid Extrudates.....	120
7.2.2. Solid Lipid Cold Extrusion.....	120
7.2.3. Lipid Spheronization .....	122
7.2.4. Orodispersible Tablets Preparation.....	123
7.2.5. Compaction Design of Experiments (DoE) .....	123
7.3. Analytical Methods.....	124
7.3.1. Loss on Drying .....	124
7.3.2. Laser Diffraction.....	124
7.3.3. Bulk and Tapped Densities, Hausner Factor, and Carr's Index .....	125
7.3.4. Differential Scanning Calorimetry (DSC) .....	125
7.3.5. X-Ray Powder Diffractometry (XRPD).....	126
7.3.6. Scanning Electron Microscopy (SEM).....	126
7.3.7. Optical Microscopy.....	126
7.3.8. Particles Flowability.....	126
7.3.9. Solid Fat Content Analysis .....	127
7.3.10. Helium Pycnometer Density.....	127
7.3.11. Drug Content of Lipid Extrudates and Micropellets.....	127
7.3.12. Dissolution Studies of Lipid Pellets and Extrudates .....	128
7.3.13. In-line Drug Release of Lipid Pellets, Extrudates, and ODTs .....	129
7.3.14. Particle Size Distribution and Particular Shape of Lipid Micropellets	130

7.3.15. Electronic Tongue Measurements.....	130
7.3.15.1. Electronic Tongue Calibration Procedure.....	131
7.3.15.2. Sample Preparation for Electronic Tongue Measurements.....	131
7.3.15.3. Data Evaluation of Taste Assessment .....	131
7.3.15.4. Euclidean Distances .....	132
7.3.16. Appearance and Dimensions of Tablets .....	132
7.3.17. Mass Uniformity of Tablets.....	132
7.3.18. Tensile Strength of Tablets.....	132
7.3.19. Disintegration Time of Tablets .....	133
7.3.20. Friability of Tablets .....	133
7.3.21. Label Claim of Tablets.....	133
7.3.22. Wetting Time and Water Absorption of Tablets.....	133
7.3.23. Dissolution Studies of Tablets.....	134
7.3.24. Dynamic Water Sorption System (SPS11).....	134
8. Annex .....	135
Annex I.....	135
Annex II.....	136
Annex III .....	137
Annex IV .....	138
Annex V.....	139
Annex VI .....	140
Annex VII.....	141
Annex VIII.....	142
Annex IX .....	143
Annex X.....	144
9. Scientific Publications Associated with this Thesis .....	145
9.1. International Peer-Reviewed Journals .....	145
9.2. Conference Presentations.....	145
10. References.....	147
11. Danksagung .....	163

---

## Abbreviations

Å	Angstrom
AAPS	American Association of Pharmaceutic Scientist
ADA	American Diabetes Association
ADI	acceptable daily intake
API	active pharmaceutical ingredient
AR	aspect ratio
AUC	area under the curve
B	width, breadth
BCS	Biopharmaceutics Classification System
CAS	Chemical Abstract Service
CI	Carr's index
D	diameter
d <sub>10</sub>	10% quantile
d <sub>50</sub>	50% quantile, median
d <sub>90</sub>	90% quantile
DM2	type 2 diabetes <i>mellitus</i>
DoE	Design of Experiment
DSC	differential scanning calorimetry
EASD	European Association for the Study of Diabetes
EDQM	European Directorate for the Quality of Medicines
F	force
FDA	Food and Drug Administration
ff <sub>c</sub>	flow function coefficient
FIP	International Pharmaceutical Federation
GFA	same direction, conveying, comb-out element
GFF	same direction, conveying, cut-free element
h	height
HCl	hydrochloride
HF	Hausner factor
HPLC	high performance liquid chromatography
HPMC	hydroxypropyl methylcellulose
IDF	International Diabetes Federation
IR	infrared
IUPAC	International Union of Pure and Applied Chemistry

J	Joule
KB	kneading block
KCl	potassium chloride
kN	kilo Newton
kPa	kilo Pascal
L	length, longest Feret diameter
LC	liquid chromatography
LOD	loss on drying
MCC	microcrystalline cellulose
MFT	minimum film forming temperature
MLR	multiple linear regression
MPa	mega Pascal
MUPS	multiple-unit pellet system
mV	millivolts
MVDA	multivariate data analysis
N	Newton
n	sample size
NIDDM	non-insulin dependent diabetes <i>mellitus</i>
ODT	orodispersible tablet
P.A.	analytical grade (per analysis)
PC1	first principal component
PC2	second principal component
PCA	principal component analysis
PEG	polyethylene glycol
Ph. Eur.	European Pharmacopoeia
Q <sup>2</sup>	goodness of prediction
r.H.	relative humidity
R <sup>2</sup>	coefficient of determination, goodness of fit
rpm	rotation per minute
RSD	relative standard deviation
S	pointless
SD	standard deviation
SEM	scanning electron microscopy
SFC	solid fat content
SLCE	solid lipid cold extrusion
TAG	triglycerides
Tg	glass transition temperature

---

u.a.	absorbance unit
UK	United Kingdom
UKPDS	United Kingdom Prospective Diabetes Study
USA	United States of America
USP	United States Pharmacopoeia
UV	ultraviolet
$V_{10}$	powder volume after 10 sequential falls
$V_{1250}$	powder volume after 1250 sequential falls
$V_{500}$	powder volume after 5000 sequential falls
$V_b$	bulk volume
$V_{is}$	visible
$V_t$	tapped volume
WHO	World Health Organization
XRPD	X-ray powder diffractometry
$\rho_{He}$	density obtained from helium pycnometric measurement
$\rho_M$	density obtained from Mercury porosimeter
$\sigma$	normal stress
$\sigma_1$	consolidation stress
$\sigma_c$	unconfined yield strength
$\sigma_T$	tensile strength
$\tau$	shear stress
$\rho_b$	bulk density
$\rho_t$	tapped density
$X_{c \min}$	particle diameter, which is the shortest chord of the measured set of maximum chords of a particle projection
$X_{Fe \max}$	particle diameter which is the longest Feret diameter of the measured set of Feret diameter of a particle





# 1. Introduction

Currently, there are about 506 million people over the age of 65 years. The estimation for 2040 reaches up to an approximate number of 1.3 billion, representing 14% of the world population. Until 2019, the number of people in the world over 65 is estimated to exceed that of children less than 5 years old (Kinsella and He, 2009). The increasing rate of the older population is more pronounced in developing countries, which is the two times higher than in developed countries and is the double of the rate of the world population.

The implications from this global change are enormous, with respect to the increase of chronic disease cases, especially in developing countries (Kinsella and He, 2009). Geriatric patients differ in many aspects from a “regular” patient, who is generally the focus of pharmaceutical companies that develop new medicines. The changes resulting from the body aging include neurological changes, alterations in the integumentary system (skin, along with hair and nails), in the sensorial perceptions, in the cardiovascular, pulmonary and gastrointestinal system, in the renal and endocrinal functions, and in the immunologic system. These physiological modifications, which contribute to the fact that people over 70 years old are the largest consumers of “over the counter” medicines and prescription medications, can affect the safety of the use of medicines by the elderly (Day, 1999; Hall, 2002).

When administering a medication, it has to be evaluated whether the patient is able to receive the dose of the drug completely, as well as comfortable and in a safe way. However, a critical analysis of available products showed that this is not the case with most medicines used in geriatric treatment. The development of suitable dosage forms for use by the elderly is a necessary trend and the issues related to the administration route, the pharmaceutical dosage form, and its composition should be carefully evaluated (Mizumoto *et al.*, 2005; Breitzkreutz and Boos, 2007). Due to the changes in physiological functions associated with aging, the use of certain traditional dosage forms, such as capsules and tablets, are often impractical (Lindgren and Janzon, 1991; Liu *et al.*, 2014).

One of the main problems is related to the difficulty in swallowing. As a result, poor patient compliance can be expected when the use of traditional formulations and pharmaceutical dosage forms by the elderly is considered. It is estimated that 35% of the general population, 30 to 40% of institutionalized elderly patients, and 18 to 22% of people in long-term care units suffer from swallowing disorders (dysphagia) (Sastry *et al.*, 2000). Furthermore, some general characteristics for geriatric medicine should be established and applied for each stage of the development of a new formulation. These characteristics include sufficient bioavailability, safe excipients, good

palatability and/or acceptable organoleptic properties, appropriate uniformity of dose, easy and safe administration, socio-cultural acceptability, and presence of clear and precise information on the formulation or the drug (Breitkreutz and Boos, 2007).

Studies show an uprising trend in research on the development of new formulations, dosage forms, and methods of administration of drugs for the elderly population (Watanabe *et al.*, 1995; Mizumoto *et al.*, 2005; Rabell-Santacana *et al.*, 2008; Arias *et al.*, 2009), as well as a growing consideration about the use and the interrelationship between drugs and the elderly (Turkoski, 1998; Hall, 2002; Breitkreutz and Boos, 2007; Yeh *et al.*, 2007; Sicras-Mainar *et al.*, 2009). Adequate formulations for the use by the elderly are those easy to swallow and easy to handle (Mizumoto *et al.*, 2005). Taking these information into account, researchers have pursued the development of dosage forms more appropriate for this patient population, for example, orally fast disintegrating tablets (orodispersible tablets or simply “ODTs”) (Mizumoto *et al.*, 2005; Khan *et al.*, 2007; Okuda *et al.*, 2009). Recently, ODTs are receiving attention as a preferred alternative to conventional solid dosage forms, such as capsules and tablets. This dosage form is placed into the oral cavity allowing the dispersion of particles in saliva, producing generally a suspension that is easily swallowed by the patient (Kundu and Sahoo, 2008). According to Bandari *et al.* (2008), the demand for ODTs is growing quickly and presents a significant impact on patient compliance to treatments. They can be easily administered to patients with dysphagia, i.e. elderly and children (Sastry *et al.*, 2000).

Comparatively, ODTs have advantages from both types of usual dosage forms, solid and liquid; they remain in solid form during storage, providing greater stability, and turn into a liquid or semi-solid form within a few seconds after administration. ODTs present high stability and accuracy of dose, are easy to manufacture also in small dimensions, facilitating storage and handling by patients. Consequently, they are the dose form of choice for elderly, pediatric patients and for institutionalized patients with mental dementia or even unconscious individuals (Bandari *et al.*, 2008). Additionally, they present only a low risk of obstruction during swallowing, and can be administered without the need of simultaneous water intake. The rapid disintegration of the tablets could also result in faster dissolution and absorption, leading to a quick onset of the pharmacological effect.

Moreover, some common diseases also present a strong influence on the necessity of medicines specifically for the elderly population. One of the most prominent examples is the type 2 diabetes *mellitus* (DM2). In general, diabetes *mellitus* is a group of disorders in the carbohydrate metabolism in which the insulin action is diminished or erased by a change in its secretion, or a decrease in its activity (due to a decreased functionality of insulin sensors in the tissues) or a combination of these two factors. As the disease progresses, damage to tissues or to the vascular system can lead to

severe complications such as retinopathy, nephropathy, neuropathy, cardiovascular problems, and alimentary ulceration (Sweetman, 2006).

Diabetes *mellitus* can be classified into several types; however, there are two main forms: type 1 (insulin-dependent) and type 2 (non-insulin dependent). The DM2 usually develops more in the adult age, affecting mainly the elderly and/or obese individuals. The secretion of insulin may seem normal or even excessive, but is still insufficient to compensate the insulin resistance (Sweetman, 2006). DM2 constitutes 85 to 95% of all diabetes cases in developed countries and has reached epidemic proportions in several nations (Zimmet *et al.*, 1997; Giannella-Neto and Gomes, 2009). In 2007, 246 million cases of diabetes were estimated in the world. Additionally, because of inefficiency, lack of professional and material resources, the public health system in developing countries will have to face an even greater number of people with this type of disease in the future (Giannella-Neto and Gomes, 2009).

In this context, the use of metformin in the treatment of DM2 patients can be highlighted. Found in its salt form, metformin hydrochloride, it is the drug of choice by the National Health System in South America, Europe, and North America (Gregorio *et al.*, 1996; Soto *et al.*, 2008). Its usual oral dose is 500 mg, administered two to three times a day, which can be increased gradually to 1000 mg (Sweetman, 2006). The efficacy of metformin HCl in the treatment of DM2 of other indications associated with insulin resistance has been shown in several studies (Campbell, 1991; Di Cianni *et al.*, 1994; Fujioka *et al.*, 2003; Soto *et al.*, 2008). On the other hand, some problems associated with the use of metformin HCl generally result in lack of adherence to treatment. The large size of the tablets containing 500 to 1000 mg of the API and its strongly bitter taste lead to difficulties in administration, especially by elderly patients or patients suffering from dysphagia, which could lead to discontinuation of the treatment (Gregorio *et al.*, 1996; Mohapatra *et al.*, 2008a; Stegemann *et al.*, 2012).

This whole set of information indicates the importance of developing new advanced formulations, specific drug dosage forms, and different modes of administration of drugs that satisfy the requirements of the elderly population in relation to physiological, biopharmaceutical, socio-cultural, and patient adherence to treatment. Thus, the aim of this project is to develop taste-masked orodispersible tablets containing high drug load of metformin HCl.



## 2. General Part

### 2.1. Type 2 Diabetes *Mellitus*

Diabetes was first described 3500 years ago by the ancient Egyptians. One of the first clinical descriptions was made by *Aretaeus*, who practiced medicine in Cappadocia around 120 A.D. (King *et al.*, 1999). The term diabetes *mellitus* describes a metabolic disorder of multiple etiology characterized by chronic hyperglycemia with disturbances in carbohydrate, fat, and protein metabolism, resulting from failings in insulin secretion, insulin action, or even both (Alberti and Zimmet, 1998).

There are three main known types of diabetes: type 1 diabetes, type 2 diabetes, and gestational diabetes. They usually occur when the body cannot produce enough insulin or cannot use insulin effectively. Insulin is a peptide hormone that regulates the metabolism of carbohydrates and fats by promoting the absorption of glucose from the blood to skeletal muscles and adipose tissue (IDF, 2013; Tibaldi, 2014). The most common type of diabetes is the type 2 (DM2), also known as non-insulin dependent diabetes *mellitus* (NIDDM). It generally occurs in adults, but it is increasingly diagnosed in children and adolescents (IDF, 2013). This particular type is characterized by impaired insulin secretion and reduced peripheral insulin sensitivity. The body is able to produce insulin but either this is not sufficient or the body is unable to respond to its effects (insulin resistance). Even though it is quite known that the pathogenesis originates from documented defects at the level of pancreatic  $\beta$ -cell, muscle, and liver, the causes or specific reasons for the development of these abnormalities are not completely understood (Bailey and Turner, 1996; Davidson and Peters, 1997; Alberti and Zimmet, 1998; Pickup and Crook, 1998).

For human health, as well as in financial terms, the burden of diabetes in the world is enormous, causing around 5.1 million deaths a year and taking up 548 billion US dollars in health spending in 2013 (11% of the total spent worldwide). DM2 represents a significant proportion of health care expenditures for treatment and prevention of complications (Dailey *et al.*, 2001). In 1997, DM2 represented the major public health issue all over the world, becoming the status of a “diabetes epidemic” (Zimmet *et al.*, 1997). Recently, an International Diabetes Federation (IDF) estimation indicates that 8.3% of the adult population (around 382 million people) suffers from diabetes; and the number of people with the disease is expected to rise to 592 million in less than 25 years (IDF, 2013). The burden of diabetes is not only reflected in the increasing number of people with diabetes, but also in the related growing number of premature deaths. In 2013, roughly half of all deaths due to diabetes in adults were related to people under the age of 60. In less developed regions, like Africa, this proportion

climbs to over 75% (IDF, 2013). Despite the public awareness, the development of innovative pharmaceutical therapies, and the implementation of new measures to improve diagnosis and treatment, diabetes persists as a cost driver in worldwide care systems (Dailey *et al.*, 2001).

Markedly, diabetes has increased alongside rapid cultural and social changes, such as aging populations, increasing urbanization, dietary changes, reduced morphological activity, and unhealthy behaviors (WHO, 1994). Obesity is considered one of the main risk factors for DM2. All over the world, the diabetes epidemic is associated to the increase of obesity, due to a “westernized” lifestyle: namely changes in nutritional habits with increased intake of saturated fats, refined sugars and alcohol, reduced intake of fibers, and at the same time, reduction in morphological activity (Virally *et al.*, 2007). Treatment options include diet, oral antihyperglycemic agents, and insulin (Davidson and Peters, 1997). When dietary treatment fails and glycemic control deteriorates, some pharmacological oral treatment must be started (Gregorio *et al.*, 1996). Although dietary management is the easiest approach, at least 50% of type 2 diabetic patients require the addition of an oral antihyperglycemic agent to achieve satisfactory glycemic control (Campbell, 1991).

Likewise, aging is becoming a risk factor for DM2 since the world population is aging and the number of elderly diabetic patients is also increasing (Gregorio *et al.*, 1996). With aging two phenomena occur: physiologic declining functions and an increase in the prevalence of diseases. Although these processes influence each other, physiologic impaired functions occur independent of illnesses (Abrass, 1990). In this context, the prevalence of DM2 related to elderlies is increasing and already affects 18 to 22% of people over 65 years old in United States, for example (Harris, 1998).

A United Kingdom Prospective Diabetes Study (UKPDS) reported that DM2 can be treated initially with an oral agent monotherapy. This study showed improved glycemic control, irrespective of the agent used (sulfonylureas, metformin, or insulin), decreased the incidence of microvascular complications (retinopathy, neuropathy, and nephropathy) (DeFronzo, 1999). However, pharmacological treatment of DM2 in elderly patients is becoming a growing and complex problem in the clinical practice, since longevity in almost every population is increasing and is accompanied with complex physiological alterations (Gregorio *et al.*, 1996). Due to physiological heterogeneity of elderly ranges from healthy and active to very frail, clinicians’ approach to what constitutes acceptable glucose control must be carefully individualized (Wallace, 1999). With the growing number of effective and available drugs and drug products, drug therapy is and will continue to be an integral part of older age (Stegemann *et al.*, 2012).

## 2.2. Metformin

Metformin is widely used for the treatment of DM2. It is a biguanide developed from galegine, a guanidine derivative found in *Galega officinallis* (Graham *et al.*, 2011). Chemically, metformin is a hydrophilic base (Figure 2.1), however, is usually present in oral dosage forms in its hydrochloride salt form. Metformin HCl has acid dissociation constant values (pKa) of 2.8 and 11.5 and, therefore, exists very large as the hydrophilic cationic species at physiological pH values ( $> 99.9\%$ ) (Graham *et al.*, 2011). The lipid solubility of the unionized species is low as shown by its low water-oil partition coefficient value ( $\log P = 1.43$ ) (Pentikainen, 1986). This chemical parameter indicates low lipophilicity and, therefore, rapid passive diffusion of metformin through cell membranes is unlikely (Graham *et al.*, 2011). Based on these properties, metformin HCl is defined as class III (low permeability, high solubility) by the Biopharmaceutics Classification System (BCS) (FDA, 2000).

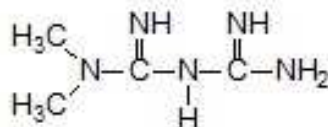


**Figure 2.1.** Chemical structure of metformin: N,N-dimethylimidodicarbonimidic diamide

Absorption from the stomach is likely to be negligible and it therefore appears that the absorption of metformin is confined largely to the small intestine with negligible absorption also from the large intestine (Graham *et al.*, 2011). The gastrointestinal absorption of metformin is incomplete with an absolute bioavailability of 40 to 60% (under fasting conditions) in combination with rapid elimination, and 20 to 30% of an oral dose is recovered in faeces. Interestingly, its absorption rate decreases as the dose increases, suggesting some form of saturable absorption or permeability/transit time-limited absorption (Tucker *et al.*, 1981) and negligible hepatic metabolism (Scheen, 1996). Passive diffusion of metformin through cell membranes is low because of the hydrophilic chemical nature of metformin. However, it is a substrate for several organic cation transporters (Graham *et al.*, 2011). Metformin is excreted unchanged in urine and the elimination half-life ( $t_{1/2}$ ) of metformin during multiple dosages in patients with good renal function is approximately 5 hours (Graham *et al.*, 2011).

Metformin is an antihyperglycemic agent which improves glucose tolerance in type 2 diabetic patients, lowering both basal and postprandial plasma glucose levels (Davidson and Peters, 1997). It is also considered an “insulin sensitizer”, since it lowers glucose levels without increasing insulin secretion. Metformin also lowers endogenous glucose production in the liver (Hundal and Inzucchi, 2003). The antihyperglycemic properties of metformin are mainly attributed to the suppression of hepatic glucose production, especially hepatic gluconeogenesis, and increased

peripheral tissue insulin sensitivity. Although the precise mechanism of hypoglycemic action of metformin remains unclear, it probably interrupts mitochondrial oxidative processes in the liver and corrects abnormalities of intracellular calcium metabolism in insulin-sensitive and cardiovascular tissue (Kirpichnikov *et al.*, 2002). Other proposed mechanisms of action include decreased hepatic glucose production, increased peripheral glucose disposal and reduced intestinal glucose absorption (Hundal and Inzucchi, 2003).

The American Diabetes Association (ADA), European Association for the Study of Diabetes (EASD), and the International Diabetes Federation (IDF) recommend metformin as first-choice treatment in all newly diagnosed patients (IDF, 2006; Nathan *et al.*, 2006). Additionally, although sulfonylureas traditionally have been used as first-line pharmacological therapy for DM2 patients, many experts and the UKPDS suggest that, in the absence of contraindications, metformin may be the agent of first choice for diabetic patients who are overweight (King *et al.*, 1999). Metformin HCl is also indicated for the treatment of type 2 diabetic patients whose hyperglycemia cannot be satisfactorily managed by diet alone (Hu *et al.*, 2006). Furthermore, studies reported antidiabetic effectiveness of metformin on the treatment of diabetic patients over 70 years old (Di Cianni *et al.*, 1994; Gregorio *et al.*, 1996).

The oral dose of metformin is considered as hydrochloride salt, but all concentrations in biological fluids are expressed as the free base (Graham *et al.*, 2011). The initial dose is generally 500 mg, two or three times daily, or 850 mg once or twice daily. Furthermore, it can be gradually increased if necessary, at intervals of at least 1 week, from 2 to 3 g daily (DeFronzo, 1999; Sweetman, 2006). In some cases, immediate-release metformin is administered in divided doses with meals to minimize gastrointestinal side effects. A dose of 500 mg has a low oral bioavailability, which decreases with higher starting doses (Pentikäinen *et al.*, 1979; Scheen, 1996; Cullen *et al.*, 2004). As is generally recommended, metformin HCl should be administered initially at a low doses in order to mitigate the adverse gastrointestinal effects. The doses should be increased to a maximum of 2.5 to 3 g daily in patients with good renal function although lower dosage may be sufficient. However, the dose of metformin HCl should be individualized because of intersubject variation in the bioavailability (Graham *et al.*, 2011).

### **2.3. Taste Issues with Metformin HCl Formulations and Patient Compliance**

Diabetes is a chronic illness requiring long-term administration of medication. Although fixed-dose antihyperglycemic medications offer less flexibility in terms of



adjustment of the dosing of the individual components, the benefits that may be achieved, such as increased acceptability, make these medications worth trying (Dailey *et al.*, 2001).

Acceptability is the overall ability of the patient and caregiver (commonly defined as “user”) to use a medicinal product as intended. The acceptability of a medicinal product has a significant impact on the patient’s adherence and consequently on the safety and efficacy of the product (Walsh *et al.*, 2014). It is generally driven by characteristics of the user (age, ability, disease type and physiologic conditions) and by the characteristics of a medicinal product such as palatability, swallowability, the required dose and frequency, the selected administration device, and the actual mode of administration (Walsh *et al.*, 2014). Notably, non-compliance is a major health care problem in all therapeutics areas, with estimates of nonadherence rates ranging from 30% to 60%, with higher rates in symptom-free patients (Dailey *et al.*, 2001).

There is no doubt that the oral route is the most preferred route in the administration of medicinal products and drug therapy. However, oral administration requires a satisfactory palatability and a functioning swallowing process. Palatability could be defined as the overall appreciation of an (often oral) medicine by organoleptic properties such as smell, taste, aftertaste and texture (mouthfeel), and possibly also vision and sound. It is determined by the characteristics of the components, the active pharmaceutical ingredient (API) and excipients, and the way the API is formulated. Not only should a medicinal product not taste and smell unpleasant, it should have acceptable mouthfeel (viscosity, grittiness) and appearance (visual aspect, size and shape) to have a positive influence on patient compliance (Walsh *et al.*, 2014).

Physiological properties such as temperature and texture affect the perception of taste. Moreover, human taste appears to change with age. Likewise, psychological factors can influence taste perception: a childhood memory of badly formulated cough medicine can significantly modify taste perception of a modern formulation. Such factors highlight the role of a taste in manufacturing a product that achieves patient compliance (Murray *et al.*, 2004). The bitterness of human pharmaceutical medicines plays a critical role in patient compliance as the oral administration of bitter drugs is often hampered by their unpleasant taste. This leads to noncompliance and thus decreases therapeutic efficacy, especially in case of children and elderlies (Schiffman *et al.*, 1994; Pandey *et al.*, 2010).

Metformin HCl is the focus of several works related to its unpleasant and bitter taste (Mohapatra *et al.*, 2008a; Bhoyar and Biyani, 2010; Gandhi *et al.*, 2010; Bhoyar *et al.*, 2011; Mostafavi *et al.*, 2014). Additionally, side effects and the need for two to three times a day administration can reduce patient compliance and hinder a more successful therapy (Hu *et al.*, 2006). Gastrointestinal side-effects, such as bloating, flatus and diarrhea, occur in about 30% of patients and therefore metformin HCl is

recommended to be taken with meals to minimize these gastrointestinal side effects (Sambol *et al.*, 1996).

Swallowing issues and the development of clinically significant dysphagia show increased prevalence with increasing age (Stegemann *et al.*, 2012). The individual swallowing capacity might differ significantly in older adults, while the overall swallowing capability is declining with increasing age (Nilsson *et al.*, 1996a). Another study performed by Nilsson *et al.* (1996b) showed that the mean oral-pharyngeal transit time in healthy adults is around 0.58 seconds. In contrast, this situation is drastically changed in the elderly population leading to an increase in swallowing time to around 1.23 seconds. Swallowing functions underlie a normal aging process and can be seriously impacted by diseases and disease progression as well as by drug substances. These age-related changes in swallowing functions are attributed to physiological, anatomical, motoric and sensory alterations. Furthermore, swallowing might also be impacted by a decline in saliva production or xerostomia, which affects bolus formation and smooth deglutination (Stegemann *et al.*, 2012).

Under those circumstances, the oral administration of metformin HCl tablets becomes a challenge since the usual doses of oral treatment with metformin HCl (500 to 1000 mg) generates tablets with relatively large dimensions (Figure 2.2). In the German market, for instance, the absence of alternative dosage forms, or age-adapted dosage forms, shows the lack of consideration to this special population: all 26 available products containing metformin HCl are film coated tablets with doses between 500 and 1000 mg (Rote Liste, 2014).

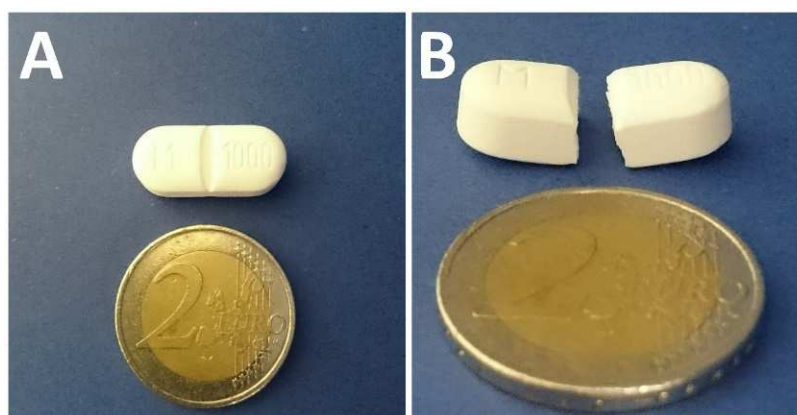


**Figure 2.2.** Available 1000 mg metformin HCl film tablet (Metformin Hexal® 1000 mg) in comparison to a two Euro coin: (a) from top view and (b) from the side view with the tablet divided

## 2.4. Taste-Masking of Solid Dosage Forms

Excessive bitterness of APIs in oral dosage form formulations is one of the major taste problems pharmaceutical scientists are facing (Zheng and Keeney, 2006). Palatability is largely dictated by taste and this is a concern as a significant number of APIs on

the market have a bitter taste. This is not considered to be a key issue when developing oral dosage forms for adults who can easily swallow tablets since such products can be film- or sugar-coated (Walsh *et al.*, 2014). However, with respect to patient acceptability and compliance, taste is one of the prime factors determining the market penetration and commercial success of oral formulations, especially in pediatric population (Jain *et al.*, 2010). Henceforth, the pragmatic approach often taken by patients and caretakers to facilitate administration of adverse taste medicines is to dilute or obscure the taste by mixing or sprinkling in food or beverages. However, there are risks associated with using this approach. For example, the entire dose of the medicinal product may not be consumed especially if the volume or quantity of food is too large or taste not appropriately masked. Hence, mixing with food or beverage should not be the primary means of taste-masking a formulation (Walsh *et al.*, 2014).

For this reason, taste-masking technology is gaining more attention in the pharmaceutical development area. The major aim of taste-masking techniques is to obscure the adverse taste of an API or formulation, or to prevent interactions of the dissolved API with the taste receptors in the mouth and throat (Walsh *et al.*, 2014) at least during the time which the dosage form or formulation remains in contact with them. The ideal approach to reduce or inhibit bitterness would be the discovery of a universal inhibitor of all bitter tasting substances without influencing the other taste modalities, such as sweetness or saltiness (Pandey *et al.*, 2010). However, until now such a substance is not discovered.

Taste-masking by using flavors and sweeteners is the foremost and the simplest approach for taste-masking, especially in the case of pediatric formulations, chewable tablets, and liquid formulations. As any compound dissolved in the saliva will interact with taste receptors and elicit a response, this approach does not work well for highly soluble and extremely bitter APIs, and for APIs with an intense lingering aftertaste (Pandey *et al.*, 2010; Walsh *et al.*, 2014). By the same token, whilst flavors and sweeteners are straight forward techniques and many of these excipients are subjected to regulatory restrictions which limit their use. Therefore, these excipients, although simple, may not sufficiently mask the taste of extremely bitter compounds (Gittings *et al.*, 2014).

Nowadays, two approaches are commonly utilized to overcome adverse taste of APIs. The first deals with a reduction of drug solubility in saliva, where a balance between reduced solubility and bioavailability must be achieved. The second is related to an alteration of the API ability to interact with taste receptors (Sajal *et al.*, 2008). The most commonly applied taste-masked techniques are shown in the Table 2.1.

**Table 2.1.** Taste-masking methodologies (Sohi *et al.*, 2004; Sajal *et al.*, 2008; Wagh and Ghadlinge, 2009; Pandey *et al.*, 2010; Gittings *et al.*, 2014; Walsh *et al.*, 2014)

Focus	Methodology
<i>Formulation</i>	Use of sweeteners and flavoring systems
	Using effervescent agent
	Taste-masking by dispersion systems (solid dispersions)
	Use of bitter blockers and taste modifiers
	Use of carbohydrates, proteins or lipids
	Rheological modifications
<i>API</i>	Salt preparation of bitter drugs
	Modification of the API solubility
	Using a prodrug approach
	Ion exchange resins
<i>Apply a morphological ‘barrier’ on the API or the dosage form</i>	Lipophilic vehicles like lipids and lecithin
	Creating a molecular barrier around the API by complexation
	Lipid or Polymer coating on the API or the dosage form
	Microencapsulation
	Multiple emulsion

Although these techniques showed positive results in several situations, they are not always useful or applicable. For example, the use capsules or coated tablets to mask the bitter taste of APIs is often uncomfortable for infants or elderly people, who have trouble in swallowing these dosage forms. Moreover, approaches such as drug coating, microencapsulation, complexation and chemical modification are not necessarily simple (coating processes are normally multi-step processes) and extensive optimization is required for their practical use (which are at least time and energy consuming) (Michalk *et al.*, 2008). Therefore the adequate dosage form, which can be easily produced and that the patients can swallow without problems may be important and valuable (Suzuki *et al.*, 2003).

There are numerous works related to the investigation of taste-masking of metformin HCl. Mohapatra *et al.* (2008a) developed ODTs prepared by direct compression of wet granules containing metformin HCl, starch 1500, croscarmellose sodium, and mannitol (using polyvinylpyrrolidone in isopropyl alcohol as binder). The tablets exhibited desired mouth feel and adequate disintegration time, water absorption ratio, and *in vitro* drug release: 85% drug release between 4 min and 8 min. The saline and bitter taste of the drug was masked using sweetener and flavor, however, the taste-masking investigation results are not presented in the work. Furthermore, the same research group developed an oral soft gel (Mohapatra *et al.*, 2008b) and soluble effervescent tablets (Mohapatra *et al.*, 2008c) containing metformin HCl. However, doses higher than 250 mg were not investigated and no improvement in the

methodology for taste-masking was reported. The same taste-masking technique was used for both dosage forms: addition of a sweetener and flavor excipient.

Likewise, Bhoyar and Biyani (2010) investigated the preparation of a sustained release tablet containing metformin HCl as well as to mask the bitter taste of the API by complexation technique using strong cation-exchange resins, indion 244 and indion 264. Resinate tablets were formulated using HPMC by direct compression. The results showed that metformin HCl was successfully taste-masked, however, the tablets showed a slow release of metformin HCl. Doses higher than 250 mg were not investigated. Interestingly, a similar work was reported by Bhoyar *et al.* (2011) presenting exactly the same development and results.

Gandhi *et al.* (2010) developed metformin HCl fast disintegrating tablets using polacrillin potassium from different sources as disintegrants. The bitter taste of the API was masked using suitable concentration of sweetener and flavor. According to the author, the taste-masked properties of the tablets were evaluated by human volunteers, however, the discussion of the results from this investigation is not reported in this work.

Furthermore, Mostafavi *et al.* (2014) developed a taste-masked chewing gum with containing metformin HCl. The API was mixed with acesulfame-isomalt as sweeteners and further spray dried, freeze dried, or directly mixed with a chewing gum base containing glycerin, xylitol, and menthol. Taste, flavor, and appearance characteristics were evaluated by using a self-made questionnaire based on the hedonic test method. The results of this questionnaire indicated that the formulation containing 250 mg of metformin HCl, obtained by freeze drying, was adequate to suppress the bitter taste of the API.

## 2.5. Lipids in Solid Oral Dosage Forms

When designing an age-appropriated medicinal product, the used excipients should be chosen according to their benefits and risks, encompassing all aspects of the proposed excipient in parallel, including: physicochemical properties, purity, toxicity, acceptable daily intake (ADI), tolerability, patient's age, patient's susceptibility, dosage regime/exposure, possible cumulative effect with excipients in concomitant medications, and regulatory status. Due to the advantage of low safety concerns or ADI restrictions, lipids are becoming an interesting and promising class of pharmaceutical excipients for taste-masking purposes (Walsh *et al.*, 2014).

There is no strict definition of the term lipid that is generally accepted (Larsson, 1966). According to Rosiaux *et al.* (2014), the term "lipid" describes a family of products with diverse physicochemical properties. Their composition includes oils,

fats, waxes, fatty acids and their derivatives, and substances related biosynthetically or functionally to these compounds (Larsson, 1966; Rosiaux *et al.*, 2014). Naturally occurring lipids are typically triglycerides, esters of glycerol and three fatty acids (triacylglycerols or triglycerides, TAGs). The basic structure of TAGs is depicted in Figure 2.3. The nature and compositions of three fatty acid radicals of a TAG molecule, defined as  $R_1$ ,  $R_2$  and  $R_3$ , determine its chemical property (Sato, 2001).

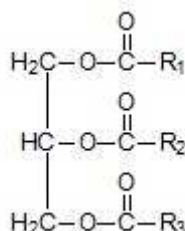


**Figure 2.3.** General structure of a triglyceride

An important characteristic of TAGs is their crystallization behavior. The specific properties of the crystallization of fats and lipids may be revealed in polymorphism on one side, and molecular interactions on the other. For example, a TAG usually possesses three polymorphs:  $\alpha$ ,  $\beta$ , and  $\beta'$  conformations. The crystallization behavior of the TAG such as crystallization rate, crystal sizes and their network, crystal morphology and crystallinity, are directly influenced by polymorphism which is influenced by molecular structure itself, and by several external factors such as temperature, pressure, solvent, rate of crystallization, impurities, etc. Due to the conformation differences, they present different melting points; the  $\alpha$  modification being the meta-stable form presenting the lowest melting point, followed by the  $\beta$  modification and the  $\beta'$  modification, which is the stable form and presents the highest melting point (Larsson, 1966; Sato, 2001).

In pharmaceuticals, short chain and unsaturated long chain fatty acids (liquids, semi-solids and some solids) are approved for use in creams, ointments, emulsions, dispersions, and suppositories (Rosiaux *et al.*, 2014). Long chain triglycerides, which have no practical ability to self-disperse, are digested rapidly in the intestine (lipolysis). Furthermore, their fatty acids and monoglycerides digestion products are solubilized by bile salt-lecithin mixed micelles, which are then absorbed (Carey *et al.*, 1983). The lipid excipients used in pharmaceutical development are derived predominantly from the food industry where they are used as additives for emulsification, solubilization, stabilization and lubrication. Besides, lipid excipients have been refined and fine-tuned for the pharmaceutical industry to provide solutions to drug delivery challenges including drug solubility, drug dissolution properties and also to resolve manufacturing issues (Rosiaux *et al.*, 2014). The most important group for commercial products are the non-polar lipids – fatty acids esters of glycerol or triglycerides (Larsson, 1966). However, over the last four decades, naturally occurring

triglycerides have been physicochemical modified to develop excipients suitable for the development of drug delivery systems (Rosiaux *et al.*, 2014).

In like manner, solid lipids became more and more interesting as pharmaceutical excipients for solid dosage forms (Saraiya and Bolton, 1990; Breitskreutz *et al.*, 2003; Jannin *et al.*, 2008; Pouton and Porter, 2008; Eckert *et al.*, 2014). They are normally crystalline in nature and have melting ranges or melting points determined by their chemical structure (and composition) (Rosiaux *et al.*, 2014). They were used primarily as lubricants to aid manufacturing of solid dosage forms. They are chemically inert and their properties such as high hydrophobicity and low density, can be used to create sustained release matrices to mask bitter tasting drugs or to solubilize lipophilic drugs (Miller and York, 1988; Pouton and Porter, 2008). Furthermore, solid lipids used as sustained release agents provide different biopharmaceutical properties compared to polymers. Fundamentally the drug release mechanism is different and this provides formulators with broader options for controlling drug release scope to develop innovative dosage forms (Rosiaux *et al.*, 2014).

Besides, they are able to enhance the solubility and permeability of drugs with poor oral bioavailability (Prabhu *et al.*, 2005), a fact that is increasingly important since a large proportion of the newly developed APIs have low solubility and permeability (Lindenberg *et al.*, 2004). Lipid excipients may be used to provide controlled/delayed release properties in medicinal products and represent an attractive alternative to polymer coatings for taste-masking (Walsh *et al.*, 2014). Several processing methods could be applied using solid lipids, such as direct compression (Singh *et al.*, 2009), dry and wet granulation (Franceschini *et al.*, 2005), melt granulation (Eckert *et al.*, 2014) and melt pelletization (Cox, 1991), molding (Rosenberg and Breitenbach, 2002), spray congealing/chilling and prilling (Passerini *et al.*, 2010), and hot melt coating (Faham *et al.*, 2000). Choosing the appropriate TAG for the use in pharmaceutical process, such as extrusion, requires an understanding of their physicochemical properties and its associated effect on API release and taste-masking effect (Walsh *et al.*, 2014). Some lipid excipients used in the pharmaceutical industry are shown in Table 2.2.

**Table 2.2.** Commonly used lipids (adapted from Walsh *et al.* (2014))

Type	Excipient name	Commercial name
Hydrogenated vegetable oils	Hydrogenated cottonseed oil	Lubritab <sup>®</sup>
	Hydrogenated palm oil	Dynasan <sup>®</sup> P60, Softisan <sup>®</sup> 154
Partial glycerides	Glyceryl monostearate	Inwitor <sup>®</sup> 191, Cutina <sup>®</sup> GMS or Tegin <sup>®</sup>
	Glyceryl distearate	Precirol <sup>®</sup> ATO 5
	Glyceryl dibehenate	Compritrol <sup>®</sup> 888 ATO
Triglycerides (TAG)	Glyceryl trimyristate	Dynasan <sup>®</sup> 114
	Glyceryl tristearate	Dynasan <sup>®</sup> 118
Polyoxyglycerides or macroglycerides	Lauryl polyoxyglycerides	Gelucire <sup>®</sup> 44/14
	Stearyl polyoxyglycerides	Gelucire <sup>®</sup> 50/13
Waxes/hard fat	Carnauba wax	Carbowax <sup>®</sup>
	Bees was	Witepsol <sup>®</sup> W35
	Polyethylene glycol (PEG)	Macrogol <sup>®</sup> 1500
	Hydrogenated coco-glycerides	Witocan <sup>®</sup> 42/44

## 2.6. Extrusion and Spheronization

### 2.6.1. Solid Lipid Cold Extrusion

Extrusion is a well-known processing technology that has been developed over the last century and spans many diverse industrial fields. The extrusion process consists of forcing the passage of a material (with plastic characteristics) through dies under controlled conditions and shaped into small cylindrical particles having a uniform diameter (Erkoboni, 1997; Mollan, 2003). Generally, the extrudate particle breaks at similar lengths under their own weight. The extrudate must have enough plasticity to deform but not so much as to adhere to other particles when collected (Erkoboni, 1997). The pharmaceutical extruders were adapted from the food and plastic industries and can be classified into three classes based on their feed mechanisms: screw, gravity, or piston (Erkoboni, 1997; Thiele, 2003).

Certainly, the most widely spread and versatile type of equipment is the co-rotating twin screw extruder. Twin-screw extruders were initially developed in the 1800s, with the concept of combining the machine actions of several available devices into a single unit (Mollan, 2003). The equipment consists of a platform, barrels, screws arranged on a screw shaft, a die, and connection to utilities and controls. Extruder barrels and screws are usually modular in arrangement as shown in Figure 2.4a. The configuration of the screws can be varied by number and arrangement of conveying and kneading elements. Usually, screw elements (Figure 2.4b-1) may be broadly classified as forwarding or conveying (Figure 2.4b-2) and kneading elements, this last being divided in mixing (Figure 2.4b-3), and zoning elements (Figure 2.4b-4). However it is



not unusual for screw pieces to have more than one of these attributes, sometimes all three (Thiele, 2003). This classical, tightly meshing screws, co-rotating system is preferred for many pharmaceutical processes. They can be operated at high screw speeds and high output and provide good mixing and conveying characteristics as well as more flexibility in screw design (Kolter *et al.*, 2012).

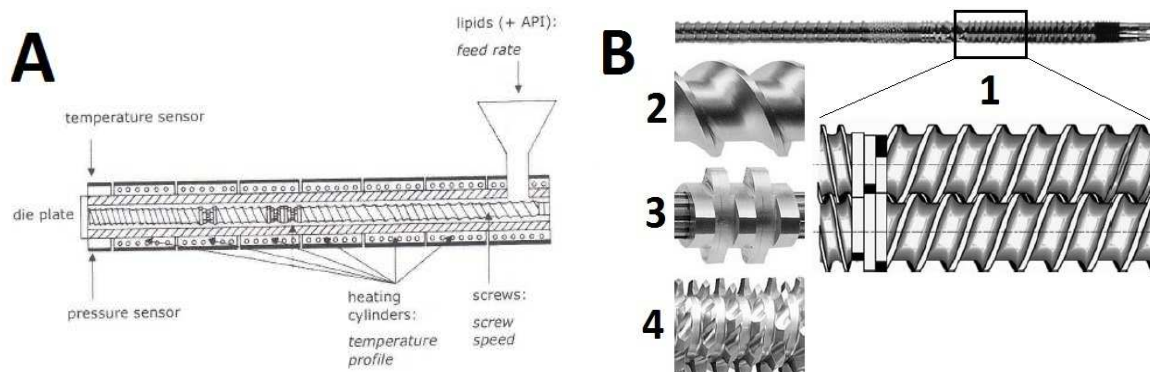


**Figure 2.4.** (A) Scheme of a twin-screw extruder (adapted from Kleinebudde (2013)) and (B) Co-rotating twin-screw elements: (1) screw overview, (2) forwarding elements, (3) mixing elements, and (4) zoning elements (adapted from Thiele (2003))

In twin screw wet extrusion, microcrystalline cellulose (MCC) is considered the standard extrusion aid and it is usually added to many formulations to achieve the desired properties. Currently, there is no other material that behaves in the same manner like MCC and possesses the same properties (Bornhöft *et al.*, 2005). Although MCC is the most used aid in extrusion processes, formulations based on it showed some disadvantages like the non-disintegration of the pellets, prolonged drug release of poorly soluble drugs, chemical incompatibility with specific drugs and/or drug adsorption onto MCC fibers (Kleinebudde, 1994; Dukić-Ott *et al.*, 2009). Moreover, according to Schröder and Kleinebudde (1996), these undesired properties cannot be overcome by the simple addition of disintegration aids. Consequently, the production of fast release pellets by extrusion/spheronization employing MCC is quite difficult.

Powdered solid lipids are a group of excipients that have recently generated substantial interest on the production of oral dosage forms. They showed a high variability in their physicochemical properties which offer various possibilities for different types of pharmaceutical formulations, especially in the pharmaceutical extrusion processes (Breitkreutz *et al.*, 2003; Chatchawalsaisin *et al.*, 2005; Windbergs *et al.*, 2009c). Currently, a particular extrusion process using solid lipids as extrusion aid (generally as binder) is becoming more attention in the development of extrudates and pellets due to the possibility of drug release modification and taste-masking of bitter APIs (Reitz and Kleinebudde, 2007b; Krause *et al.*, 2009; Vaassen *et al.*, 2012). The solid lipid cold extrusion (SLCE), also known as “solvent-free cold extrusion” or simply cold extrusion, is an innovative preparation method for matrices which takes place some degrees Celsius below the melting point or melting range of the used lipid

(or mixture of lipids) (Reitz *et al.*, 2008; Kleinebudde, 2013). In contrast to other similar processes, such as hot melt lipid extrusion, the lipids are not molten but “softened” due to a specific thermo-mechanical treatment. The process is performed under moderate pressure and temperature, resulting in a plastic moldable lipid mass (Reitz and Kleinebudde, 2007b). The material plasticity, in this case called “softening”, is achieved without melting the bulk part of the lipid. Depending on the melting point of the lipid, the extrusion process can be performed at room temperature or up to approximately 70 °C. The lipid is not removed and usually forms a matrix, which can influence the drug release from the extrudate. In the simplest case, binary mixtures of lipid and API are extruded. The API load in the extrudate can be as high as 80% or even higher in some cases (Kleinebudde, 2013).

Because of its solvent-free characteristic, SLCE is an advantageous method for the development of pediatric and geriatric dosage forms, since the residual solvent burden is reduced to zero. As no water is used, water sensitive or hygroscopic APIs can be used and the risk of microbial contamination is also reduced. Likewise, as the process is held at low temperatures and no further drying step is required, the process is suitable for evaporating API and also for thermolabile substances. As changes in the solid state of lipids can affect critical product properties (Larsson, 1966; Sato, 2001; Choy *et al.*, 2005), the temperature can be considered the major issue for development of formulations based on solid lipids. SLCE has a major advantage over techniques working with molten lipids, such as hot melt extrusion. However, the advantages are only valid, if the starting material is the stable modification of the lipid. It is unlikely that the API itself melts and issues regarding recrystallization of metastable modifications of the API can be avoided (Breitkreutz *et al.*, 2003; Kleinebudde, 2013; Walsh *et al.*, 2014).

The most employed solid lipids in SLCE using twin-screw extruder are described in Table 2.3. Among them, the most used is the Witocan<sup>®</sup> 42/44 (also known as hard fat) which is also widely employed as special hard fat in chocolate and confectionery industry (Suzuki *et al.*, 2004). Equally important, pure monoacid triglycerides, such as trilaurin, tripalmitin, and tristearin showed good stability of the dosage form (Reitz *et al.*, 2008; Windbergs *et al.*, 2009b), however they are brittle and have a narrow melting range. Therefore, they are difficult to handle in a solid lipid extrusion process. On the other hand, monoglycerides, diglycerides and multiacid glycerides mixtures have a smooth consistency and broader melting range, resulting in robust and less complicated extrusion processes (Krause *et al.*, 2009; Witzleb *et al.*, 2011b).

**Table 2.3.** Most used solid lipids in SLCE (adapted from Krause (2008))

	Hard fat	Glyceryl trimyristate (trimyristin)	Glyceryl distearate	Glyceryl dibehenate
<i>Commercial name</i>	Witocan® 42/44	Dynasan® 114	Precirol® ATO 5	Compritol® 888 ATO
<i>Quality</i>	Ph. Eur.	Food grade	Ph. Eur.	Ph. Eur.
<i>Composition</i>	90% < triglycerides	95% < triglycerides	25-35% triglycerides 40-60% diglycerides 8-22% monoglycerides	21-35% triglycerides 40-60% diglycerides 13-21% monoglycerides
<i>Melting point</i>	42-44 °C	55-58 °C	53-57 °C	69-74 °C
<i>Hydroxyl number</i>	15	10	100	100
<i>Related works</i>	Breitkreutz <i>et al.</i> (2003); Krause <i>et al.</i> (2009); Reitz and Kleinebudde (2009); Vaassen <i>et al.</i> (2012); Witzleb <i>et al.</i> (2011b)	Güres and Kleinebudde (2011); Krause <i>et al.</i> (2009); Reitz and Kleinebudde (2007a); Reitz and Kleinebudde (2007b); Reitz and Kleinebudde (2009); Vaassen <i>et al.</i> (2012); Witzleb <i>et al.</i> (2011a)	Breitkreutz <i>et al.</i> (2003); Krause <i>et al.</i> (2009); Reitz and Kleinebudde (2007a); Reitz and Kleinebudde (2007b); Vaassen <i>et al.</i> (2012); Yan <i>et al.</i> (2012)	Krause <i>et al.</i> (2009); Michalk <i>et al.</i> (2008); Witzleb <i>et al.</i> (2011a); Witzleb <i>et al.</i> (2011b); Witzleb <i>et al.</i> (2012); Yan <i>et al.</i> (2012)

### 2.6.2. Solid Lipid Spheronization

In the pharmaceutical industry, pellets can be defined as small, free-flowing, spherical particles manufactured by agglomeration of fine powders or granules of drug substances and excipients using appropriate processing equipment (Ghebre-Sellassie and Knoch, 2006). Pellets as a drug delivery system offer not only therapeutic advantages such as less irritation of the gastro-intestinal tract and lowered risk of side effects due to dose dumping but also technological advantages, for example, better flow properties, less friable dosage form, narrow particle size distribution, superior quality for coating application and uniform powder packing characteristics (Reynolds, 1970; Erkoboni, 1997; Rahman *et al.*, 2009).

Pellets offer a high degree of flexibility in the design and development of oral dosage forms. They can be divided into desired dose strengths without formulation or processing changes and can also be blended to deliver incompatible bioactive agents

simultaneously and/or to provide different release profiles at the same or different sites in the gastrointestinal tract. In addition, orally taken pellets disperse freely in the gastrointestinal tract, maximize drug absorption, minimize local irritation of the mucosa by certain irritant drugs, improve the safety and efficacy of the active ingredient, and reduce inter- and intra-patient variability (Ghebre-Sellassie and Knoch, 2006; Hu *et al.*, 2006). Pellets are typically filled into hard gelatin capsules, but can also be compressed into tablets (Erkoboni, 1997). In addition, they can be further dispersed in a pleasant tasting suspension base or administered with food (Walsh *et al.*, 2014), or even be used in the development of tablets or ODTs.

There are several methods to produce pellets. One of the most employed is the extrusion followed by spheronization. Extrusion/spheronization technique was first reported by Reynolds (1970), but it was originally invented and copyrighted by Nakahara in 1964 (Nakahara, 1966). In the spheronization step the starting material, generally extrudates or irregular granules, is subsequently rounded into pellets as there is adequate surface plasticity under stress for remodeling and yet the mass is sufficiently cohesive to remain as an entity under the frictional stresses during the spheronization process (Heng, 2005). The major advantage of extrusion/spheronization over other methods of producing drug-loaded spheres or pellets is the ability to incorporate high levels of actives without producing an excessively large particle (Erkoboni, 1997).

Regarding the spheronization process, it is carried out in a relatively simple piece of equipment. The working parts consist of a bowl having fixed sidewalls with a rapidly rotating bottom plate or disk. The rounding of the extrudate into spheres or pellets is dependent on frictional forces which are generated by particle-particle and particle-equipment interactions. For this reason, the disk is generally machined to have a grooved surface that increases the forces generated as particles move across its surface (Figure 2.5) (Erkoboni, 1997).

The friction plate (or rotational plate/disk) can present frequently two geometrical surface patterns: a cross-hatched pattern with the grooves running at right angles to one another (which is more commonly used) (Figure 2.5a), and a radial pattern with the grooves running radially from the center (Figure 2.5b) (Erkoboni, 1997). Studies showed that the pattern of the friction plate used in the spheronization of extrudates could affected in some extent the morphological properties of the pellets, such as pellet size distribution, yield, mechanical strength, and density. However, the pellet shape do not seems to suffer influence by the plate pattern (Michie *et al.*, 2012). Other variables in the spheronization process include equipment size, material amount, plate rotational speed, temperature, and residence time. Each one of the variables has the potential to play a major role in influencing the morphological characteristics of the resulting product (depending on the material composition).

During the spheronization step, the extrudate is transformed from rod-shaped into spherical particles. This transition occurs in several and sequential stages. Once placed into the spheronizer, the extrudates are drawn to the walls of the extruder by centrifugal forces. Under ideal conditions, the extrudate breaks into smaller and more uniform pieces. Within a short time period, the length of each piece is approximately equal to the diameter of the initial extrudate, owing to attrition and rapid movement of the bottom plate. Due to the difference in particle velocity, as they move outward to the walls, the particles begin to climb the walls and fall back onto the rotating bed along with the angular motion of the friction plate, results in a rope-like formation (Figure 2.5c) (Erkoboni, 1997).

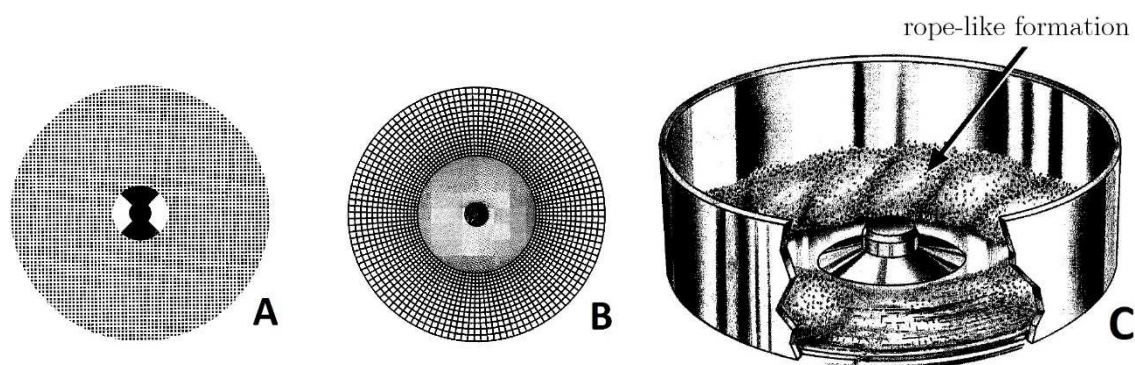


**Figure 2.5.** Friction plate surface geometry patterns: (A) cross-hatched pattern with the groves running at right angles to one another, (B) a radial pattern with the groves running radially from the center and circular grooves, and (C) particle’s bed movement on a spheronizer depicting a rope-like formation (adapted from Erkoboni (1997))

In literature there are two main models that describe the mechanisms of pellet formation by spheronization: one proposed by Rowe (1985) and a posterior, proposed by Baert *et al.* (1993). A graphic representation of this mechanisms is depicted in Figure 2.6. The previous model describes a transition from cylindrical particles (a1) into cylindrical particles with rounded edges (a2), a known “dumb-bell” form (a3), ellipsoid particles (a4), until a spherical shape is achieved (a5). The model proposed by Baert *et al.* (1993) describes a similar mechanism. However, in this mechanism, the transition from the initial cylindrical particle (b1) pass through different phases: a bent rope (b2), a “twisted” dumb-bell form (b3), and a two spherical particles with a hollow cavity (b4), until finally the formation of spheres is achieved (b5) (Erkoboni, 1997). Recently, new complementary mechanisms were proposed, such as the “mass transfer mechanism” by Koester and Thommes (2010) and the spheronization mechanism of MCC II-based pellets by Krueger *et al.* (2013). However, all these mechanisms are related to the spheronization of wet extrudates, generally based on microcrystalline cellulose or other commonly used spheronization aids which require water to achieve adequate plasticity.

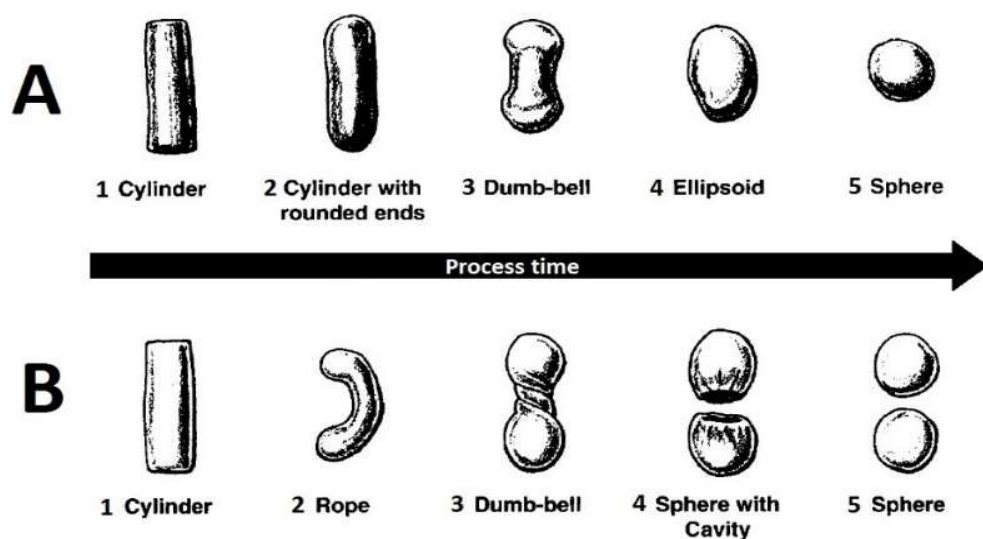


**Figure 2.6.** Graphic representation of the two proposed models to describe the mechanism of spheronization: (A) the model proposed by Rowe (1985) and (B) the model proposed by Baert *et al.* (1993) (adapted from Erkoboni (1997))

In the same fashion, lipid spheronization is a pelletization technique developed to round solid lipid based extrudates. The solid lipids are used as binders during the extrusion step and can be employed alone or in a mixture of different lipids. This specific method is performed under similar conditions to traditional spheronization. However, an additional thermo-mechanical treatment of the extrudates is required, since the rounding process necessitates a certain plasticity of the mass. This specific condition is achieved by raising the temperature during spheronization to a suitable temperature in order to plastify the mass by partly or completely melting (or “softening”) of lipid components. Usually, the temperature can be raised by friction between the particles during spheronization or by heating the spheronizer wall using a double jacket wall (Kleinebudde, 2013). For this purpose, mixtures of high and low melting lipids are generally suggested (Krause *et al.*, 2009; Reitz and Kleinebudde, 2009).

There are very few reports on literature about investigation of the spheronization process of solid lipid based extrudates. Most of them worked with the lipid binders described in Table 2.3 (item 2.6.1, see page 19). Breitzkreutz *et al.* (2003) developed sodium benzoate coated lipid pellets, using SLCE followed by spheronization. Aiming to the production of slow release characteristics of the API, they investigated pellets containing 10-25% of a mixture of stearic acid, glyceryl distearate and hard fat as lipid binders. However, during the spheronization step, uncontrolled agglomeration of the material was observed after 5 min, especially when the material temperature reached 39 °C. Due to these short spheronization times, ideal spherically shaped pellets were not obtained.

Krause *et al.* (2009) used the same spheronization parameters and equipment to round sodium benzoate extrudates based on 20% of hard fat or mixtures containing different solid lipid binders. Parameters like the friction plate speed and spheronizer wall jacket temperature were also evaluated in some extent. It was observed that temperatures closer than 8 °C to the melting point of the binder were inadequate for the production of suitable shaped pellets since material agglomeration was observed. In summary, equipment jacket temperature of 33 °C, friction plate speed of 1500 rpm and process time of 15 min were reported as more suitable for spheronization of lipid extrudates containing hard fat in the formulation. However, depending on the lipid binders used, these parameters were still not sufficient to obtain adequate spherical pellets due to material agglomeration.

The impact of the jacket temperature on the spheronization process was investigated by Reitz and Kleinebudde (2009). In their work, the spheronization of lipid based extrudates, containing theophylline and 45% of binary mixtures of glyceryl trimyristate and hard fat in different proportions, was investigated. They observed that the variation on the lipid binders' proportion, especially the increase of hard fat content in the extrudate, strongly influenced the spheronization process time. Due to material agglomeration, the spheronization process of some compositions needed to be stopped after 5 to 9 min, especially at material temperatures around 39 °C. It was concluded that the temperature sensitive nature of the process still requires further elucidation especially of problems with respect to material temperature. The temperature which results was primarily from friction and shear forces showed to be formulation dependent and difficult to control (Reitz and Kleinebudde, 2009).

## 2.7. Orodispersible Tablets

Recently, ODTs are receiving special attention as an alternative to conventional solid dosage forms, such as capsules and tablets, due to the improvement on patient compliance (Uko-Ekpenyong, 2006; Navarro, 2010). Orodispersible tablets are uncoated tablets containing medicinal substances intended to be placed in the mouth where they disperse rapidly, usually within a matter of seconds, before being swallowed generally not requiring water to their administration (USP 34, 2011; Ph. Eur., 2014). Furthermore, according to the Ph. Eur. (2014), ODTs are characterized by disintegrating within not more than 3 min. They are commonly also denominated as orally disintegrating tablets, quick disintegrating tablets, mouth dissolving tablets, fast disintegrating tablets, fast dissolving tablets, rapid dissolving tablets, and porous tablets (Bandari *et al.*, 2008).

Over a decade, the demand for development of ODTs has enormously increased as it has significant impact on patient compliance since they offer an advantage for

populations who have difficulty in swallowing. They are placed into the oral cavity allowing the fast dispersion of the drug in saliva, producing a suspension that can be easily swallowed (Kundu and Sahoo, 2008). They present themselves as an ideal form of administration to people with dysphagia, which is common among children and elderly (Sastry *et al.*, 2000). As ODTs are unit solid dosage forms, they provide good stability, accurate dosing, easy manufacturing, small packaging size, and are easy to handle by patients (Sastry *et al.*, 2000; Fu *et al.*, 2004). Moreover, they do not present a risk of obstruction of dosage form, which is beneficial for traveling patients who do not have access to water (Bandari *et al.*, 2008).

To highlight the importance of this dosage form and its different characteristics, the American Agency FDA released a guidance to provide pharmaceutical manufacturers with an Agency perspective on the definition of ODTs and also providing recommendations to applicants who would like to designate proposed products as ODTs (FDA, 2007). However, they have different monographs for ODTs compared to the European Pharmacopoeia.

Regarding the technologies related to the production of ODTs by compression, similar excipients to traditional direct compression are used, such as fillers, diluents, lubricants, binders, and disintegrants. There are several excipients developed to the production of ODTs, however the most commonly employed excipient is mannitol. Mannitol is a sugar alcohol, which presents high water solubility (1:5; w/V), low hygroscopicity, a moderate sweetness and a pleasant mouthfeel, since it has a sweet taste (approximately as sweet as glucose and half as sweet as sucrose) and imparts a cooling sensation in the mouth (Daoust and Lynch, 1963; Bauer *et al.*, 2000). However, this excipient presents inadequate flowability properties and high adhesion to the compaction tools during tableting (Bauer, 2000; Rowe *et al.*, 2012).

To overcome these issues, co-processed excipients (also called “ready-to-use” excipients) can be employed. Co-processed excipients are a mixture of two or more existing excipients at subparticle level which offers substantial benefits of the incorporated excipients and minimize their drawbacks (Saha and Shahiwala, 2009). The aim of these co-processed excipients is to provide a synergy of functionality improvements as well as masking the undesirable properties of individual excipients (Reimerds, 1993). Most of them are based on mannitol or modified mannitol with addition of a disintegrant, i.e. Ludiflash<sup>®</sup>, Parteck<sup>®</sup> ODT, Orocell<sup>®</sup>, and Pearlitol<sup>®</sup>. Since ODTs are designed to present a fast disintegration time, the disintegrant plays an important role in the formulation. Generally, in direct compression there is only the need to blend the co-processed excipient with the API, however in some cases a lubricant or an anti-adherent is still required.

There are few works reported in literature about the development of ODTs containing metformin HCl. Mohapatra *et al.* (2008a) developed ODTs containing 250 mg of



metformin HCl from granules obtained by wet granulation. The co-processed excipients were starch 1500, croscarmellose sodium, mannitol, and polyvinylpyrrolidone binder. Sweetener and flavor excipients were used to taste-mask the bitter taste of metformin HCl. According to the authors, the ODT showed fast disintegration time and fast *in vitro* drug release, releasing more than 85% of metformin HCl after 4-8 min.

Gandhi *et al.* (2010) investigated the use of polacrillin potassium from different sources as disintegrant to obtain 250 mg metformin HCl fast disintegrating tablets. The ODTs were prepared by direct compression. Lactose was used as a diluent, and magnesium stearate as flow promoter. All investigated formulations showed disintegration times below 30 seconds. The rapid *in vitro* drug dissolution of 100% metformin HCl released after 5 min, was justified due to the easy breakdown of particles and rapid absorption of drugs into the dissolution medium. As already reported in other works, the bitter taste of metformin HCl was masked using saccharin as sweetening agent and vanillin as flavor.

Furthermore, Maniyar *et al.* (2010) investigated the production of metformin HCl tablets containing 250 mg of the API, by the direct compression method. In this study, ODTs were prepared using a combination of disintegrants: sodium starch glycolate and polacrillin potassium. In the investigation, a 2<sup>3</sup> full factorial design was used to investigate the joint influence of three formulation variables: amount of camphor, sodium starch glycolate and polacrillin potassium. The strong saline and slight bitter taste of the drug was masked using mannitol as sweetener. The results of analysis revealed that for obtaining a rapidly disintegrating dosage form, tablets should be prepared using an optimum concentration of camphor and a lower percentage of each sodium starch glycolate and poliacrilin potassium.

The development of ODTs based on solid lipid pellets was never investigated before. Therefore, the feasibility of producing ODTs with lipid based micropellets employing co-processed excipients will be investigated in the present work.



### 3. Aim of the Study

The major aim of this study is the development and characterization of taste-masked orodispersible tablets containing metformin HCl. Initially, this work has been focused in the development of metformin HCl high drug loaded lipid based small diameter pellets. Solvent-free cold extrusion followed by spheronization should be investigated as methodology to obtain pellets with taste-masked properties and fast drug release. This particular methodology was never employed before to taste mask metformin HCl. Therefore, different formulations based on traditionally used lipid binders should be investigated as well as the influence of process parameters on the material. Characteristics as particle size distribution, shape, drug release, taste-masking properties should be investigated to define the more adequate formulation for producing solid lipid pellets of metformin HCl.

Furthermore, the metformin HCl lipid based pellets presenting acceptable shape characteristics, fast drug release, and adequate taste-masked properties should be used for the development of orodispersible tablets. The incorporation of solid lipid pellets into ODTs, to obtain a multiple unit pellet system, has never been investigated before. Two co-processed excipients based on mannitol, Ludiflash® and Parateck® ODT, should be investigated by a Design of Experiment (DoE), where the influence of the compression force and excipient proportion on the tablets properties should be evaluated. Thus, tablet disintegration time, tensile strength and friability should be evaluated. The aim of this works is the development of ODTs containing 500 mg of metformin HCl presenting taste-masked properties.



## 4. Results and Discussion

### 4.1. Material Characterization

#### 4.1.1. Introduction

Morphological and physicochemical characteristics of APIs and excipients have an important influence on the development and production of pharmaceutical dosage forms. Regarding the development of solid dosage forms, morphological properties of the formulation components, such as flowability or particle size distribution, can influence the production processes and, consequentially, the final product quality. Likewise, their physicochemical properties also exert an important influence on the stability of the dosage form (or its components), resulting in alterations in the bioavailability, drug release profile and even in the API activity. Equally, studies have shown that solid lipophilic binders may present a complex behavior depending on the sample treatment (i.e. aged, freshly) influencing the stability or the properties of lipid based dosage forms (Laine *et al.*, 1988; Sutananta *et al.*, 1994; Hamdani *et al.*, 2003).

The characterization of the raw material consists of morphological and physicochemical evaluation of the used raw materials to assure the quality and to understand the implications of such properties on further dosage form development steps. Their morphological form (the packing of the molecules and the size and shape of the particles) can have an influence on the way the material will behave (Buckton, 2013). Therefore, metformin HCl, hard fat, trimyristin and glyceryl distearate should be characterized individually. Their morphological characteristics, such as particle shape, particle size and size distribution and powder flow should be investigated by scanning electron microscopy (SEM), laser diffractometry and ring shear cell, respectively. Indirect powder compactability indicators for metformin HCl, such as Carr's index and Hausner factor, should also be evaluated. Likewise, the physicochemical properties of the substances should be investigated by differential scanning calorimetry (DSC), X-ray powder diffractometry (XRPD) and the water content by loss on drying.

#### 4.1.2. Particle Shape and Size Characterization

The particle size distribution of raw materials present an important influence on the initial phases of a dosage form development. It can influence the solid mixture step,

the manufacturing process and furthermore, the final dosage form properties, such as the drug release profile. Powders with different particle sizes have different flow and packing properties, which could alter the volume of the powder during encapsulation or compression process (Staniforth and Taylor, 2013). Moreover, a difference in particle size of components of a formulation is the main cause of segregation in powder mixes in practice. Small particles tend to fall through the voids between larger ones and move to the bottom of the mass, a phenomenon known as powder segregation. This phenomenon arises because powder mixes generally are not composed of monosized spherical particles, but contain particles that differ in size, shape, density and surface properties (Twitchell, 2012).

The particle size distribution quantiles based in the Feret diameter and the true density values of the investigated powders are shown in Table 4.1. Regarding the 10%, 50%, and 90% quantiles ( $d_{10}$ ,  $d_{50}$ , and  $d_{90}$ , respectively). The materials can be considered, from a technological point of view, as presenting similar particle size distributions. The median particle diameter ( $d_{50}$ ) corresponds to the point that separates the cumulative frequency curve into two equal halves, above and below which 50% of the particles lie (Staniforth and Taylor, 2013). Taking this value as reference, it is possible to define the trimyrustin as the finest powder of all evaluated and metformin HCl presenting the biggest particles together with glyceryl distearate. However, all materials are considered “very fine powders” according to the classification of the USP 34 (2011). Interestingly, although statistically different particle sizes, in terms of powder density, metformin HCl presents a similar value as trimyrustin, and hard fat presents a similar value when compared to glyceryl distearate, which could indicate a good miscibility between these materials during a mixing step.

Standard deviation is the preferred value to describe the width or breadth of particle size distribution, however, it is applicable only for normal distribution patterns (monomodal distribution). In the present work the “span” value was used, in order to express, quantify and compare particle size distribution widths (Table 4.1). Generally span is related to  $d_{10}$ ,  $d_{50}$  and  $d_{90}$  quantiles, and therefore, the higher the span value, the wider is the particle size distribution of the powder. Hard fat presents the highest span value among the materials, while glyceryl distearate showed the smallest, representing a variety of material particles sizes.

**Table 4.1.** Particle size distribution and true densities

Material	Mean $\pm$ SD (n = 3)				True density (g·cm <sup>-3</sup> )*
	d <sub>10</sub> (μm)	d <sub>50</sub> (μm)	d <sub>90</sub> (μm)	Span	
Metformin HCl	10.66 $\pm$ 0.12	33.76 $\pm$ 0.17	89.94 $\pm$ 0.15	2.35 $\pm$ 0.01	1.39 $\pm$ 0.01
Hard fat	9.36 $\pm$ 0.17	22.92 $\pm$ 0.68	90.59 $\pm$ 10.45	3.54 $\pm$ 0.36	1.00 $\pm$ 0.02
Trimyristin	1.79 $\pm$ 0.02	19.95 $\pm$ 0.17	66.16 $\pm$ 0.97	3.23 $\pm$ 0.02	1.39 $\pm$ 0.01
Glyceryl distearate	3.89 $\pm$ 0.32	33.84 $\pm$ 2.55	71.21 $\pm$ 1.74	1.99 $\pm$ 0.09	1.00 $\pm$ 0.03

The size distribution and the cumulative distribution curves are depicted in Figure 4.1. Metformin HCl powder (Figure 4.1a) presents a monomodal particle size distribution, while trimyristin (Figure 4.1c) and glyceryl distearate (Figure 4.1d) are negatively skewed due to a large proportion of fine particles. Thus, the skewness showed by trimyristin indicates a higher proportion of fines compared to glyceryl distearate. In contrast, hard fat (Figure 4.1b) presents a bimodal frequency distribution, which is typical for a powder which has been subjected to milling. Some of the coarser particles from the unmilled population remain unbroken and produce a mode towards the highest particle size, whereas the fractured particles have a new mode which appears lower down the size range (Staniforth and Taylor, 2013).

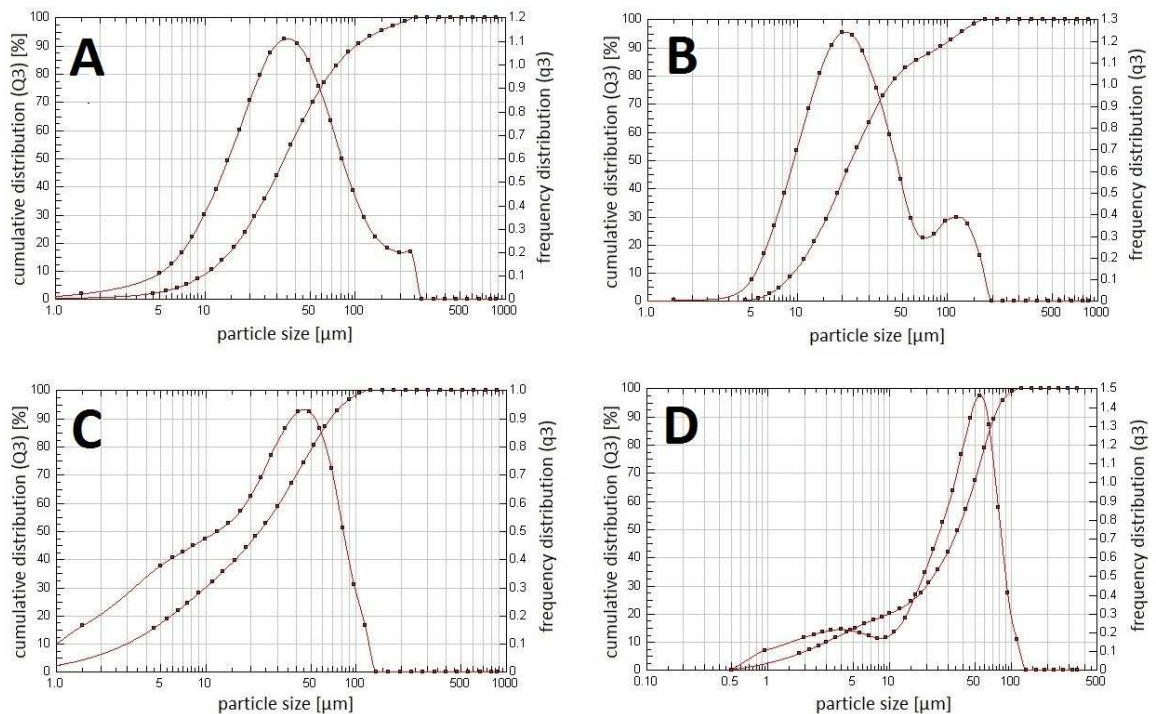


**Figure 4.1.** Particle size: percent frequency and cumulative distributions of (A) metformin HCl, (B) hard fat, (C) trimyristin and (D) glyceryl distearate obtained by laser diffraction

From the particle size distribution logarithmic curve it is possible to extrapolate the mean diameter and the geometric standard deviation of powders (Wells, 1988; Lantz, 1989). Metformin HCl particles presents a mean diameter of  $47.48 \pm 0.25 \mu\text{m}$ , while hard fat, glyceryl distearate and trimyristin showed  $39.46 \pm 2.89 \mu\text{m}$ ,  $29.91 \pm 0.47 \mu\text{m}$  and  $39.58 \pm 1.73 \mu\text{m}$ , respectively. According to Wells (1988), a standard deviation of the particle mean diameter higher than 2 represents a wide particle size distribution range. Under those circumstances, the SD values corroborate the calculated values of the distribution “span” (Table 4.1): hard fat showing a wide range size distribution, while the other materials present narrow particle size distribution.

The SEM images of metformin HCl particles (Figure 4.2a) show crystalline irregular shaped particles, with sharp edges, displaying a variety of particle sizes. Hard fat (Figure 4.2b), trimyristin (Figure 4.2c), and glyceryl distearate (Figure 4.2d) also showed irregular shaped particles, however, not presenting protuberances. Trimyristin SEM image shows, when compared to the other materials, exceptionally small particles, with presence in a smaller amount of large ones, as observed in the percent frequency distribution graphic for this material (Figure 4.1c). The SEM images corroborate the particle size characterization results previously discussed.

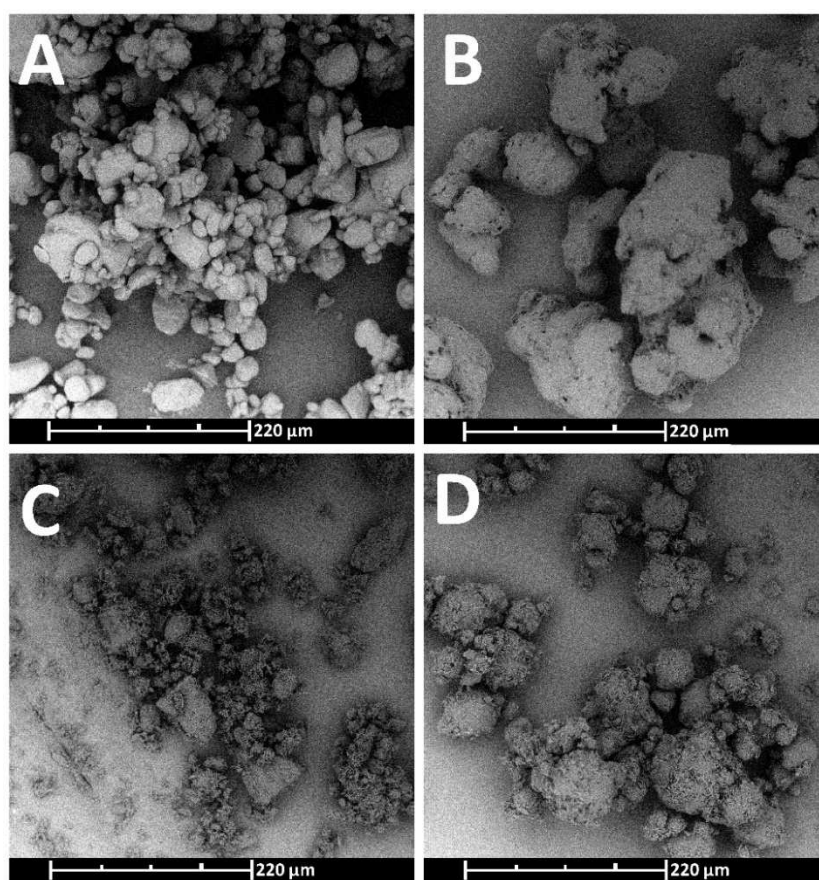


**Figure 4.2.** SEM images taken at 600x magnification (scale represents 220  $\mu\text{m}$ ): (A) metformin HCl, (B) hard fat, (C) trimyristin, and (D) glyceryl distearate



### 4.1.3. Powder Properties

The measurement of packing geometry by an assessment of percentage compressibility and changes in bulk density have proven to be useful indirect methods to estimate powder flow in an industrial manufacturing process (Aulton, 2013). The powder compactability and flow properties characterization of metformin HCl is presented in Table 4.2. The results indicate strongly cohesive particles, presenting a poorly particular flow. As metformin HCl is a crystalline powder, the irregular flow property could probably be attributed to its small particle size and relatively irregular particle shapes. The particle's shape also presented strong influence on the compactability and compressibility properties of the powder due to its void in the particular accommodation and interface, which is explained by its high Carr's index and Hausner factor. Hausner (1967) described that the ratio between bulk volume and tapped volume ( $V_b$  and  $V_t$ , respectively) is related to interparticulate friction. It was reported that powders with low interparticulate friction, such as coarse spheres, had ratios of less than 1.2, whereas more cohesive and less free flowing powders showed ratios greater than 1.5, which is the case of metformin HCl.

The presence of molecular forces produces a tendency for solid particles to stick to themselves and to other surfaces. Adhesion and cohesion can be considered as two aspects of the same phenomenon. Adhesive and cohesive forces acting between particles in a powder bed are composed mainly of short-range non-specific van der Waals forces, which increase as particle size decreases since the interparticulate contact points increases. (Aulton, 2013).

**Table 4.2.** Direct and indirect flow characteristics of metformin HCl

Parameter	Mean $\pm$ SD (n = 3)
Powder bulk density (g·mL <sup>-1</sup> )	0.42 $\pm$ 0.01
Powder tapped density (g·mL <sup>-1</sup> )	0.79 $\pm$ 0.01
Hausner factor	1.86 $\pm$ 0.04
Carr's index (%)	46.29 $\pm$ 1.11
Flow function coefficient (ff <sub>c</sub> )	1.27 $\pm$ 0.01

Complementarily, the percentage of compressibility (estimated by Carr's index) is a direct measure of the potential powder arch or bridge strength and stability of the material (Aulton, 2013). Carr's index above 15% characterize materials as presenting poor flowability and problems in packing (Augsburger and Vuppala, 1997). Change in the bulk volume is produced by rearrangement of the packing geometry of the particles. In general, such geometric rearrangements result in a transition from loosely packed particles to more tightly packed ones. According to Aulton (2013), this also means that more tightly packed powders require a higher driving force to produce powder flow than more loosely packed particles of the same powder.

The powder flow function coefficient ( $ff_c$ ) of metformin HCl is shown in Table 4.2. Irregular or needle-shaped particles may become interlocked, decreasing the tendency to segregate once mixing has occurred. Non-spherical particles will also have a greater specific surface area, which will tend to decrease segregation by increasing contact surface area (Twitchell, 2012). Because adhesion and cohesion are phenomena that occur at surfaces, particle size influences the flowability of a powder. The observed value of  $ff_c$  of metformin HCl powder characterizes it as “very cohesive material”, a property which could also be visually observed when the material stays in storage (Figure 4.3). The hypothesis that this agglomeration or strong adhesion could be formed due to high humidity of the material was not confirmed by the loss on drying assay. Although metformin HCl was reported to present hygroscopic characteristics (Bretnall and Clarke, 1998), the powder showed a low humidity content ( $0.25 \pm 0.02$ ; w/w), a lower value than 4.9 to 5.3% (w/w), which is specified in the Ph. Eur. (2014). Furthermore, the observed results corroborate other works, which reported that metformin HCl exhibits reduced flowability and poor compressibility properties during compaction, often resulting in weak and unacceptable tablets with high tendency to cap (Mohapatra *et al.*, 2008a; Barot *et al.*, 2010).



**Figure 4.3.** Metformin HCl powder: handling before use

#### 4.1.4. Thermal Properties

Figure 4.4 and Table 4.3 depicts the thermograms obtained by differential scanning calorimetry (DSC) showing the melting point/range of the lipids and metformin HCl. The melting point is the temperature at which the crystal lattice breaks down, due to the molecules having gained sufficient energy from the heating process to overcome the attractive forces that hold the crystal together (Buckton, 2013). Metformin HCl thermal profile showed only one endotherm event at 230.4 °C referencing to the melting of the substance, value slightly higher when compared to bibliographic values

(222 – 225 °C) (Ph. Eur., 2014). As no other thermic signal is observed, there is no indication of the presence of other substances or impurities in the sample.

The presence of metastable forms can be elucidated by DSC observing alterations on their thermal profile. The melting points or ranges encountered in literature and the observed values, for the investigated solid lipids, are depicted in Table 4.3. According to Larsson (1966), TAGs polymorphic forms can be distinguished by their melting points/ranges: the  $\alpha$ -modification having the lowest melting point, followed by metastable  $\beta'$ -modification and the  $\beta$ -modification with the highest melting point. Hard fat and trimyristin present similar values to the literature.

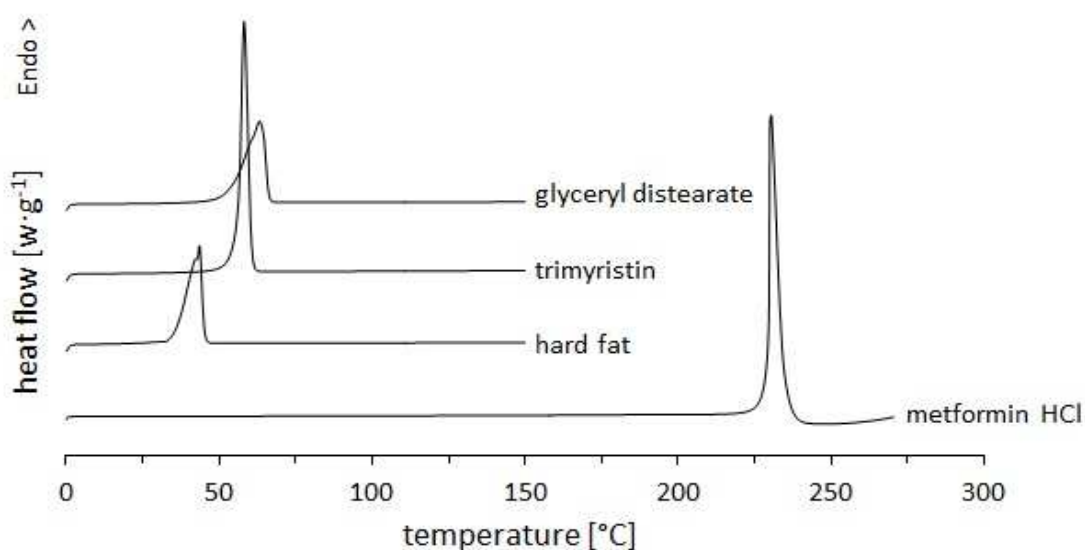


**Figure 4.4.** DSC thermograms of metformin HCl, hard fat, trimyristin and glyceryl distearate (heating rate: 10 K·min<sup>-1</sup>)

Glyceryl distearate showed a slightly elevated temperature peak compared to the literature value. Glyceryl distearate is a mixture of diglycerides and triglycerides, which behave differently under specific conditions (aging, temperature). Nevertheless, observing its onset temperature, it is still in the range reported in literature to glyceryl distearate. This result was also reported by Krause *et al.* (2009), who observed a melting range between 53 to 67 °C for glyceryl distearate. Though, this higher melting temperature could indicate the presence of another metastable polymorphic form or crystallographic re-organization in the material or a different ratio between the diglyceride and triglyceride fraction.

**Table 4.3.** Thermal properties of the powder materials (n = 2)

	Onset temp.		Peak temp.		Heat of fusion		Literature values (°C)
	(°C)		(°C)		(J·g <sup>-1</sup> )		
	1	2	1	2	1	2	
Metformin HCl	229.1	229.1	230.4	230.3	344.5	337.3	222-225
Hard fat	35.4	35.3	43.4	43.6	156.0	159.0	42-44
Trimyristin	55.8	55.7	58.1	58.1	214.0	212.2	55-58
Glyceryl distearate	53.2	54.5	63.1	63.1	200.7	201.6	53-57

#### 4.1.5. Crystallographic Properties

As metformin HCl and TAG are crystalline materials (which was depicted by the presence of endothermic peaks for the substances), X-ray powder diffractometry (XRPD) could also provide important information about the presence of polymorphic forms of TGAs and be a complementary assay to DSC measurements. The diffractograms of the materials are shown in Figure 4.5. Metformin HCl presents a more crystalline structure when compared to the lipids. Glyceryl distearate and hard fat present only two breadth peaks in the region between 17 and 25 degrees.

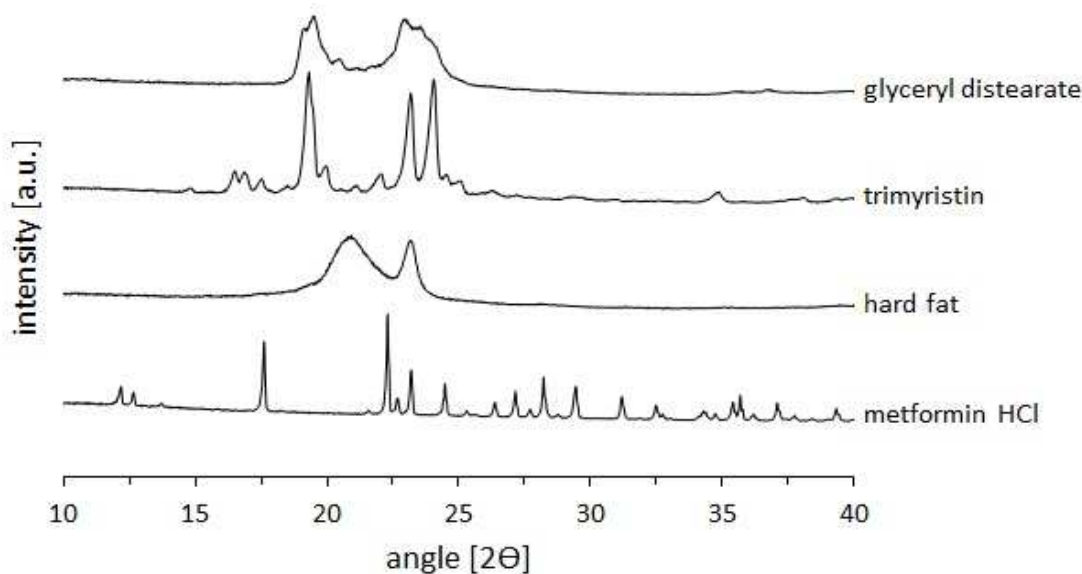


**Figure 4.5.** Diffractograms of metformin HCl, hard fat, trimyristin, and glyceryl distearate in the  $2\theta$  interval of 10 to 40 degrees (increment of 0.02 degrees, reading time of 1 s per point)

However, according to literature, glyceryl distearate shows only one crystallographic peak at the region of 20 to 30 degrees (Hamdani *et al.*, 2003), which indicates that the used glyceryl distearate could present two polymorphic forms or a different diglyceride/triglyceride proportion, corroborating the DSC results. No report in literature describing diffractogram of hard fat (Witocan<sup>®</sup> 42/44) was found, therefore, it is not possible to compare the observed results. On the other hand, the observed

diffractogram of trimyristin is similar to what is reported in literature (van Langevelde *et al.*, 2001; Reitz and Kleinebudde, 2007a).

#### 4.1.6. Conclusions

The starting materials, metformin HCl powder and the lipid binders, were investigated and characterized according to their morphological and physicochemical properties. All the materials showed very fine particle sizes and a wide particle size distribution or presented a high proportion of fines, which can influence further steps or processes such as mixture and extrusion. In the case of metformin HCl powder, their particle size characteristics lead to very cohesive powder characteristics demonstrated by its low  $f_c$  and high Hausner factor and Carr's index. The observed powder characteristics reinforce the necessity of a granulation step, since the materials exhibit inappropriate properties for direct compression.

Regarding the lipid binders, XRPD and DSC investigations showed no polymorphic unstable forms. However, a higher melting temperature of glyceryl distearate and a different crystallographic pattern were observed compared to that reported in literature, which could indicate the presence of another metastable polymorph of this TAG. On the other hand, metformin HCl presents thermal and crystallographic properties according to what is reported in literature or defined in its monograph in official compendia.

## 4.2. Pre-Formulation Studies for the Extrudates Development

### 4.2.1. Introduction

The physicochemical properties of a molecule affect the processing of the material, its stability, its interaction with excipients, how it will transfer to solution and, ultimately, may determine its bioavailability. However, its intrinsic properties can be altered by chemical modification and its properties are the result of intermolecular interactions. They can be affected by solid-state form, interaction with other molecules (i.e. excipients), and the environment among other factors (Gaisford, 2013).

Pre-formulation studies should be carried out to evaluate existent morphological or physicochemical interactions between the lipophilic binders and the API. For this reason, morphological mixtures should be prepared based on different drug-excipient ratios and further investigated by DSC and XRPD. The initial formulations and solid mixture ratios should be based on the investigations of Krause (2008), who evaluated

the feasibility of development of lipid based pellets containing sodium benzoate by SLCE followed by spheronization.

#### 4.2.2. Thermal Properties

The thermograms of the solid mixtures in comparison to the pure substances are shown in Figure 4.6 and the values of the endothermic events are depicted in Table 4.4. In all solid mixture thermograms the endothermic event of the melting of metformin HCl is present between 229 and 231 °C. This range is similar to the observed one for the pure substance and slightly higher than the values of the Ph. Eur. (2014). The heat of fusion, which is the change in enthalpy due to heating of a quantity of substance altering its state from solid to liquid (Netz and Ortega, 2002), showed similar values in all solid mixtures of metformin HCl. However, the mixture based on the same ratio of the three lipids and metformin HCl, the heat of fusion of metformin HCl increases although its melting point is the same (Table 4.4).

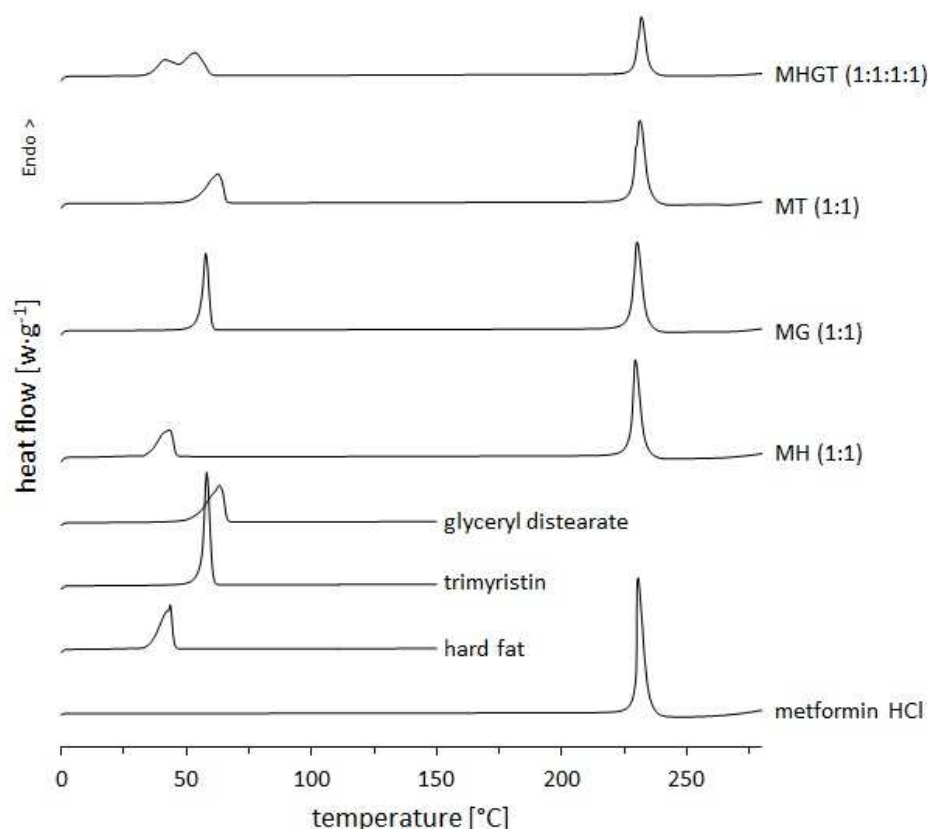


**Figure 4.6.** DSC thermograms of mixtures in comparison to pure metformin HCl and lipids (heating rate: 10·K·min<sup>-1</sup>). M = metformin HCl; H = hard fat; T = trimyristin; G = glyceryl distearate

Observing the DSC curve of the mixture containing all components at the same ratio (MHGT), there are only two endothermic events at the temperature range relative to the melting of the lipids (Figure 4.6). The first peak is related to the hard fat, since

the melting range of this event coincides with the value for this lipid. The second peak is related to trimyristin and/or glyceryl distearate. As reported in literature, these both lipids melt in similar temperature ranges, which could explain the observation of only one endothermic peak at this temperature range (Krause, 2008). However, this melting temperature presents a lower temperature (53.4 °C) compared to observed values for trimyristin and glyceryl distearate alone. This decrease reinforces the hypothesis of a possible interaction between the components in this mixture sample.

**Table 4.4.** Thermal characteristics of solid powder mixtures and substances

Metformin HCl characteristics						
Substances (ratio)	Onset temp. (°C)		Peak temp. (°C)		Heat of fusion (J·g <sup>-1</sup> )	
	1	2	1	2	1	2
Metformin HCl	229.1	229.1	230.4	230.3	344.5	337.3
MH (1:1)	227.0	226.9	229.4	229.4	343.1	333.4
MT (1:1)	226.9	226.9	230.0	230.1	341.4	338.1
MG (1:1)	227.7	227.5	231.0	230.9	352.1	359.2
MHGT (1:1:1:1)	228.9	228.9	231.7	231.7	408.6	437.7
Lipid characteristics						
Substances (ratio)	Onset temp. (°C)		Peak temp. (°C)		Heat of fusion (J·g <sup>-1</sup> )	
	1	2	1	2	1	2
Hard fat	35.4	35.3	43.4	43.6	156.0	159.1
MH (1:1)	35.0	35.0	43.2	42.7	158.3	159.4
Trimyristin	55.8	55.7	58.1	58.1	214.0	212.2
MT (1:1)	55.2	55.2	57.9	57.8	214.3	216.8
Glyceryl distearate	53.2	54.5	63.1	63.1	200.7	201.6
MG (1:1)	53.6	53.6	62.7	62.2	186.7	191.2
MHGT (1:1:1:1)	(a) 33.3	(a) 35.3	(a) 41.5	(a) 41.5	(a) 223.2	(a) 215.2
	(b) 43.0	(b) 46.7	(b) 53.4	(b) 53.4	(b) 318.5	(b) 322.9

M = metformin HCl; H = hard fat; T = trimyristin; G = glyceryl distearate. (a) First endothermic peak; (b) second endothermic peak. n = 2

Likewise, the fusion enthalpy value of metformin HCl showed a small increase in the binary mixture with glyceryl distearate (MT), while the value of the lipid decreases. This result could indicate the occurrence of a physicochemical interaction between these substances. A change in the fusion enthalpy was not observed for the binary mixture of metformin HCl and trimyristin (MG) or hard fat (MH), indicating that only glyceryl distearate interacts with the API. The heat of fusion value of metformin HCl is higher in the mixture of the API with the three lipids (MHGT). A similar energy increase is also observed in the second melting event referent to glyceryl distearate or trimyristin. However, by these results alone it is not possible to infer if this temperature alteration is due to some interaction or due to the concomitant melting of the lipids, which could also explain the increase of the fusion enthalpy

value. However, it is important to point that the used lipids binders (Witocan® 42/44, Dynasan® 114, and Precirol® ATO 5) are in fact a complex mixture of mono-, di- and triglycerides in different proportions, which could also result in different DSC results.

According to Sato (2001), in general, three typical phases may occur in lipid binary solid mixtures when the components are miscible in all proportions in a liquid state: solid solution phase, eutectic phase and compound formation. Mohamed and Larsson (1992) reported an effect of glyceryl distearate isomers on trimyristin phase transition. It was observed that low concentrations of distearin (0.1% to 8%) induced a transition to the  $\beta$ -form of trimyristin at temperatures as low as 20 to 30 °C after 24 hours in a binary mixture. A eutectic behavior was confirmed by XRPD investigations. As a decrease in the melting temperature was observed, a eutectic phase formation due to miscibility of lipids could be the explanation to the observed event on the mixture MHGT. According to Mohamed and Larsson (1992), this phenomenon is due to a co-crystallization of distearin into the triglyceride crystal as a solid solution. In this event, the lattice energy is changed acting as the driving force behind the polymorphic transition.

To investigate this hypothesis, a binary mixture of glyceryl distearate and trimyristin in a 1:1 ratio (w/w) was analyzed by DSC (Figure 4.7). Two endothermic events were observed at the same temperature range, with an onset temperature of 54.91 °C and two maximum temperatures: 58.43 and 59.98 °C. These values are similar to those encountered in literature to the melting of glyceryl distearate (53-57 °C) and trimyristin (55-58 °C). However, the decrease in the melting temperature of the lipids was not observed. Likewise, a mixture of the three lipids also in similar ratios was analyzed and the decrease in the melting temperature was than observed (Figure 4.7). This result show that the presence of metformin HCl is not the cause of this temperature alteration.

Another hypothesis could rely to the fact that hard fat in its used quality melts at lower temperatures compared to the other lipid binders. Therefore, hard fat is in liquid form in the mixture MHGT before the other substances, it could dissolve the monoglycerides, diglycerides and TAGs from glyceryl distearate (Precirol® ATO 5 is a mixture of tri-, di-, and monoglycerides; Table 2.3, see page 19) and trimyristin, which explains the decrease of the melting temperature observed in the DSC (Figure 4.7). This hypothesis was also suggested by Krause (2008).



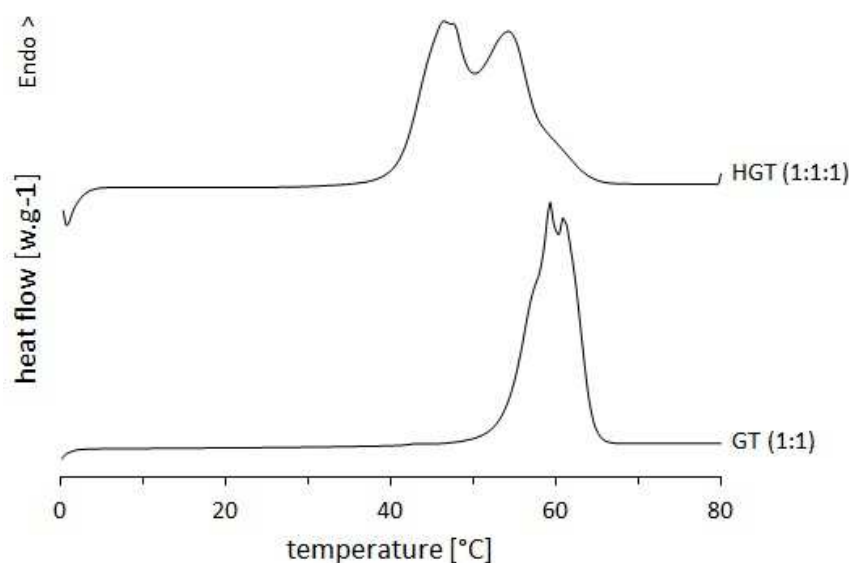


**Figure 4.7.** DSC of a powder mixture of glyceryl distearate and trimyristin (1:1 ratio; w/w) and a powder mixture of hard fat, glyceryl distearate, and trimyristin (1:1:1 ratio; w/w). Heating rate: 10 K·min<sup>-1</sup>. H = hard fat; G = glyceryl distearate; T = trimyristin

However, these results do not explain the change in the heat of fusion observed in the mixture between metformin HCL and glyceryl distearate. Surprisingly, there are no reports in literature about interactions between this API and TAGs nor about what can causes an increase in the fusion enthalpy of metformin HCL.

### 4.2.3. Crystallographic Properties

To further investigate the results observed by DSC, the same solid mixtures were evaluated by XRPD. The diffractograms of solid mixtures of API and lipid binders in comparison to pure powders are illustrated in Figure 4.8. It is not possible to identify any crystallographic pattern alteration in the diffractograms of the mixtures, as the peaks of metformin HCL do not shift and the lipids peaks are difficult to identify.

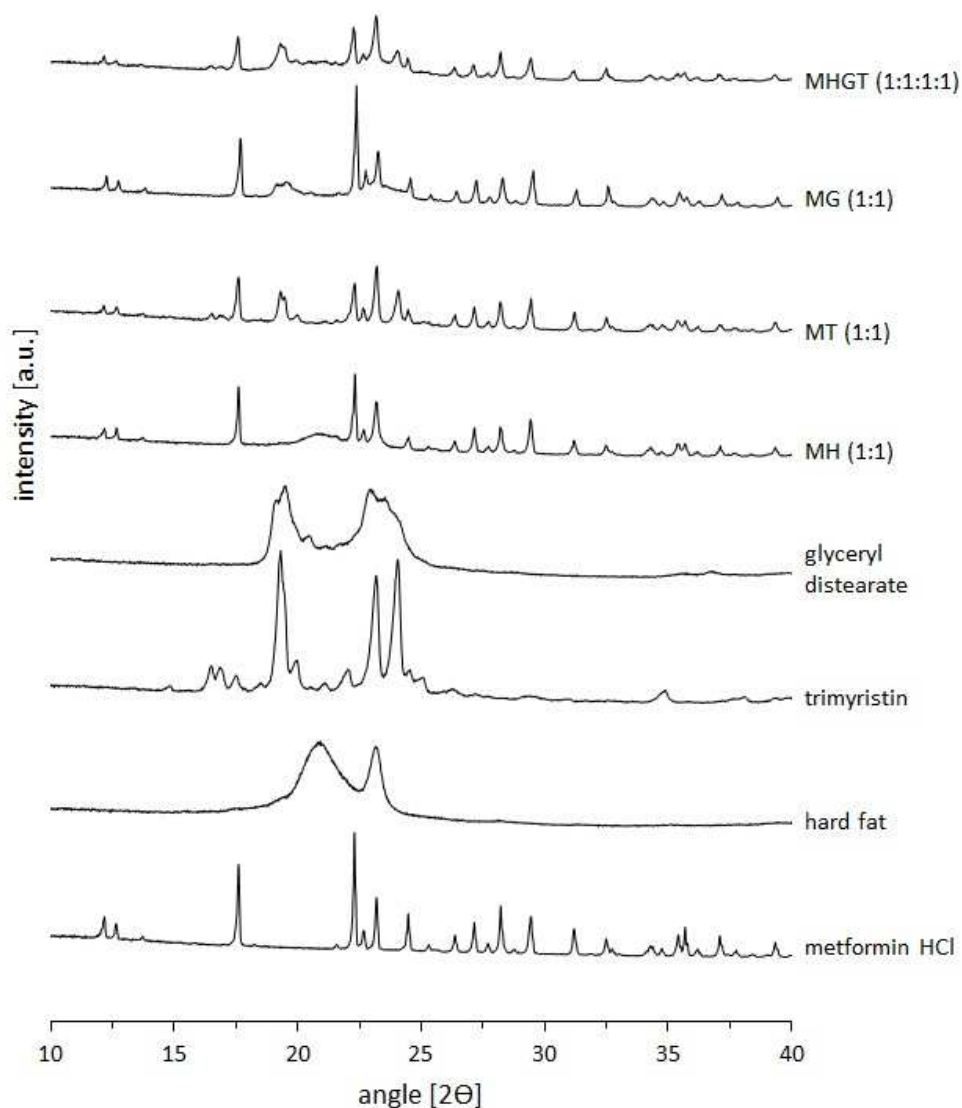


**Figure 4.8.** Diffractograms of metformin HCl, solid lipids, and mixtures with lipophilic binders in different ratios (w/w) in the  $2\theta$  interval from 10 to 40 degrees (increment of 0.02 degrees, reading time of 1 s per point). M = metformin HCl; H = hard fat; T = trimyrustin; G = glyceryl distearate

Therefore, to elucidate if the interaction observed in the DSC thermograms and to evaluate if only glyceryl distearate is interacting with metformin HCl, the diffractograms of metformin HCl and glyceryl distearate or trimyrustin were plotted together with their binary mixture (Figure 4.9). By analyzing the overlapped diffractograms, it is possible to identify the absence of one peak relative to metformin HCl in the  $2\theta$  interval between 25 and 26 degrees in the binary mixture between metformin HCl and trimyrustin (when compare to pure metformin HCl; Figure 4.9a). In the mixture of metformin HCl and glyceryl distearate the peak is not completely absent but decreased probably due to the small relative intensity of the signal. However, similarly to the mixture between metformin HCl and trimyrustin, in the mixture MHGT this peak is also absent (Figure 4.9c), which reinforces the hypothesis that an interaction occurs between metformin HCl and these lipids.

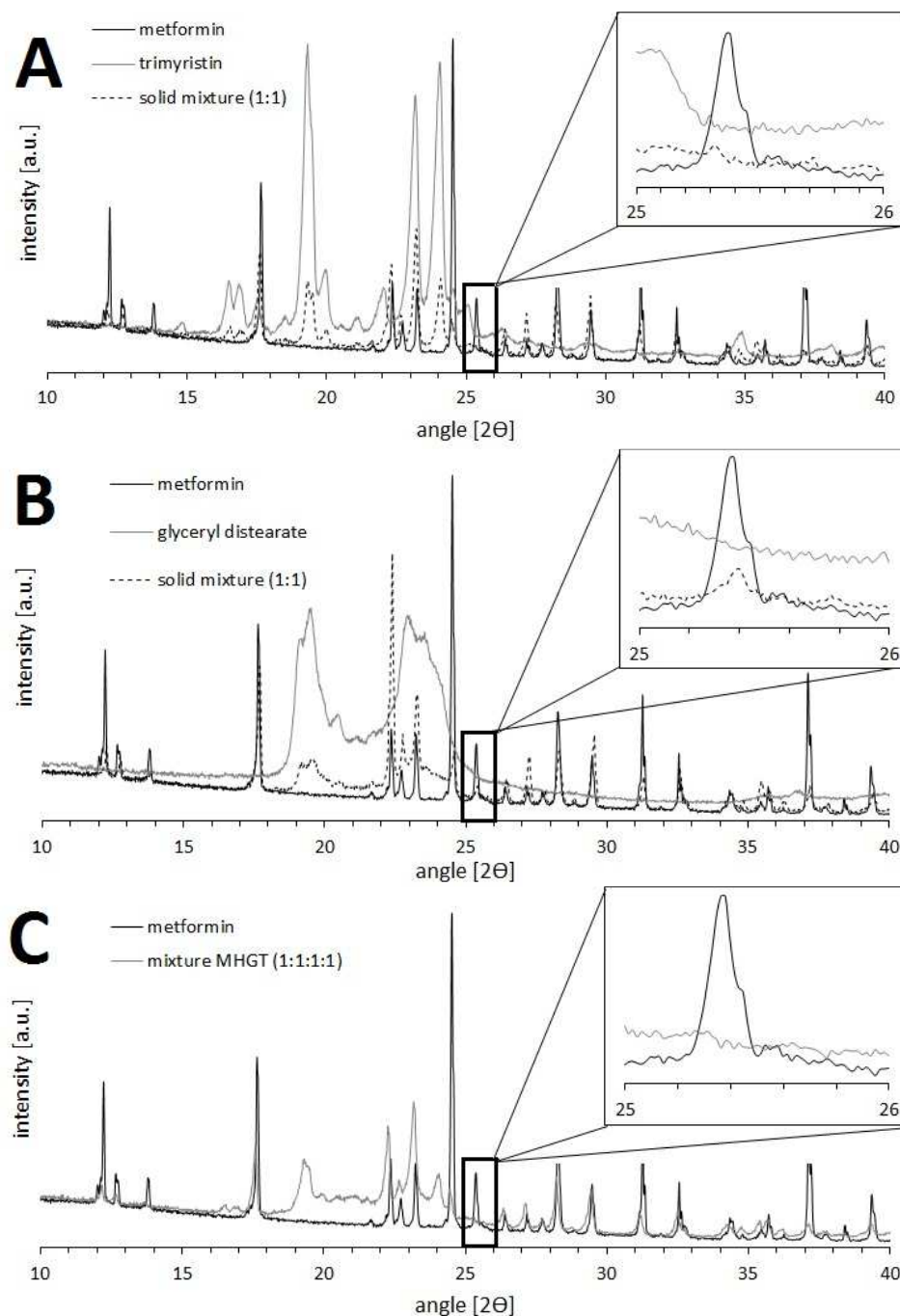


**Figure 4.9.** Diffractograms of (A) metformin HCl and glyceryl distearate and (B) metformin HCl and trimyristin and their respective solid mixtures, and (C) metformin HCl and the mixture with the three lipids (increment of 0.02 degrees, reading time of 1 s per point)

#### 4.2.4. Conclusions

Solid mixtures in various ratios of metformin HCl, hard fat, glyceryl distearate, and trimyristin were investigated. The DSC investigation showed a decrease in the melting range of glyceryl distearate or trimyristin in a quaternary mixture. This temperature decrease was not observed in a mixture of glyceryl distearate and trimyristin only, indicating that the presence of metformin HCl is necessary to observe this

phenomenon. Moreover, an interaction between glyceryl distearate and metformin HCl was confirmed due to an alteration in the fusion enthalpy value of metformin HCl and glyceryl distearate in a binary mixture.

XRPD investigation also revealed a physicochemical interaction between metformin HCl and trimyristin and likewise between metformin HCl and glyceryl distearate in binary mixtures and in a quaternary mixture. This was confirmed by the absence of a peak of metformin HCl in the  $2\theta$  interval of 25 to 26 degrees. Further investigations are still required for a better understanding of these interactions, especially if this phenomenon impact in further process steps such as extrusion and/or spheronization.

## 4.3. Solid Lipid Cold Extrusion

### 4.3.1. Introduction

In order to develop taste-masked micropellets, solid lipid cold extrusion (SLCE) should be employed. SLCE is a process where solid lipid excipients are used as binders and are treated below their melting points to obtain a plastified mass which passes through a defined diameter die. This technique has some advantages, when compared to other traditional extrusion processes, such as low process temperatures and absence of water or organic solvents. Moreover, it was reported that this method can be used to obtain extrudates with taste-masking properties (Michalk *et al.*, 2008; Witzleb *et al.*, 2011b). These properties could be further improved through a sequential spheronization step (Krause, 2008).

The process parameters should be adjusted according to other works dealing with SLCE, which employed screw configurations based only on conveying elements, process temperature of 25 to 33 °C, and screw rotational speed of 50 rpm (Breitkreutz *et al.*, 2003; Krause *et al.*, 2009). However, a die plate with die diameter of 0.5 mm should be used to produce small diameter lipid extrudates. Initially, the formulations investigated in the pre-formulation studies should be extruded. The morphological characteristics of the obtained extrudates should be characterized by SEM. Likewise, their physicochemical properties and possible alterations of metformin HCl or lipid binders due to the extrusion process should be investigated by DSC and XRPD. The drug release characteristics should be evaluated for further investigation during the next development steps.

### 4.3.2. Preparation of Lipid Extrudates

High drug loadings were aimed for the development of lipid based extrudates. All extrudate formulations should contain hard fat. Its presence was reported as advantageous since it melts between 42-44 °C and therefore lower process temperatures can be applied to the process (Breitkreutz *et al.*, 2003; Krause, 2008; Krause *et al.*, 2009). The basic formulation was analogue to the works of Breitkreutz *et al.* (2003) and Krause *et al.* (2009): 80% of API and 20% (w/w) of hard fat. In the present work, extrudates based on a ternary lipid mixture were also investigated and were designed regarding a fixed ratio between hard fat, glyceryl distearate, and trimyristin of 4:1:1 (w/w), respectively (Table 7.5, see page 120). Some studies reported that formulations based on these lipids are suitable for cold extrusion and produced adequate extrudates with a variety of properties (Reitz and Kleinebudde, 2007b; Krause *et al.*, 2009).

In the present study, the temperatures of the first six extruder segments were adjusted to 25 °C and the last cell (where the die plate is positioned) was set to 33 °C. Regarding the melting temperature of hard fat (43.5 °C), 33 °C is around 10 °C below it and 2 °C below its onset temperature (35.4 °C). This temperature was reported to be sufficient to achieve the desired plastic deformation characteristic of the mass during the passage through the dies for formulations based on hard fat (Krause *et al.*, 2009).

The first extrusion experiments (which will not be discussed in the present work) with a die plate with 1 mm dies showed that all formulations were feasible to be extruded under these conditions. However, the main aim of the present work is to obtain ODTs based on small diameter pellets to improve mouth feeling during administration. After disintegration, the pellets should remain intact in the oral cavity, consequently, the influence of the particles size on the mouth feeling is an important aspect to patient compliance (Jeong *et al.*, 2008). Micropellets present smaller risk of suffocation in airways due to morphological obstruction when swallowed. Therefore, to obtain small diameter pellets, a die plate with dies of 0.5 mm in diameter was used.

Employing only conveying elements and the 0.5 mm die plate during the extrusion a complete blockage of the dies was observed for all formulations after a few minutes of process time (Figure 4.10a). Barot *et al.* (2010) reported that metformin HCl can consist of needle-shaped, large crystals. This aspect becomes important since needle-shaped drugs can cause problems during SLCE and sometimes APIs presenting such characteristics cannot be processed (Witzleb *et al.*, 2011a; Witzleb *et al.*, 2011b). Figure 4.10b depicts an optical microscopy photo of the used metformin HCl particles. As observed in the SEM photos (Figure 4.2a, see page 32), crystals in different sizes can be seen, however, needle-shaped particles are not present. Thus, the metformin HCl particle shape is not the reason for the die blockage during the extrusion.

Another possible reason is related to the particle size of the components in the powder mixtures. During the blending of different materials, particles exhibiting similar sizes could aggregate, forming regions in the powder bed with a higher concentration of a particular component (Twitchell, 2012). If such a region is formed previously to the extrusion by metformin HCl particles during blending or during the transport into the extruder barrels, the passage of the material through the small diameter dies could be blocked. However, metformin HCl and the lipids showed different particle size distributions (Figure 4.1, see page 31) not support this hypothesis. On the other hand, these particle size differences could lead to segregation of components during the mixture step or during feeding in the extruder barrel. This phenomenon could influence the particle packing at the point of maximum pressure at the extruder die and block the dies (Twitchell, 2012).

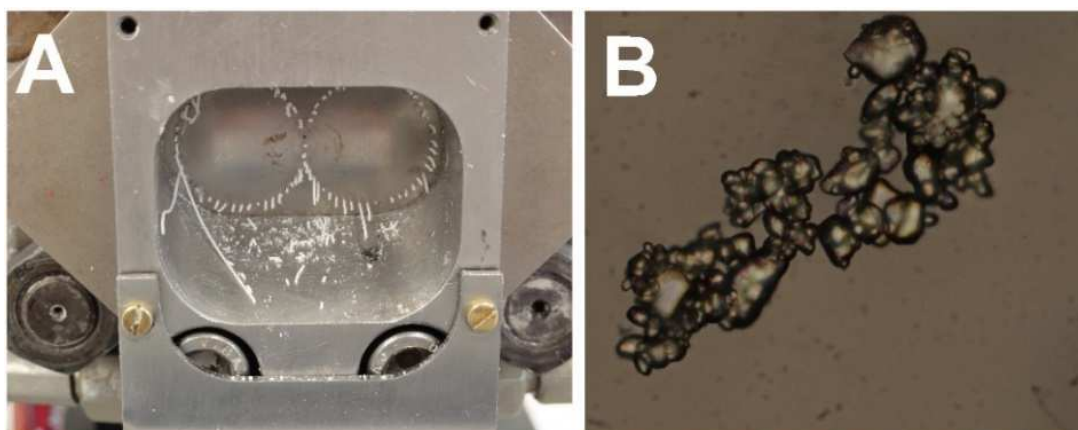


**Figure 4.10.** (A) Material blockage of the die plate during extrusion and (B) microscopic images of metformin HCl particles taken at 10x magnification

To avoid die blockage, two mixing zones were incorporated in the screw configuration to improve distribution and disaggregation properties (Figure 4.11). Employing this new configuration no blockage of the dies was observed, even for formulations containing high metformin HCl content (EMH<sub>80</sub> and EMHGT<sub>80</sub>).

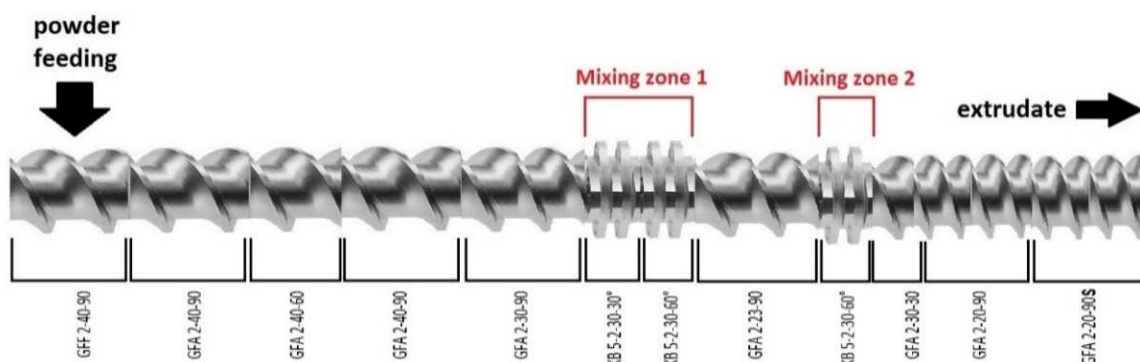


**Figure 4.11.** Extruder screw configuration used in the solvent solid lipid cold extrusion (adapted from Thiele (2003)). GFF = same direction, conveying, cut-free; GFA = same direction, conveying, comb-out; KB = kneading block; S = pointless; 2 = two flighted

### 4.3.3. Morphological Characterization of Extrudates

According to Witzleb *et al.* (2011b), some properties of solid lipid extrudates can be inferred by observing the extrudate surfaces. SEM images of the extrudates are depicted in Figure 4.12. The extrudates showed smooth surfaces where the solid lipid matrix can be recognized. Some pores are observed leading further into the extrudate. Small particles of metformin HCl are present at the surfaces embedded in the solid lipid matrix.

With the increase of lipid content in the extrudate formulation a proportionally higher matrix surface is formed as shown in figure 4.12. Moreover, extrudates based on 50% (w/w) of lipids (EMH<sub>50</sub> and EMHGT<sub>50</sub>) present a slightly irregular surfaces compared to the other extrudates. The higher the amount of low melting fat, the lower is the bulk viscosity during the extrusion, and the wider is the melted layer at the boundary layer of the extrudate. This phenomenon can be visualized by differences in extrudate surfaces and their core structures (Figure 4.12 and Figure 4.13). Moreover, the presence of two high-melting temperature lipids (glyceryl distearate and trimyristin) in the extrudate formulations does not seem to influence the surface characteristics when compared to the extrudates based on a same proportion of hard fat.

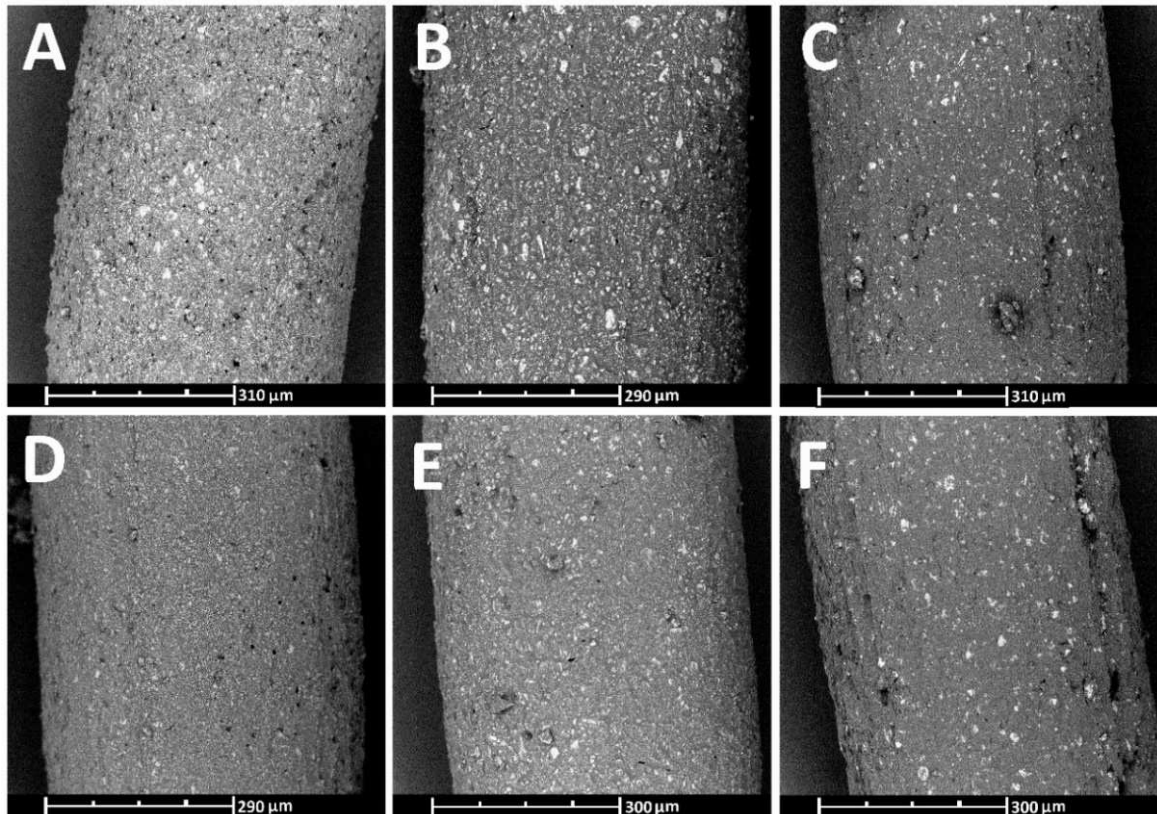


**Figure 4.12.** SEM photos of the lipid extrudates surfaces taken at 440x magnification (scale represents around 300  $\mu\text{m}$ ): (A) EMH<sub>80</sub>, (B) EMH<sub>70</sub>, (C) EMH<sub>50</sub>, (D) EMHGT<sub>80</sub>, (E) EMHGT<sub>70</sub> and (F) EMHGT<sub>50</sub>



Photos of cross-sections of the lipid extrudates are shown in Figure 4.13. The extrudate cores present a different structure when compared with their surfaces. However, the lipid matrix is also present, showing that the lipids in the core of the extrudates are also influenced by the extrusion process. The crystals of metformin HCl are still intact and fully embedded in the lipid matrix, which show a porous structure.

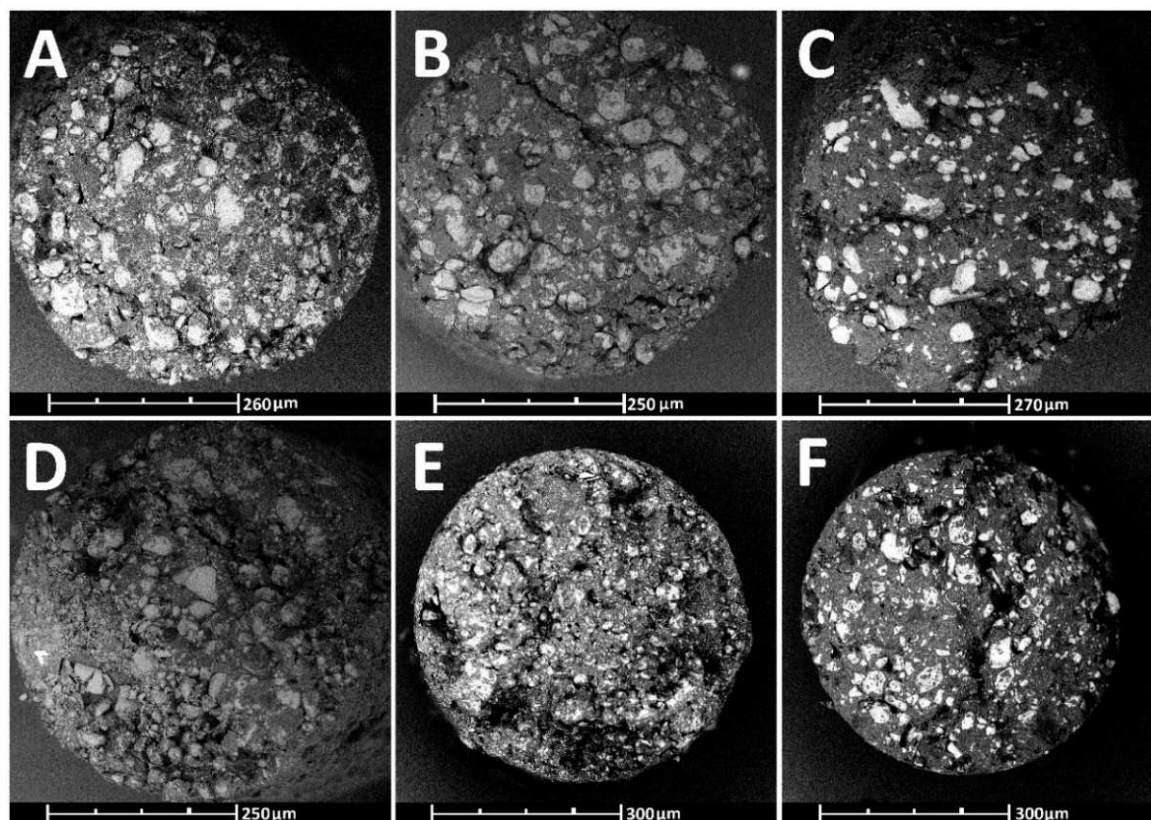


**Figure 4.13.** SEM photos of sectioned lipid extrudates taken at 490x magnification: (A) EMH<sub>80</sub>, (B) EMH<sub>70</sub>, (C) EMH<sub>50</sub>, (D) EMHGT<sub>80</sub>, (E) EMHGT<sub>70</sub> and (F) EMHGT<sub>50</sub>

#### 4.3.4. Thermal properties

Properties of TAGs, such as crystal sizes and their lattice, crystal morphology and crystallinity, are directly influenced by polymorphism. Polymorphism is influenced by their molecular structure itself, and by several external factors such as temperature exposure, shear forces, and pressure, which are generally encountered in the extrusion process (Sato, 2001; Reitz and Kleinebudde, 2007a). Besides, the temperature with the extrudate leaves the die plate was reported to be a key factor determining the crystallization behavior from molten components in the extruded mass (Windbergs *et al.*, 2009a). Due to the friction in the extruder and/or in the die plate, the temperature at the inner surface of the extruder barrel is higher, since that is where the shear rate is maximal (Barnes, 1995). This can result in a partial melting of the lipid and change the morphology due to recrystallization.



In the present work, the use of kneading elements in the screw configuration could lead to an increase in the shear rate, which could culminate in an increase of the material temperature in these zones. Additionally, as discussed in Section 4.2, a possible interaction between metformin HCl and glyceryl distearate and trimyristin is observed. Therefore, to elucidate if this interaction also occurs during the extrusion step and to investigate possible influences of the employed extrusion parameters on the material properties, DSC and XRPD analysis of the extrudates were performed.

The thermograms for the lipid based extrudates are shown in Figure 4.14. Two endothermic events are evidenced in all samples. The first endothermic peak refers to the melting of the hard fat, since the onset and peak temperature values coincides with its previous characterization (Table 4.6) and literature values. The second endothermic event refers to the melting point of metformin HCl, which occurs between 227.10 and 230.38 °C. The melting temperature is the same to that observed of pure metformin HCl in the material characterization. The melting peaks referent to glyceryl distearate and trimyristin in extrudates EMHGT were not visible. Probably as hard fat is completely melted before them, these lipids, which are present in small amounts in the formulations (2.5 to 6.25%; w/w), are dissolved in the melted hard fat and therefore do not showed a melting peak in the DSC. A similar behavior was observed in pellets containing sodium benzoate based on the same lipids (Krause, 2008).

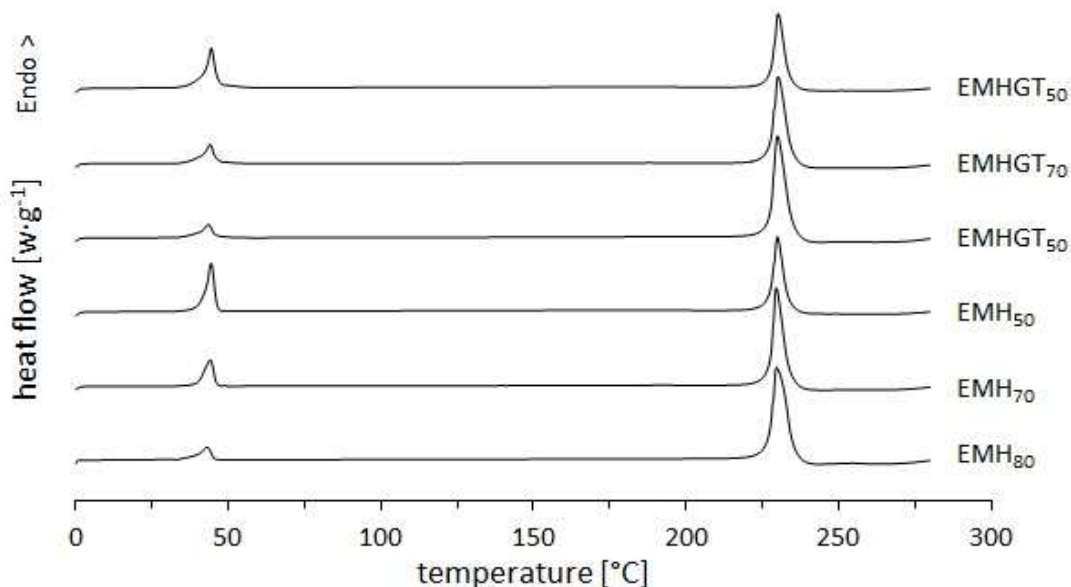


**Figure 4.14.** DSC thermograms of lipid extrudates (heating rate: 10 K·min<sup>-1</sup>). E = extrudate; M = metformin HCl; H = hard fat; T = trimyristin; G = glyceryl distearate

The fusion enthalpy values observed for metformin HCl and for hard fat are presented in Table 4.6. There is no substantial alteration in the heat of fusion of metformin HCl in the extrudates containing glyceryl distearate and trimyristin (EMHGT<sub>80</sub>, EMHGT<sub>70</sub>, and EMHGT<sub>50</sub>) compared to the results for the pure substance

(highlighted in Table 4.6). It is possible that the interaction between these lipids and metformin HCl does not take place under the extrusion conditions.

Regarding hard fat, the heat of fusion values are quite similar among the extrudates. However, they are slightly higher compared to pure hard fat. This effect could be due to the presence of glyceryl distearate and trimyristin in these formulations, which could be dissolved in the melted hard fat at lower temperatures, and therefore their melting events were not recognized. This hypothesis could explain these different values and also why the melting peaks from these both lipids have not been visible in the thermograms.

**Table 4.6.** Thermal characteristics of the lipid based extrudates

	Metformin HCl					
	Onset temp. (°C)		Peak temp. (°C)		Heat of fusion (J·g <sup>-1</sup> )	
	1	2	1	2	1	2
Metformin HCl	229.1	229.1	230.4	230.3	344.5	337.3
EMH <sub>80</sub>	226.9	227.3	229.4	229.6	347.5	344.2
EMH <sub>70</sub>	227.0	227.2	229.6	229.5	354.1	355.7
EMH <sub>50</sub>	227.2	227.2	229.8	229.9	338.6	332.8
EMHGT <sub>80</sub>	227.3	226.9	229.9	230.0	354.8	351.1
EMHGT <sub>70</sub>	227.3	227.3	230.2	229.7	354.8	351.1
EMHGT <sub>50</sub>	227.7	227.5	230.2	230.1	340.2	342.0

	Hard fat					
	Onset temp. (°C)		Peak temp. (°C)		Heat of fusion (J·g <sup>-1</sup> )	
	1	2	1	2	1	2
Hard fat	35.4	35.3	43.4	43.6	156.0	159.1
EMH <sub>80</sub>	40.0	39.8	43.4	43.5	168.5	167.2
EMH <sub>70</sub>	39.8	39.9	44.0	44.0	170.8	169.6
EMH <sub>50</sub>	42.0	41.6	44.4	44.3	168.1	163.9
EMHGT <sub>80</sub>	39.8	39.9	43.5	43.5	175.3	175.3
EMHGT <sub>70</sub>	40.5	40.3	43.9	43.9	168.7	174.5
EMHGT <sub>50</sub>	41.3	41.6	44.4	44.4	170.2	178.1

E = extrudate; M = metformin HCl; H = hard fat; T = trimyristin; G = glyceryl distearate. n = 2

The DSC investigations indicate no interaction between metformin HCl and glyceryl distearate and trimyristin. However, it is not possible to conclude if these results are due to the absence of this phenomenon or due to the low amount of the lipids within the extrudates based on the ternary mixture.

#### 4.3.5. Crystallographic properties

Therefore, XRPD investigations were performed. The diffractograms of the extrudates are depicted in Figure 4.15. The results did not show any alteration on their chromatographic pattern results compared to each other, even plotted overlapped

(Figure 4.16). The only difference among the diffractograms relies on the peaks related to hard fat, in the region from 20 to 22.5 degrees, which intensity increases with the increase in hard fat content in the extrudate formulation. As glyceryl distearate and trimyristin are in a small amount in the extrudates (2.5 to 6.25%, w/w), their peaks cannot be recognized due to their low intensity.

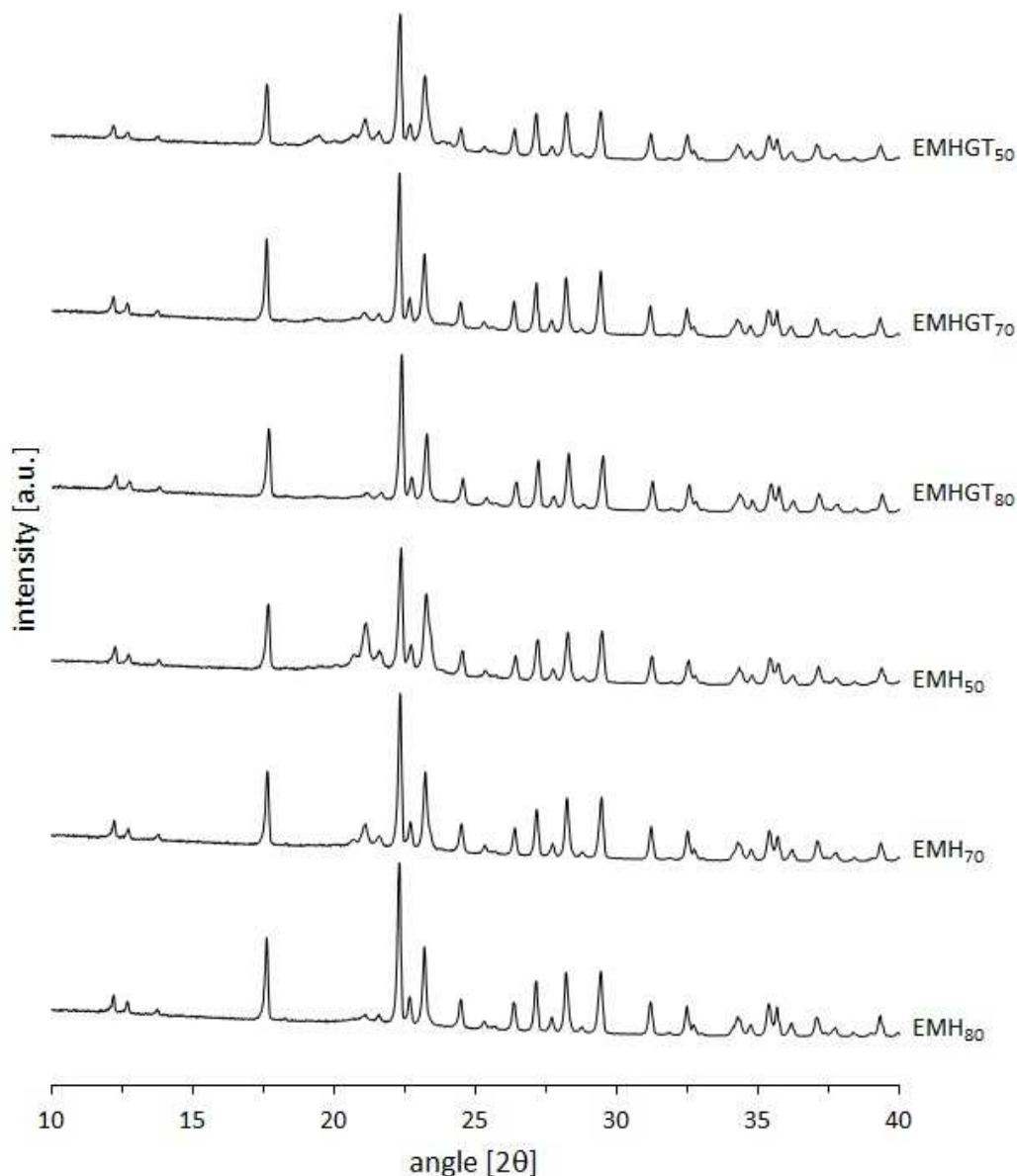


**Figure 4.15.** Diffractograms of the lipid extrudates degrees (increment of 0.02 degrees, reading time of 1 s per point). E = Extrudate, M = Metformin HCl, H = hard fat, T = trimyristin, G = glyceryl distearate

Surprisingly, the peak relative to metformin HCl at 25-26 degrees is present in all extrudates, even those with glyceryl distearate and trimyristin (Figure 4.16). Thus, the presence of this peak indicates that the interaction observed during the pre-formulation studies does not take place during the extrusion process or that the lipids did not melt.

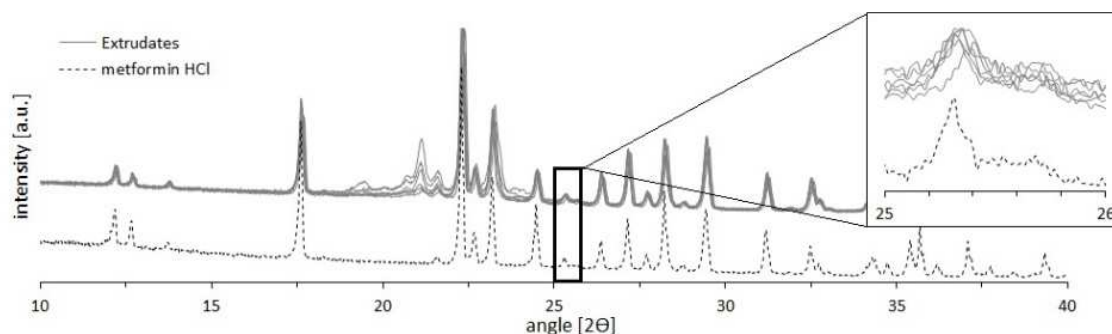


**Figure 4.16.** Overlapped diffractograms of lipid extrudates in comparison to the diffractogram of metformin HCl

### 4.3.6. Drug content of Extrudates

To ensure the drug content uniformity, every unit in a batch should have a drug substance content within a narrow range around the label claim, according to the Ph. Eur. (2014). Considering extrudates as single-dose unit preparations, the uniformity of dosage units can be demonstrated by either of two methods: content uniformity or weight variation (Ph. Eur., section 2.9.6). To investigate the drug content on the lipid extrudates, a liquid chromatographic method was used. Using the methodology described in section 7.3.13, metformin HCl showed a retention time of around 5.7 min. The calibration curve and its values are presented in Table 7.1 and Figure 7.1 (Annex I).

The content of metformin HCl in the lipid extrudates is depicted in Table 4.7. Interestingly, only the extrudate EMH<sub>50</sub> presented the expected amount of API. This difference between the “theoretical” amount of metformin HCl and the observed could be due to segregation of material during the blending step (as discussed in section 4.1.2) or even due to material adherence to the screws and barrel walls (Vervaet and Remon, 2005).

The content uniformity investigation of the extrudates was performed based on the Ph. Eur., section 2.9.6 test B (Ph. Eur., 2014), which defines a preparation as complying with the test if the content is inside the limits of 85% to 115% of the average content. The individual extrudates presented  $\pm 5\%$  (w/w) of metformin HCl content variation from the powder mixture content (Table 7.5, see page 120) within the defined limits of the Pharmacopeia. Additionally, from the technological point of view, as the extrudates are not the intended final dosage form, these observed content variations can be considered acceptable of next development steps.

**Table 4.7.** Metformin HCl content in the lipid based extrudates

	Mean $\pm$ SD (%; w/w; n = 10)					
	EMH <sub>80</sub>	EMH <sub>70</sub>	EMH <sub>50</sub>	EMHGT <sub>80</sub>	EMHGT <sub>70</sub>	EMHGT <sub>50</sub>
Drug Content	77.07 $\pm$ 0.73	66.39 $\pm$ 0.32	50.97 $\pm$ 1.75	76.77 $\pm$ 3.74	69.12 $\pm$ 0.62	48.21 $\pm$ 1.99

E = extrudate; M = metformin HCl; H = hard fat; T = trimyristin; G = glyceryl distearate

### 4.3.7. Dissolution Studies

Dissolution tests were performed for all lipid based extrudates batches. The basket method was used to prevent flotation of the extrudates and to ensure complete wetting during the assay. Additionally, 0.001% (w/w) polysorbate 20 was added to the medium to improve the surface wettability and to avoid material agglomeration in the basket. According to Krause (2008), the rotation speed of the basket did not influence the release profile during the dissolution studies of lipid pellets, therefore a rotational speed of 150 rpm was chosen to avoid particle agglomeration.

The drug release profiles of the lipid extrudates are depicted in Figure 4.17. Different dissolution profiles are observed, which are related to the lipid content in the extrudates. Extrudates based on 20% (w/w) of hard fat or the ternary lipid mixture (EMH<sub>80</sub> and EMHGT<sub>80</sub>, respectively) showed a first order release kinetic, releasing 100% (w/V) of metformin HCl after 40 min, characterizing them as immediate-release dosage forms.

An increase of 10% (w/w) in the lipid content leads to a slight decrease in drug release in the first minutes, however still 100% (m/V) of metformin HCl are released after 48 min (EMH<sub>70</sub>) and 58 min (EMHGT<sub>70</sub>). As immediate-release is defined as at least 80% release of an API within 45 min in a standard dissolution apparatus according to the USP 34 (2011), these profiles can still be considered as immediate-release.

The observed kinetic indicates a diffusion-controlled mechanism which is explained due to two factors: (1) the high water solubility of metformin HCl and (2) the insoluble lipid matrix. In this case, the fast dissolution of the particles located on the extrudate surfaces produces a burst effect and the particles without direct contact with the medium dissolve slowly. Moreover, the rate diffusion is then controlled by the concentration gradient, which is higher at the matrix extrudate surface, at sink conditions, and lower within the matrix due to hindered exchange with the release medium because of fine pore capillaries (Reitz *et al.*, 2008). Moreover, this explains the observed differences in the drug release profiles due to the increase of lipid content in the extrudate formulation, since the lipid matrix porosity decreases obstructing the diffusion of the dissolved API to the exterior of the extrudate (Güres *et al.*, 2011; Rosiaux *et al.*, 2014)

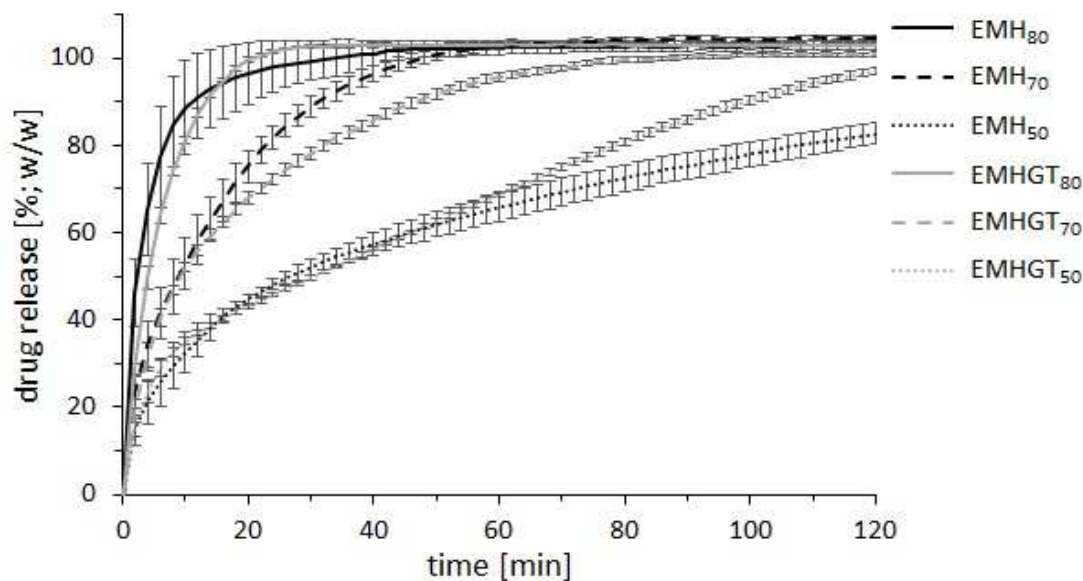


**Figure 4.17.** Drug release of metformin HCl from lipid based extrudates. Dissolution media: 900 mL purified water containing 0.001% (w/w) polysorbate 20, temperature of  $37\text{ }^{\circ}\text{C} \pm 0.5$ , 150 rpm, basket method,  $\lambda = 232\text{ nm}$  (mean  $\pm$  SD,  $n = 6$ ). E = extrudate; M = metformin HCl; H = hard fat; T = trimyristin; G = glyceryl distearate

The extrudates EMH<sub>50</sub> and EMHGT<sub>50</sub> showed a different drug release kinetic due to a relative higher lipid amount (50%; w/w). A faster initial release followed by slower sustained release of metformin HCl is observed. This profile is characteristic of Higuchi release kinetic and was confirmed by plotting the cumulative amount of drug released against the square root of time, since sink conditions were maintained (Siepmann and Peppas, 2011). This significant kinetic alteration could be related to a lower extrudate porosity generated by a higher amount of lipids. In these extrudates, water needs more time to penetrate into the porous system, delaying the drug dissolution.

Solid lipid based extrudates produced by SLCE are known for remaining intact during drug release without gel formation or erosion of the dosage form (Pinto and Silverio, 2001; Güres *et al.*, 2011). This behavior suggests pure Fickian diffusion mechanism, where: (1) water penetrates into the matrix, (2) dissolves the drug, (3) occupies the pores generated by the diffusion of dissolved drug particles and (4) creates water-filled channels which increase matrix porosity and drug mobility, allowing for continuous drug diffusion out of the dosage form and into the release medium (Siepmann and Peppas, 2011; Siepmann and Siepmann, 2011; Rosiaux *et al.*, 2014). The extrudate surfaces after dissolution are shown in Figure 4.18 and confirm that the lipid matrix is kept unaltered after the complete release of metformin HCl.

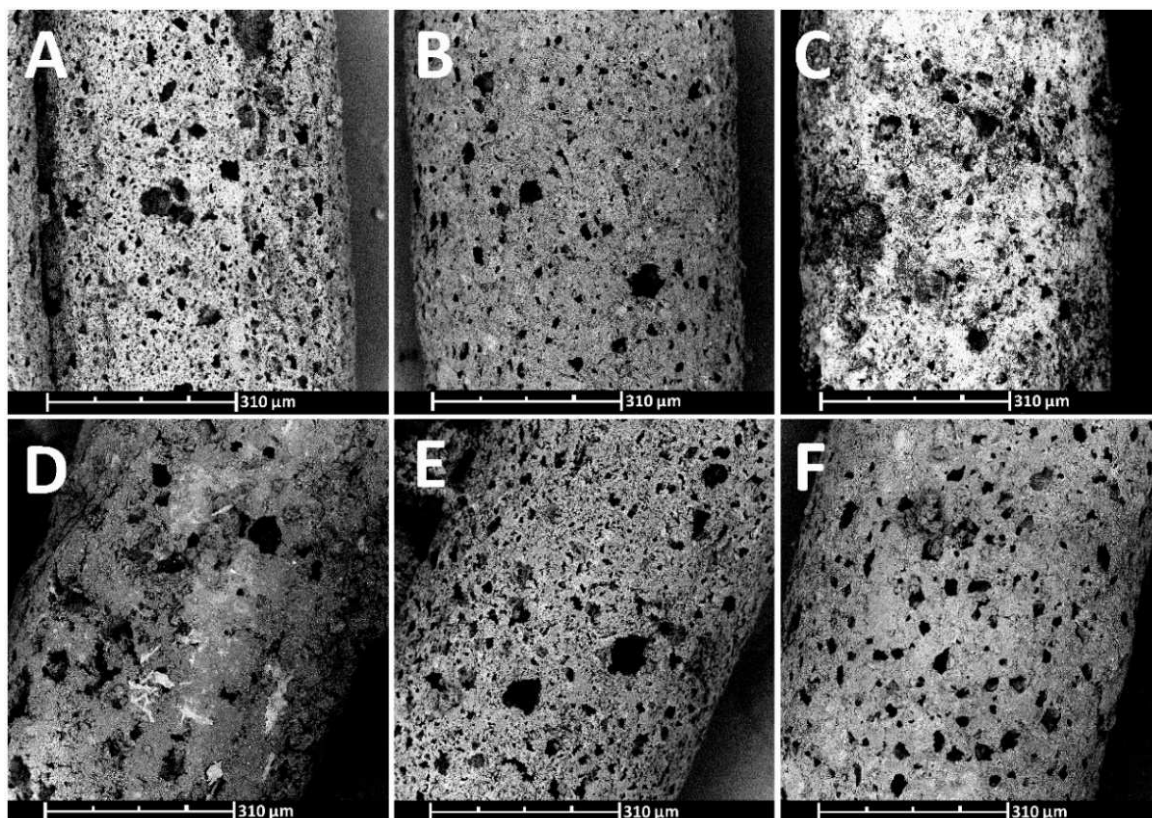


**Figure 4.18.** SEM photos of the lipid extrudates surfaces after dissolution taken at 420x magnification (scale represents 310  $\mu\text{m}$ ): (A) EMH<sub>80</sub>, (B) EMH<sub>70</sub>, (C) EMH<sub>50</sub>, (D) EMHGT<sub>80</sub>, (E) EMHGT<sub>70</sub> and (F) EMHGT<sub>50</sub>

Generally, taste-masking properties are attributed to extrudates and pellets obtained by solid lipids, which are related to the presence of a lag time or a slow drug release within the first minutes (Witzleb *et al.*, 2011b; Vaassen *et al.*, 2012; Kharb *et al.*, 2014). Therefore, the drug release from the extrudates in the first minutes was investigated using an in-line UV probe. The results are depicted in Figure 4.19. Considering the AAPS/FIP guideline (Siewert *et al.*, 2003), which suggests that taste-masked dosage forms are characterized by not more than 10% of API release within 5 min, the extrudates cannot be considered as taste-masked.

After 5 min all the extrudates showed a metformin HCl release higher than 30% (w/V). Similarly to the dissolution assay, differences between the extrudates, regarding their lipid content can be observed. The extrudates EMH<sub>80</sub> and EMHGT<sub>80</sub> released almost 100% (w/V) of metformin HCl in 5 min, while EMH<sub>70</sub> and EMHGT<sub>70</sub> released around 60% (w/V). Comparatively, the extrudates based on the higher content of lipids (EMH<sub>50</sub> and EMHGT<sub>50</sub>) showed a slower drug release, releasing less than 40% (w/V) after 5 min.



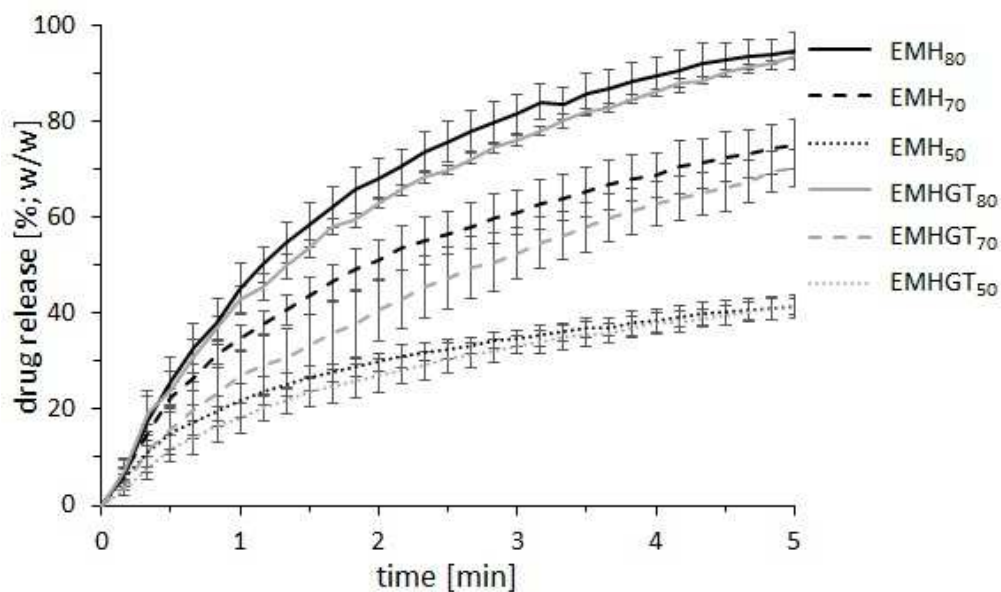


**Figure 4.19.** Drug release from the lipid extrudates using UV/Vis probe equipment. Dissolution media: 900 mL purified water containing 0.001% (w/w) polysorbate 20, temperature of  $37\text{ }^{\circ}\text{C} \pm 0.5$ , 100 rpm, paddle method using a sinker,  $\lambda = 232\text{ nm}$  (mean  $\pm$  SD,  $n = 3$ ). E = extrudate; M = metformin HCl; H = hard fat; T = trimyristin; G = glyceryl distearate

### 4.3.8. Conclusions

Initial extrusion experiments employing commonly used parameters presented die blockage during the process using a die plate of 0.5 mm in diameters. An alteration of the commonly used screw configuration, by adding two mixing zones, proved to improve the extrusion process avoiding blockage in the die plate. None of the investigated formulations showed any impairment during extrusion. Small diameter extrudates based on different lipid binders at different proportions, containing high drug load of metformin HCl, were successfully produced.

XRPD and DSC investigations of the extrudates did not detect alterations in their crystallographic or thermal properties, which indicate that the extrusion process does not influence the physicochemical properties of the lipid binders or metformin HCl in these formulations. However, more investigations are still needed to confirm these results, since unexplained interactions were observed in powder mixtures between metformin HCl and the used lipid excipients during the pre-formulation studies.

The lipid extrudates showed immediate and sustained-drug release in dependence of the lipid content. It was observed that 50% of lipid content led to an alteration on the drug release kinetic of metformin HCl from the extrudates. Furthermore, the presence of high-melting lipids did not influence the drug release profiles of the extrudates. Taste-masked properties of the lipid pellets were not confirmed, since they released more than 30% (w/w) of metformin HCl within the first 5 min of dissolution.



## 4.4. Lipid Spheronization

### 4.4.1. Introduction

Spheronization is a subsequent step to extrusion where the rod particles are rounded due to particle collision and frictional forces generated by a friction plate. Beside, centrifugal and frictional forces and temperature play an important role in the spheronization of solid lipid based extrudates. The process temperature influences the softening of the material until a certain plasticity is achieved and the spheronization of the extrudates can take place. There are few reports in literature about the investigation of the spheronization of lipid extrudates (Krause *et al.*, 2009; Reitz and Kleinebudde, 2009; Vaassen *et al.*, 2012; Yan *et al.*, 2012). All these studies investigated the spheronization of lipid based extrudates with diameter above 1.0 mm. The spheronization process and its influence on the pellets characteristics was never investigated for small diameter lipid based extrudates.

Furthermore, issues related to the control of the material temperature during the spheronization were reported as the most critical problem of the process (Krause *et al.*, 2009; Reitz and Kleinebudde, 2009). Fast material agglomeration and material adhesion at equipment walls, due to high material temperature during the process were reported, especially for extrudates based on high amounts of lipid binders.

So far, the works dealing with the spheronization of lipid based extrudates could not completely solve this problem. Therefore, the aim of this part of the work is to investigate the influence of the spheronization parameters on the material temperature of small diameter lipid based extrudates containing metformin HCl and propose a new approach to control the high material temperature problems reported in recent literature.

### 4.4.2. Investigation of the Spheronization Process

#### 4.4.2.1. Influence of Spheronization Parameters on Material Temperature and Process Time

Spheronization of batches of 300 g lipid extrudates were investigated using process parameters reported by Krause *et al.* (2009) and Reitz and Kleinebudde (2009). The rotational speed of the friction plate was set to 1500 rpm and the process temperature was adjusted to 33 °C by a water jacket system. This temperature was reported as ideal to process lipid extrudates based mainly on hard fat since this lipid has a melting range of 42-44 °C, which is around 10 K higher than the process temperature.

However, as there are no reports in literature about the spheronization of lipid based extrudates containing metformin HCl, a previous investigation of the ideal temperature to spheronize the extrudates was performed. A spheronization was performed for each formulation (Table 7.6, see page 121), samples were collected every minute and their surfaces were evaluated by SEM. All extrudates showed an initial alteration of the morphology of their surfaces at temperatures around 32 and 33 °C. To demonstrate the point where the surface morphology suffer this alteration, SEM photos of the extrudate EMH<sub>80</sub> surface are depicted in Figure 4.20. It is possible to recognize an alteration in the lipid matrix morphology from a rugose and irregular (Figure 4.20a) to a smooth and more homogeneous surface (Figure 4.20b).

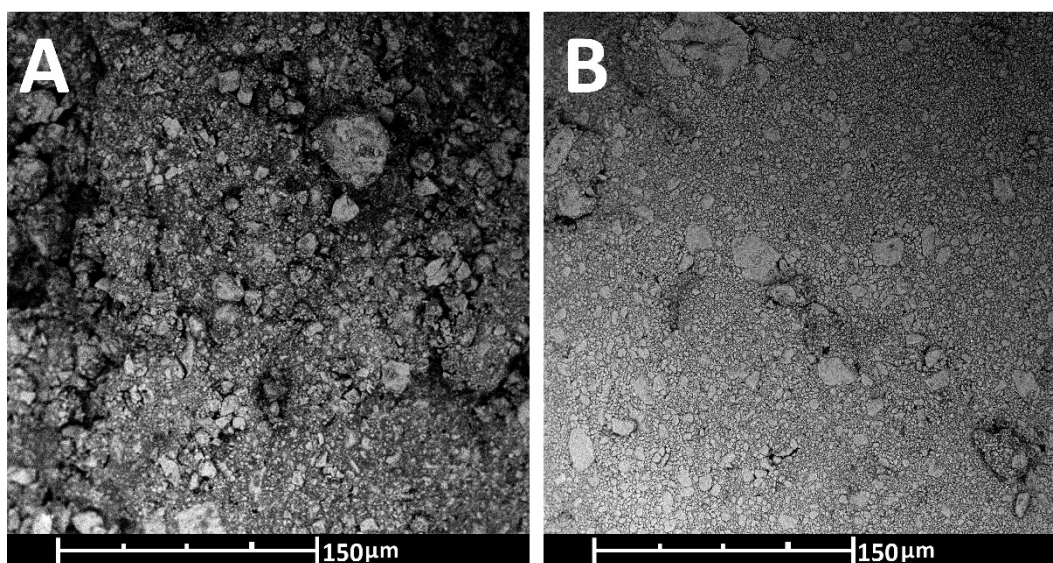


**Figure 4.20.** SEM pictures of the surface morphology of extrudate EMH<sub>80</sub> taken at 890x magnification (scale represents 150 µm) at different material temperatures: (A) 28.8 °C and (B) 32.9 °C

The material temperature variations during the spheronization for the extrudate formulations are depicted in Figure 4.21. The material temperature increases exponentially within the first minutes until a temperature is reached, where the lipids in the surface start to melt and, furthermore, the particles begin to stick together and generate big agglomerates. At this point it is not possible to continue with the spheronization.

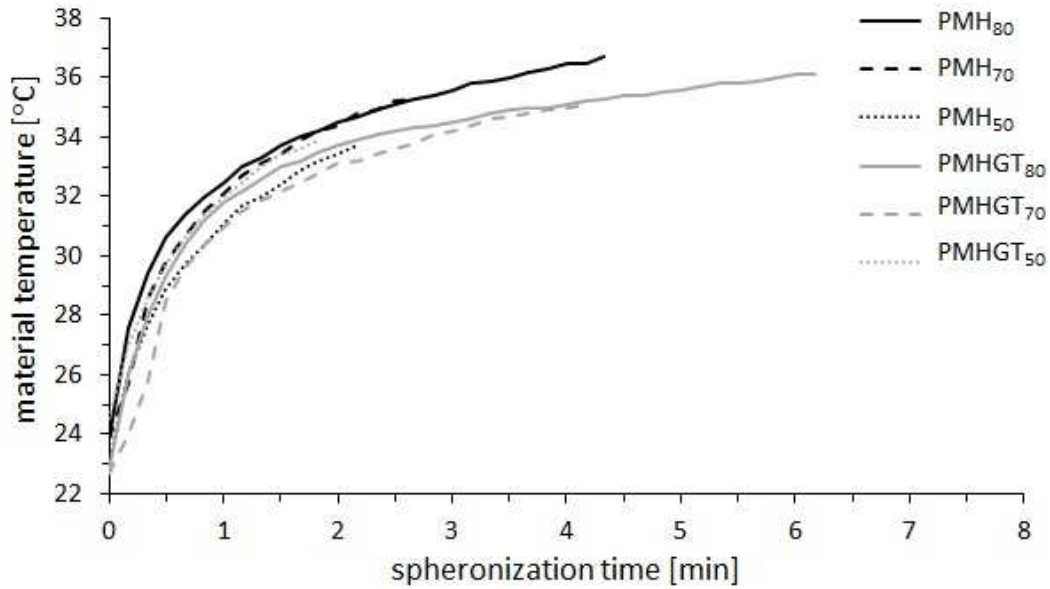


**Figure 4.21.** Material temperature during the spheronization process (water jacket: 33 °C; rotational plate speed: 1500 rpm). P = pellet; M = metformin HCl; H = hard fat; T = trimyristin; G = glyceryl distearate

This material temperature increase curve is similar to that reported by Reitz and Kleinebudde (2009). The authors described a three phase temperature increase curve which could be also recognized in Figure 4.21. The first phase is characterized by a low material temperature, where the lipid extrudates are still brittle and are broken into short fragments. A second phase where a fast increase in the material temperature takes place can be highlighted. The material temperatures increase greatly due to friction and shear forces as well as tempering of the spheronizer water jacket. After reaching of a specific material temperature, the extrudates show sufficient plasticity to be rounded. The last phase is characterized by a slower and constant increase in the temperature. At this phase the material temperature increases until a temperature where the material starts to stick at the equipment walls and the particles start to form big agglomerates. At this point, the free-flowing of the particles is impaired and the process was stopped. This phenomenon is schematically shown in Figure 4.22.

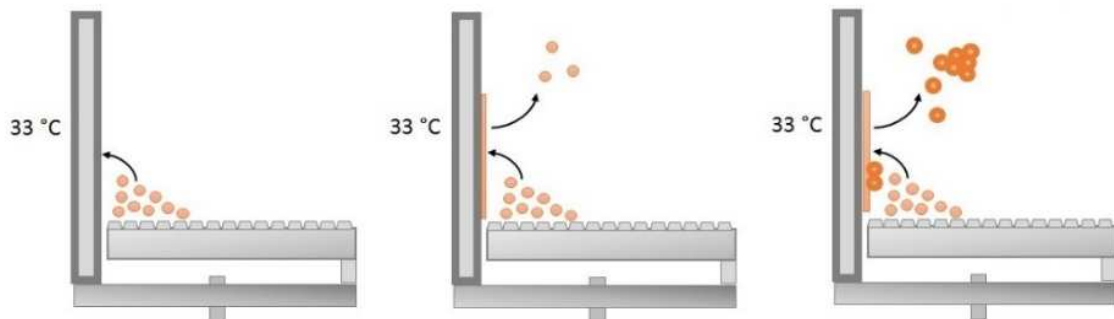


**Figure 4.22.** Scheme of agglomeration of material during the spheronization

The time until material agglomeration and the material temperature at this process time are shown in Table 4.8. Process times of more than 6.2 min were not feasible for any formulation. Moreover, a relation between the lipid content in the extrudate, the material temperature and the process time until material agglomeration was observed. The higher the content of lipids, the faster the agglomeration of the material occurs. The formulations based on 50% (w/w) of lipids showed agglomeration times around 2 min, denoting a strong influence of the lipid proportion on the spheronization process. The extrudates based on hard fat as the only lipid binder showed agglomeration at shorter process times compared to formulations based on the ternary lipid mixture. As hard fat melts at lower temperature compared to glyceryl distearate and trimyristin, this result could be explained by the proportionally lower amount of hard fat in the extrudates EMHGT<sub>80</sub>, EMHGT<sub>70</sub>, and EMHGT<sub>50</sub>.

Interestingly, the observed “agglomeration temperatures” are clearly lower than those reported by other authors for other lipid extrudate formulations (around 39 °C), also for extrudates based on lower amounts of hard fat (Breitkreutz *et al.*, 2003; Krause *et al.*, 2009; Reitz and Kleinebudde, 2009). Moreover, for the formulations MH<sub>50</sub> and MHGT<sub>50</sub> this temperature is near to the defined process temperature, considered as ideal (33 °C). Similar agglomeration temperatures were observed for the formulations based on the same content of lipids, indifferent of based on only hard fat or on the ternary lipid mixture.

**Table 4.8.** Temperature and agglomeration time during spheronization

Formulation	Lipid content (%; w/w)	Time until agglomeration (min)	Observed agglomeration temperature (°C)
PMH <sub>80</sub>	20	4.3	36.7
PMH <sub>70</sub>	30	2.7	35.3
PMH <sub>50</sub>	50	2.2	33.7
PMHGT <sub>80</sub>	20	6.2	36.1
PMHGT <sub>70</sub>	30	4.2	35.1
PMHGT <sub>50</sub>	50	1.8	34.0

P = pellet; M = metformin HCl; H = hard fat; T = trimyristin; G = glyceryl distearate

The rounding of lipid extrudates into spheres is strongly influenced by frictional forces, which are generated by particle-to-particle and particle-to-equipment interactions. In addition to the occurring friction forces, also the energy input by the friction plate is consequently converted into heat, which then leads to an increasing material temperature during the process (Erkoboni, 1997; Chatchawalsaisin *et al.*, 2005; Reitz and Kleinebudde, 2009). These events produces an increase in the material temperature, which then leads to a partial melting of lipid binders at the surface of the particles. Likewise, the equipment jacket temperature also plays an important role, since the material temperature is also influenced by the equipment wall temperature during the contact of the particles with it.

These specific agglomeration temperatures are also influenced by the heat conductivity of the substances in the extrudate formulation. Each formulation presents a different heat conductivity resulting in different energy needed to start the melting of the lipid fraction. Moreover, the heat conductivity is influenced by inter- and intra-particle material contact at the surface and interior of the extrudates. According to Chatchawalsaisin *et al.* (2005), it generally increases with a high amount of liquid components or if low melting temperature lipids are presented in high proportions at the particle surface.

To elucidate the reason of these low agglomeration temperatures in the studied extrudate formulations, the solid fat content variation (SFC) of the formulations was investigated. The SFC results are depicted in Figure 4.23. The extrudates based on the ternary lipid mixture start to melt at temperatures around 33 °C while the formulations based on hard fat at 34-35 °C. The initial decrease in the SFC of extrudates containing high-melting temperature lipids are less accentuated compared to the extrudates containing hard fat only. The extrudates MHGT present a second and fast melting phase which starts at 40 °C. Comparatively, the extrudates MH do not present this secondary phase, however, they have an accentuated alteration in their SFC starting at 38°C. Still, the formulations based in three lipids present a slower melting (100% SFC variation in a 7 °C interval) compared to the formulations based on hard fat (100% SFC variation in a 4 °C interval).

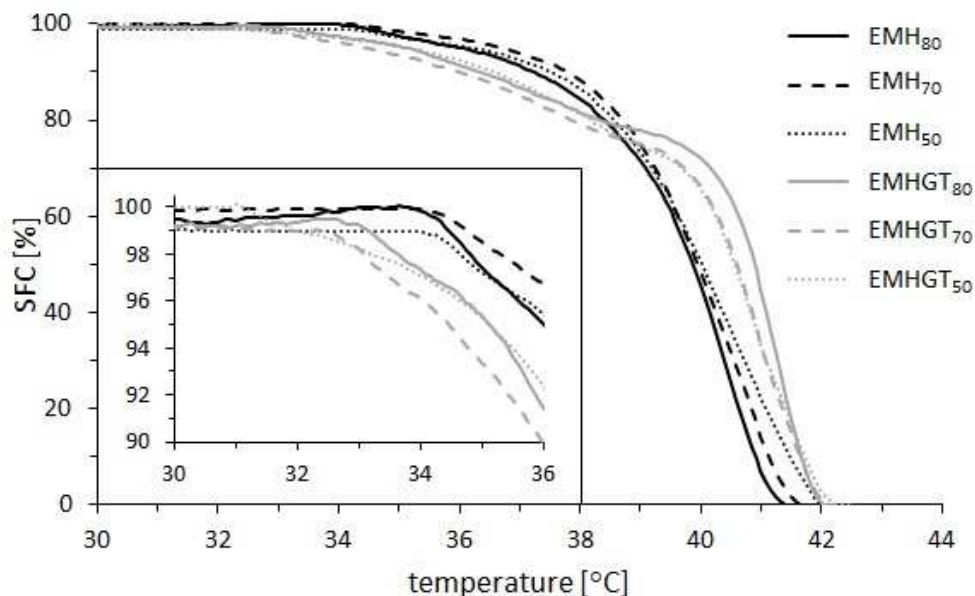


**Figure 4.23.** Solid fat content (SFC) variation of the lipid extrudates during heat (DSC, 25 to 50 °C, heating rate: 1 K·min<sup>-1</sup>). E = extrudate; M = metformin HCl; H = hard fat; T = trimyristin; G = glyceryl distearate

Although the SFC results help to explain the difference in the agglomeration temperatures between extrudates based on hard fat and extrudates based on the ternary lipid mixture due to the presence of different melting kinetics, these behaviors

do not clarify the temperature differences related to the lipid amounts in the extrudates. The fusion enthalpy for the SFC assay are depicted in Table 4.9. The values were further adjusted according to the amount of lipids present in the formulation. As expected, the higher the content of lipids in the extrudate, the higher the energy required to complete the melting of the lipids. However, adjusting these values to the amount of lipids in the extrudate formulations, an inverse relation is observed. This result indicates that the higher the amount of lipids in the formulations, the lower will be the total required energy to melt the same amount of extrudates and the lower will be the temperature where this process takes place.

**Table 4.9.** Heat of fusion of lipids in the extrudates in the SFC assay

	Heat of fusion ( $\text{J}\cdot\text{g}^{-1}$ )		Adjusted heat of fusion ( $\text{J}\cdot\text{g}^{-1}$ )	
	1	2	1	2
EMH <sub>80</sub>	150.8	148.2	7.5	7.4
EMH <sub>70</sub>	153.5	154.5	5.1	5.1
EMH <sub>50</sub>	151.4	155.7	3.0	3.1
EMHGT <sub>80</sub>	157.5	159.4	7.9	8.0
EMHGT <sub>70</sub>	164.7	161.9	5.5	5.4
EMHGT <sub>50</sub>	160.9	157.4	3.2	3.1

E = extrudate; M = metformin HCl; H = hard fat; T = trimyristin; G = glyceryl distearate

To investigate if these process times are sufficient to spheronize lipid extrudates, the particle shape was characterized. Several factors can be used to characterize the shape of round particles, i.e. circularity, radial shape factor, mass shape factor and sphericity. During the present work the aspect ratio (AR), a length-width ratio based on Feret diameter, was used. According to Kleinebudde (1995), a mean AR lower or equal to 1.2 is considered as sufficient for pharmaceutical pellets. The obtained ARs for the lipid based pellets are shown in Table 4.10. Although the formulation PMH<sub>80</sub> showed a value near to the reported, none of the formulations presented AR below 1.2. Furthermore, a relation between the lipid amount and the AR of the pellets can be seen: the higher the amount of lipids, the shorter is the spheronization time, and the more irregular is the pellet shape. The AR values characterize the pellets as irregular and non-spherical shaped and indicate that the spheronization times were not sufficient to achieve adequate shape of the pellets.

**Table 4.10.** Lipid pellets aspect ratios obtaining by commonly used spheronization parameters

	PMH <sub>80</sub>	PMH <sub>70</sub>	PMH <sub>50</sub>	PMHGT <sub>80</sub>	PMHGT <sub>70</sub>	PMHGT <sub>50</sub>
AR	1.24	1.66	1.63	1.53	1.47	1.57

P = pellet; M = metformin HCl; H = hard fat; T = trimyristin; G = glyceryl distearate

Images of the produced pellets are presented in Figure 4.24. The photos corroborate the AR values, where it is possible to identify that the particles are not adequate rounded, in especial the formulations MH<sub>50</sub> and MHGT<sub>50</sub>, where the cylindrical form



of the original extrudates are perceived and only the edges were broken. Furthermore, although the AR value for the formulation  $MH_{80}$  showed a value near to described as sufficient by Kleinebudde (1995), it is possible to see that the particles are still in an intermediate formation phase called “dumb-bell” (Rowe, 1985).

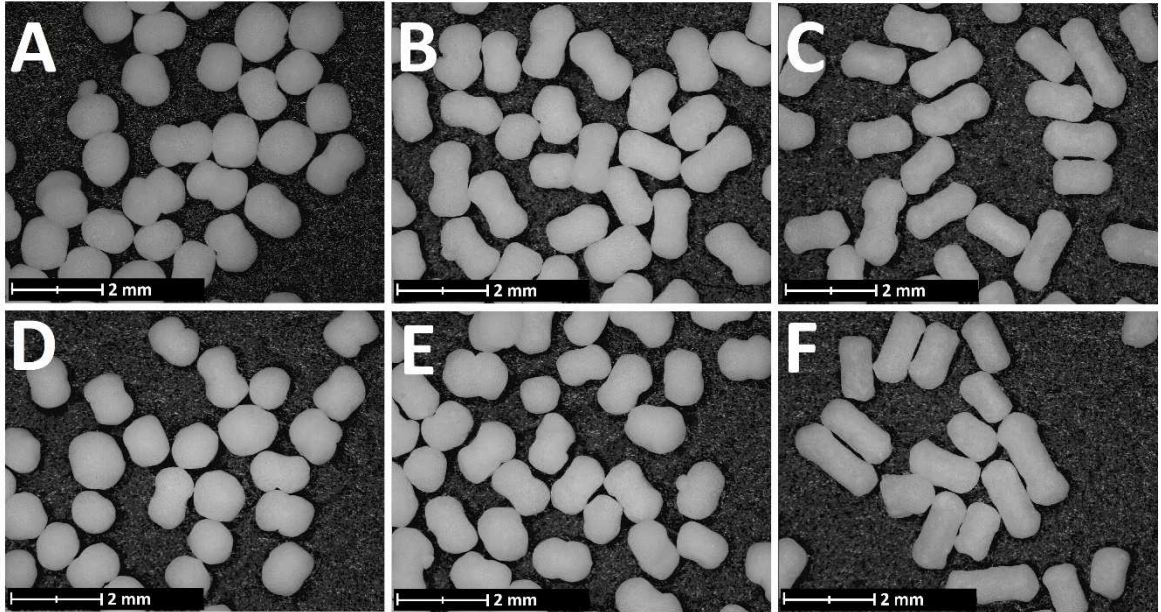


**Figure 4.24.** Optic microscope photos of the pellets taken at 4.5x magnification: (A)  $PMH_{80}$ , (B)  $PMH_{70}$ , (C)  $PMH_{50}$ , (D)  $PMHGT_{80}$ , (E)  $PMHGT_{70}$ , and (F)  $PMHGT_{50}$

A closer look of the particle surfaces (Figure 4.25) also shows that the spheronization parameters are not sufficient to achieve a complete morphology change in the surface of the extrudates, probably due to the low exposition time to the temperature. Furthermore, the photos reveal that a partial melting of the lipids on the edges of the particles slightly covers the central part of the extrudate indicating a similar mechanism of shape formation as described by (Rowe, 1985).

As shown above, the used parameters are not adequate to control the material temperature during the process, since all the formulations agglomerate at lower process times, especially the formulations based on more than 20% (w/w) of lipids, and adequate sphericity is not achieved.

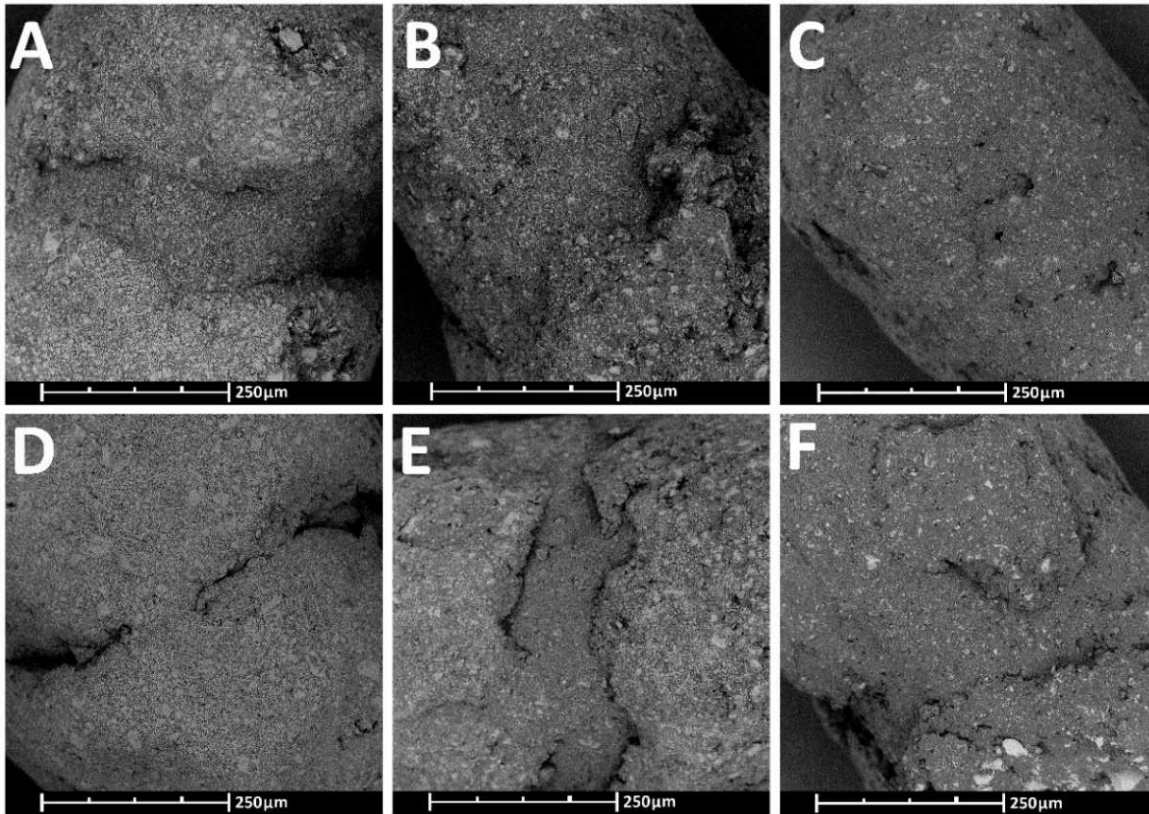


**Figure 4.25.** SEM of the particles surfaces taken at 520x magnification (scale represents 250  $\mu\text{m}$ ): (A) PMH<sub>80</sub>, (B) PMH<sub>70</sub>, (C) PMH<sub>50</sub>, (D) PMHGT<sub>80</sub>, (E) PMHGT<sub>70</sub>, and (F) PMHGT<sub>50</sub>

#### 4.4.2.2. Influence of Friction Plate Temperature on Material Temperature

The main heating sources in the lipid spheronization, as outlined in Figure 4.26, are (1) the equipment water jacket and (2) the frictional forces generated by the friction plate. However, the friction plate temperature could also play an important role in the heat transferred from the equipment to the extrudates during the process.

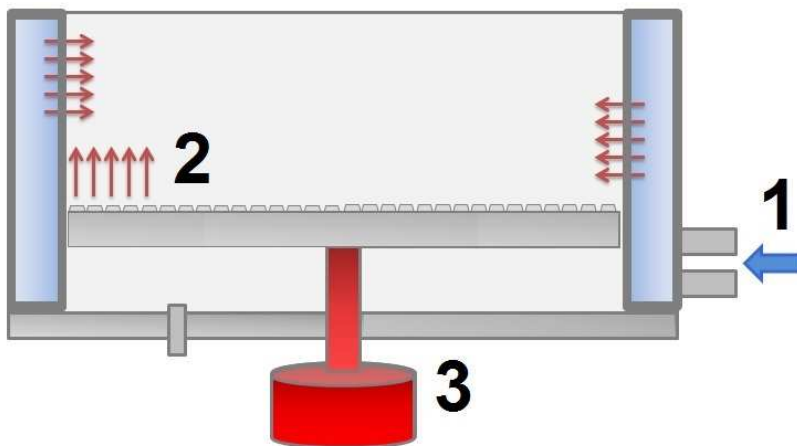


**Figure 4.26.** Schematic heat sources in the spheronizer: (1) water jacket temperature, (2) frictional forces due to the rotation of the friction plate, and (3) motor heating



To investigate the influence of the friction plate temperature on the material temperature, the temperature of the plate was initially measured in the absence of extrudates, while the spheronizer jacket temperature was set to 33 °C. The temperature increased by more than 3 K after 60 min of continuous running of the equipment (Figure 4.27a). This increased temperature can be related to the construction of the spheronizer, where the motor is positioned directly below the friction plate. When the motor runs, heat is generated, which is transported by heat transduction from the bottom of the plate to its surface (Figure 4.26-3). This increasing temperature is subsequently transferred to the material during the process, which could influence the observed fast partial melt of lipids present in the particles.

One component of the employed spheronizer model is a pressurized air entrance located under the friction plate. This device is generally used to produce flow air current from the bottom of the plate to the internal chamber walls and avoid small particles to escape the spheronization chamber through the gap between the plate and walls. The studies about spheronization of lipid based extrudates employing the same model of this equipment did not report the use of this device in the investigations (Breitkreutz *et al.*, 2003; Krause *et al.*, 2009; Reitz and Kleinebudde, 2009). This device provides pressurized air at 0.25 bar and temperature of 20 °C. By using this pressurized air device in the aforementioned setup, the plate temperature variation was reduced to less than 0.5 K after 60 min of continuous running of the spheronizer (Figure 4.27b). It is interesting to note that the plate temperature is kept relatively low and constant in the first 20 min of operation comparatively to the heating curve presented without the use of the air device. This time windows is important since 15 min was reported was necessary for obtaining adequate shaped lipid pellets (Krause *et al.*, 2009; Reitz and Kleinebudde, 2009).

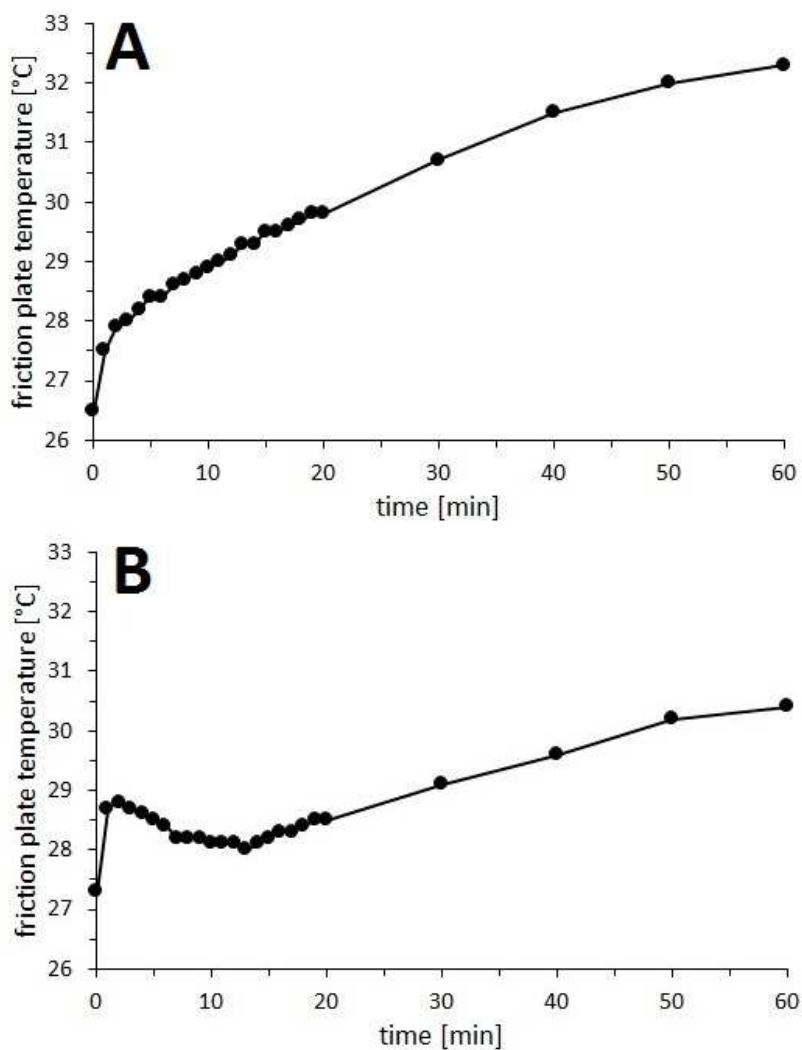


**Figure 4.27.** Friction plate temperature variation (A) without using pressurized air and (B) with pressurized air, at 1500 rpm, in empty spheronizer, and water jacket set to 33 °C

To investigate a potential advantage of this pressurized air on the spheronization process, and consequently on the material temperature, the same lipid extrudates were processed using the same parameters, however, with the presence of pressurized air. The material temperature variations during the spheronization for the extrudates are presented in Figure 4.28. A similar temperature increase pattern is observed compared to the first spheronization investigations. The extrudates EMH<sub>80</sub> and EMHGT<sub>80</sub> were successfully spheronized until 15 min. However, the extrudates based on 70% and 50% (w/w) of lipids still showed agglomeration at shorter process times.

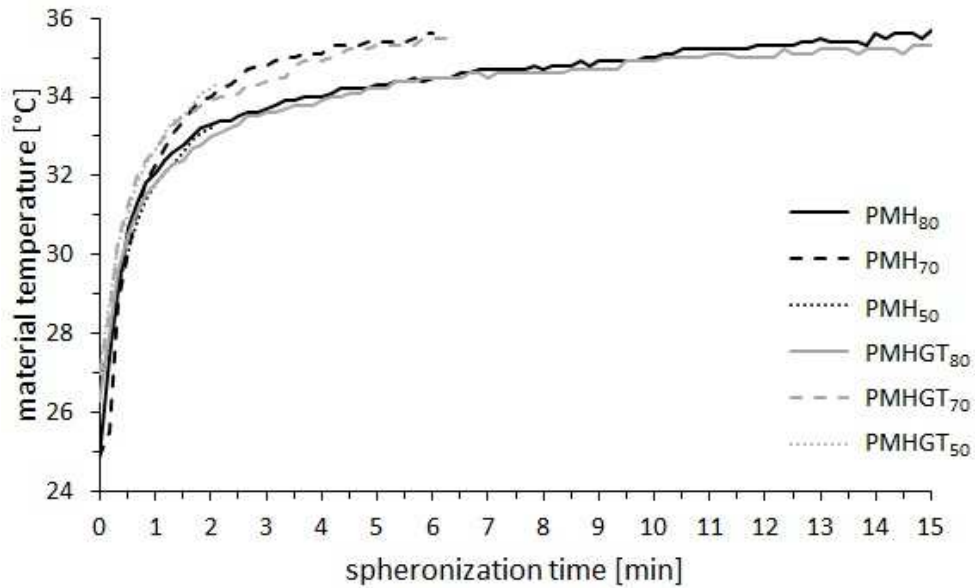


**Figure 4.28.** Material temperature during the spheronization process using pressurized air (water jacket: 33 °C; rotational speed: 1500 rpm). P = pellet; M = metformin HCl; H = hard fat; T = trimyristin; G = glyceryl distearate

Table 4.11 displays the observed times until agglomeration of the extrudates and the material temperature at this point. The spheronization times for extrudates based on 20% (w/w) of lipids (MH<sub>80</sub> and MHGT<sub>80</sub>) were increased and no agglomeration or material adherence on the equipment walls was observed. The process time increase observed for these extrudates is related to the material temperature, which was kept below the defined agglomeration temperatures (36.7 °C and 36.1 °C, respectively). Unfortunately, this improvement provided by the cooling air was not sufficient to avoid the increase in the material temperature of other formulations until high temperatures, still leading the material to adhere to the equipment walls and agglomeration at short spheronization times.

**Table 4.11.** Temperature and agglomeration time during spheronization

Formulation	Lipid content (%; w/w)	Time until agglomeration (min)	Observed agglomeration temperature (°C)
PMH <sub>80</sub>	20	15.0*	35.7**
PMH <sub>70</sub>	30	6.0	35.6
PMH <sub>50</sub>	50	2.0	33.2
PMHGT <sub>80</sub>	20	15.0*	35.3**
PMHGT <sub>70</sub>	30	6.3	35.5
PMHGT <sub>50</sub>	50	2.2	34.2

\*No agglomeration was observed. \*\*Final material temperature. P = pellet; M = metformin HCl; H = hard fat; T = trimyristin; G = glyceryl distearate

Table 4.12 summarizes the AR for the obtained lipid pellets. The prolonged spheronization times observed for the formulations MH<sub>80</sub> and MHGT<sub>80</sub> resulted in a

small improvement in their ARs compared to the previous process. Regarding the extrudates based on 70% and 50% (w/) of lipids, as the spheronization times were similar (around 2 min), no shape improvement was achieved.

**Table 4.12.** Lipid pellets aspect ratios obtaining using cooling air

	PMH <sub>80</sub>	PMH <sub>70</sub>	PMH <sub>50</sub>	PMHGT <sub>80</sub>	PMHGT <sub>70</sub>	PMHGT <sub>50</sub>
AR	1.24	1.45	1.65	1.31	1.43	1.62

P = pellet; M = metformin HCl; H = hard fat; T = trimyristin; G = glyceryl distearate.

AR results are corroborated by microscope images of the pellets, which are shown in Figure 4.29. Different shapes can be observed for the formulations. Slightly spherical shape pellets were obtained for the formulations based on 20% of lipids (PMH<sub>80</sub> and PMHGT<sub>80</sub>). The AR values indicates an improvement in the pellet shape of these formulations compared to those obtained by spheronization without using the pressurized air device. However, their AR values still characterize them as not sufficiently shaped regarding the value suggested by Kleinebudde (1995).

The extrudates based on 30% (w/w) of lipids were spheronized until an ellipsoid shape particle and some dumb-bell structures can also be seen. On the other hand, due to the extremely short spheronization times, the extrudates based on 50% (w/w) of lipids did not presented alteration on their initial cylindrical forms, suffering only deformation on their edges due to friction forces generated by the friction plate and collision against the equipment walls.

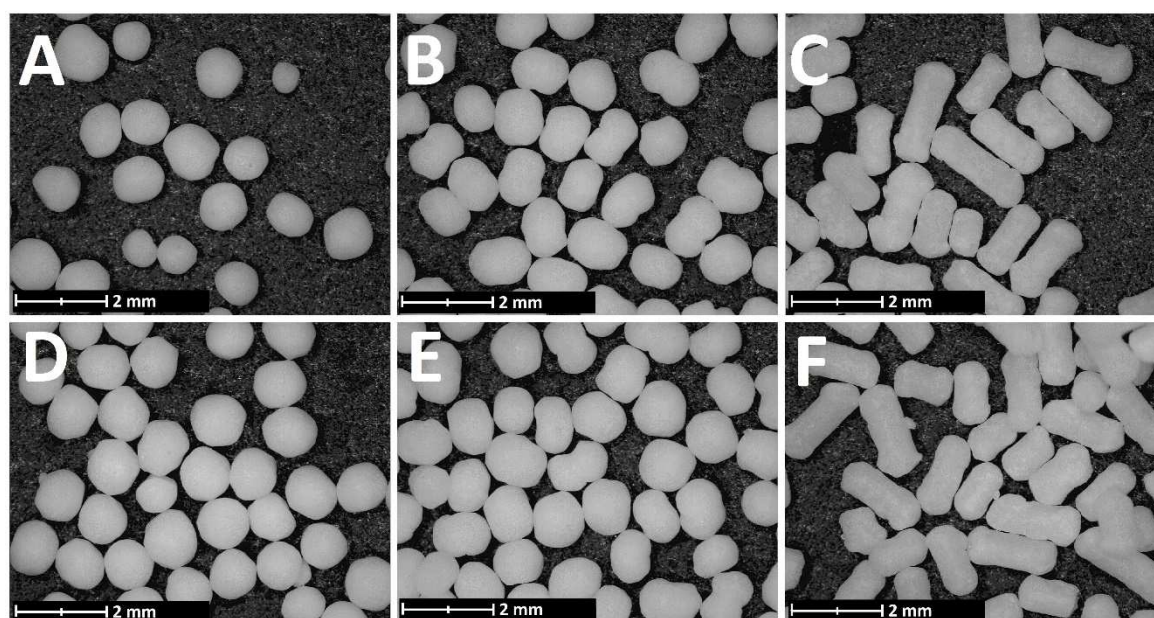


**Figure 4.29.** Optical microscope photos of the pellets taken at 4.5x magnification: (A) PMH<sub>80</sub>, (B) PMH<sub>70</sub>, (C) PMH<sub>50</sub>, (D) PMHGT<sub>80</sub>, (E) PMHGT<sub>70</sub>, and (F) PMHGT<sub>50</sub>

The pellets surfaces are depicted in Figure 4.30. The SEM images of PMH<sub>80</sub> and PMHGT<sub>80</sub> (Figure 4.30a and 4.30d, respectively) show smooth and homogeneous surfaces compared to surface morphology of the pellets based on 70% and 80% (w/w)

of lipids, which shown irregular surfaces and non-spheroidal particles which seems to be in a pellet formation shape. The images allied to the AR values corroborate the necessity of 15 min of spheronization to achieve spherical pellets. On the other hand, the SEM images of the pellets based on 70% and 50% (w/w) of lipids show clearly that the process time is too short to change the shape of the extrudates. Besides, although the optimal spheronization temperature was achieved, no surface alteration is perceived in the formulations  $EMH_{50}$  and  $EMHGT_{50}$ .

For the extrudates based on 20% (w/w) of lipids the use of the air device showed a positive improvement on the process time due to the decreased influence of the plate temperature on the material temperature. Still, these parameters were insufficient to increase the process time for extrudates based on 30% or 50% (w/w) lipids, since they still agglomerated due to high material temperatures after short process times.

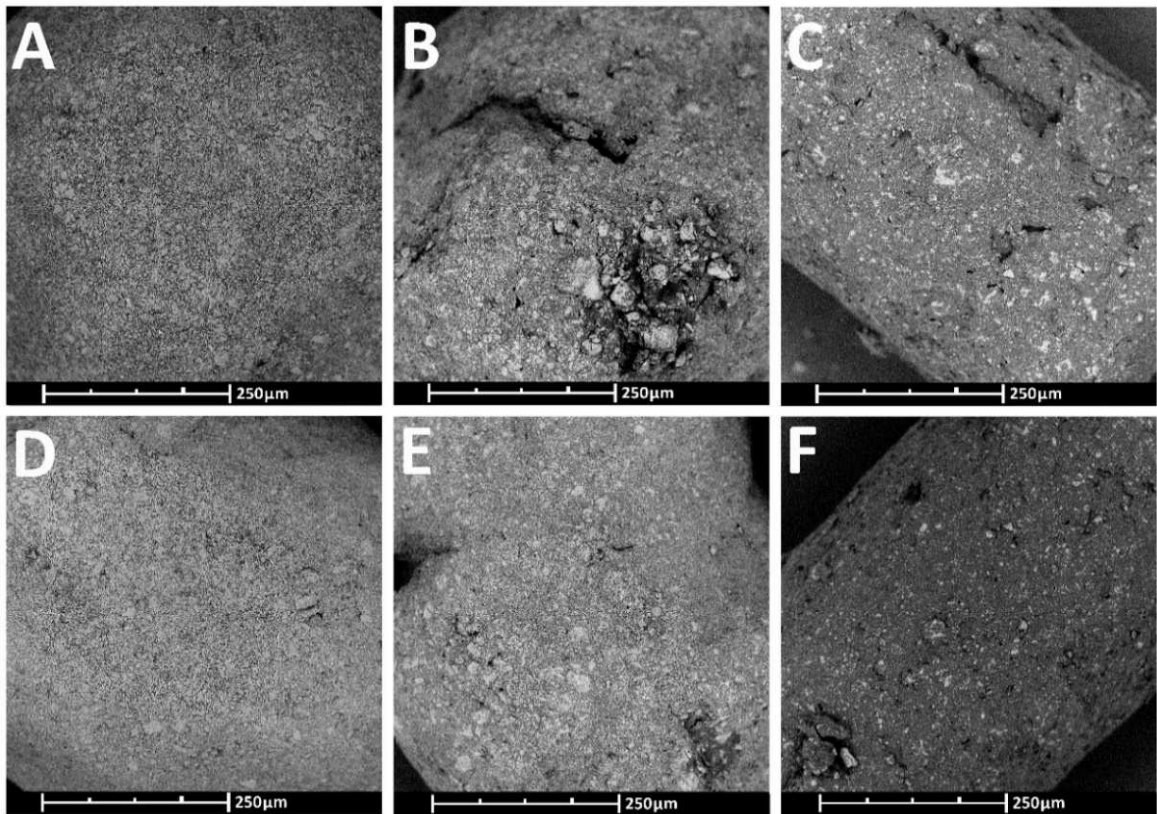


**Figure 4.30.** SEM of the particles surfaces taken at 520x magnification (scale represents 250  $\mu\text{m}$ ): (A)  $PMH_{80}$ , (B)  $PMH_{70}$ , (C)  $PMH_{50}$ , (D)  $PMHGT_{80}$ , (E)  $PMHGT_{70}$ , and (F)  $PMHGT_{50}$

#### 4.4.2.3. Improved Equipment Setup

To overcome the issues related to the agglomeration of material due to uncontrolled temperature, such as material adhesion at the equipment walls and particle agglomeration, a new equipment setup was developed (Figure 4.31). Process parameters, such as process time, plate rotational speed, and extrudates amount were maintained. The process heating source was removed from the equipment walls

(decreasing the jacket temperature to 30 °C) and a new heating source - an infrared (IR) light - was employed. This IR light was installed at the upper shell of the spheronizer to heat only the superior surface of the moving particle bed as depicted in Figure 4.31a. The light was plugged to a “power control unit” that allowed the adjustment of the temperature of the lamp and therewith the material temperature during the spheronization. In the other edge of spheronizer chamber, an IR contact-free thermometer was placed to measure the material temperature during the process without interference of the light (Figure 4.31b). A defined and smaller heating area is then generated at the surface of the particle moving bed as shown in Figure 4.30a. This modification in the heating source and the size of the heating zone allied to a constant and quick adjustment of the IR light power supply should enable a more precise control of the material temperature during the process.

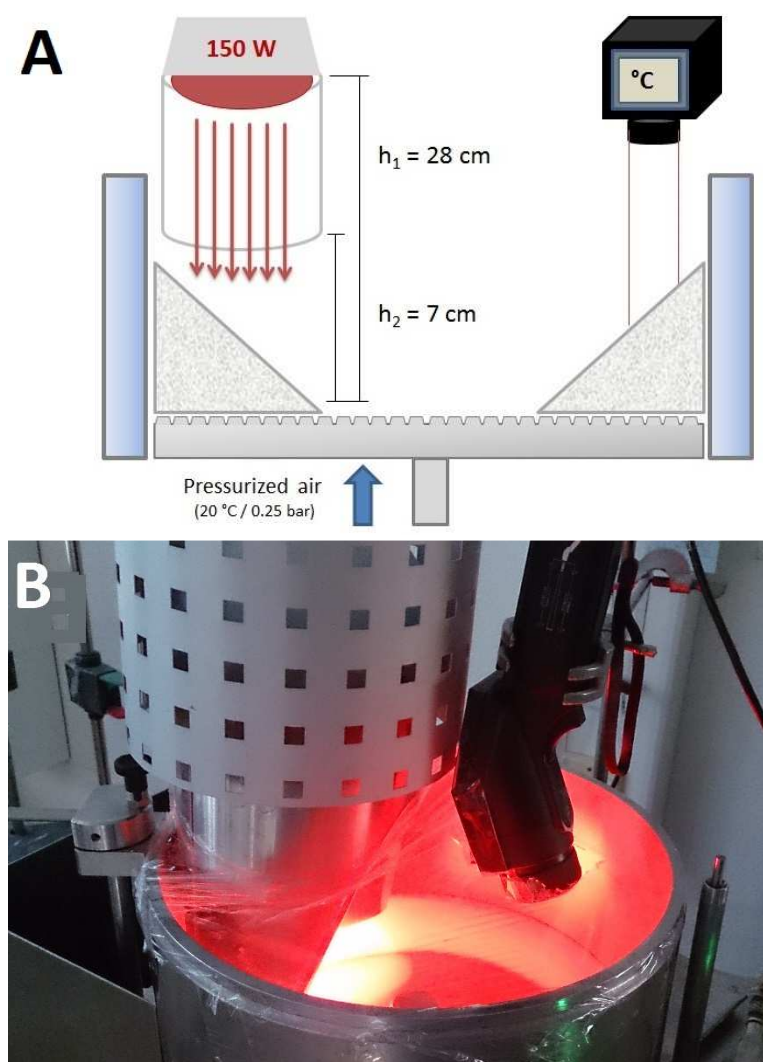


**Figure 4.31.** (A) Schematic setup of the spheronizer and (B) equipment photo

Furthermore, to minimize possible external temperature influences on the process, the environment temperatures were measured using thermometers. Likewise, the internal chamber wall and friction plate temperatures were measured using the contact-free



IR thermometer. The temperature values for the spheronization of the lipid extrudates are presented in Table 4.13. The spheronization was initiated at relative similar temperature conditions for each extrudate formulation.

**Table 4.13.** Temperatures measured in spheronization processes (°C)

	PMH <sub>80</sub>	PMH <sub>70</sub>	PMH <sub>50</sub>	PMHGT <sub>80</sub>	PMHGT <sub>70</sub>	PMHGT <sub>50</sub>
Room temp.	24.2	22.4	21.2	24.6	23.2	23.7
Chamber temp.	27.1	26.7	26.1	27.4	26.6	26.8
Starting chamber wall temp.	29.6	28.7	27.8	29.3	28.2	27.9
Final chamber wall temp.	30.7	30.4	30.1	31.2	30.7	30.5
Starting plate temp.	26.1	26.0	24.8	26.5	25.4	24.9
Final plate temp.	30.7	29.7	29.3	31.3	30.4	29.9
Starting material temp.	23.6	22.9	22.8	24.5	23.6	23.8

P = pellet; M = metformin HCl; H = hard fat; T = trimyristin; G = glyceryl distearate

The initial agglomeration temperature values (Table 4.8, see page 60) were used as critical temperature limits for the respective formulations. Since extrudates based on 50% (w/w) of lipids showed agglomeration temperatures around 33 °C, a material temperature range of 32-33 °C was defined as adequate. For the other formulations, a range of 33-34 °C was defined as adequate to achieve the desired characteristics of the material avoiding stickiness. When the material temperature approached this value, the potency of the IR light was reduced and adjusted until the material temperature was constant. The material temperature variation during the spheronization using this new set up are shown in Figure 4.32. The temperature curves show an asymptotic profile with a fast temperature increase within the first minutes, behavior similar to previously observed without the use of the pressurized air device. However, due to the control of the IR lamp power, a constant and controlled temperature phase is observed. Comparatively, the spheronization under commonly used conditions does not exhibit such a phase, presenting a constant temperature increase (Figure 4.28, see page 67).

With the new setup all the formulations were successfully spheronized to longer process times. No agglomeration tendencies or material adhesion at the equipment walls were observed, not even at spheronization times of 15 min. Moreover, the material temperature control led to similar thermal behavior for formulations based on different lipids or lipid amount. The rounding process and the final micropellets obtained using this new approach were then further investigated and will be discussed in details.

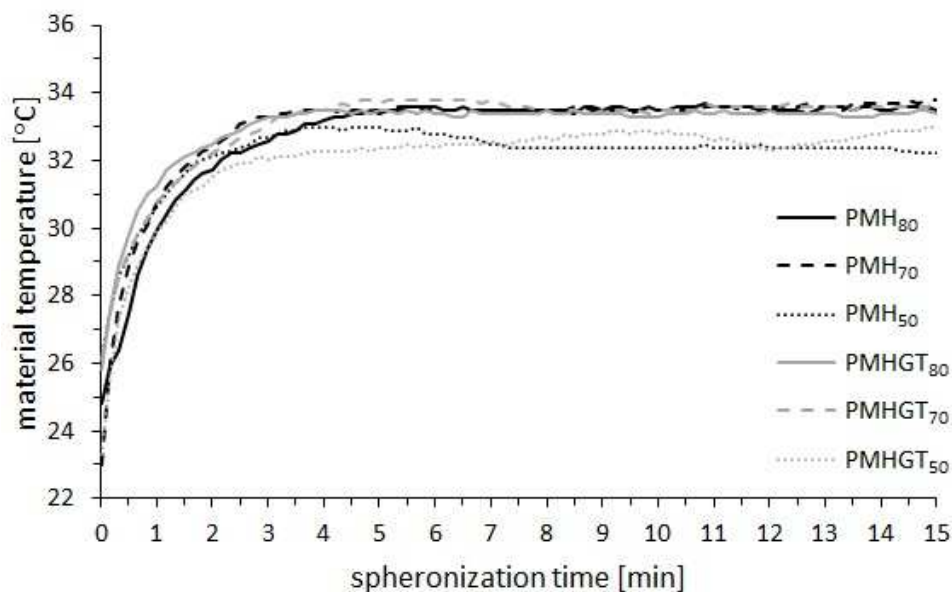


**Figure 4.32.** Material temperature during spheronization using the new heating approach. P = pellet; M = metformin HCl; H = hard fat; T = trimyristin; G = glyceryl distearate

#### 4.4.3. Particle Size Distribution, Shape Characterization, and Flow Properties of Lipid Pellets

In literature, some authors defined “micropellets” as aggregates with mean diameter below 500  $\mu\text{m}$  or below 1.0 mm (Kleinebudde, 1997; Parkin, 2007). In the present work, pellets presenting a median around 700  $\mu\text{m}$  should be referred as micropellets. The particle size distribution values and shape parameters are depicted in Table 4.14. The particle size of the different micropellets formulations presents quite similar values. However, the micropellets based on 20% (w/w) of lipids showed lower  $d_{10}$  values compared to other pellet formulations. This difference could be related to the higher loss of particles observed for these extrudates. As the amount of lipid binders in these formulations is relatively lower, the contact area between the lipids and the metformin HCl particles is reduced and could lead to a weaker binding between the particles. Consequently, due to the frictional forces generated by the rotation of the plate and the collision among particles and the walls fines a higher production of fines is formed compared to the formulations based on higher lipid amounts.

All the lipid micropellets showed median values ( $d_{50}$ ) below 700  $\mu\text{m}$ , with exception of the formulation  $\text{PMH}_{50}$ , which showed a slightly higher value. Span values indicate a narrow particle size distribution for all formulations, however, the micropellets  $\text{PMH}_{80}$  and  $\text{PMHGT}_{80}$  showed a relative wider span, probably due to the already mentioned loss of fines during the spheronization process.



**Table 4.14.** Particle shape and size distribution of micropellets obtained by the new approach

	Mean $\pm$ SD (n = 3 batches)				
	d <sub>10</sub> ( $\mu$ m)	d <sub>50</sub> ( $\mu$ m)	d <sub>90</sub> ( $\mu$ m)	AR	Span
PMH <sub>80</sub>	409.25 $\pm$ 31.61	668.50 $\pm$ 2.26	736.30 $\pm$ 1.98	1.21 $\pm$ 0.00	0.52 $\pm$ 0.07
PMH <sub>70</sub>	610.07 $\pm$ 1.69	694.20 $\pm$ 1.64	767.20 $\pm$ 1.13	1.15 $\pm$ 0.00	0.23 $\pm$ 0.00
PMH <sub>50</sub>	618.60 $\pm$ 7.43	707.17 $\pm$ 11.49	798.70 $\pm$ 14.32	1.29 $\pm$ 0.02	0.25 $\pm$ 0.01
PMHGT <sub>80</sub>	340.03 $\pm$ 17.65	637.27 $\pm$ 2.38	713.23 $\pm$ 1.37	1.25 $\pm$ 0.01	0.59 $\pm$ 0.03
PMHGT <sub>70</sub>	613.13 $\pm$ 1.97	693.87 $\pm$ 2.18	764.23 $\pm$ 1.76	1.22 $\pm$ 0.01	0.22 $\pm$ 0.00
PMHGT <sub>50</sub>	564.53 $\pm$ 3.99	627.40 $\pm$ 4.12	702.70 $\pm$ 2.98	1.37 $\pm$ 0.00	0.22 $\pm$ 0.00

Aspect ratio (AR) was calculated to the fraction between 250 and 1000  $\mu$ m. d<sub>10</sub>, d<sub>50</sub>, and d<sub>90</sub> = 10%, 50%, and 90% quantiles, based on Feret diameter. P = pellet; M = metformin HCl; H = hard fat; T = trimyristin; G = glyceryl distearate

Regarding the micropellets shape, ARs below 1.3 were achieved for all lipid micropellets, even for the formulations based on high amounts of lipids, with exception of the formulation PMHGT<sub>50</sub>. The micropellets showed a higher value than the threshold defined by Kleinebudde (1995), however, in the present work, AR below 1.3 were considered as sufficient since these pellets presented adequate particle flow properties, characteristic required for a further compaction step. Figure 4.33 depicts the shape of the micropellets after 15 min of spheronization. Spheroid shapes can be seen and correlated to the AR values resulted from the spheronization process. Figure 4.33f shows the micropellets PMHGT<sub>50</sub>, which depicts still irregular shaped particles and corroborate the AR showed by this formulation. This result indicates that for this particular formulation a longer process time is still required to obtain more spherical particles.

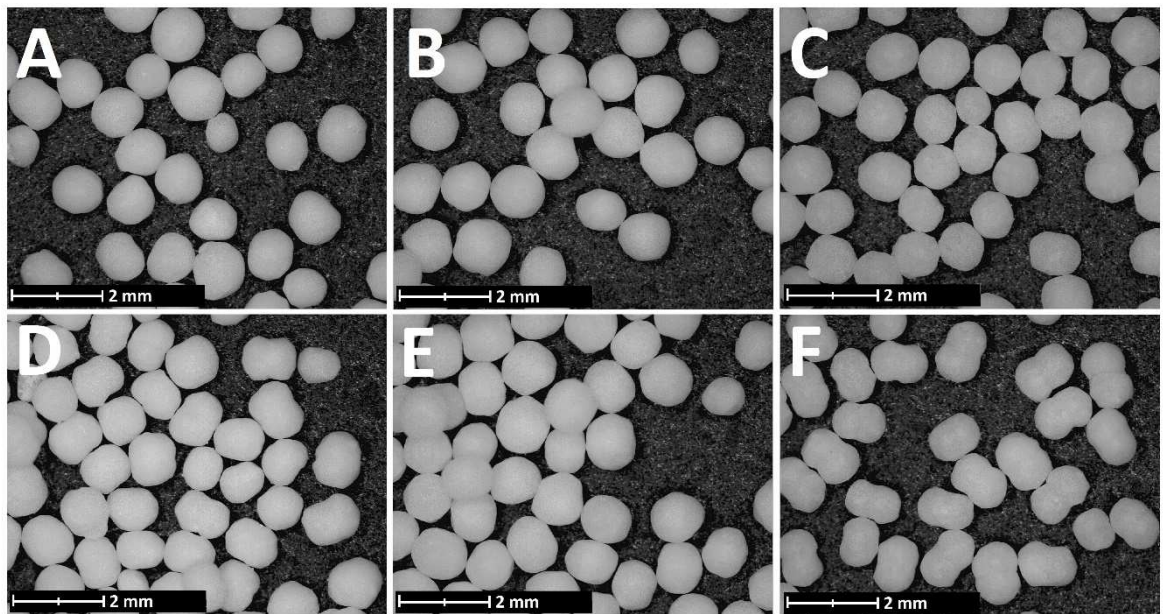


**Figure 4.33.** Optic microscope photos of the micropellets taken at 4.5x magnification: (A) PMH<sub>80</sub>, (B) PMH<sub>70</sub>, (C) PMH<sub>50</sub>, (D) PMHGT<sub>80</sub>, (E) PMHGT<sub>70</sub>, and (F) PMHGT<sub>50</sub>

The SEM images of the micropellets show smoother and more regular surfaces compared to the original extrudates (Figure 4.34 and Figure 4.12, respectively). The lipid matrix is easily visible and represents the major extent of the lipid surfaces. Small visual differences can be seen comparing the pellets based on 20%, 30%, and 50% (w/w) of lipids. The micropellets PMH<sub>80</sub> and PMHGT<sub>80</sub>, which contain a lower amount of lipids on their formulations, exhibit smoother surfaces and apparently less crystals of metformin HCl embedded on it. Notably, all micropellets present metformin HCl particles at their surfaces, although, embedded in the lipid matrix and not completely exposed. In the micropellets PMH<sub>50</sub> and PMHGT<sub>50</sub> the particles of metformin HCl are more prominently seen. This difference could rely on the fact that the material temperature needed to be maintained below 33 °C to avoid material agglomeration. Furthermore, the partial melting of the lipids on their surfaces did occur at the same extent for the other pellet formulations.

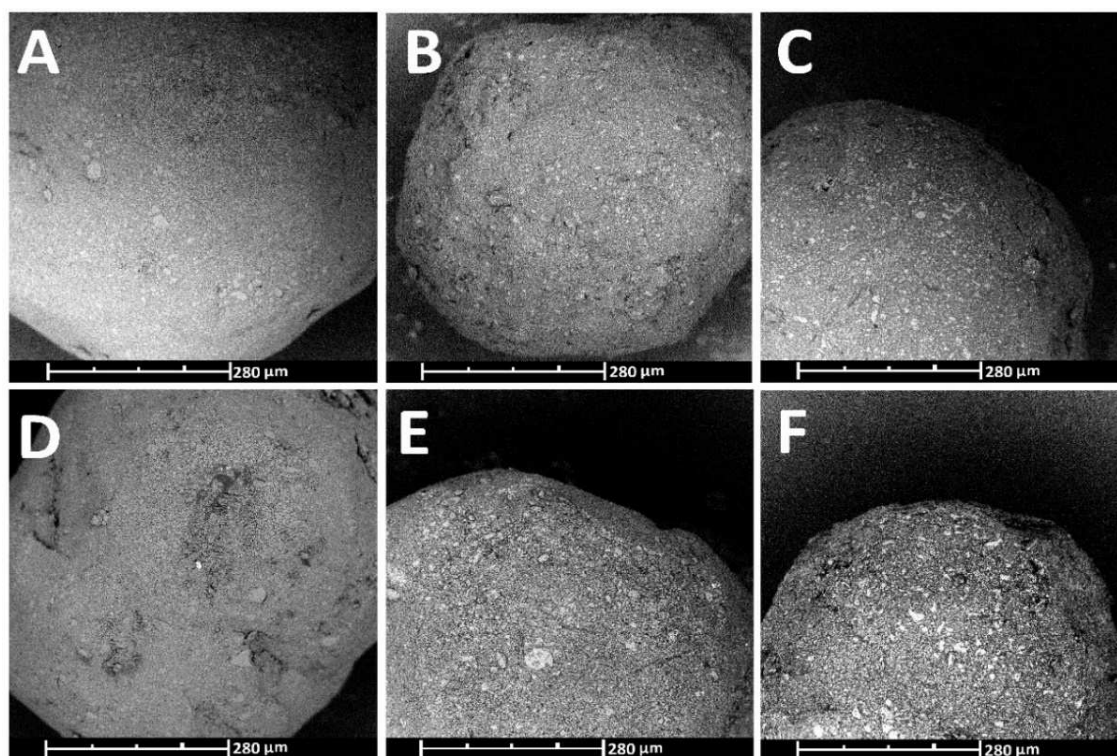


**Figure 4.34.** SEM photos of the lipid micropellets taken at 450x magnification (scale represents 280  $\mu\text{m}$ ): (A) PMH<sub>80</sub>, (B) PMH<sub>70</sub>, (C) PMH<sub>50</sub>, (D) PMHGT<sub>80</sub>, (E) PMHGT<sub>70</sub>, and (F) PMHGT<sub>50</sub>

The indirect flow indicators and packing properties of the micropellets are depicted in Table 4.15. CI below 15% and HF below 1.18 indicates good or excellent material flow properties. Low and quite similar HF values for the micropellets can be highlighted. HF describes the ratio between the tapped and bulk density of materials, and this relation depends on interparticular friction, size, and particle shape, among others. The micropellets particle size distribution showed similar values. HF values near 1.0 mean a more stable packing system and according to the results it is highly correlated to the spherical particle shape. Spheres present smaller contact

points between each other compared to irregular granules and occupied better the spaces due to an easy accommodation among the particles. This explains the small difference between their bulk and tapped densities. As HF and CI are based on this volume variation, they indicate that the pellets should exhibit high capability to flow freely (Carr, 1965; Thomas and Pourcelot, 1991; Aulton, 2013).

**Table 4.15** Micropellets characteristics: indirect flow properties

	Mean $\pm$ SD (n = 3)	
	HF	CI
PMH <sub>80</sub>	1.08 $\pm$ 0.00	7.76 $\pm$ 0.36
PMH <sub>70</sub>	1.05 $\pm$ 0.01	4.56 $\pm$ 0.80
PMH <sub>50</sub>	1.06 $\pm$ 0.01	5.79 $\pm$ 0.64
PMHGT <sub>80</sub>	1.08 $\pm$ 0.01	7.14 $\pm$ 1.08
PMHGT <sub>70</sub>	1.04 $\pm$ 0.01	3.52 $\pm$ 0.70
PMHGT <sub>50</sub>	1.07 $\pm$ 0.02	6.71 $\pm$ 1.34

HF = Hausner factor; IC = Carr's index. P = pellet; M = metformin HCl; H = hard fat; T = trimyristin; G = glyceryl distearate

#### 4.4.4. Shape Formation Mechanism

The lipid spheronization can be described by three phases, which are correlated with the material temperature and its properties. During the spheronization samples of around 1 g were collected and the particle size and AR were measured by Camsizer equipment. Figure 4.35a depicts the particle size distribution variation according to the material temperature during the spheronization of PMHGT<sub>70</sub>. The same results for the other lipid micropellets formulations are depicted in Annex III. The first phase which lasts around 1 min is characterized by low material temperature and a fast temperature increase. In this phase the extrudates are broken into small fragments due to the brittle properties of the extrudates (Figure 4.36). The second phase which lasts approximately 2 min is characterized by an initial decrease in the material temperature until the intended temperature is reached. This phase can be visualized in Figure 4.36 (2 to 5 min). In this phase there is a fast increase in the particle sizes until a certain peak that could be due for a short particle adhesion, as the lipids in the micropellets surfaces started to partially melt. At this phase a fast decrease in the AR of the particles occurs (Figure 4.35b).

The third phase is characterized by constant material temperature and constant increase in particle diameter. At 6 min process, the IR lamp temperature was adjusted to keep the material temperature constant. At this point, the particle size still increases, but in a slower velocity. This increase in particle diameter can be visualized in Figure 4.35. The edges of the extrudate start to deform and this material starts to move to the center of the particle.

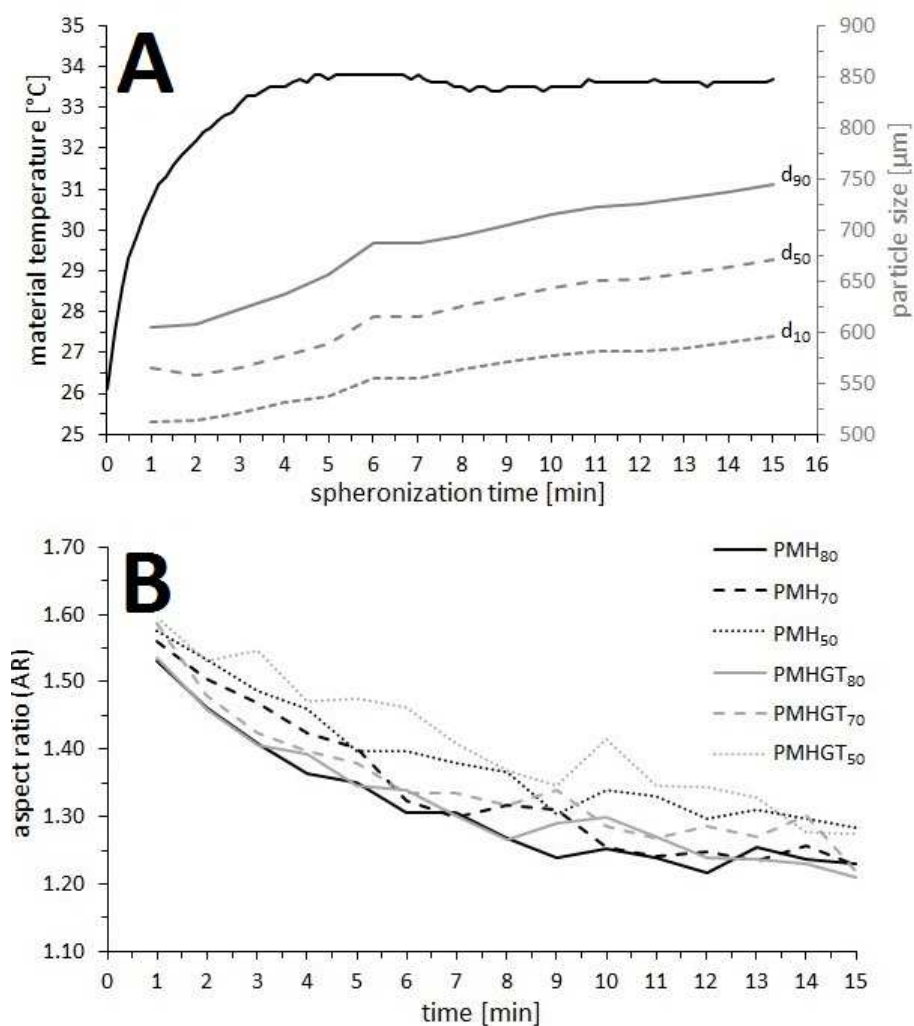


**Figure 4.35.** (A) Material temperature and particle size distribution variation (10, 50, and 90% quantiles) of PMHG<sub>70</sub>, (B) AR variation of the micropellets during spheronization. P = pellet; M = metformin HCl; H = hard fat; T = trimyristin; G = glyceryl distearate

This phenomenon can be well recognized by SEM images of the micropellets (Figure 4.37). Rowe (1985) describes these specific shape as “dumb-bell” form. The rounding process, from this specific shape until a spherical particle starts at around 6 min and takes until the end of the spheronization process. At this stage the AR of the micropellets decreases slowly and starts to become more constant among the particles.

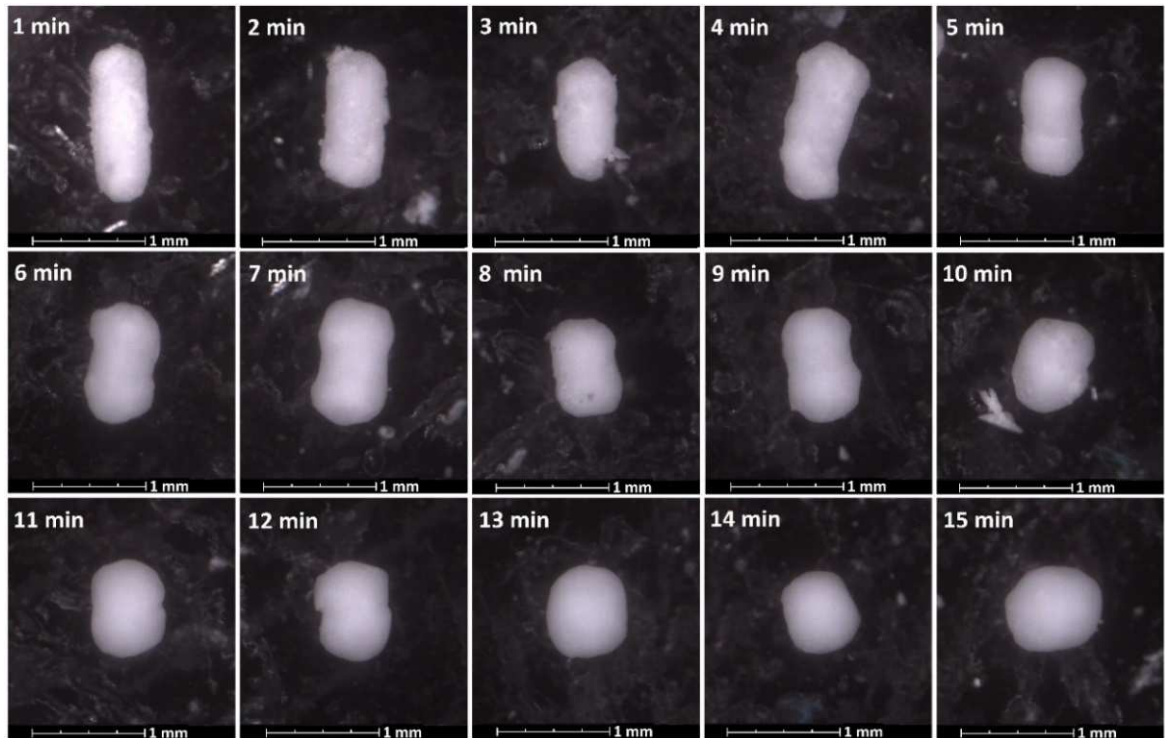


**Figure 4.36.** Particle shape changes during the spheronization process (PMHGT<sub>70</sub>). Optical microscope images taken at 120x magnification

The SEM images of the particle surface alteration during the spheronization for the pellet PMHGT<sub>70</sub> are presented in Figure 4.37. The shape and surface morphology modification of the micropellets PMH<sub>80</sub>, PMH<sub>70</sub>, PMH<sub>50</sub>, PMHGT<sub>80</sub>, and PMHGT<sub>50</sub> are shown additionally in Annex IV, V, VI, VII, and VIII, respectively. The morphological alteration starts around 3 to 4 min when the material temperature reaches 32-33 °C. The surface changes from a rough to a smoother surface. At this process time the lipids located at the surface partially start to melt. Under this condition, the materials at the extrudate edges, due to particle collisions and frictional forces are “compressed” and starts to deform in direction towards the center of the particle. As the heat at the edges is probably higher than in the center, the cylindrical form is kept slightly constant in the central region, and the softened material starts to form further two small connected spheres (Figure 4.37, 11 to 13 min). This material deforms until a spherical shape is achieved.



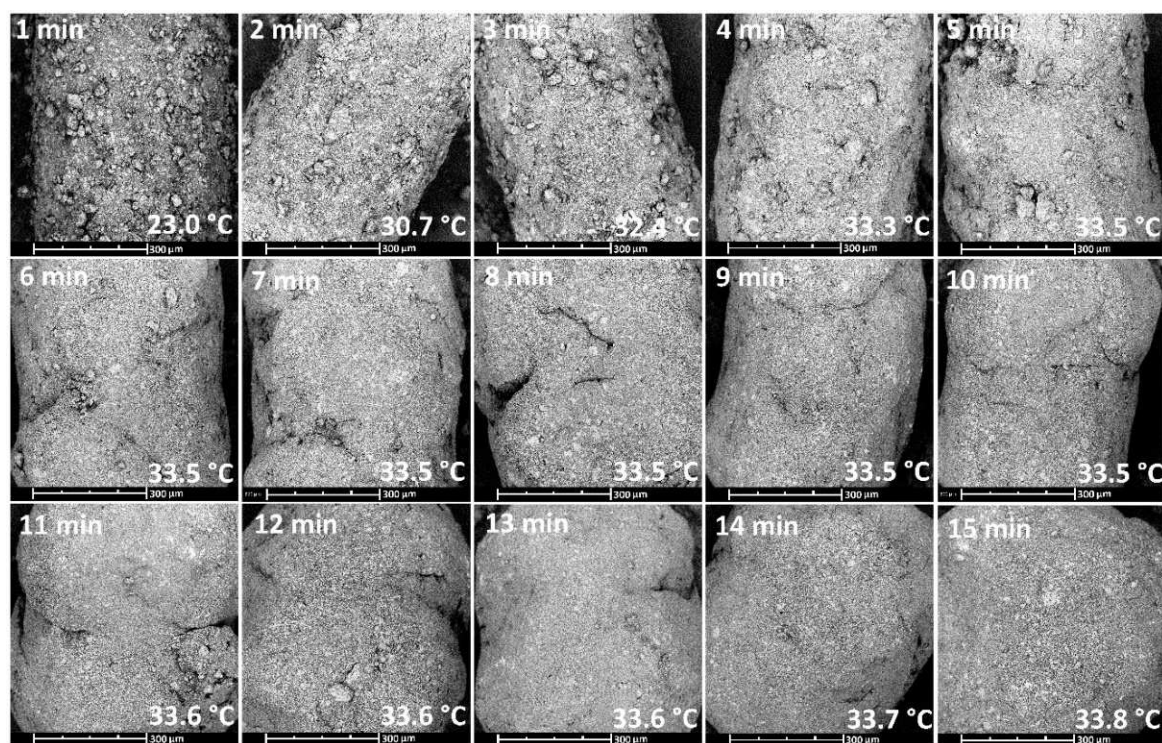


**Figure 4.37.** SEM photos of the surface modification and temperature during the spheronization process for the formulation PMHGT<sub>70</sub> taken at 450x magnification (scale represents 300  $\mu\text{m}$ )

#### 4.4.5. Thermal and Crystallographic Properties

DSC thermograms of the lipid micropellets are depicted in Figure 4.38. Two endothermic events are depicted, the first at 38-44  $^{\circ}\text{C}$  referent to the melting of the lipids, and the second around 230  $^{\circ}\text{C}$  relative to the melting of metformin HCl. The results are similar to those observed for the lipid extrudates. In comparison with the extrudates, the DSC results indicates no alteration on the thermal properties of the micropellets due to the temperature used in the spheronization step. Moreover, no differences are observed comparing the micropellets with each other. As expected, the heat of fusion of metformin increases with the increase of the API content. The same occurs with hard fat. However comparing the adjusted heat of fusion according to the amount of metformin in the micropellets, no alterations were observed (Table 4.16).

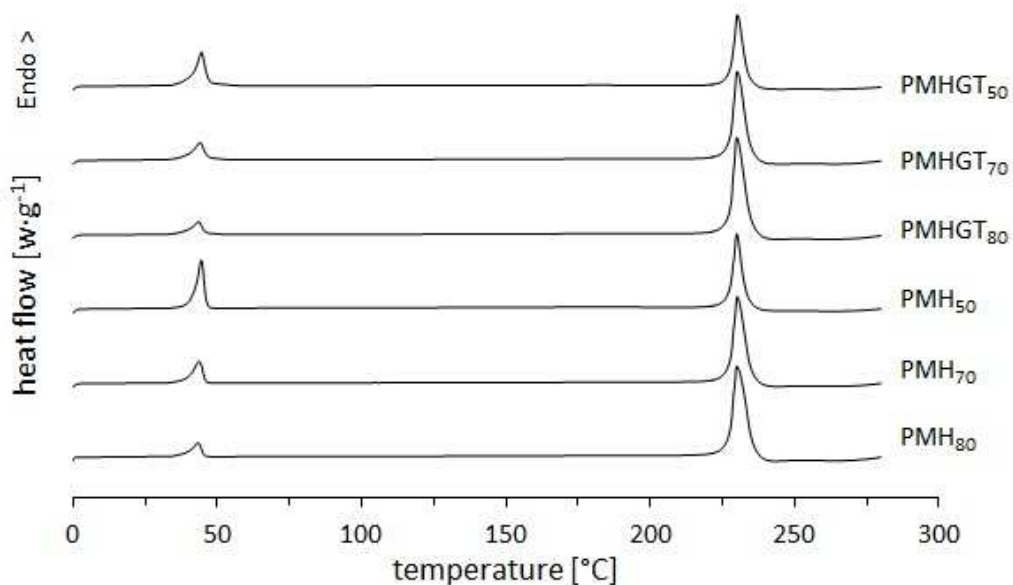


**Figure 4.38.** DSC thermograms of lipid micropellets (heating rate: 10 K·min<sup>-1</sup>). P = pellet; M = metformin HCl; H = hard fat; T = trimyristin; G = glyceryl distearate

**Table 4.16.** Thermal characteristics of the lipid based micropellets in comparison with starting materials

	Metformin HCl					
	Onset temp. (°C)		Peak temp. (°C)		Heat of fusion (J·g <sup>-1</sup> )	
	1	2	1	2	1	2
Metformin HCl	229.1	229.1	230.4	230.3	344.5	337.3
PMH <sub>80</sub>	228.3	228.2	230.6	230.7	349.0	341.5
PMH <sub>70</sub>	228.4	228.3	231.1	230.7	351.2	358.3
PMH <sub>50</sub>	227.7	227.7	230.8	230.8	351.0	347.4
PMHGT <sub>80</sub>	228.4	228.6	231.4	231.5	341.9	342.5
PMHGT <sub>70</sub>	228.2	228.5	231.2	231.0	343.5	349.7
PMHGT <sub>50</sub>	229.0	228.7	231.3	231.3	362.6	363.3

Figure 4.39 depicts the XRPD diffractograms of the micropellets and metformin HCl. No differences in the crystallographic pattern of metformin HCl are observed in the micropellets as no shifting nor new peaks are present in the micropellets diffractograms. The peaks referent to hard fat are also noticed in the region between 20 and 22.5 degrees. The phenomenon observed for the powder mixture that led to the absence of a peak of metformin in the region between 25 to 26 degrees is not observed, which indicates that this phenomenon does not occur during the spheronization.

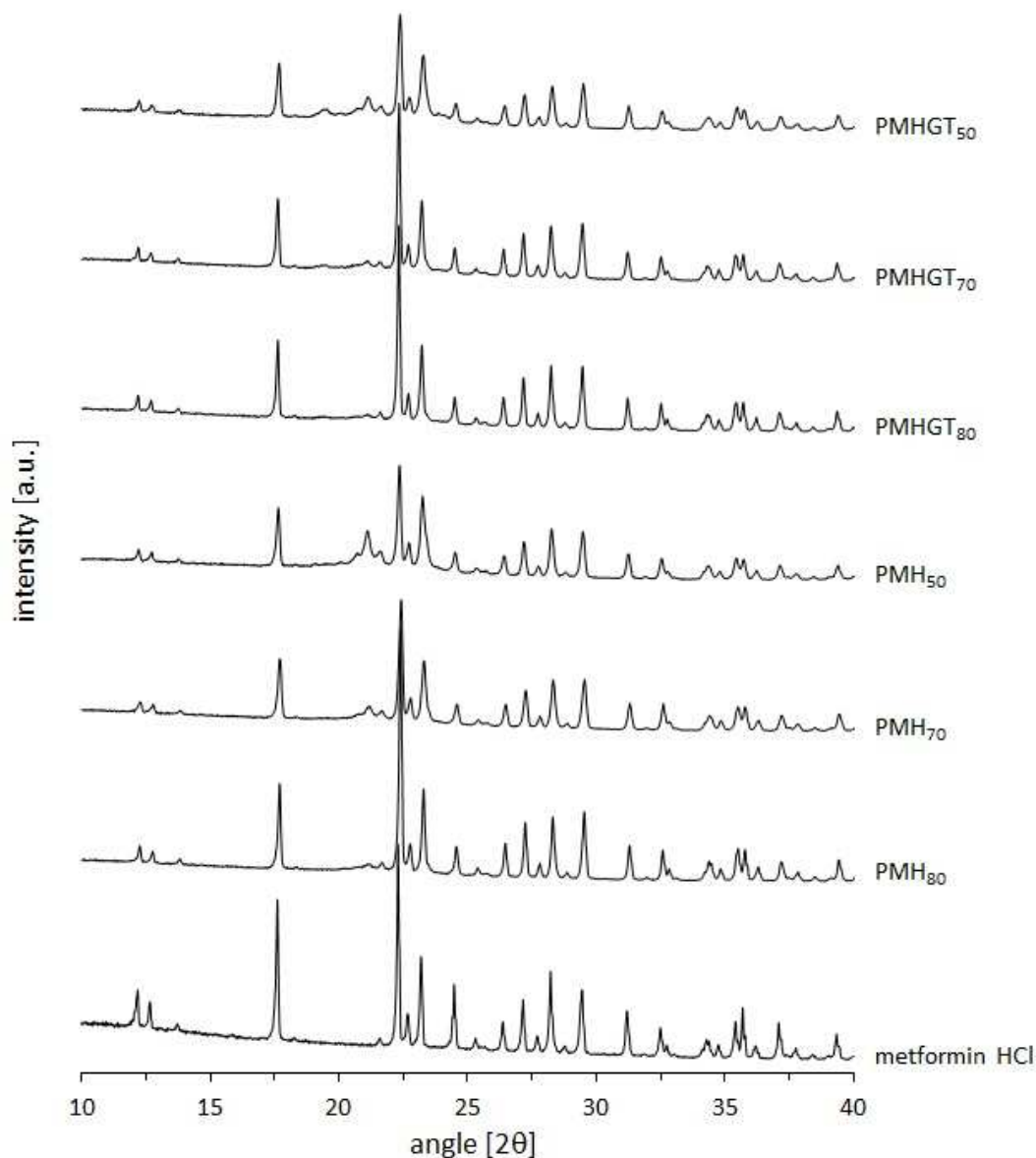


**Figure 4.39.** Diffractograms of the lipid micropellets and metformin HCl powder (increment of 0.02 degrees, reading time of 1 s per point). P = Extrudate, M = Metformin HCl, H = hard fat, T = trimyristin, G = glyceryl distearate

#### 4.4.6. Drug Content of Lipid Micropellets

The metformin HCl content in the lipid micropellets is shown in Table 4.17. A drug content increase around 5% (w/w) is observed. As the drug content increases compared to original extrudates, it is possible to assume that the loss of fines during the first phase of the spheronization process could be the main reason. However, this observed variation is within the limits of 85 to 115% of the uniformity content of single-dose preparations defined on Ph. Eur. (2014) (Section 2.9.6, test B).



**Table 4.17.** Metformin HCl content in the lipid based micropellets

	Mean $\pm$ SD (%; n = 10)					
	PMH <sub>80</sub>	PMH <sub>70</sub>	PMH <sub>50</sub>	PMHGT <sub>80</sub>	PMHGT <sub>70</sub>	PMHGT <sub>50</sub>
Drug content	83.53 $\pm$ 1.73	75.13 $\pm$ 1.51	53.36 $\pm$ 3.36	85.42 $\pm$ 1.67	74.69 $\pm$ 2.80	55.07 $\pm$ 3.59

P = pellet; M = metformin HCl; H = hard fat; T = trimyristin; G = glyceryl distearate. 80, 70, and 50: amount of metformin HCl in the pellet formulation

#### 4.4.7. Drug Dissolution Studies of Lipid Micropellets

The drug release profiles of the lipid micropellets are depicted in Figure 4.40. The micropellets based on 20 and 30% (w/w) of lipids present a fast drug release. Their profiles can be classified as immediate-drug release according to the definition in the USP 34 (2011) since they release 85% (w/w) of metformin HCl in around 10 and 22 min (PMH<sub>80</sub> and PMHGT<sub>80</sub>, respectively); 36 and 54 min (PMH<sub>70</sub> and PMHGT<sub>70</sub>, respectively). Likewise, the complete drug release (100%; w/w) was achieved after 20 to 25 min to the micropellets based on 20% (w/w) of lipids, and 58 to 80 min to the micropellets based on 30% (w/w) of lipids.

On the other hand, as previously reported for the lipid extrudates, the increase in the amount of lipids to 50% (w/w) led to a complete alteration on the drug release kinetic. The micropellets PMH<sub>50</sub> and PMHGT<sub>50</sub> showed a Higuchi kinetic, characterized by a short burst release followed by a constant and slower drug release. This kinetic was confirmed by plotting the amount of API commutative released against the root of the time (Siepmann and Peppas, 2011). After 2 hours the released metformin HCl reached around 64 to 58% (w/w), respectively.

As already discussed in the section 4.3.6 the dissolution of high soluble APIs from triglyceride matrices is completely diffusion controlled since the matrix stays intact after the release of the drug and is therefore strongly influenced by the matrix formulation (Reitz *et al.*, 2008; Windbergs *et al.*, 2009c). Therefore the amount of lipids in the formulations influence the matrix amount and therefore the metformin HCl release kinetic.

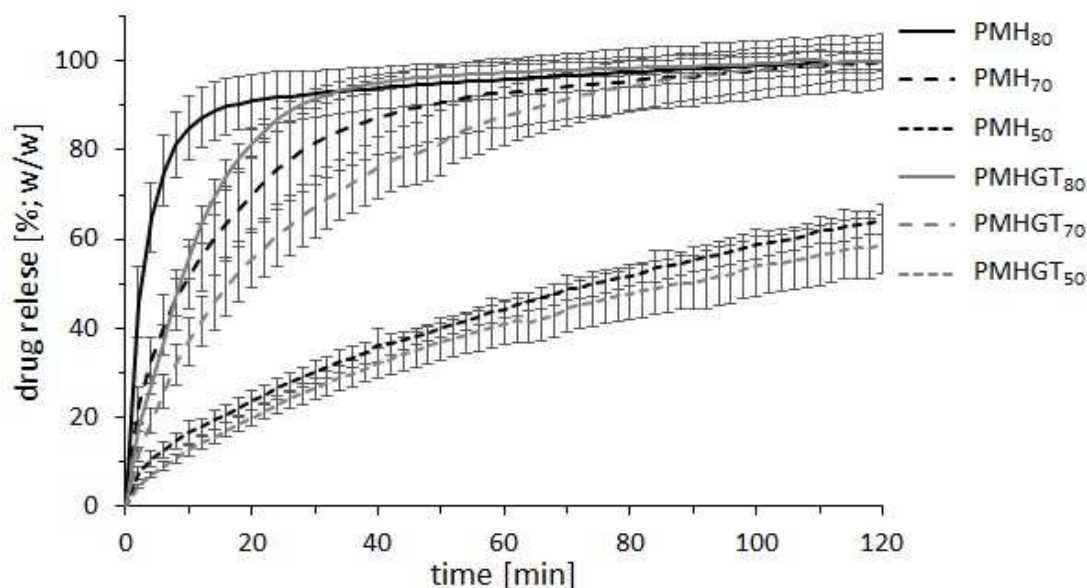


**Figure 4.40.** Drug release profiles of the lipid micropellets. Dissolution media: 900 mL purified water containing 0.001% (w/w) polysorbate 20, temperature of  $37\text{ }^{\circ}\text{C} \pm 0.5$ , 150 rpm, basket method,  $\lambda = 232\text{ nm}$  (mean  $\pm$  SD,  $n = 6$ ). P = pellet; M = metformin HCl; H = hard fat; T = trimyristin; G = glyceryl distearate

According to Krause (2008), the lipid spheronization process represents a self-coating mechanism, which occurs due the presence of low melting lipids in the extrudate formulations. The melting of the lipids during the process generates a thin lipid layer at the pellet surface. This mechanism led to an alteration on the drug release pattern. Although no complete coating layer was observed by SEM for the micropellets (Figure 4.34, see page 74), since particles of metformin HCl were observed fully embedded in the lipid matrix. However, the spheronization altered the morphology of their surfaces, which could lead to an alteration on the drug release (the reason of the use of this methodology to obtain taste-masked pellets). Metformin HCl release comparison between the micropellets and the extrudates are shown in Figure 4.41.

Although a small decrease in the drug release is observed for almost all the micropellets, the profiles can be considered similar since the amount of metformin HCl released did not change significantly. On the other hand, the micropellets PMH<sub>50</sub> and PMHGT<sub>50</sub> showed a decrease in the drug release of metformin HCl. These micropellets release around 19% and 39% (w/w) less API compared to the extrudates, after 120 min, respectively. Interestingly, for these both specific formulations, the presence of glyceryl distearate and trimyristin exert a stronger influence on the drug release of metformin HCl after the spheronization process compared to the micropellets based on hard fat only.

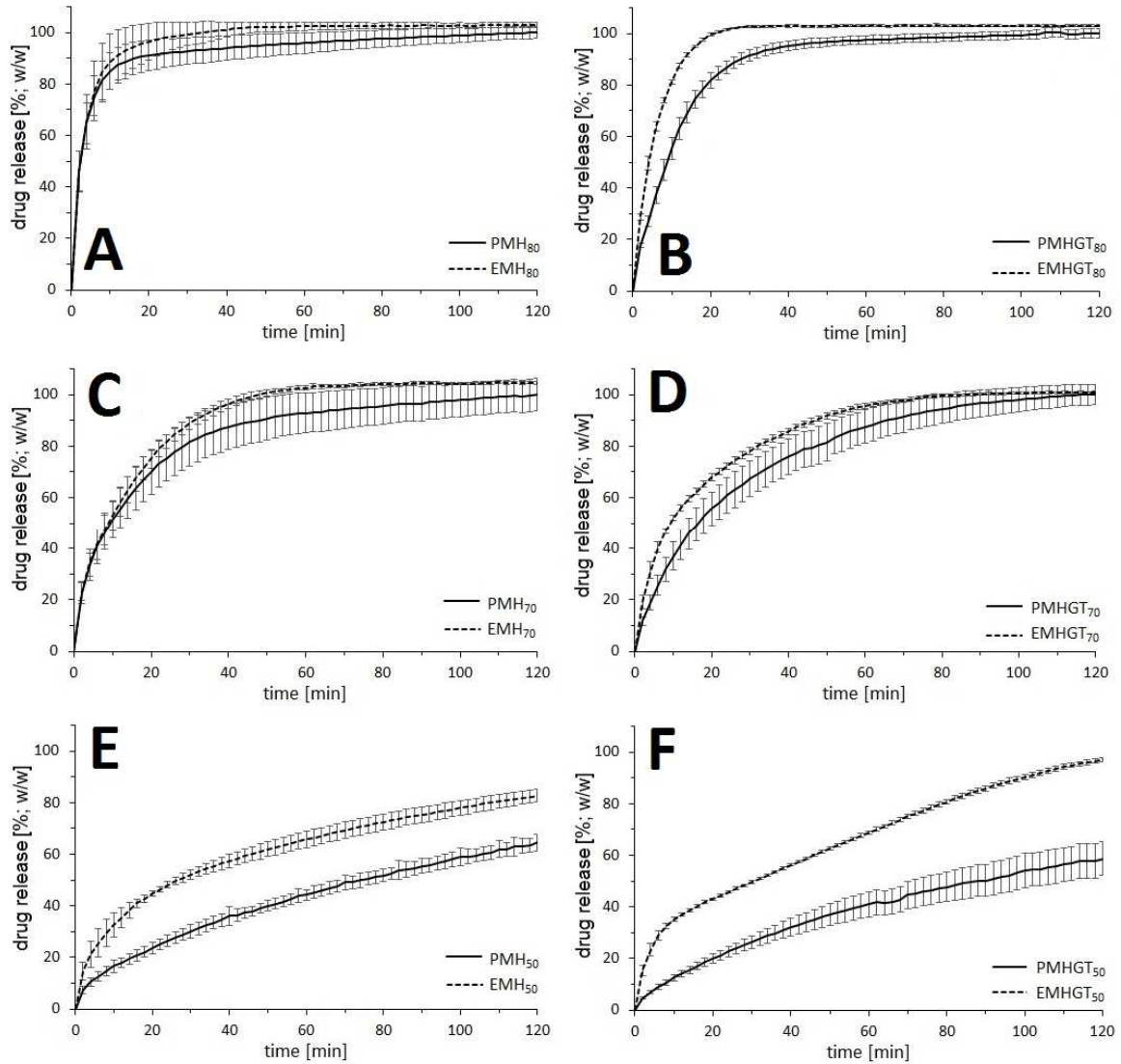


**Figure 4.41.** Drug release comparison between lipid based micropellets and their original extrudates: (A) MH<sub>80</sub>; (B) MHGT<sub>80</sub>; (C) MH<sub>70</sub>; (D) MHGT<sub>70</sub>; (E) MH<sub>50</sub>; and (F) MHGT<sub>50</sub>. Dissolution medium: 900 mL purified water containing 0.001% (w/w) polysorbate 20, temperature: 37 °C ± 0.5, 150 rpm, basket method,  $\lambda = 232$  nm (mean ± SD, n = 6). E = extrudate; P = pellet

Although no self-coating mechanism was observed after the spheronization, an alteration of the morphology of the micropellets surface compared to its interior needs to be highlighted. This is shown for micropellet PMH<sub>80</sub> in Figure 4.42. Differences of the external to internal structure/morphology can be distinguished and could also play an important role in the drug release kinetics.

Furthermore, compared to pellets, extrudates are cylindrically shaped and exhibit complete uncovered surfaces at its two base areas. The dissolution of the drug is enhanced at these uncovered surfaces compared to covered surfaces, where the drug has to diffuse through the thin lipid layer before getting into solution (Michalk *et al.*, 2008; Reitz *et al.*, 2008). As the micropellets present a more regular surface compared

to the extrudates, it could influence the differences observed for the formulations based on 50% (w/w) of lipids, since a bigger lipid matrix is present

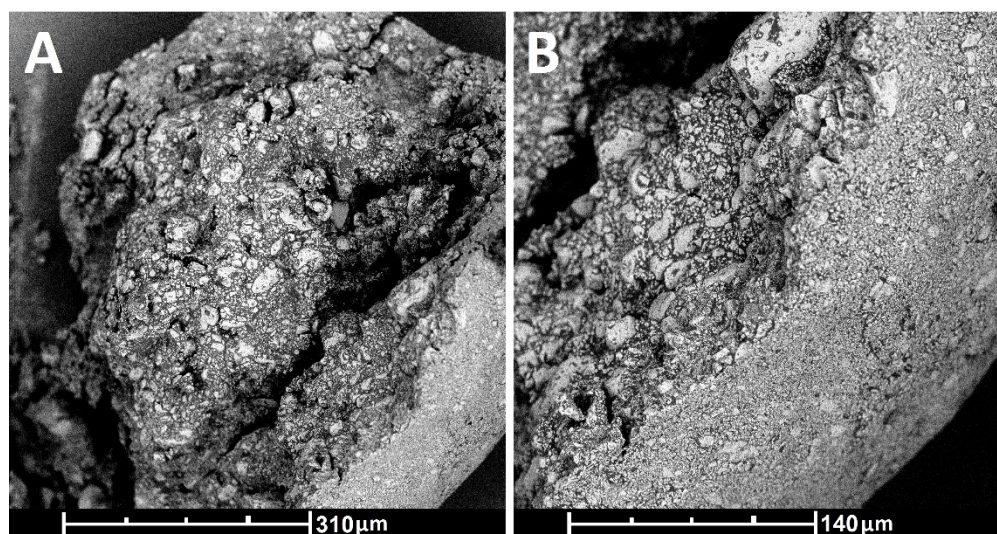


**Figure 4.42.** SEM images of lipid pellet cuts (PMH<sub>50</sub>): taken at (A) 420x and (B) 920x magnification (scale represents 310 and 140  $\mu\text{m}$ , respectively)

Another factor that could impact the observed small drug release alterations for the other micropellets is related to the different dimensions of the extrudate and pellets. Indeed larger dimensions will lead to longer diffusion pathways. In this case, water needs more time to penetrate the system, which delays drug dissolution, pore creation and drug diffusion. Smaller matrixes such as micropellets have shorter lengths of the diffusion pathways (Rosiaux *et al.*, 2014). However, it is stated that the effect of device dimension on the entire drug release kinetics becomes minor with drugs being extremely water soluble since the API require very little water to be completely dissolved and released (Rosiaux *et al.*, 2014). This could explain the small difference on the drug release of the pellets compared to the extrudates.

The SEM images of the micropellets after the drug release assay are depicted in Figure 4.43. A highly porous structure can be seen in all the micropellets. However, the pellets based on lower amounts of lipids seem to present higher diameter pores, which corroborate the drug release results observed. The images also support the drug release mechanism, since the lipid matrix is kept intact after the dissolution of the API.

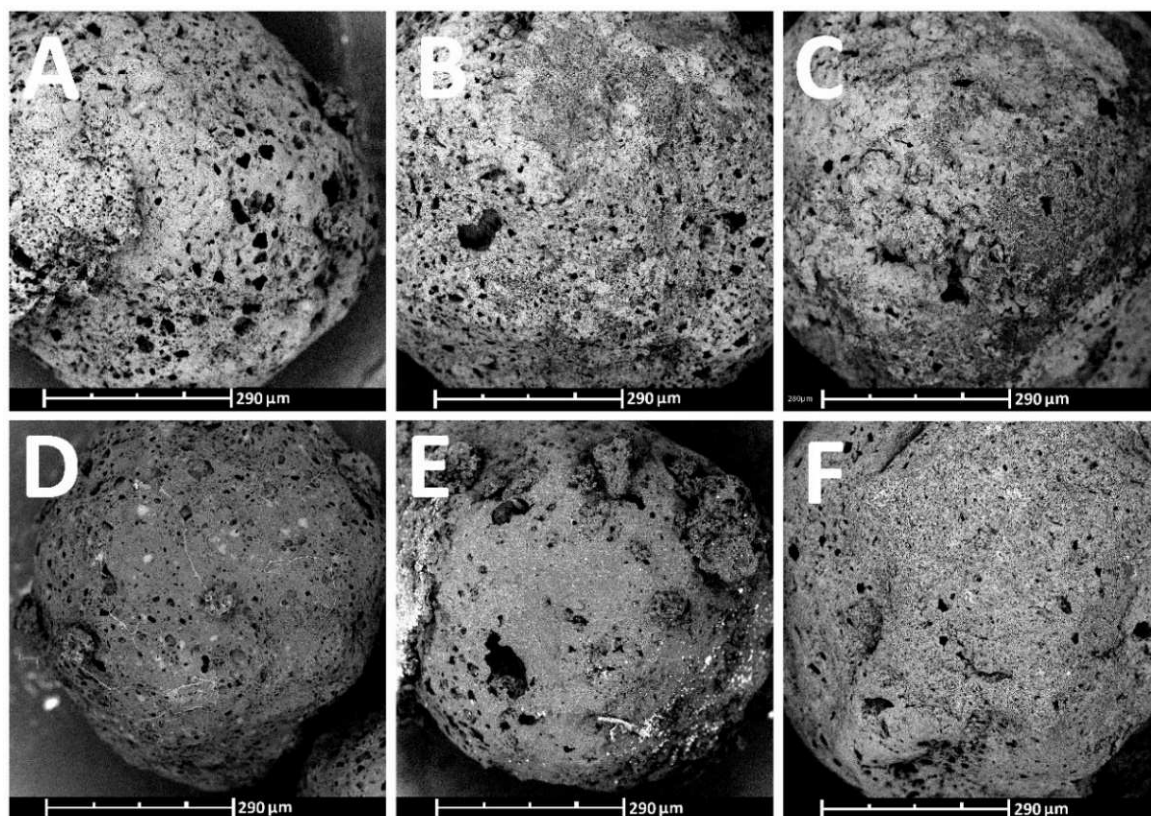


**Figure 4.43.** SEM images of the lipid micropellets after the dissolution assay, taken at 450x magnification (scale represents 290  $\mu\text{m}$ ): (A) PMH<sub>80</sub>, (B) PMH<sub>70</sub>, (C) PMH<sub>50</sub>, (D) PMHGT<sub>80</sub>, (E) PMHGT<sub>70</sub>, and (F) PMHGT<sub>50</sub>

According to a former FIP/AAPS guideline, a drug release  $\leq 10\%$  within the first 5 min of dissolution is proposed as indicative of a successful taste-masking (Siewert *et al.*, 2003). Although it is obvious that this specification is not based on *in vivo* investigations and is mainly influenced by the taste recognition of the compounds, an investigation of metformin HCl release within this period was performed using an UV probe. The rational use of UV spectroscopy to determine taste-masking effects is based on two assumptions: a substance needs to be dissolved to cause an unpleasant taste, and in most cases the unpleasant taste of the drug formulation is related to the included API (Pein *et al.*, 2014). The first 5 min drug release assay results are depicted in Figure 4.44. The micropellets based on hard fat only showed similar results to previous dissolution studies, where the increase of the amount of lipid led to a decrease in the drug release of metformin HCl.

The micropellets containing glyceryl distearate and trimyristin showed a different behavior in this time period. Small differences in the drug release kinetic are observed due to the increase of the lipid amount comparatively to the micropellets based on hard fat only. Similar observations were described by Krause *et al.* (2009), who reported the influence of these lipid binders on the drug release kinetic of a highly soluble API. The micropellets PMHGT<sub>80</sub> showed not more than 40% (w/w) of metformin HCl released after 5 min, while PMH<sub>80</sub> releases around 90% (w/w) of the



API. On the other hand, the micropellets PMHGT<sub>70</sub> and PMHGT<sub>50</sub> showed similar drug releases profiles within these first 5 min, releasing 19.6 and 15.9% (w/w) of metformin, respectively. These previous results could indicate that the spheronization of the formulations based on the ternary lipid mixture could lead to micropellets presenting taste-masked properties even at high drug loads compared to formulations based on only hard fat.

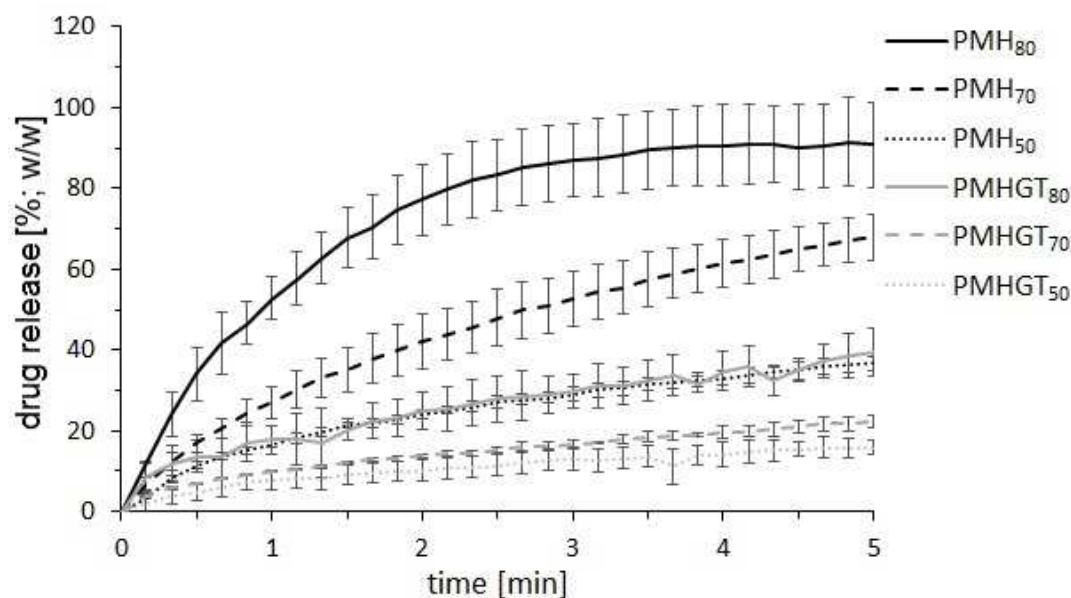


**Figure 4.44.** In-line lipid micropellets drug release by UV/Vis probe equipment: Dissolution media: 900 mL purified water containing 0.001% (w/w) polysorbate 20, temperature of  $37\text{ }^{\circ}\text{C} \pm 0.5$ , 150 rpm, paddle method using a sinker,  $\lambda = 232\text{ nm}$  (mean  $\pm$  SD,  $n = 3$ ). P = pellet; M = metformin HCl; H = hard fat; T = trimyristin; G = glyceryl distearate

This conclusion is supported by the comparison of metformin HCl release from the micropellets and their original extrudates (Figure 4.45). A clear difference in the metformin HCl release is seen in the formulations based on the ternary lipid mixture (Figure 4.45a, b, and c) compared to the extrudates and compared to the formulations based on hard fat only. According to Siepmann and Siepmann (2011), water penetration into the lipid system might play a major role for the control of drug release. The hypothesis could rely on the wettability of the micropellets. Since the lipid matrixes presents different compositions and lipid amount and glyceryl and trimyristin present different lipophilicity compared to hard fat, these factors could influence the water penetration on the pellet (Koennings *et al.*, 2007). Further investigations are needed to elucidate the results and their relation with the pellets wettability. Interestingly, after 5 min the drug release profile of the micropellets based on hard fat and based on the ternary lipid mixture become quite similar (Figure 4.42, see page 84) which could be the influence of the polysorbate 20 present in the dissolution media.

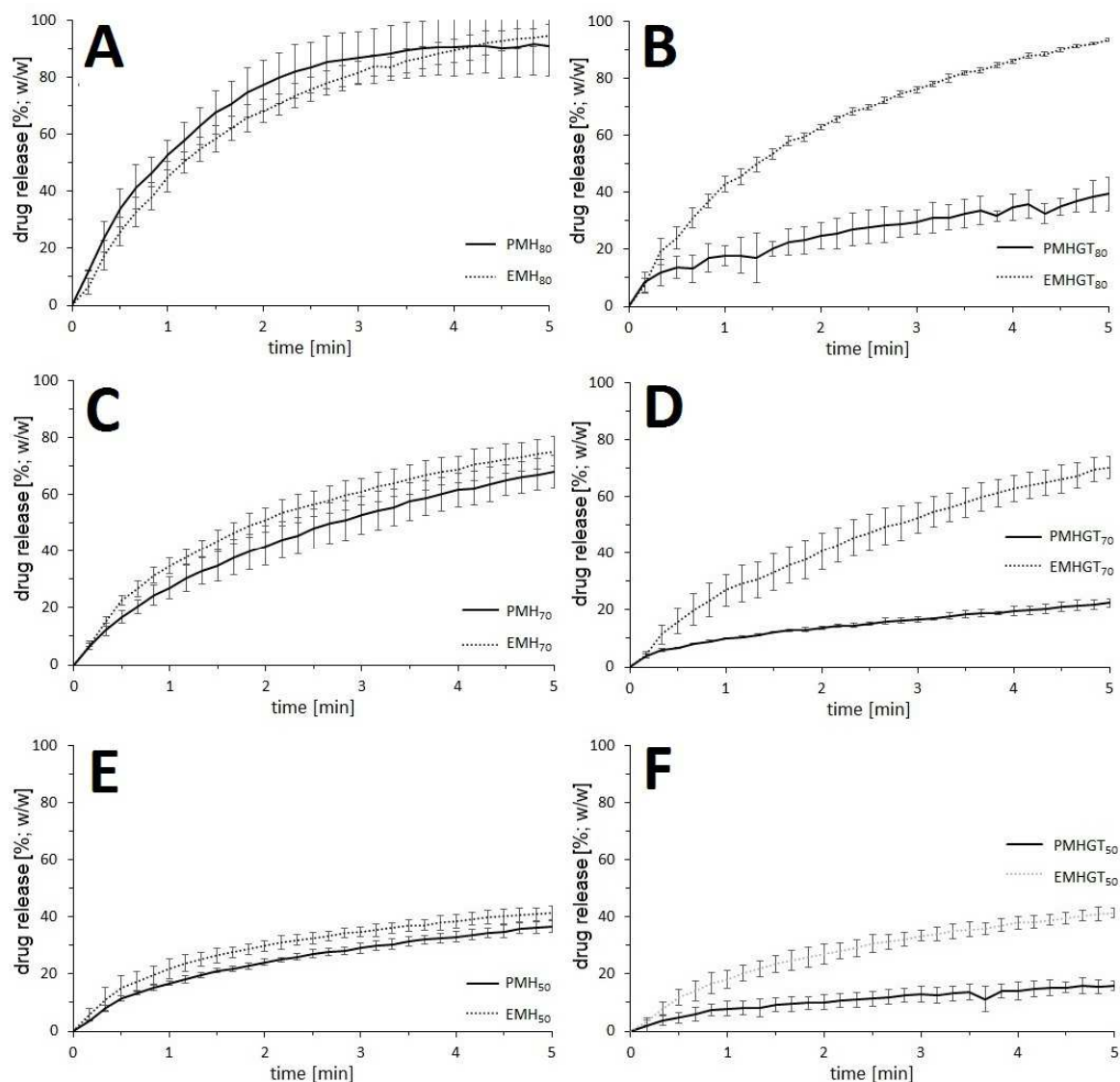


**Figure 4.45.** Drug release comparison between lipid based micropellets and their original extrudates: (A) MH<sub>80</sub>; (B) MHGT<sub>80</sub>; (C) MH<sub>70</sub>; (D) MHGT<sub>70</sub>; (E) MH<sub>50</sub>; and (F) MHGT<sub>50</sub>. E = extrudate; P = pellet. Dissolution medium: 900 mL purified water containing 0.001% (w/w) polysorbate 20, temperature: 37 °C ± 0.5, 150 rpm, basket method using an UV probe,  $\lambda = 232$  nm (mean ± SD, n = 3)

## 4.4.8. Electronic Tongue Investigations

### 4.4.8.1. Electronic Tongue Calibration

There is no report in literature about the evaluation of the pure drug metformin HCl or dosage forms containing this API using electronic sensing systems. To evaluate the response of the used sensor set of the Insent system to metformin HCl, a previous “calibration” was performed. According to Woertz *et al.* (2010), the results of an electronic tongue investigation need to be interpreted in relation to a preliminary performed calibration in order to assess the taste information of the substance. The

relative sensor responses to different metformin HCl concentrations are presented in Figure 4.46. Log-linear ranges of the log of the metformin HCl concentration and the relative sensor responses were observed in the range of 0.5 to 1.5 mg·mL<sup>-1</sup>. The value of 0.5 mg·mL<sup>-1</sup> showed to be the limit of detection for the most of the sensors. The sensors SB2AE1 and SB2AC0 showed the lowest limits of determination to the variation of metformin HCl concentration (Table 4.18) compared to the other sensors.

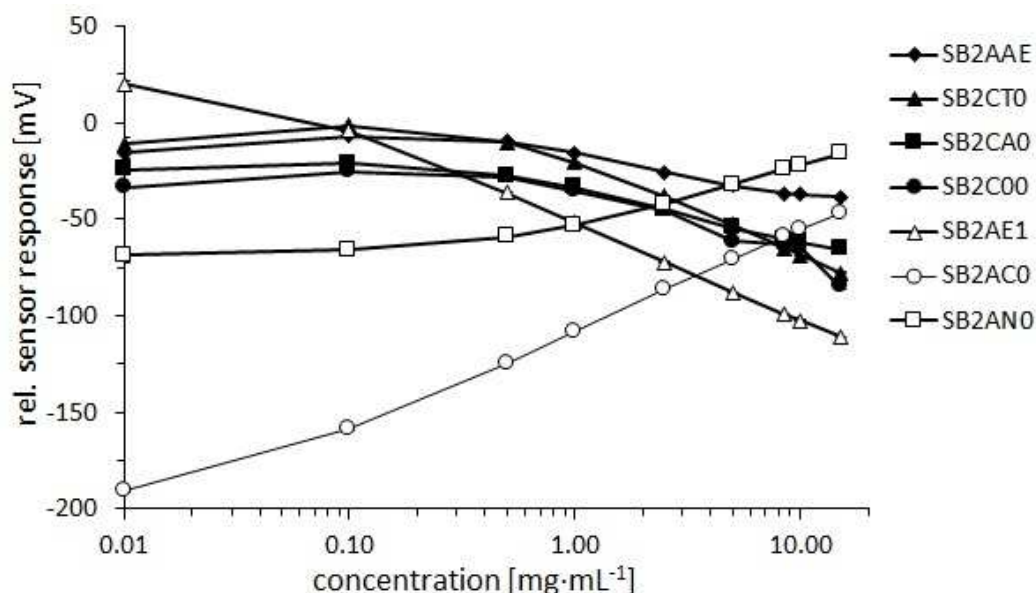


**Figure 4.46.** Sensor responses to different concentrations of metformin HCl ( $n = 3$ , mean  $\pm$  SD)

Both sensors showed a linear range starting at lower API concentrations. High correlation coefficients were obtained for almost all sensors. The sensor SB2AN0, which according to the equipment manufacturer provides information about bitterness of cationic and neutral substances, presented also a good response to the calibration. Moreover, the slope of calibration curves for the sensors relative bitterness responses (SB2AN0 and SB2AC0) was positive, whereas a negative slope was exhibited by the remaining sensors. These results could provide information about further taste alterations of formulations containing metformin HCl and support the reports about the unpleasant taste of this API (Mohapatra *et al.*, 2008a; Bhoyar and Biyani, 2010; Gandhi *et al.*, 2010; Bhoyar *et al.*, 2011; Mostafavi *et al.*, 2014).



**Table 4.18.** Data evaluation of sensor responses to metformin HCl within the linear range

Sensor	Concentration range of linearity (mg·mL <sup>-1</sup> )	Sensor sensitivity (mV)	Slope of the regression line	Coefficient of determination (R <sup>2</sup> )
SB2AAE	0.5 – 1.5	28.74	-8.94	0.9875
SB2CTO	0.5 – 1.5	67.48	-20.09	0.9960
SB2CA0	0.5 – 1.5	38.18	-11.73	0.9965
SB2C00	0.5 – 1.5	57.10	-15.03	0.9371
SB2AE1	0.1 – 1.5	106.68	-21.57	0.9994
SB2AC0	0.01 – 1.5	143.76	20.47	0.9903
SB2AN0	0.5 – 1.5	42.96	12.95	0.9938

A multivariate data analysis (MVDA) of the information descendant from the calibration, regarding the role set of sensors, was performed and the obtained PCA map is depicted in Figure 4.47a. The first principal component (PC1) shows 96.2% of the data information on the horizontal axis. The results showed that the set of sensor is able to efficiently discriminate between differences in the amount of metformin HCl. Moreover, the PCA map also depicts the influence of the concentration linear range since the samples containing 1 and 10 mg of metformin HCl (0.01 and 0.1 mg·mL<sup>-1</sup>, respectively) showed a difference position pattern in the second principal component (PC2). No data outliers were detected by the DModX and Hotelling's T<sup>2</sup> test ( $\alpha = 0.05$ ).

The loading plot of the set of sensors in the calibration is depicted in Figure 4.47b. It allows a quantitative and visual analysis of relations between the sensors and their importance. Regarding the first principal component (PC1), the sensors SB2AC0 and SB2AN0 are correlated (positive increase in the sensor response), however the sensor SB2AC0 presents more importance and more influence on the results of the PCA regarding the increase of metformin HCl amount. The loading plot corroborate the values of the electronic tongue calibration presented in Table 4.18, which also indicate the sensors SB2AC0 as the presenting highest sensitivity to metformin HCl.

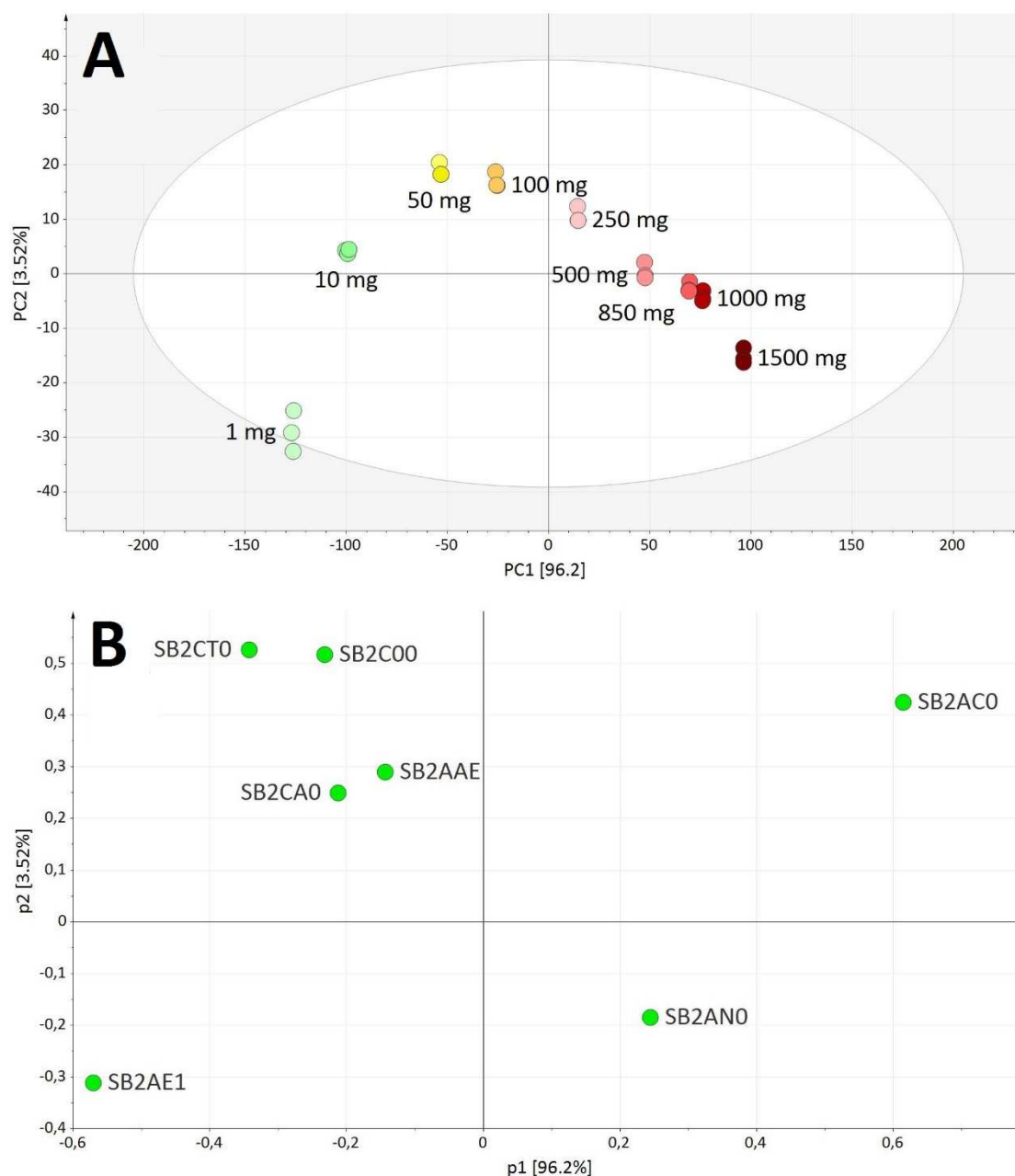


**Figure 4.47.** (A) Principal component analysis representing sensor responses to metformin HCl and (B) loadings plot of the set of sensors (data was mean centered)

#### 4.4.8.2. Electronic Tongue Investigation of Lipid Based Micropellets

The micropellets based on hard fat lonely (PMH<sub>80</sub>, PMH<sub>70</sub>, and PMH<sub>50</sub>) and the micropellets based on the ternary lipid mixture (PMHGT<sub>80</sub>, PMHGT<sub>70</sub>, and PMHGT<sub>50</sub>) were evaluated separately by an electronic tongue. To investigate the taste-masking properties of these micropellets, samples containing 500 mg of metformin HCl (625 mg, 714 mg, and 1000 mg for pellets based on 20%, 30%, and 50% of lipids, respectively) were stirred in 80 mL of purified water for 30 and 60 s. These times were suggested as more adequate to investigate taste-masking properties of dosage forms intended to be placed in the oral cavity (Pein *et al.*, 2014).

Furthermore, as the lipid micropellets were employed to the development of ODTs, these time intervals are consistent to the defined disintegration time of such a tablets in the oral cavity (USP 34, 2011; Ph. Eur., 2014).

The PCA representing sensor responses to the micropellets PMH, metformin HCl, and drug-free pellets based on hard fat is depicted in figure 4.48a. The PC1 contains 90.5% of the MVDA information, therefore, the horizontal distance differences among the samples contains the most important data of the set of relative sensor responses to the investigated formulations. The pure metformin HCl is positioned on the left corner while the drug-free formulation on the right corner, indicating a complete different response from the set of sensor. The loading plot of the set of sensors regarding the MVDA is shown in Figure 4.48b. Similarly to the calibration step, as metformin is the bitter taste sample, it results in more responses from the sensors SB2AN0 (bitterness sensor 2) and SB2AC0 (bitterness sensor 1), while the drug-free formulation is located in the opposite side to these sensors. Interestingly, the drug free sample (hard fat) promote a positive response of the sensors SB2AE1 and SB2CT0, referent to astringency and saltiness, respectively. This result indicate that hard fat itself presents an intrinsic response by the set of sensor. Taste of hard fat was reported by Suzuki *et al.* (2004) based on the recognition by human volunteers showing a low but recognized taste intensity.

The lipid micropellets PMH<sub>80</sub> is positioned near to the metformin HCl sample in the PCA map and a small difference between the samples of 30 and 60 s is observed. This effect results from the fast drug release showed by this formulation, which released more than 35% (w/w) of metformin HCl after 30 s and around 60% (w/w) after 60 s (Figure 4.44, see page 86). The results indicate that this formulation does not present taste-masking properties, although a small decrease in the sensor responses was observed. The micropellets PMH<sub>70</sub> are positioned in the central part of the PCA map, indicating a sensor response alteration compared to pure metformin HCl. The MVDA results showed that, similarly to PMH<sub>80</sub>, no great difference between the 30 and 60 s is perceived.

The PC2 contains 5.69% of the MVDA information. In the vertical direction (y-axis) a small difference between these samples can be highlighted. The formulation PMH<sub>50</sub> showed the highest proximity to the drug-free pellets indicating the most taste-masked formulation among them micropellets based on hard fat lonely. This results are in agreement with the drug release investigations, since a relation between the lipid amount in the micropellets and their drug release kinetic was found. However, PMH<sub>70</sub> (after 30 s of stirring) and PMH<sub>50</sub> are positioned in the same quadrant on the PCA map, indicating that these samples are positively correlated, which could mean a similar sensor response to these samples and, therefore, relative similar taste-masked properties. The amount of micropellets used to prepare the samples was calculated to

contain 500 mg of metformin HCl, the same amount used to prepare the reference metformin HCl sample.

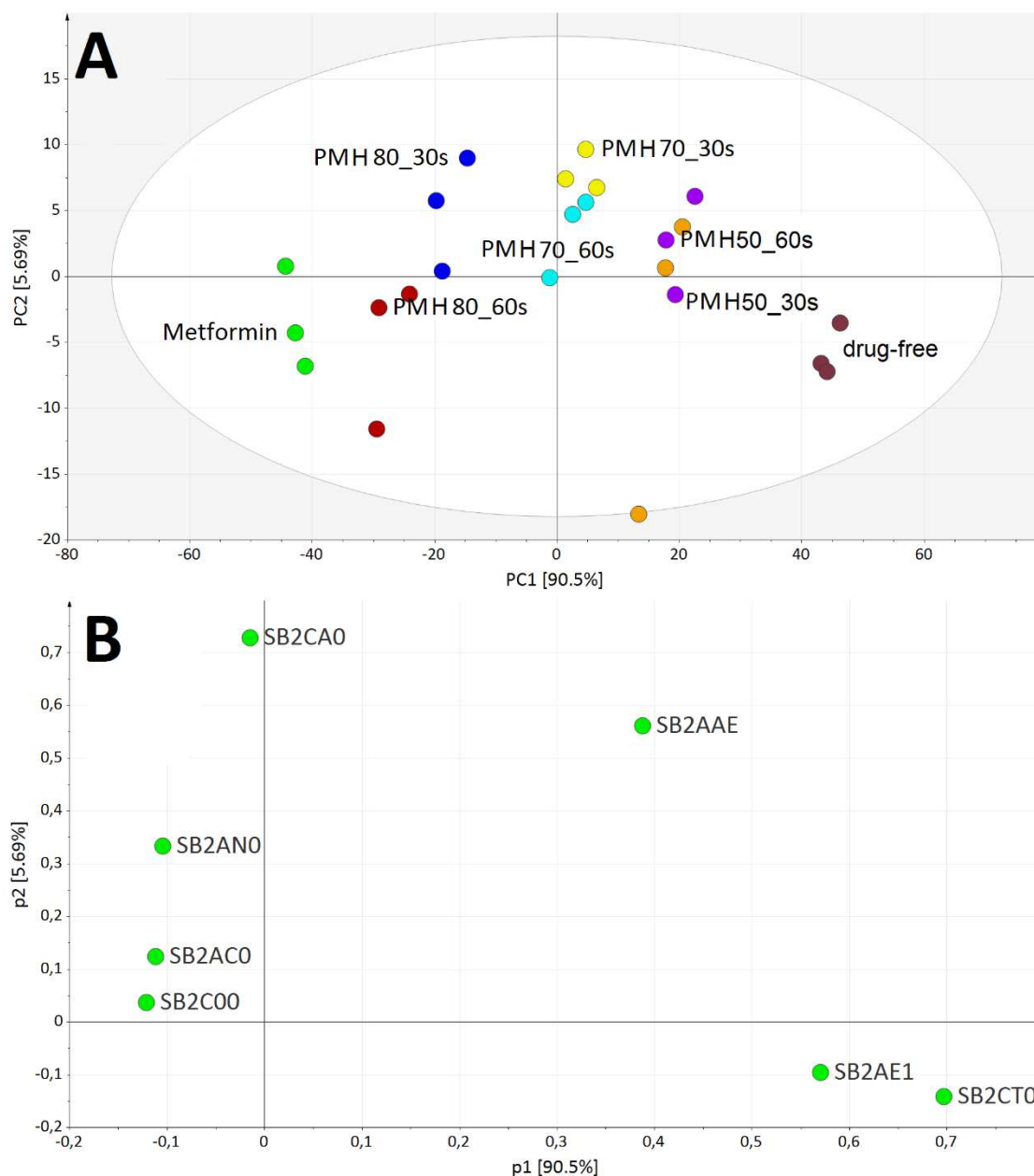


**Figure 4.48.** Multivariate data analysis of metformin HCl lipid micropellets based on hard fat only (PMH) performed by electronic tongue: (A) PCA representing sensor responses to the micropellets and (B) loadings plot of set of sensors (data was mean centered)

The PCA representing sensor responses to the micropellets PMHGT, metformin HCl, and drug-free pellets based on hard fat, glyceryl distearate, and trimyristin is depicted in figure 4.49a. The PC1 includes 80.0% of the MVDA information and the PC2 contains 9.88%. For this assay the PC2 also contains important information about the set of sensor responses to the samples and therefore need to be considered. A similar loading plot is generated (Figure 4.49b) compared to the observed in the MVDA of PMH micropellets (Figure 4.48b), showing a similar correlation between

the bitter taste of metformin and the sensors SB2AC0 and SB2AN0. Interestingly, the drug-free formulation promoted a higher response by the sensor SB2AEE (umami) probably due to the presence of different lipids or accompanying fatty acids in the drug-free pellets composition.

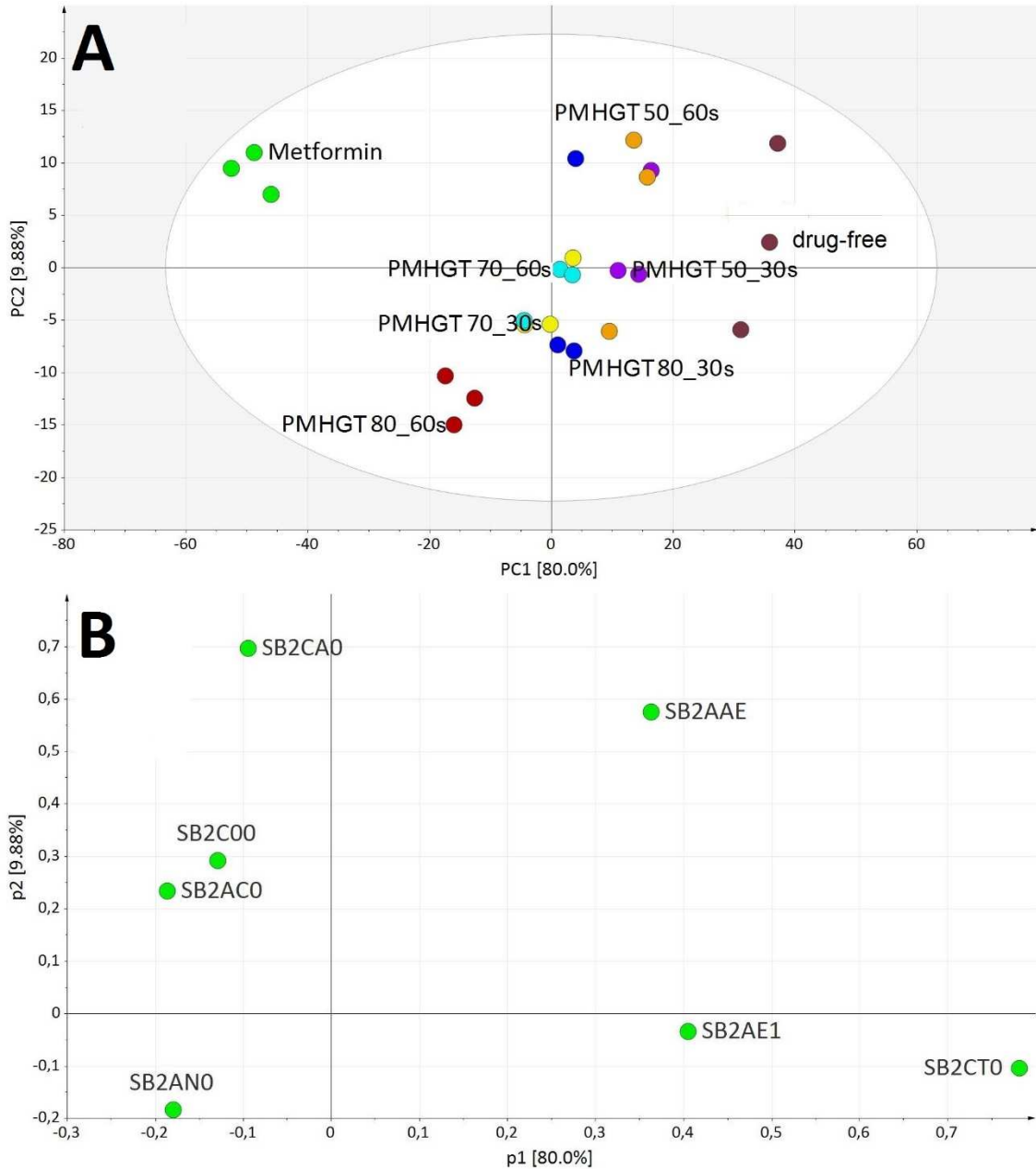


**Figure 4.49.** Multivariate data analysis of metformin HCl micropellets based on the lipid mixture (PMHGT) performed by electronic tongue: (A) PCA map and (B) loadings plot (data was centered scaled)

Concerning the PCA results, and initially regarding the PC1 (x-axis) information, a similar pattern compared to the pellets based on only hard fat can be observed and are related to the amount of lipids within the micropellets and the proximity to the drug-free formulation. Higher is the amount of lipids, closer is the sample to the drug-free formulation.

These results also can be correlated with the drug release results discussed previously in the section 4.4.7, since slower metformin HCl releases were observed for formulations based on higher amounts of pellets (Figure 4.40, see page 82). As less metformin HCl is released, lower is the responses of the sensors SB2AN0 and SB2AC0 to the metformin HCl concentration and, furthermore, lower should be the unpleasant taste of the formulation. This premise can be supported by the differences between the samples after 30 and 60 s. The higher is the exposure time of the micropellets to water, the closer is the sample to pure metformin HCl in the PCA map.

Considering the whole PCA map (PC1 and PC2), similar results were observed compared to the PCA of the micropellets based on hard fat only. The results indicate prominent taste-masking properties by the micropellets PMHGT<sub>50</sub>, which are positioned at the same Cartesian quadrant as the drug-free formulation. The micropellets PMHGT<sub>70</sub> are located in the central position on the PCA map, indicating that this formulation shows average properties and presents taste-masked properties compared to the micropellets PMHGT<sub>80</sub>.

#### 4.4.8.3. Euclidean Distances

The Euclidean distance is the closest distance between two Cartesian points and the use of this equation allows the conception of a metric space using the PCA map results. These calculated distances can be used to compare formulations in different PCA plots allowing a better visual comparison. Employing this approach, the distance between metformin HCl and a drug-free formulations can be considered as 100% of “unpleasant taste variation” or the achievement of an adequate taste-masking effect. However, this premise is only valid considering metformin HCl as the bitter and unpleasant taste sample while the drug-free formulation is considered as good tasting.

Euclidean distances for the samples of 30 and 60 s for micropellets PMH and PMHGT are depicted in Figure 4.50. A relation between the amount of lipids and the distance to the drug-free formulation is evidenced. The higher is the amount of lipids, the closer is the position of the sample to the pleasant taste reference. Moreover, the micropellets based on hard fat only presented lower Euclidean distances to the drug-free pellets compared to micropellets based on ternary lipid mixture, which indicates the micropellets PMH as presenting better taste-masked properties. It is interesting to point out that the micropellets PMHGT showed a slower drug release of metformin HCl within 5 min compared to the micropellets based on hard fat. The Euclidean distance results indicate that the presence of glyceryl distearate and trimyristin negatively influences the taste-masking properties of these formulations compared to the use of hard fat only.

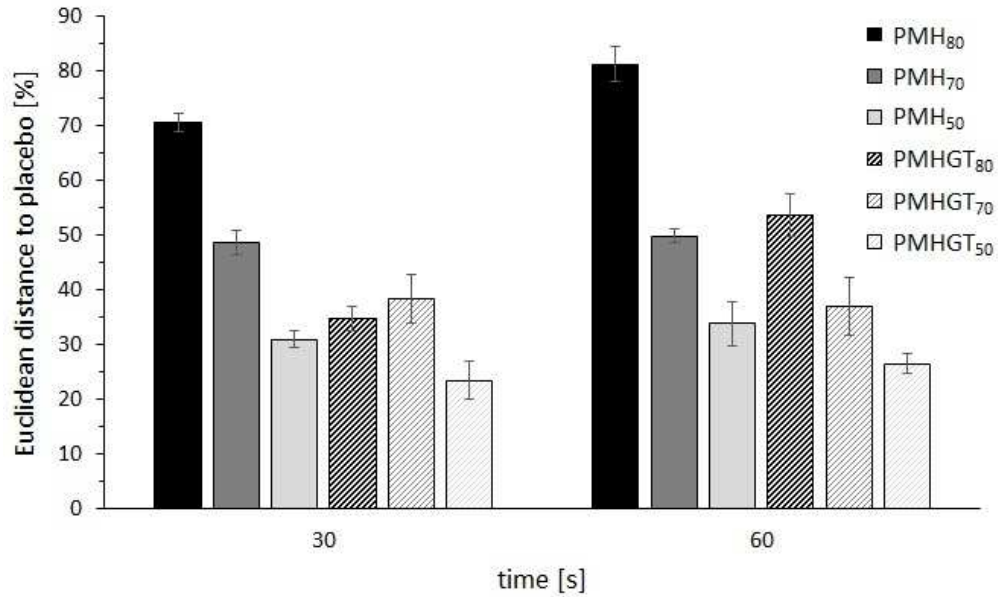


**Figure 4.50.** Euclidean distances of the micropellets to the drug-free formulation normalized in percentage ( $n = 3$ , mean  $\pm$  SD). P = pellet; M = metformin HCl; H = hard fat; T = trimyristin; G = glyceryl distearate

#### 4.4.9. Preparation and characterization of Lipid Micropellets for ODT Development

The decision about the characteristics of the investigated micropellets was based on their characteristics. Spheronization feasibility, immediate-drug release profile, taste-masked properties and slow release in the first 2 to 5 min of dissolution were the aimed criteria to choose the most adequate micropellets for the ODT development studies. The characteristics of the micropellets regarding these criteria are schematically depicted in Figure 4.51. In this mainframe the micropellets that showed the most adequate or prominent properties or characteristics compared to each other are present. The pellet PMHGT<sub>70</sub> was the only micropellet formulation that showed all aimed characteristics and therefore was chosen to the development of the ODTs.

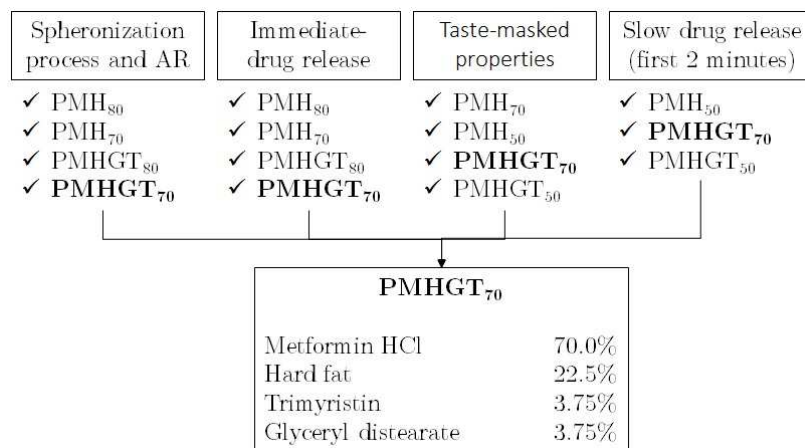


**Figure 4.51.** Decision mainframe for the selection of lipid based micropellets to the ODT development

16 batches of 300 g of micropellets based on this formulation were produced. The micropellets were sieved and the fraction between 250 and 1000  $\mu\text{m}$  were further characterized (Annex X). The lipid pellet batches were then blended for 15 min at 25 rpm, and the final batch was named “LP<sub>70</sub>” (lipid micropellet containing 70% (w/w) of metformin HCl). The LP<sub>70</sub> particle size distribution in comparison to the PMHGT<sub>70</sub> is presented in Table 4.19. Similar particle size distribution and AR were obtained.

**Table 4.19.** LP<sub>70</sub> particle size distribution and shape compared to PMHGT<sub>70</sub>

	Mean $\pm$ SD (n = 3)				
	d <sub>10</sub> ( $\mu\text{m}$ )	d <sub>50</sub> ( $\mu\text{m}$ )	d <sub>90</sub> ( $\mu\text{m}$ )	AR	Span
PMHGT <sub>70</sub>	613.13 $\pm$ 1.97	693.87 $\pm$ 2.18	764.23 $\pm$ 7.76	1.22 $\pm$ 0.01	0.22 $\pm$ 0.00
LP <sub>70</sub>	598.90 $\pm$ 4.17	680.90 $\pm$ 1.20	748.10 $\pm$ 1.25	1.18 $\pm$ 0.01	0.22 $\pm$ 0.00

The drug release profile of LP<sub>70</sub> is depicted in Figure 4.52. The micropellet released 85% (w/w) of metformin HCl within 34 min and 100% (w/w) after around 60 min (Figure 4.52a), values that characterize it as immediate-release. Regarding the UV probe results the micropellets showed a drug release of 22.57% (w/w) of metformin HCl after 2 min (Figure 4.52b), slightly higher than the value showed by the PMHGT<sub>70</sub>. Based on the FIP/AAPS guidelines, which considered a maximal drug release of 10% after 5 minutes as taste-masked dosage form, the dissolution results indicate that the LP<sub>70</sub> initially cannot be classified as taste-masked. However further investigations are still needed to better support this statement.

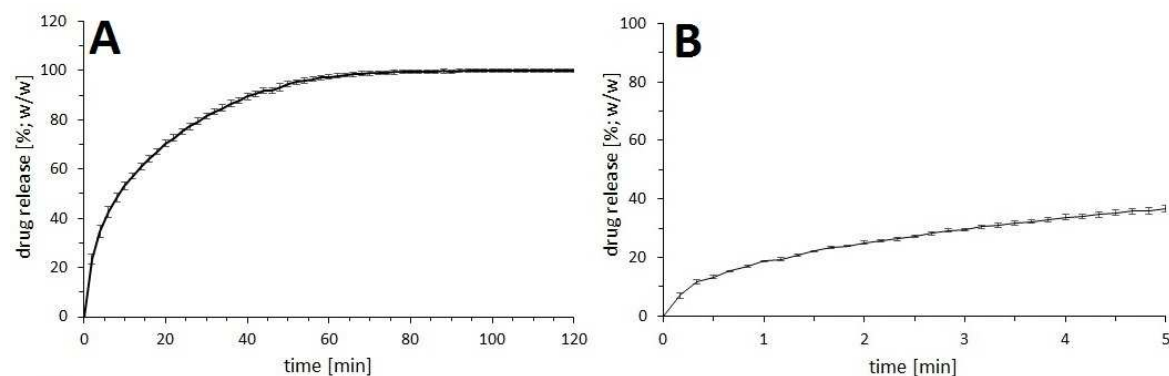


**Figure 4.52.** (A) LP<sub>70</sub> drug release profile. Dissolution media: 900 mL purified water containing 0.001% (w/w) polysorbate 20, temperature of 37 °C  $\pm$  0.5, 150 rpm, basket method,  $\lambda$  = 232 nm (mean  $\pm$  SD, n = 6). (B) LP<sub>70</sub> drug release by UV probe. Dissolution media: 900 mL purified water containing 0.001% (w/w) polysorbate 20, temperature of 37 °C  $\pm$  0.5, 150 rpm, paddle method using a sinker,  $\lambda$  = 232 nm (mean  $\pm$  SD, n = 3)



#### 4.4.10. Conclusions

Material temperature control is considered to be the most critical factor on the spheronization of solid lipid based extrudates. During the process, high material temperatures lead to stickiness of material at the equipment walls and a fast agglomeration of particles, avoiding the obtainment of adequate spherical micropellets. The implementation of an alternative setup on the conventional spheronizer was investigated. This new control allowed to maintain the material temperature in a pre-determined and adequate range, even for extrudates based on higher lipid proportions. Particle agglomeration and material adhesion in the equipment walls were not observed and process times up to 15 min were achieved. Micropellets with similar shape and narrow particle size distributions showing ARs below 1.3 were successfully obtained.

The micropellets presented different drug release profiles influenced by the amount of lipid binder in their formulations. The presence of 20 to 30% (w/w) of lipids resulted in immediate-drug release profiles. The increase to 50% (w/w) led to an alteration on the drug release kinetic, producing micropellets with slower and sustained drug release. Furthermore, taste-masked micropellets were obtained since the drug release of pellets based on more than 30% (w/w) of lipids showed to be low at the first 5 min of dissolution, especially for the micropellets based on ternary lipid mixtures. Electronic tongue investigations supported the drug release results, elucidating different taste-masking properties of the micropellets based on their lipid amounts.

Based on the set of results of the pellets characterization, regarding drug release profile, taste-masking properties, particle shape, and spheronization feasibility, the micropellet formulation PMHGT<sub>70</sub> presented the prominent characteristics compared to the other formulations and therefore was chosen to the development of ODTs.

### 4.5. Orodispersible Tablets Development

#### 4.5.1. Introduction

Compaction of pellets into conventional tablets and in particular, into orodispersible tablets (ODTs), is a challenging area. There are no reports in the present literature about investigations of the development of multiple unit pellet system (MUPS) or ODTs based on solid lipid pellets produced by SLCE/spheronization. Further, to avoid problems arising from compaction of pellets, formulation scientist must have a comprehensive knowledge of how the pellets behave during tableting as well as how the material and/or process-related parameters affect the performance of that formulation as a drug delivery system (Abdul *et al.*, 2010).

To produce ODTs there are several ready-to-use excipients in the market which are designed to improve the disintegration process of the dosage form. Most of them are co-processed mixtures based on mannitol, such as Ludiflash® and Parteck® ODT. Mannitol is a low-digestible carbohydrate, which shows supplementary benefits as pharmaceutical excipients such as reduced caloric content, reduced, low glycemic response, and a non-cariogenic effect (Walsh *et al.*, 2014). Mannitol has been used as filler in chewable tablets due to its pleasant taste. Furthermore, mannitol exhibits a negative heat of solution and imparts a cooling sensation when sucked or chewed (Alderborn, 2013).

The co-processed excipient should be used to fill the void space between the pellets to be compressed and to act as cushioning agent to absorb the compression force. At the same time, the filler materials should be used to separate the individual pellets to preventing direct contact forming a layer around the pellets. This function should be investigated to avoid adhesion between the lipid micropellets and furthermore the formation of a monolithic matrix, which could influence negatively the disintegration of the ODTs.

Therefore, a DoE should be performed to investigate the influence of compression force and a qualitative and quantitative variation of co-processed excipients on the properties of ODTs containing 500 mg of metformin HCl. The ODTs should be characterized according to their friability, tensile strength, and disintegration times. The ODTs formulation presenting the most prominent characteristics in the DoE should be further characterized according to morphological aspects, water uptake, drug release, and taste-masking properties. The general aim of this chapter is investigate the development of ODTs with metformin HCl presenting immediate-release profiles and taste-masked properties.

## 4.5.2. Design of Experiments (DoE)

### 4.5.2.1. Factors

The experimental plan was designed using two factors with three levels each (Table 4.20). The type and amount of co-processed excipient and compression force were considered the most relevant parameters to the production of ODTs containing pellets.

**Table 4.20.** Factors of the DoE

Factors	Factor level		
	-1	0	+1
Compression force (kN)	2.5	5.0	7.5
Co-processed excipient (%; w/w)	30	40	50

### 4.5.2.2. Quality of the Model

A 2<sup>3</sup> statistical design was performed. Three repetitions were made at the center point of the DoE to estimate the repetition error, resulting in 22 experiments. The ODTs were characterized regarding their tensile strength, disintegration time and friability as most important oral tablet quality attributes (Alderborn, 2013). The results of the DoE investigation using Ludiflash® and Parateck® ODT are shown in Table 4.21.

**Table 4.21.** DoE of ODTs: factors and responses

Ludiflash®						
Factors			Responses			
Excipient content (%)	Compression force (kN)	Mean ± SD (n = 10)				
		Tensile strength (MPa)	Crushing force (N)	Disintegration time (min)**	Friability (%)	
N1	30	2.5	0.182 ± 0.046	24.0 ± 6.1	3.22 ± 0.97	12.95
N2	30	5.0	0.452 ± 0.111	57.1 ± 14.2	7.68 ± 4.21	0.38
N3	30	7.5	0.748 ± 0.044	91.4 ± 5.8	7.05 ± 3.60	0.26
N4	40	2.5	0.041 ± 0.014	7.0 ± 2.3	0.68 ± 0.14	100.00
N5	40	5.0	0.310 ± 0.126	47.4 ± 19.0	2.12 ± 1.02	2.17
N6*	40	7.5	0.518 ± 0.061	72.9 ± 8.5	3.88 ± 1.96	0.31
N19*	40	5.0	0.269 ± 0.090	38.9 ± 12.8	2.74 ± 1.36	4.19
N20*	40	5.0	0.289 ± 0.141	42.8 ± 19.4	1.89 ± 0.43	1.67
N7	50	2.5	0.041 ± 0.014	8.3 ± 2.9	0.61 ± 0.14	100.00
N8	50	5.0	0.226 ± 0.031	41.8 ± 5.7	1.60 ± 0.83	3.39
N9	50	7.5	0.466 ± 0.080	79.5 ± 12.7	1.78 ± 0.36	0.89
Parateck® ODT						
Factors			Responses			
Excipient content (%)	Compression force (kN)	Mean ± SD (n = 10)				
		Tensile strength (MPa)	Crushing force (N)	Disintegration time (min)**	Friability (%)	
N10	30	2.5	0.184 ± 0.028	23.5 ± 3.5	1.12 ± 0.44	11.7
N11	30	5.0	0.398 ± 0.078	49.9 ± 9.7	5.76 ± 1.90	0.45
N12	30	7.5	0.586 ± 0.192	71.7 ± 22.9	6.36 ± 1.29	0.34
N13	40	2.5	0.039 ± 0.029	10.0 ± 1.7	0.60 ± 0.23	100.0
N14	40	5.0	0.238 ± 0.114	36.2 ± 16.6	1.96 ± 1.79	5.82
N15*	40	7.5	***	***	***	***
N21*	40	5.0	0.194 ± 0.089	28.9 ± 13.0	1.6 ± 0.60	***
N22*	40	5.0	0.185 ± 0.044	27.7 ± 6.1	2.09 ± 1.19	6.18
N16	50	2.5	0.059 ± 0.021	11.2 ± 4.0	1.18 ± 1.02	7.49
N17	50	5.0	0.138 ± 0.024	25.0 ± 4.3	1.13 ± 0.56	23.08
N18	50	7.5	***	***	***	***

\* Center points; \*\* n = 6; \*\*\* Not measured due to tablet lamination.

Some batches based on Parateck® ODT could not be evaluated. Tablet lamination phenomenon was observed at 5.0 and 7.5 kN of compression forces only for the formulations containing Parateck® ODT (Figure 4.53). Therefore, was not possible to characterize these tablets. According to Alderborn (2013), lamination is highly dependent of the properties of the material and to the design and conditions of the press and the tooling. The difference in the investigated co-processed excipients rely in the different binder used and probably in the different proportions among the adjuvants (Table 7.3, see page 119). Since no information about the quantitative composition of Parateck® ODT is available, this phenomenon will not be discussed in the present work.



**Figure 4.53.** Lamination of tablets produced with Parateck® ODT

Therefore, the model based on the experiments with Ludiflash® was evaluated separately. The data were analyzed by regression analysis (least squares fit), which provides a model relating the changes in the factors (compression force and excipient amount) to changes in the responses (friability, disintegration time, and tensile strength).

Furthermore, to improve the model quality, the effects on the disintegration time and friability were logarithmic transformed. The quality of the obtained model for the investigated responses is shown in Table 4.22. The quality of the model was evaluated according their goodness of fitness ( $R^2$ ), goodness of prediction ( $Q^2$ ), model validity, and reproducibility. According to Eriksson *et al.* (2008),  $R^2$  alone is not sufficient for probing the validity of a model and a much better indication of the usefulness of the model is given by  $Q^2$ . These both indicator results reflect on the model validity value exhibit by the model, which indicates that the models fits appropriately. Generally, values higher than 0.25 suggest a valid model.

The indicators for the used models suggest a good quality for the fitting and prediction of the effect on the tablets tensile strength, disintegration time, and friability, since their  $R^2$  and  $Q^2$  are higher than 0.5 and do not diverge more than 0.2 – 0.3 from each other (Eriksson *et al.*, 2008).

**Table 4.22.** Quality of the experimental design: using Ludiflash® as co-processed excipient

	Tensile strength	Disintegration time	Friability
Goodness of fit ( $R^2$ )	0.9964	0.9506	0.9680
$R^2$ adjusted	0.9929	0.9176	0.9360
Goodness of prediction ( $Q^2$ )	0.9836	0.8115	0.7631
Model validity	0.9013	0.7664	0.7925
Reproducibility	0.9906	0.9453	0.9491

### 4.5.2.3. Results

The importance of the compression force and Ludiflash® amount was evaluated in terms of a plot of regression coefficients for disintegration time, tensile strength, and friability. Figure 4.54a displays the regression coefficients with confidence intervals regarding the disintegration time responses. Both investigated factors showed an impact on the disintegration time of the tablets. However, comparatively, the increase in Ludiflash® amount produces a higher influence on the disintegration of the tablet. The negative coefficient indicates an inverse influence, in other words, the higher the amount of the excipient, the lower the disintegration time. As Ludiflash® is based on 90% (w/w) of mannitol, a disintegrant excipient, higher will be the contact with water, and faster will be the disintegration of the tablet. On the other hand, at lower Ludiflash® content, the contact among the lipid pellets is increased, and solid lipid bridges could be form, retarding the disintegration process. The interaction coefficient (Exc\*Com) indicated a statistical insignificant interaction between the both factors since the uncertainty of this effect is relatively high due to its high confidence interval. The interaction coefficient was therefore removed from the model to improve its quality. Moreover, the quadratic effect coefficient shows a significant and higher impact of lower compaction forces and lower amounts of Ludiflash® on the disintegration time of the tablets compared to higher values.

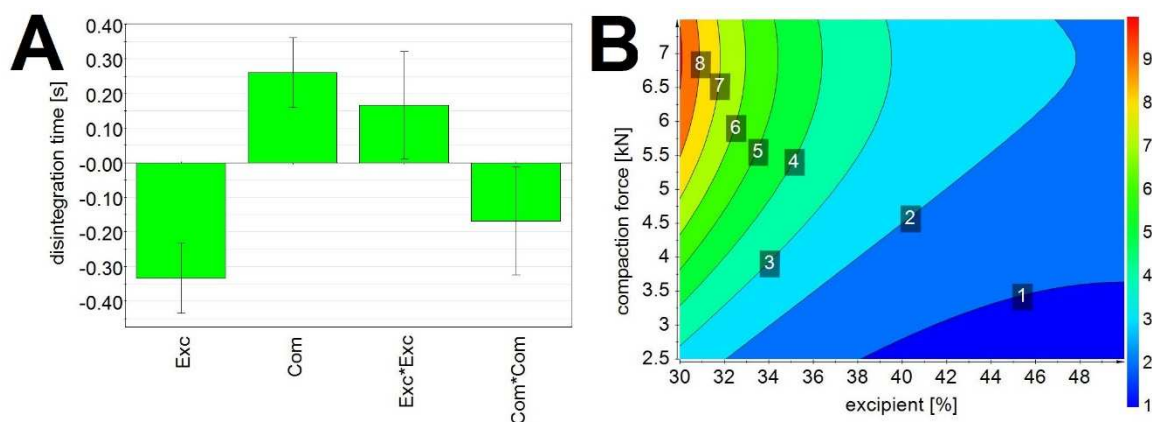


**Figure 4.54.** Investigation results regarding the tablet disintegration time: (A) regression coefficients and (B) response contour plot (data centered and scaled)

Comparatively, the increase in the compression force exhibit its influence mainly due to the increase in particle rearrangement and contact points among particles, increasing surface interactions, i.e. Van der Waals forces (Führer, 1995; Nyström and Karehill, 1995). Therefore, it shows a positive coefficient, indicating that the higher the compression force, the slower the disintegration process.

The contour plot of the model is depicted in Figure 4.54b. As previously discussed, higher mounts of Ludiflash® and lower compaction forces led the tablets to exhibit a faster disintegration time. However, the disintegration time of an ODTs needs to be interpreted considering the specified limits provided by Official compendiums. Basing the observations on the ODTs definition of the Ph. Eur. (2014), which defines ODTs as presenting a disintegration time inferior to 3 min, amounts superior to 30% (w/w) of Ludiflash are required. Regarding the compression, its effect do not seems to influence strongly the disintegration process, since disintegration times below 3 min were obtained with compression in the whole studied range (From 2.5 to 7.5 kN). On the other hand, considering 30 s as aimed disintegration time, as defined in the USP 34 (2011), concentrations of more than 38% (w/w) of Ludiflash® are required and compression forces inferior to 3.5 kN need to be employed.

The mechanical strength of the tablets are represented by the tensile strength and it is associated with the resistance of the tablet to fracture and attrition (Aldernborn, 2013). The regression coefficients of the effect of compression force and Ludiflash® amount on the tensile strength are depicted in Figure 5.55a. The plot depicts a higher impact of the compression force on the tensile strength of the tablets compared to the amount of co-processed excipient. This result rely by the fact that the increase in the compaction force generates an increased proximity in the particles and also material deformation. The effect of this alteration leads to an increase in molecular and particular surface interactions among the components on the tablet, increasing its resistance to fracture (Nyström and Karehill, 1995). The coefficient of the two-factor interaction shows a significant and negative interaction between the compression force and the amount of Ludiflash® regarding the tensile strength of the tablet. However, the impact on this tablet characteristics is lower than those showed by the linear coefficients for the same factors influence.

The quadratic effect of the compression force shows a high uncertainty of the coefficient due to its confidence interval that crosses the zero of the x-axis. On the other hand, the quadratic effect of the amount of Ludiflash indicates that lower amounts of the excipient present a higher and positive impact on the tablet tensile strength compared to higher quantities.

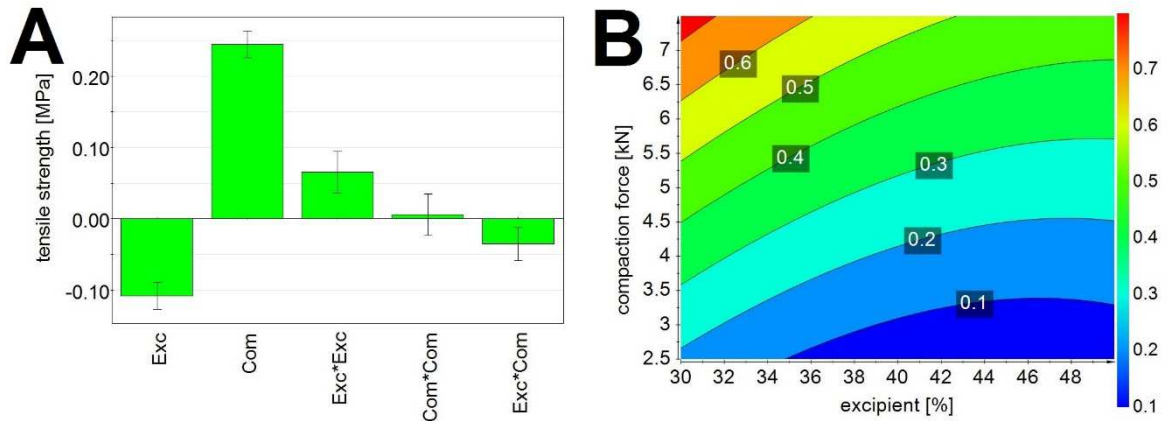


**Figure 4.55.** Investigation results regarding the tablet tensile strength (ODTs with Ludiflash®): (A) regression coefficients and (B) response contour plot (data centered and scaled)

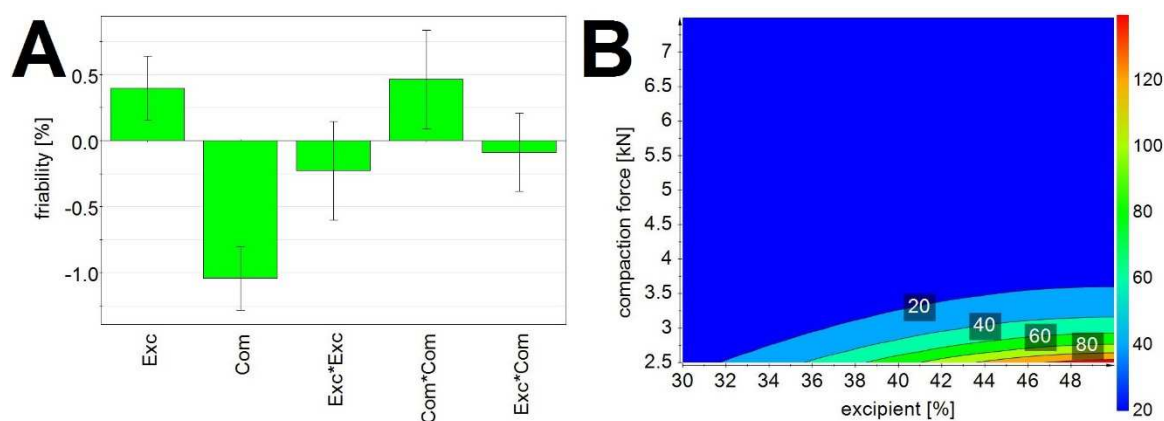
The contour plot for the model related to the effect on the tablet tensile strength is shown in Figure 5.55b. There is no specified limit for tablet tensile strength or resistance to fracture of tablets in Ph. Eur. (2014). Herewith, considering tablet further processes such as blistering, transportation, and further handling, the higher the tensile strength, the better the tablet mechanical strength to withstand fracture and erosion, and therefore its quality regarding its physical integrity (Alderborn, 2013). However, a high tensile strength value should be only considered adequate since this attribute does not influence other properties such as the drug release. For this reason, higher tensile strengths are obtained in the region of high compression forces and Ludiflash® amounts below 42% (w/w), since the presence of the excipients showed a negative impact on the tablet tensile strength. The observed effect of the compression force on the tablet tensile strength containing mannitol as main excipient is in accordance as reported in literature (Rowe *et al.*, 2012).

Figure 4.56a displays the regression coefficients regarding the impact of the investigated factors on the friability of the tablets. Similarly to the influence on the tensile strength, the compression force shows a higher impact on the tablet friability compared to the amount of Ludiflash. However, regarding this effect, the compaction force shows a negative coefficient, indicating that the increase in its value generates a decrease in the loss of material from the tablet. According to this coefficient, an increase in 2.5 kN in the compaction force, produces a decrease of around 1% of friability, when the amount of Ludiflash is kept constant. Moreover, the two factor interaction effect coefficient and the quadratic effect coefficient of the Ludiflash amount on the tablet friability showed high confidence intervals and are statistical insignificant. However, the quadratic effect coefficient of the compression force indicates a higher impact on the friability of the tablets at lower values compared to higher ones. At lower compression forces higher material losses are expected.

The response contour plot regarding the ODTs friability is depicted in Figure 4.56b. A region of high material loss is observed at higher Ludiflash® proportions (> 36%;

w/w) and compression force below 3.5 kN. The higher presence of mannitol could be the reason, since it does not present sufficient binder properties against breakage compared to the ODTs based on less excipient. At low Ludiflash® amount, there are higher amount of lipid binders and the resistance of the tablets to material loss is therefore higher.

Comparing the results to the acceptance value of 1% (w/w) of maximal material loss for tablets defined in the Ph. Eur. (2014), only the tablets produced at 7.5 kN of compression force showed weight loss below this limit, denoting that this force is required to achieved the adequate quality of tablets. The amount of Ludiflash® did not impact strongly on this tablet property, since formulations based on 30, 40 and 50% (w/w) of the excipient exhibited adequate values at this compaction force level, which corroborates the results observed in the regression coefficient plot (Figure 4.56).



**Figure 4.56** Investigation results regarding the tablet friability: (A) regression coefficients and (B) response contour plot (data centered and scaled)

### 4.5.3. ODT with Ludiflash®

Based on the results of the DoE, a batch of 1,000 tablets were produced using a compression force of 7.5 kN and based on 50% (w/w) of Ludiflash® as co-processed excipient. These ODTs were further characterized.

#### 4.5.3.1. Morphological Characterization of the ODTs

Ideally, compacted pellets of a multiple-unit pellet system should not fuse into a non-disintegrating matrix during compaction (Abdul *et al.*, 2010). Compaction of lipids showed the formation of a monolithic and inert matrix which influences the drug release from the tablet (Barakat *et al.*, 2009). Therefore, the use of specific excipients should present two important main functions: (1) to avoid the formation of this monolithic lipid matrix between the micropellets and (2) to improve the disintegration properties of the ODTs. These functions could further avoid alterations in the pellet units such as drug release profile and taste-masked properties. This goal can be



achieved with an optimum amount and type of excipient, which was the aim of the previously performed DoE.

Microscopical image of the ODT surface and a SEM image of a lipid micropellets at the ODT surface are depicted in Figure 4.57. It is possible to recognize the micropellets dispersed at the tablet surface and surrounded by the excipient (Figure 4.57a). A closer look in the tablet surface shows that the lipid micropellet structure remains intact after compression (Figure 4.57b). No cracks in the micropellet surface are perceived. Due to the plastic properties of the lipids in their structure they are not crushed but being deformed. According to the mechanistic conception proposed by York and Pilpel (1973) regarding the compression process of pellets, typical plastic deformable material presents a volume reduction of the pellet by local surface deformation involving flattening of pellets. This phenomenon can be recognized in the SEM images (Figure 4.57).

Moreover, according to Abdul *et al.* (2010), the pellets may deform but should not rupture, since, for example, the existence of cracks in the pellet surface may have undesirable effects on the drug release properties of that subunit. Moreover, the maintenance of the micropellets main structure after compression indicates that the properties of the micropellets such as taste-masking was not influenced by the compression process.

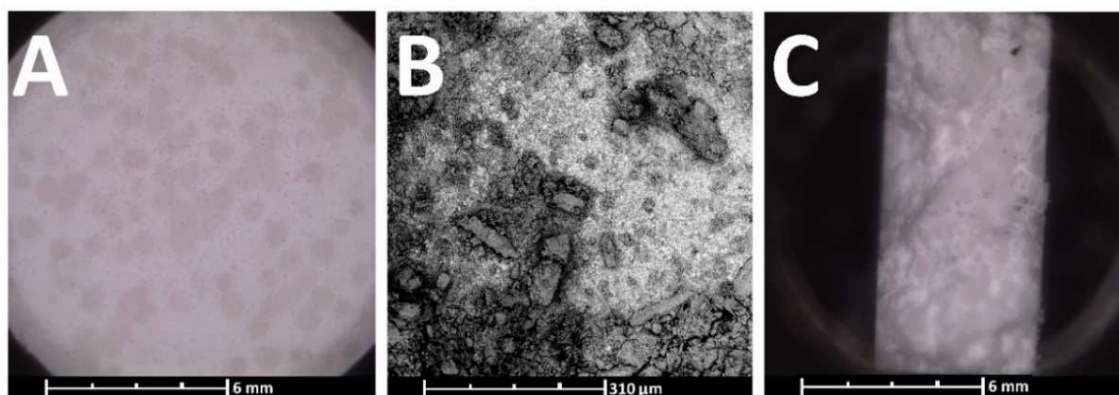


**Figure 4.57.** SEM images of the ODT surface taken at (A) 20x magnification, (B) 430x magnification and (C) tablet sectional cut at 20x magnification (scale represents 6 mm, 310  $\mu$ m, and 6 mm, respectively)

The morphological characteristics of the ODTs are depicted in Table 4.23. According to the Ph. Eur. (2014), the mass variation of single-dose preparations cannot present individual masses deviating from the average by more than 5% (w/w). The present ODTs showed a mean mass variation of 1.42 g (1.51%; w/w) which is in accordance with the limits defined in the pharmacopeia. Regarding the tablet dimensions, the ODTs thickness can be considered too high for a regular oral tablet, however, as the tablets were developed to be swallowed only after complete disintegration into the oral cavity, the thickness size influence during administration can be neglected.

**Table 4.23.** Morphological characteristics of the ODTs

	Mean $\pm$ SD			
	Porosity (%) <sup>*</sup>	Mass variation (g) <sup>**</sup>	Dimensions (mm) <sup>***</sup>	
			Thickness	Diameter
ODTs	19.38 $\pm$ 0.82	1.42 $\pm$ 0.02	7.19 $\pm$ 0.13	15.13 $\pm$ 0.02

\* n = 6; \*\* n = 20; \*\*\* n = 10

The friability, tensile strength, and disintegration time of the ODTs are depicted in Table 4.24. The values are similar to those observed to the same ODT formulation during the DoE. A friability below 1% (w/w) and a disintegration time below 3 min were observed and are in accordance with the limits for these properties in the Ph. Eur. (2014).

**Table 4.24.** Friability, tensile strength, and disintegration time

	Friability (%; w/w)	Mean $\pm$ SD	
		Tensile strength (MPa) <sup>*</sup>	Disintegration time (min) <sup>**</sup>
ODTs	0.41	0.53 $\pm$ 0.06	1.27 $\pm$ 0.13

\* n = 10; \*\* n = 6; \*\*\* n = 20

#### 4.5.3.2. Uniformity of Dose of the ODTs

To ensure the consistency of dosage units, each tablet in a batch should have a drug substance content within a narrow range around the label claim (USP 34, 2011). The ODTs were designed to contain a dose of 500 mg of metformin HCl. The content of metformin HCl in the ODTs are shown in Table 4.25. The label claim assay performed by HPLC showed a metformin HCl content average of 99.54%  $\pm$  4.72 (w/w). No tablet unit showed less than 85.0% and more than 115.0% (w/w) of API as specified in the Ph. Eur. (2014).

**Table 4.25.** Label claim of the ODTs containing 500 mg of metformin HCl

	Metformin HCl (%; w/w)									
	1	2	3	4	5	6	7	8	9	10
ODTs	101.72	91.23	102.72	97.97	103.71	101.76	101.58	94.83	94.26	105.65

#### 4.5.3.3. Loss on Drying, Water absorption and Wetting Test of the ODTs

The visual start and endpoint of the simulated wetting test are shown in Figure 4.58. It is possible to observe that the water absorption starts from the surroundings of the tablet (Figure 4.58b) until a complete wetting is achieved (Figure 4.58d). The water absorption process took about 3.02 min  $\pm$  0.90 (mean  $\pm$  SD; n = 10). Under this assay conditions and considering the water density as 1.0 g·mL<sup>-1</sup>, a water absorption rate of 0.20 g·min<sup>-1</sup> was calculated. A final tablet mass increase of 43.39%  $\pm$  1.85 (w/w; mean  $\pm$  SD; n = 6) was observed after 6 min of exposure to 1.75 mL of water. This means that after the assay almost 50% (w/w) of the tablet weight is absorbed water. It is

interesting to point that the initial water content of the ODTs showed a value of  $0.73\% \pm 0.02$  (w/w; mean  $\pm$  SD;  $n = 6$ ).

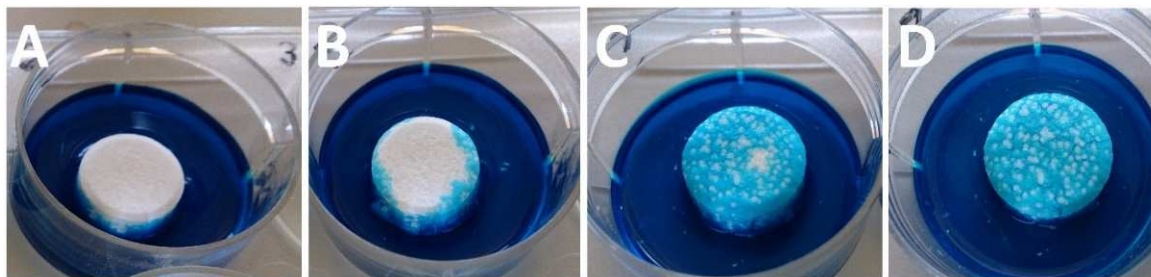


**Figure 4.58.** Simulated wetting test visual observations: (A) starting point and (D) end point

As lipids are mainly hydrophobic, and are present in a proportion of around 15% (w/w) in the final formulation of the ODTs, they do not seem to influence the wettability of the tablets significantly. This is due to the fact that the amount of material in the tablet that absorb water (considering only metformin HCl and mannitol) represents around 80% (w/w) of the total formulation. Considering the crospovidone also present in the co-processed excipient these amount increased to 83% (w/w). Although crospovidone is water-insoluble, it exhibits high capillary activity and pronounced hydration capacity (Schiermeier and Schmidt, 2002).

The water sorption and desorption isotherms exhibit by the ODTs and the micropellets are depicted in Figure 4.59. LP<sub>70</sub> showed a weight increase of  $1.73\% \pm 0.02$  (w/w; mean  $\pm$  SD) after the exposure to a relative humidity of 90%. This water sorption could be pointed as mainly caused by metformin HCl, which exhibits hygroscopic characteristics. On the other hand, the ODTs which is based on 50% of LP<sub>70</sub> showed a mass variation of  $3.61\% \pm 0.04$  (w/w; mean  $\pm$  SD), value relatively low compared to the results of the simulated wetting test. These values represent an increase of 47.92% in the tablet weight compared to the micropellets which is a similar value regarding the proportion of micropellets and excipient.

Although the micropellets exhibit a higher superficial area compared with one tablet, it is important to highlight that the ODTs showed a porosity around 19% (w/w), which plays an important role in the water adsorption isotherm. The ODTs presented a slight increase in its mass until a relative humidity of 80% is achieved. At this point a fast water adsorption was observed until equilibrium was achieved. Interestingly, a similar pattern is also shown by the micropellets, which indicates that the metformin HCl plays an important role on the water adsorption occurrence. In contrast, the water desorption of the ODTs showed a small hysteresis, probably due to the tablet dimensions, since the water vapor requires more time (due to a longer path compared to the micropellets) to exit the inner core of the ODTs. Still, after decreasing the relative humidity the complete water vapor is removed which indicates that superficial adsorption is the main water adsorption mechanism.

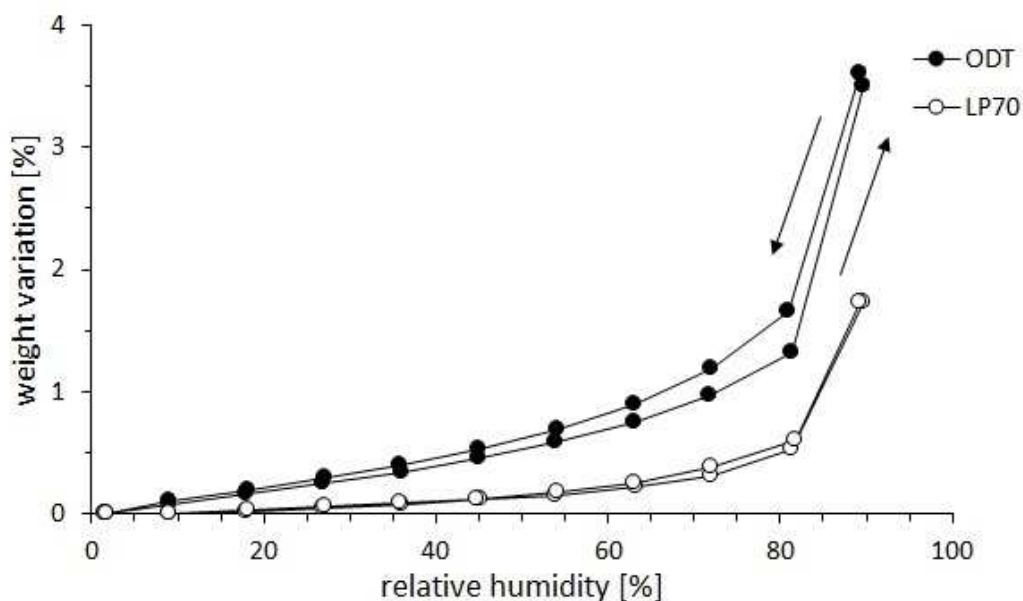


**Figure 4.59.** Water sorption and desorption curves of ODTs in comparison with the lipid micropellets LP<sub>70</sub> (n = 3; mean  $\pm$  SD)

#### 4.5.3.4. Drug Release of the ODTs

The drug release profile of the ODTs is shown in Figure 4.60. According to Klancke (2003), taste-masked ODTs should be formulated in such a manner that the delay in drug release is long enough to pass through the oral cavity, followed by fast and complete release as for any immediate release dosage form. The ODTs showed drug release results according to this statement, releasing 85% (w/w) of metformin after around 28 min and 100% (w/w) after 40 min. These results characterize them as immediate-release tablets.

On the topic of MUPS, the drug release of the multiple-units (micropellets) should not be affected by the compaction process (Abdul *et al.*, 2010). A comparison between the ODTs and the LP70 drug release profiles is also depicted in Figure 4.60. Comparatively, it is possible to notice that the compression process did not influence the drug release profile of micropellets. However, a relative lag time is observed within the first minutes of dissolution, probably related to the disintegration process of the tablet. This slight alteration in the drug release profile can be remarkably considered since the lag time could influence positively the taste-masked properties of the tablet (Vaassen *et al.*, 2012).

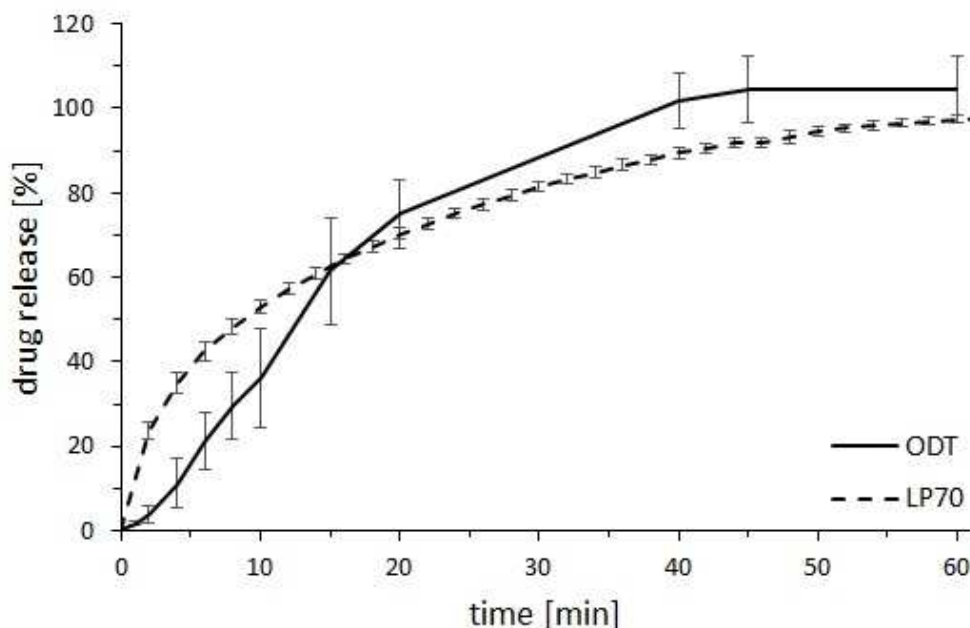


**Figure 4.60.** Metformin HCl release from ODT and from LP<sub>70</sub>. Dissolution media: 900 mL purified water containing 0.001% (w/w) polysorbate 20, temperature of 37 °C ± 0.5, LP<sub>70</sub> using basket method (150 rpm) and ODT using paddle method (50 rpm),  $\lambda = 232$  nm (mean ± SD, n = 6)

An in-line drug release assay was performed to investigate the extension of the lag time produced by the compression step. The results are depicted in Figure 4.61. ODTs releases 0.20% (w/w) of metformin HCl after 30 s of dissolution and around 0.90% (w/w) after 60 s. After 2 min only 2.4% (w/w) of metformin HCl is released. The results characterize the ODTs as presenting taste-masked properties according to the FIP/AAPS guideline, which suggests a successful taste-masking by a drug release below 10% (w/w) within the first 5 min of dissolution (Siewert *et al.*, 2003). However, according to Pein *et al.* (2014) this arbitrary threshold is highly dependent on the human perception threshold of each individual drug substance and dissolution methods as such are not applicable individually to judge about taste-masking effects.

Unfortunately, using the UV probe, longer dissolution times could not be measured due to a high concentration of metformin HCl released after 2 min, which exceeded the Lambert-Beer linear range.

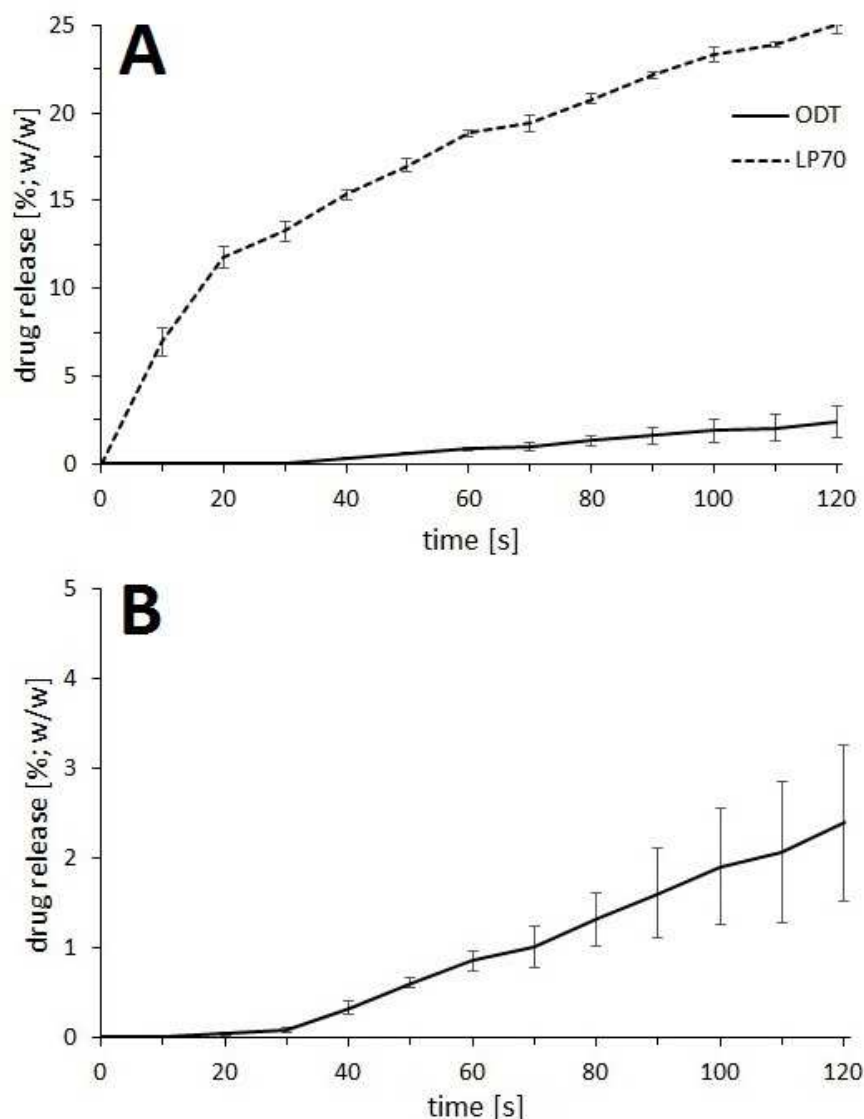


**Figure 4.61.** In-line drug release (A) a comparison between the ODTs and LP<sub>70</sub> drug release and (B) of metformin HCl from the ODTs, by UV/Vis probe. Dissolution media: 900 mL purified water containing 0.001% (w/w) polysorbate 20, temperature of 37 °C ± 0.5. LP<sub>70</sub> by basket method and the ODTs by paddle method, 100 rpm,  $\lambda = 232$  nm (mean ± SD, n = 3)

#### 4.5.3.5. Electronic Tongue Investigations

The taste-masked properties of the ODTs were investigated by electronic tongue and parallel compared to pure metformin HCl powder and a tablet (placebo or pleasant taste reference) produced by direct compression with a mixture of Ludiflash®, hard fat, glyceryl distearate, and trimyristin in the ratio of 10:4:1:1 (w/w), respectively. Similarly to perform with the micropellets, ODTs samples were prepared based on times of 30 and 60 s, since these values represent a more realistic residence time of a orodispersible tablet in the oral cavity before swallowing (Carnaby-Mann and Crary, 2005; Pein *et al.*, 2014). The MVDA results of the sensor responses are depicted in Figure 4.62. The PCA of the data resulted in a bi-dimensional map where 85.5% of

the data information are contained in the PC1 and 13.2% in the PC2. The correlated loading plot is additionally showed in Figure 4.63b.

Regarding only the PC1, which contains most of the MVDA information, a clear proximity of the ODTs samples to the placebo compared to metformin HCl is seen. The ODTs sample of 30 s showed the most prominent taste-masked properties, since it is closer to the placebo. This result was expected regarding the drug release results of the ODTs that showed a slight metformin release within 30 s (0.20%; w/w) compared to 60 s (0.90%; w/w).

On the other hand, taking into account the PC2 information, the ODTs samples of 30 and 60 s present a similar response to the set of sensors and can be considered as presenting taste-masked properties due to their position on the PCA map. These results indicate that the taste information after 30 and 60 s result in a slight different response by the set of sensors, especially compared to pure metformin HCl. This similarity in the sensor responses is directly related to the low drug release amount of metformin HCl within this time window observed in the drug release assays. Interestingly, pure metformin HCl showed a strong interrelation with the sensors for bitterness (SB2AN0 and SB2AC0) which are located in the opposite side in the loading plot in relation to the ODTs samples and likewise the placebo formulation.

The placebo formulation showed a higher response by the sensors SB2AE1 (astringency) and SB2CT0 (saltiness), result similar to presented by the drug-free formulations based on lipids only during the investigation of the micropellets (Figure 4.48 and Figure 4.49, see page 92 and 93, respectively). Due to stability problems, the sweetness sensor was not used, which would influence the sensor set responses and further the position of the placebo formulation on the PCA map due to the presence of mannitol (a sugar alcohol). The insertion of such a sensor probably could provide more accurate information about the taste-masked properties of the ODTs.

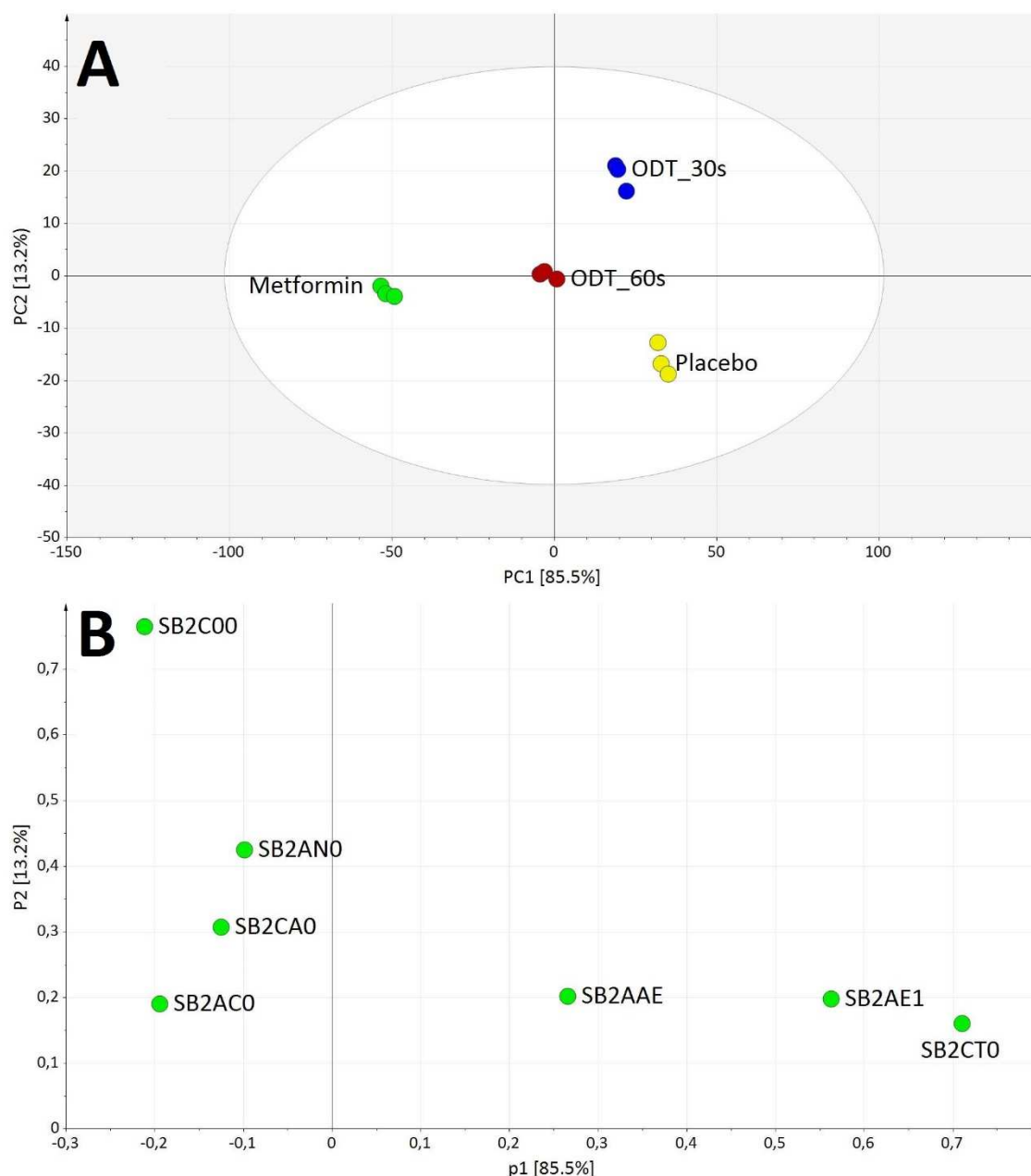


**Figure 4.62.** Multivariate data analysis of metformin HCl ODTs performed by electronic tongue: (A) PCA map and (B) loadings plot (data was previously mean centered)

Comparing the ODTs to its original lipid pellet (Figure 4.63), the ODTs sample of 30 s showed significant improved taste-masked properties, even compared to the LP<sub>70</sub> sample of 30 s. Interestingly, at longer times (60 s) the ODTs and the LP<sub>70</sub> (30 s) are near positioned in the central region of the PCA map, indicating a relatively similar taste response among these samples. These results do not corroborate the observed drug release results for these samples, which showed a slower drug release from the ODTs within 30 and 60 s (0.20 and 0.90%, respectively) compared to the LP<sub>70</sub> at the same times (13.2 and 18.8%, respectively). This observation indicates that the presence of Ludiflash® in the ODTs formulation influences the used set of sensor responses in a way that the electronic tongue does not differentiate significantly these



samples regarding the bitter taste of metformin HCl. Moreover, the taste-masked properties of the ODTs were confirmed regarding the proximity of the samples with the pleasant reference, the placebo formulation.

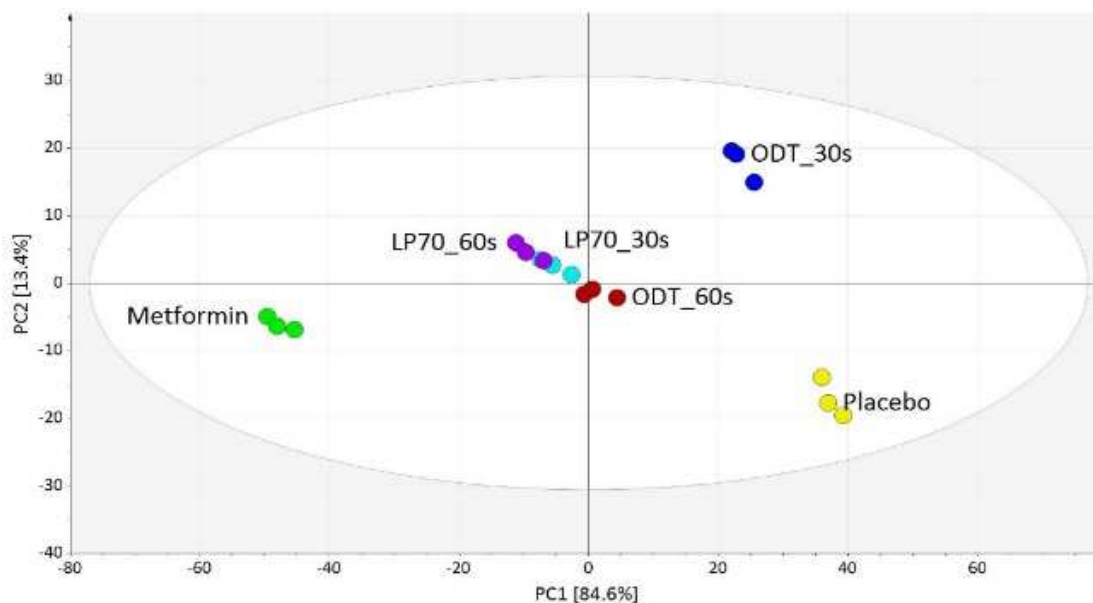


**Figure 4.63.** PCA map obtained by multivariate data analysis of metformin HCl ODTs compared to LP<sub>70</sub> performed by electronic tongue (data was mean centered)

A further aspect, that needs to be considered, is that the bitterness threshold by elderly patients also plays a role in the taste-masking abilities of a formulation. The elderly have elevated thresholds for bitter taste due to a decreased taste perception (Cowart *et al.*, 1994) specially in comparison with adults and teenagers. Sometimes the average threshold difference is increased comparatively by a factor of 5 (Schiffman *et al.*, 1994). Therefore, further taste assessment investigations, such as human taste panel, are still required to correlate the results discussed on the present work to the human perception.

#### 4.5.4. Conclusions

The main aim of the present work is the development of ODTs containing 500 mg of metformin HCl presenting immediate drug release profile and taste-masked properties. A DoE was performed to investigate the influence of the compression force and the amount of two co-processed excipients on the properties of ODTs. During the compression investigations a strong lamination of the tablets containing Parteck® ODT was observed. This phenomenon was prominently observed when higher compression forces and higher excipient amounts were used. Therefore, it was not possible to evaluate the influence of this excipient on the production of ODTs.

The DoE using Ludiflash® as compression excipient showed a positive influence of the compression force on the tensile strength, friability, and disintegration time of the tablets regarding values specified in the Ph. Eur. (2014) for tablets. Likewise, the increase in the amount of this excipient resulted in fast disintegrant tablets, however, a negative influence on the tensile strength was shown.

Tablets presenting adequate friability and tensile strength were obtained at higher compression forces and high amounts of co-processed excipient. Moreover, disintegration times below 3 min successfully characterized the tablets as orodispersible according to the Ph. Eur. (2014). The compression process did not generate breakage of the lipid based micropellets which led the ODTs to maintain similar properties of the lipid micropellets. A lag-time in the drug release profile of metformin HCl due to the compression was observed. However, the presence of this lag-time did not influence the drug release profile and tablets presenting an immediate-drug release kinetic were obtained.

Electronic tongue results showed a significant alteration on the sensor responses of the tablets compared to pure metformin HCl. Relating this effect with the low drug release showed by the tablets within the first minutes of dissolution, these results indicate the successful taste-masking of the unpleasant taste of the API in the ODTs.

## 5. Summary

Metformin HCl tablets encountered in the market show relatively inconvenient dimensions, decreasing the patient compliance during the treatment of type 2 diabetes *mellitus*. Furthermore, the crushing and dispersion of such a tablets in food or beverages exposes the unpleasant bitter taste of the API, which increases even more the nonadherence to treatment, especially by elderly patients. Therefore, this work focused on the development, manufacturing, and characterization of ODTs containing taste-masked lipid based micropellets of metformin HCl.

To obtain pellets presenting taste-masked properties a recently extrusion/spheronization methodology using solid lipids excipients was employed: solid lipid cold extrusion followed by spheronization (SLCE). The manufacturing of small diameter extrudates based on different quantitative and qualitative solid lipid binders were investigated. Extrudates presenting different drug release kinetics, correlated with the amount of lipid binders, were obtained. As the taste-masking principle of the SLCE is to modify the drug release of the API, reducing its contact with the taste buds in the oral cavity after drug administration, all extrudate formulations, even those presenting sustained release profiles, were further spheronized.

The material temperature during the spheronization of lipid based extrudates was reported the most critical factor in SLCE/spheronization method. Although this issue was recently investigated, there are no reports in the literature suggesting a solution for this problem, especially if the formulation is based on a high amount of lipid binders. During the spheronization step process, high material temperatures led to stickiness of material fast particles agglomeration. Longer process times could not be achieved, avoiding the obtainment of spherical pellets. Therefore, a new approach to control this parameter was suggested. The employment of an alternative heating source on the conventional spheronizer was investigated. An IR light was used as external source of heat.

The control of the IR light power supply provided an improved control of the material temperature during the entire process. This new control allowed to maintain the material temperature constant in a pre-defined and adequate range, avoiding material stickiness and the formation of agglomerates, even for extrudates based on higher lipid proportions. Despite qualitative and quantitative differences in the investigated formulations, the material temperature of each lipid extrudate was maintained at similar ranges. Micropellets exhibiting comparable shape and narrow particle size distributions were obtained and ARs below 1.3 were successfully achieved for the all investigated formulations, with exception of the PMHGT<sub>50</sub>, which showed a slightly

higher value. Furthermore, the lipid micropellets based on more than 70% (w/w) of a lipid mixture containing hard fat, glyceryl distearate, and trimyristin showed prominent taste-masked properties due to a slower drug release within the first 2 min of dissolution.

The micropellet formulation showing most prominent taste-masked properties and immediate drug release profile was chosen to the development of the ODTs. For the investigation of the impact of compression force and amount of two mannitol based ready-to-use excipients (Ludiflash® and Parateck® ODT) on the properties of tablets produced with these lipid micropellets, a DoE was performed. An eccentric press machine dotted of 15 mm flat-faced punches was used. The tablets based on Parateck® ODT showed a strong lamination phenomenon during the ejection phase. Therefore, it was not feasible to characterize these tablets and produce a DoE model to investigate the Parateck® ODT influences. Under those circumstances, only the DoE for the formulations based on Ludiflash® was evaluated. The increase in the compaction force led to an increase in the tensile strength and disintegration time of the tablets. On the other hand, the increase in the amount of Ludiflash® generates tablets exhibiting faster disintegration times and lower tensile strengths. Considering the specifications for tablets and ODTs in the Ph. Eur. (2014) regarding friability and disintegration time, a formulation containing 50% (w/w) of Ludiflash® and a compaction force of 7.5 kN were required to obtain adequate ODTs.

Taste-masked properties and immediate drug release profile showed by the lipid micropellets were not influenced by the compression process. Moreover, the taste-masked properties of the ODTs were further improved by the establishment of a lag-time in the drug release profile. The presence of mannitol in the ready-to-use excipient showed a change on electronic tongue sensor responses, which indicated an improvement in the taste-masked properties. SEM images depicted that the lipid micropellets are deformed and do not suffer crush or breakage during the compaction step. ODTs presenting disintegration times below 2 min and exhibiting low friability and 500 mg of metformin were successfully produced.

To conclude, SLCE/spheronization using a new spheronization process showed to be a robust method to better control the material temperature during the process and the quality of the produced pellets. A further direct compression of the lipid micropellets using Ludiflash® as disintegration excipient showed to be a feasible methodology to produce adequate taste-masked ODTs containing high drug load of metformin HCl.

## 6. Zusammenfassung

Handelsübliche Metformin HCl Tabletten weisen eine besonders große Dimension auf, wodurch die Patienten Compliance während der Behandlung von Diabetes mellitus negativ beeinflusst wird. Darüber hinaus wird durch das Zerkleinern und Untermischen solcher Tabletten in Speisen und Getränke der bittere Geschmack des Wirkstoffs wahrgenommen, wodurch die Chance auf eine erfolgreiche Einnahme des Medikaments, insbesondere bei älteren Patienten, weiter reduziert wird. Daher liegt der Fokus der vorliegenden Arbeit auf der Entwicklung, Herstellung und Charakterisierung von orodispersiblen Tabletten (ODTs), hergestellt aus geschmacksmaskierten, lipidbasierten Mikropellets mit Metformin HCl.

Um Pellets mit geschmacksmaskierenden Eigenschaften zu erhalten, wurde eine neu entwickelte Extrusions/Spheronisations-Methode für feste Lipide benutzt: die festen Hilfsstoffe werden hierbei zusammen mit dem Arzneistoff extrudiert und im Folgenden spheronisiert. Die Herstellung von Extrudaten mit kleinem Durchmesser, basierend auf festen Lipiden verschiedener Qualität und Zusammensetzung, wurde untersucht. Extrudate mit unterschiedlichen Freisetzungskinetiken und korrelierenden Mengen an eingesetzten Lipiden wurden erhalten. Da das Prinzip der Geschmacksmaskierung der SLCE auf der Modifizierung der Wirkstofffreisetzung und der damit verbundenen Reduktion des Kontakts des Wirkstoffs mit den Geschmacksrezeptoren auf der Zunge und der Mundhöhle beruht, wurden alle Extrudatformulierungen, auch die mit einer verzögerten Wirkstofffreisetzung, spheronisiert.

Die Materialtemperatur während der Spheronisation der lipidbasierten Extrudate war dabei der kritischste Faktor der entwickelten Methode. Während des Spheronisationsschrittes führen hohe Materialtemperaturen zu klebrigen Partikeln und ferner zu Agglomeration. Längere Prozesszeiten können daher nicht erreicht werden, was ein Erhalten von sphärischen Partikeln verhindert. Auch wenn diese Aspekte kürzlich beschrieben wurden, gibt es keine Problemlösungsansätze in der Literatur, insbesondere wenn die Formulierung auf einem hohen Anteil an Lipid basiert. Der Einbau einer alternativen Heizquelle in Form einer IR-Wärmelampe, in einen konventionellen Spheronizer wurde in der vorliegenden Arbeit untersucht.

Die Kontrolle der Energieversorgung des IR Lichts ermöglichte eine verbesserte Kontrolle der Materialtemperatur während des gesamten Prozesses. Dies erlaubte das Einhalten konstanter Materialtemperaturen in einem vordefinierten und adäquaten Bereich, was die Klebrigkeit des Materials verringerte und die Formation von Agglomeraten verhindern konnte. Dies galt auch für Extrudate mit einem höheren Lipidanteil. Trotz der Unterschiede in Qualität und Zusammensetzung der untersuchten Formulierungen, konnte die Materialtemperatur aller Lipidextrudate im

gleichen Bereich gehalten werden. Mikropellets vergleichbarer Form und mit einer engen Partikelgrößenverteilung wurden auf diese Weise hergestellt, die für alle untersuchten Formulierungen eine aspect ratio (AR) von weniger als 1.3 zeigte. Des Weiteren zeigten die Mikropellets basierend auf mehr als 70% (m/m) Lipidmischung, bestehend aus Hartfett, Glyceroldistearat und Trimyristin, ausreichende geschmacksmaskierende Eigenschaften als Folge einer verzögerten Wirkstofffreisetzung in den ersten 2 Minuten.

Die Mikropellet-Formulierung mit den besten geschmacksmaskierenden Eigenschaften und einem schnellfreisetztenden Freisetzungsprofil wurde für die Herstellung der orodispersiblen Tabletten verwendet. Für die Untersuchungen des Einflusses der Kompaktierkraft und dem Anteil zweier, auf Mannitol basierende koprozessierter Hilfsstoff-Fertigmischungen (Ludiflash® und Parateck® ODT) auf die Eigenschaften von Tabletten, hergestellt aus den Lipidmikropellets, wurde ein Statistischer Versuchsplan (DoE) erstellt. Tabletten wurden mit einer Exzenterpresse mit 15 mm biplanen Stempeln hergestellt. Die Tabletten mit Parateck® ODT zeigten ein starkes Deckeln während der Auswurfphase. Daher war es nicht möglich diese Tabletten zu charakterisieren und ein sinnvolles DoE Modell für Parateck® ODT zu erstellen. Aufgrund dessen wurden nur die Zubereitungen mit Ludiflash® für die Erstellung eines DoE Modells verwendet. Eine Erhöhung der Kompaktierkraft führte hierbei zu einer Steigerung der Bruchkraft und der Zerfallszeit der Tabletten. Auf der anderen Seite zeigte eine Erhöhung des Ludiflash® Anteils eine Erniedrigung der Zerfallszeit und der Bruchkraft. Aufgrund der Spezifikationen des Ph. Eur. für Tabletten und ODTs bezüglich der Friabilität und der Zerfallszeit wurde eine Zubereitung mit 50% (m/m) Ludiflash® und einer Kompaktierkraft von 7,5 kN für die Herstellung von ODTs mit adäquaten Eigenschaften ausgewählt.

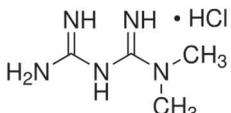
Geschmacksmaskierende Eigenschaften und ein schnelles Freisetzungsprofil der Lipidmikropellets wurden auch nach der Tablettierung beibehalten. Zusätzlich wurden diese Eigenschaften durch den Kompaktiervorgang und dem zusätzlichen Einsatz von Mannitol innerhalb des gebrauchsfertigen Hilfsstoffs verstärkt. REM Aufnahmen zeigten, dass die Lipidmikropellets zwar deformiert wurden, aber während des Kompaktiervorgangs weder zerdrückt noch zerbrochen werden. ODTs mit einer Zerfallszeit von weniger als 2 Minuten und einer niedrigen Friabilität mit 500 mg Metformin HCl wurden erfolgreich produziert.

Zusammenfassend lässt sich sagen, dass Lipidextrusion/Spheronisation mit einer neuen Spheronisationsmethode eine robuste Methode zur besseren Kontrolle der Materialtemperatur während des Prozesses darstellt. Eine anschließende Kompaktierung der Lipidmikropellets mit Ludiflash® als Zerfallhilfsmittel zeigte eine praktikable Methode, um erstmalig adäquat geschmacksmaskierte ODTs mit einer hohen Wirkstoffbeladung von Metformin HCl zu herzustellen.

## 7. Material and Methods

### 7.1. Materials

**Table 7.1.** Employed API

Properties	Metformin hydrochloride
Chemical name	1,1-Dimethylbiguanide hydrochloride*
IUPAC name	1-carbamimidamido-N,N-dimethylmethanimidamide
Source	Wanbury, Maharashtra, India
Used batch	MSB-0450112
Primary reference standard (CRS)	EDQM, European Pharmacopoeia; batch: 3.0; ld: 00098Y3
Molecular formula	C <sub>4</sub> H <sub>11</sub> N <sub>5</sub> .HCl
Molecular weight	165.63
CAS	657-24-9 (metformin); 1115-70-4 (metformin hydrochloride)
Melting point	222 - 225 °C*
Chemical structure	
Solubility	Soluble in water (50 mg·mL <sup>-1</sup> ), ethanol, and DMSO
Description	(50 mM)** White crystals. Freely soluble in water; slightly soluble in alcohol; practically insoluble in acetone and in dichloromethane**

\*Ph. Eur. (2014)

\*\*Bretnall and Clarke (1998)

**Table 7.2.** Excipients used in the extrusion process

Substance	Commercial name	Batch	Company
Hard fat	Witocan® 42/44 Mikrofein	911028	Cremer Oleo, Witten, Germany
Glyceryl distearate	Precirol® ATO 5	195303	Gattefossé, Weil am Rhein, Germany
Glyceryl trimyristate	Dynasan® 114	007168	Cremer Oleo, Witten, Germany

**Table 7.3.** Pharmaceutical excipients used in the ODT development

Substance	Commercial name	Batch	Company
Co-processed excipient	Ludiflash®	1670090T0	BASF, Ludwigshafen, Germany
Co-processed excipient	Parteck® ODT	F1562390926	Merck, Darmstadt, Germany

**Table 7.4.** Other used substances

Substance	Commercial name	Batch	Company
Methanol HPLC grade		1497081	Fisher Scientific, Loughborough, UK
Polysorbate 20		80479398	Caesar & Loretz, Hilden, Germany
Phosphoric acid	Rotipuran®	269103931	Carl Roth, Karlsruhe, Germany
Potassium dihydrogen phosphate		3M000923	AppliChem, Darmstadt, Germany
Brilliant blue 85 E 133	Sicovit®	70-3998	BASF, Ludwigshafen, Germany

## 7.2. Preparative Methods

### 7.2.1. Pre-Formulation Studies of Solid Mixtures for the Preparation of Lipid Extrudates

To investigate possible morphological, chemical and/or morphological-chemical interactions, as well as potential incompatibilities between the excipients and metformin HCl, pre-formulation studies were performed using mixtures of metformin HCl and solid lipid binders chosen for the production of extrudates. Metformin HCl was milled using a centrifugal mill (ZM 200, Retsch, Haan, Germany) doted of a 1.0 mm sieve, at 6000 rpm. The lipid powders were sieved manually trough a 350 µm sieve. Mixtures in ratios of 1:1 (w/w) and other proportions (Table 7.5) were prepared in porcelain capsules.

**Table 7.5.** Mixture ratios

Mixture	Proportion (w/w)
Hard fat : metformin HCl (MH)	1:1
Trimyristin : metformin HCl (MT)	1:1
Glyceryl distearate : metformin HCl (MG)	1:1
Hard fat : trimyristin : glyceryl distearate : metformin HCl (MHGT)	1:1:1:1

### 7.2.2. Solid Lipid Cold Extrusion

The solid lipid cold extrusion was performed in a (Figure 7.1) co-rotating twin screws extruder (Micro 27GL-28D, Leistritz, Nuremberg, Germany). The excipients and the API were previously sieved through a 350 µm sieve and blended in a laboratory mixer (LM20, Bohle, Ennigerloh, Germany) for 15 min, at 25 rpm. The investigated formulations are described in Table 7.6. The powder blend (500 g) was transferred to a gravimetric powder feeder (KT20 K-Tron Soder, Lenzhard, Switzerland), coupled to the extruder. For the extrusion process, an axial screen plate with 91 dies of 0.5



mm in diameter and length of 1.35 mm was used. This extruder model is equipped with co-rotating screws of 850 mm length and seven individual barrels that allow the control of the process temperature in different segments of the equipment. As screw configuration a setup of only conveying elements was initially chosen regarding the work of Krause *et al.* (2009).



**Figure 7.1.** Leistritz Micro 27GL-28D extruder

**Table 7.6.** Investigated formulations for the lipid extrusion process

Batch name	Proportion (%; w/w)					
	MH <sub>80</sub>	MH <sub>70</sub>	MH <sub>50</sub>	MHGT <sub>80</sub>	MHGT <sub>70</sub>	MHGT <sub>50</sub>
Metformin HCl	80.0	70.0	50.0	80.0	70.0	50.0
Hard fat	20.0	30.0	50.0	15.0	22.5	37.5
Trimyrustin	-	-	-	2.5	3.75	6.25
Glyceryl distearate	-	-	-	2.5	3.75	6.25

M = metformin HCl; H = hard fat; T = trimyrustin; G = glyceryl distearate

The applied screw configuration is depicted schematically in Figure 7.2. Conveying elements (GFA and GFF) were inserted in order to decrease the pitch size from 40 to 20 mm. This setup consists in three distinct zones: zone (1) with elements of a pitch size of 40 mm, zone (2) with elements of a pitch size of 30 mm, and zone (3) with elements of a pitch size of 20 mm, representing, respectively, 44.4%, 22.2% and 33.3% of length of the total screw set. Six of the seven barrels were set to 25 °C during the process. As no direct temperature control of the screen plate is possible, the barrel next to the axial screw was adjusted to 33 °C. The extrusion was performed at a constant screw speed of 50 rpm and powder feed rate of 40 g·min<sup>-1</sup>. For each batch, 300 g of extrudates were collected.

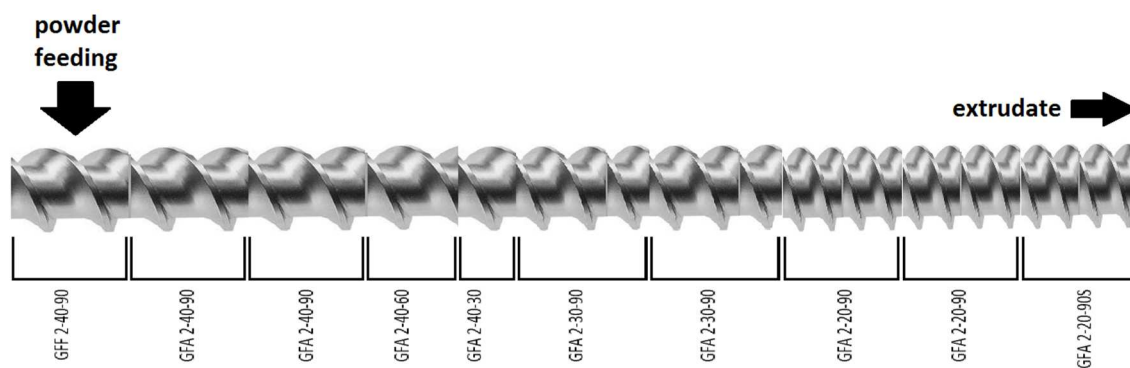


**Figure 7.2.** Extruder screw configuration used for solid lipid extrusion (adapted from Thiele (2003))

### 7.2.3. Lipid Spheronization

Batches of 300 g of lipid extrudates were transferred into a spheronizer (RM-300, Schlüter, Neustadt, Germany). The device was equipped with a cross-hatched rotor plate of 300 mm in diameter (Figure 7.3) and a water jacket heating system. The lipid extrudates were spheronized for 15 min at 1500 rpm. The spheronizer jacket temperature was adjusted to 33 °C with the help of a refrigerated heating circulator (Haake K40-DC50, Thermo Fisher Scientific, Karlsruhe, Germany). Samples of around 2 g were collected each minute for further evaluation of particle size distribution and particle shape during the process. The material temperature was measured contact-free using an infrared thermometer (LaserSight, Optris, Berlin, Germany). During the temperature measurements, the thermometer was positioned at the upper shell of the spheronizer. The spot size with a constant diameter of 16 mm was aimed at the surface of the rotating particles bed at a distance of approximately 17 cm. The temperature measurements were recorded using the software Optris Connect® v. 2.0.5 (Optris, Berlin, Germany). The temperature precision of the equipment is  $\pm 0.75$  °C. The obtained pellets were sieved and the fraction between 250  $\mu\text{m}$  and 1000  $\mu\text{m}$  was further evaluated.

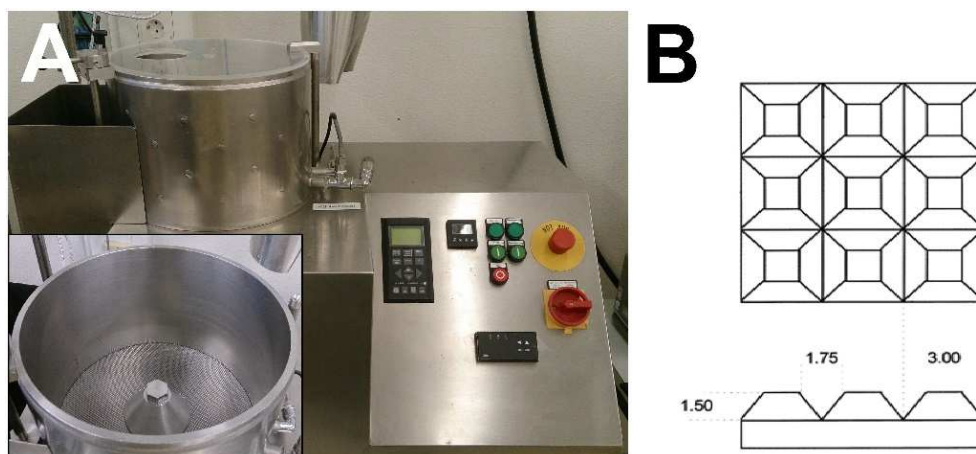


**Figure 7.3.** (A) Spheronizer Schlüter RM-300 with the spheronization chamber highlighted and (B) the used cross-hatched friction plate (figure adapted from Schmidt and Kleinebudde (1998))

### 7.2.4. Orodispersible Tablets Preparation

The tablets were developed on an instrumented single-punch press machine (EK0, Korsch, Berlin, Germany) using 15 mm flat-faced punches. For the investigation of the ODT production, the lipid based pellets presenting the most adequate properties were selected. The amount of pellets was adjusted for ODTs containing a dose of 500 mg of metformin HCl. Two co-processed excipients based on mannitol for the production of ODT by direct compression were investigated (Ludiflash® and Parateck® ODT). Their composition are shown in Table 7.7. The excipient and the lipid pellets were blended in a laboratory mixer (LM20, Bohle, Ennigerloh, Germany) for 15 min, at 25 rpm. Batches of 100 tablets were produced.

**Table 7.7.** Investigated co-processed disintegrants composition (Chaudhary *et al.*, 2010)

	Ludiflash®	Parateck® ODT
Composition	90% mannitol	mannitol
	5% crospovidone (Kollidon® CL-SF)	croscarmellose sodium
	5% polyvinyl acetate (Kolliccoat® SR 30D)	

### 7.2.5. Compaction Design of Experiments (DoE)

Tablets containing 500 mg of metformin HCl were aimed. The influence of the compression force and amount of two commonly used co-processed excipients (Ludiflash® and Parateck® ODT) on the tablet disintegration time, friability, and tensile strength was investigated. The conception and statistical evaluation of the experimental project to the development of metformin HCl containing ODTs was performed with help of Software Modde v. 9.0 (Umetrics, Umea, Sweden). The quality of the design was described by the goodness of fit ( $R^2$ ), goodness of prediction ( $Q^2$ ), reproducibility, and validity. The complete model equation for the tablet friability and tensile strength contains 2 factors, 2 quadratic and one interaction term as shown in the following equation:

$$y = \beta_0 + \beta_{Exc \cdot Exc} + \beta_{Com \cdot Com} + \beta_{Exc \cdot Exc} X_{Exc}^2 + \beta_{Com \cdot Com} X_{Com}^2 + \beta_{Exc \cdot Com} X_{Exc} X_{Com} \quad \text{Equation 7.1}$$

Due to the significant error ( $\alpha = 0.005$ ) of the interaction effect on the disintegration time, this term was removed and a new model equation was used (Equation 7.2).

$$y = \beta_0 + \beta_{Exc \cdot Exc} + \beta_{Com \cdot Com} + \beta_{Exc \cdot Exc} X_{Exc}^2 + \beta_{Com \cdot Com} X_{Com}^2 \quad \text{Equation 7.2}$$

## 7.3. Analytical Methods

### 7.3.1. Loss on Drying

The loss on drying assay was performed in accordance with the method 2.2.32 described in the Ph. Eur. (2014). Samples of 1.0 g of metformin HCl were weighed using an analytical balance (Sartorius, Göttingen, Germany) and transferred to a previously tared weighing glass. The samples were placed in a circulating air oven (Kelvitron® T, Heraeus Instruments, Hanau, Germany) at 105 °C for a period of 5 hours. Furthermore, the sample was cooled in desiccator, containing dried silica gel beads, and weighed again. This procedure was repeated until constant weight. For metformin HCl a maximum of 0.5% (w/w) is defined as acceptable (Ph. Eur., 2014). The assay was carried out in triplicate. For the ODTs the same procedure was performed with 6 tablets, measured individually.

### 7.3.2. Laser Diffraction

The particle size and size distribution were determined by laser diffractometry. The laser diffraction particle size analyzer (Helos H1402+, Sympatec, Clausthal-Zellerfeld, Germany) was equipped with a helium-neon laser, which emits a coherent monochromatic light at a wavelength of 632.8 nm. A Fourier lens is located on the other edge of the measuring zone and capture the diffraction pattern produced by the particles that flow through the measuring zone. For the characterization of metformin HCl and the excipients the set of lens R5 was chosen (particle size range: 0.5/4.5-875 µm; focal distance: 500 mm).

The equipment is equipped of a vibratory feeder (Sympatec, Clausthal-Zellerfeld, Germany), which was adjusted to 50% of vibration rate, and a dry dispersing system (Rodas, Sympatec, Clausthal-Zellerfeld, Germany). The dispersing pressurized air need to be adjusted to the characteristics of the investigated material to achieve the splitting of agglomerates without milling the primary particles. To the characterization of the metformin HCl powder, the dispersion pressure was adjusted to 4.0 bar to split existent agglomerates and to properly disperse the particles. The amount of used material was adjusted until an optical concentration between 5 and 10% was achieved. The results were recorded and evaluated using Windox® 4.0 software (Sympatec, Clausthal-Zellerfeld, Germany).

The provided particle size distribution values 10%, 50%, and 90% quantile ( $d_{10}$ ,  $d_{50}$  and  $d_{90}$ , respectively), were used to calculate the width of the particle size distribution (span) according to the following equation (Heng *et al.*, 2001):

$$\text{span} = \frac{d_{90} - d_{10}}{d_{50}} \quad \text{Equation 7.3}$$

### 7.3.3. Bulk and Tapped Densities, Hausner Factor, and Carr's Index

The determination of the tapped and bulk densities was performed using a tapped density tester (STAV II, J. Engelsmann, Ludwigshafen am Rhein, Germany) according to the Ph. Eur. (2014). 100 g of the material was previously weighed on a semi-analytic balance (KB BA 100, Sartorius, Göttingen, Germany) and was carefully transferred to a 200 mL glass cylinder. The bulk volume ( $V_b$ ) was measured. The cylinder was positioned in the equipment and five taps were performed. The material volume was measured and recorded as tapped volume ( $V_t$ ). Furthermore, the material was submitted to sequential 10 ( $V_{10}$ ), 500 ( $V_{500}$ ) and 1250 ( $V_{1250}$ ) taps. The volumes were recorded respectively. The assay was continued until a difference smaller than 0.1 mL was observed, and this volume was recorded as the material tapped volume ( $V_t$ ). The bulk and tapped densities ( $d_b$  and  $d_t$ , respectively) were calculated using the values of the  $V_b$  and  $V_t$ , respectively, and the mass of the sample.

The Hausner factor (HF) was determined by the ratio of the tapped and bulk densities (Equation 7.4) (Hausner, 1967). For the calculation of the compressibility index or Carr's index (CI) (Equation 7.5) the data obtained for bulk and tapped densities was used as well (Carr, 1965). The evaluation was carried out in triplicate.

$$\text{HF} = \frac{d_t}{d_b} \quad \text{Equation 7.4}$$

$$\text{CI} = \left(1 - \frac{1}{\text{HF}}\right) \cdot 100 \quad \text{Equation 7.5}$$

### 7.3.4. Differential Scanning Calorimetry (DSC)

The thermal characteristics of the substances were investigated using differential scanning calorimeter (DSC1, Mettler Toledo, Columbus, USA). For the characterization, samples of 2 to 5 mg were weighed in a 40  $\mu\text{L}$  aluminum pan with help of a micro balance (XP56, Mettler Toledo, Giessen, Germany). The pan was hermetically closed. An empty aluminum pan was used as reference. A heating rate of 10  $^{\circ}\text{C}\cdot\text{min}^{-1}$  and nitrogen gas flow of 50  $\text{mL}\cdot\text{min}^{-1}$  were applied. For the assay of metformin HCl and obtained lipid extrudates and pellets, a heating range from 0 to 300  $^{\circ}\text{C}$  was set; and for the lipids assay a heating range from 0 to 150  $^{\circ}\text{C}$  was adjusted.

The measurements were conducted in duplicate. Indium and Zinc were used to calibrate the temperature and the melting enthalpies. The plot of the results was carried out considering the weighted sample mass.

### **7.3.5. X-Ray Powder Diffractometry (XRPD)**

The crystallographic profile characterization was held in an X-ray diffractometer (X'Pert Pro MPD, PANalytical, Almelo, the Netherlands). The sample was placed in a sample-holder with a 13 mm matrix and pressed manually. The equipment geometry setup is based on the Bragg-Brentano principle, in which the height of the X-ray radiation source and the detector adjust themselves separately. The sample-holder was placed in the center of the equipment and is kept in a horizontal position, while it moves itself at one rotation per second in its own axis. The analysis was performed in transmission mode and a copper anode with  $K\alpha$  radiation was used ( $\lambda = 1.5406 \text{ \AA}$ ). The analysis range was performed from 10 to 70 degrees; with an increment of 0.02 degrees and reading time of 1 second per point.

### **7.3.6. Scanning Electron Microscopy (SEM)**

The surface morphology was evaluated using a scanning electron microscope (Phenom<sup>®</sup> G2 PRO Desktop SEM, Phenom-World, Eindhoven, the Netherlands). A small amount of material was placed on a bi-adhesive tape, which was attached to a sample-holder. The sampler-holder consists of a small metal disc that is attached to a height adjustable connector. The images were taken at acceleration voltage of 10 kV and acquisition rate of 5.8 Hz.

### **7.3.7. Optical Microscopy**

Images were taken using a system consisting of a stereomicroscope (Leica KL 1500, Cambridge, UK), a digital camera (D300, Nikon, Langen, Germany), and the image software Leica QWin<sup>®</sup> (Leica Microsystems Cambridge, Cambridge, UK).

### **7.3.8. Particles Flowability**

The evaluation of metformin HCl powder flow behavior was performed using a ring shear cell (RST-01.pc, Dr. Dietmar Schulze Schüttguttechnik, Wolfenbüttel, Germany). The sample was submitted to a normal pressure of 5.0 kPa and to sequential shearing force of 1.0, 2.0, 3.0 and 4.0 kPa. The collected data was evaluated by Control 95 software provided by the manufacturer. The evaluation was performed in triplicate.

Flowability of a bulk solid is characterized mainly by its unconfined yield strength ( $\sigma_c$ ) in dependence on consolidation stress ( $\sigma_1$ ). Usually the ratio of consolidation stress to unconfined yield strength ( $ff_c$ ) is used to characterize flowability numerically according to the Equation 7.6 (Jenike, 1964).

$$ff_c = \frac{\sigma_1}{\sigma_c} \quad \text{Equation 7.6}$$

The larger the  $ff_c$  is, the smaller the ratio of the unconfined yield strength to the consolidation stress, the better a bulk solid flows (Table 7.8).

**Table 7.8.** Powder flowability classification (Jenike, 1964)

$ff_c$	Flowability
$ff_c < 1$	not flowing
$1 < ff_c < 2$	very cohesive
$2 < ff_c < 4$	cohesive
$4 < ff_c < 10$	easy-flowing
$ff_c > 10$	free-flowing

### 7.3.9. Solid Fat Content Analysis

Solid fat content (SFC) measurements of the lipids extrudates were performed using a differential scanning calorimeter (DSC1, Mettler Toledo, Columbus, USA). Samples of approximately 5 mg were prepared as described in section 7.3.4, and heated in a temperature range from 25 to 100 °C, at a heating rate of 1 °C·min<sup>-1</sup>. The SFC was determined as the total fat content minus the amount of the melted lipid. The measurement was performed in duplicate. The values were determined by the area under the curve in the respective temperature ranges according to Khan and Craig (2004).

### 7.3.10. Helium Pycnometer Density

Helium density measurements were performed using a helium pycnometer (AccuPyc® 1330, Micromeritics, USA). A sample cylinder with a volume of 10 cm<sup>3</sup> was used. The sample was placed in the cylinder until a maximum 2/3 of its volume and flushed with helium tenfold with a pressure of 134.55 kPa. The measurements were performed at 25 ± 0.1 °C. The density was determined as average of three measurements.

### 7.3.11. Drug Content of Lipid Extrudates and Micropellets

Liquid chromatography was carried out on a Hitachi HPLC (LaChrom Elite, Hitachi, San Jose, USA). Isocratic mobile phase: methanol-phosphate buffer (0.01 mol·L<sup>-1</sup>, pH

4.0) in the ratio of 80:20 (V/V), at a flow rate of  $1 \text{ mL} \cdot \text{min}^{-1}$  (LaChrom Elite L-2130, Hitachi, San Jose, USA). A Hypersil ODS column (250 x 4.6 mm, 5  $\mu\text{m}$  particle size) was employed and heated to 30 °C by a column oven (LaChrom Elite L-2300, Hitachi, San Jose, USA). Injection of 20  $\mu\text{L}$  were performed by an auto sampler (LaChrom Elite L-2200, Hitachi, San Jose, USA.). The detection was performed by UV detection at a wavelength of 232 nm (LaChrom Elite UV-Vis detector L-2400, Hitachi, San Jose, USA).

A calibration was previously performed. A standard solution was prepared dissolving 50 mg of metformin HCl (EDQM primary standard reference) in 500 mL methanol-water solution (80:20; V/V). Volumetric aliquots of the standard solution were separately diluted with 100 mL of the methanol-water solution to obtain concentrations of 0.01, 0.02, 0.03, 0.04, 0.05 and 0.06  $\text{mg} \cdot \text{mL}^{-1}$ . The calibration was performed in triplicate.

Sample preparation: amounts of extrudates or pellets containing around 0.1 g of metformin HCl were dissolved in 250 mL of purified water using an ultrasound bath at 40 °C for 40 min. 1 mL aliquots were volumetrically taken and diluted to 10 mL with a methanol-water solution (80:20; V/V) to achieve a concentration of 0.04  $\text{mg} \cdot \text{mL}^{-1}$  of metformin HCl. The samples were filtrated and placed in HPLC vials. Each sample was prepared 10 times.

### **7.3.12. Dissolution Studies of Lipid Pellets and Extrudates**

The metformin HCl release assay from lipid based extrudates and micropellets was performed in a dissolution tester (AT7 Smart, Sotax, Loerrach, Germany) using basket apparatus according to Ph. Eur. (2014). Amount of extrudates containing 10 mg of metformin HCl were weighted. The basket method was employed to prevent the flotation of the extrudates and to ensure complete wetting during dissolution assay. The assay was performed during 2 hours at 150 rpm with sample measurement each 2 min. The dissolution media consisted of 900 mL of demineralized water containing 0.001% (w/w) polysorbate 20, at  $37 \pm 0.5$  °C. The measurement of the drug release was performed using an UV/Vis spectrophotometer (Lambda 40, Perkin Elmer, Rodgau, Germany) in a continuous flow-through cuvette of 1.0 mm, at a wavelength of 232 nm. Previously, a calibration was performed (considering the Lambert-Beer absorption linear range between 0.1 and 1.2) (Annex II). Solutions of metformin HCl in demineralized water containing 0.001% (w/w) polysorbate 20, at concentrations from 0.025 to 0.15  $\text{mg} \cdot \text{mL}^{-1}$ , were prepared. Each solution was evaluated at a wavelength of 232 nm. Three calibrations were performed.



### 7.3.13. In-line Drug Release of Lipid Pellets, Extrudates, and ODTs

For in-line measurements an UV transmission probe (T300-RT-UV-VIS, Ocean Optics, Ostfildern, Germany) with a path length of 10 mm, connected via an optical fiber with a deuterium light source (Mikropak<sup>®</sup> DH-2000, Ocean Optics, Ostfildern, Germany), was used. A previously calibration was performed considering the Lambert-Beer absorption linear range between 0.1 and 1.2 (Annex II). Solutions of metformin HCl in demineralized water containing 0.001% (w/w) of polysorbate 20 at concentrations from 0.001 to 0.015 mg·mL<sup>-1</sup>, were prepared. Each solution was evaluated using the UV probe, at a wavelength of 232 nm. The calibration was performed in triplicate.

A pre-defined sample amount of lipid extrudate or pellets (corresponding to 10 mg of metformin HCl) was placed in a cylindrical metallic sinker (diameter: 16 mm, height: 19 mm) with a mean mesh size of 0.25 mm. Regarding the ODTs samples, individual tablets were placed manually at the bottom of the vessel before starting the assay. The dissolution media consisted of 900 mL of demineralized water containing 0.001% (w/w) polysorbate 20 at 37 ± 0.5 °C. A paddle apparatus set up was employed (Figure 7.4a). The UV probe was positioned 1 cm away from the paddle and paddle rod (Figure 7.4b). The base of the paddle was adjusted to a distance of 2.5 cm from the bottom of the vessel and set to 100 rpm. The UV light intensity was previously adjusted to a value between 40,000 and 60,000 through adjustment of the integration time of the measurements. The data was collected using SpectraSuite<sup>®</sup> v.2.0.162 Software (Ocean Optics, Ostfildern, Germany).

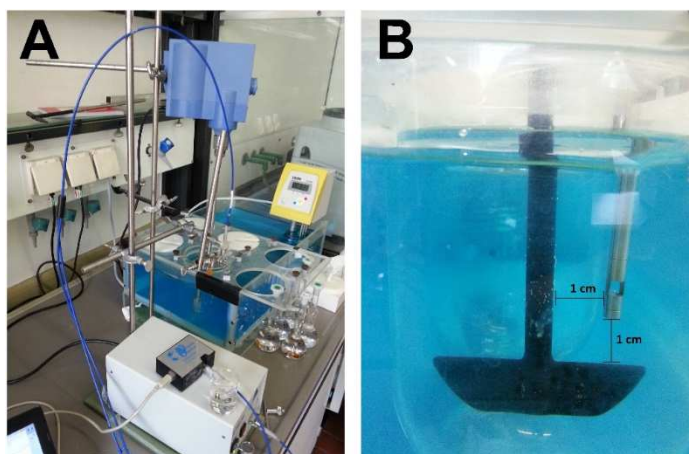


**Figure 7.4.** In-line drug release assay: (A) equipment set up and (B) positioning of the UV probe in the vessel

### 7.3.14. Particle Size Distribution and Particular Shape of Lipid Micropellets

The particle size distribution was determined using a Camsizer<sup>®</sup> XT (Retsch Technology, Haan, Germany). The 10%, 50% and 90% quantile ( $d_{10}$ ,  $d_{50}$ , and  $d_{90}$ , respectively) were recorded, and the aspect ratio (AR) was determined as the ratio between the particle Feret diameter which is the longest chord of the measurement particle projection (particle width, B) and the particle diameter which is the longest Feret diameter of the measured particle projection (particle length, L) according to the following equation:

$$AR = \frac{L}{B} \quad \text{Equation 7.7}$$

The 10%, 50% and 90% quantile and the AR are calculated and recorded by the CamiszerXT64 software v.7.3.12 (Retsch technology, Hann, Germany). Samples of around 50,000 particles were measured in triplicate. The particle size distribution width (span) was calculated according to the Equation 7.3, as described in section 7.3.2 (see page 124).

### 7.3.15. Electronic Tongue Measurements

All measurements were performed using a taste sensing system (TS-5000Z, Insent, Atsugi-Chi, Japan). This so called electronic tongue is equipped membrane sensors providing different taste qualities (umami, saltiness, sourness, astringency, bitterness and sweetness) and corresponding reference electrodes. However, only seven sensor were used; the sweetness sensor was not used. The employed set of sensors is shown in Table 7.10.

Standard solution of 30 mM KCl and 0.3 mM tartaric acid and different washing solutions for sensors with positive and negative charged membranes were prepared. Sample measurement followed a standard procedure, according to Woertz *et al.* (2010). The first phase included the washing of the sensors for 330 s in three different beaker sets containing ethanol washing solutions or the standard solution. The second phase consists of conditioning the sensor output for 30 s in the next set of standard solution. Each sample was measured for 30 s and the sensor outputs after this time were recorded, afterwards the sensors were dipped shortly (3 s) in two standard solution beaker sets for cleaning. Each sample was tested four times and the first measurement was discarded.

**Table 7.10.** Sensors for the taste sensing system and corresponding taste sensations

Sensor type	Sensor name	Corresponding taste sensation
SB2AAE	umami sensor	umami
SB2CT0	saltiness sensor	saltiness
SB2CA0	sourness sensor	sourness
SB2AE1	astringency sensor	astringency
SB2AC0	bitterness sensor 1	bitterness of cationic substances
SB2AN0	bitterness sensor 2	bitterness of cationic and neutral substances
SB2C00	bitterness sensor 3	bitterness of anionic substances
Reference electrode		

### 7.3.15.1. Electronic Tongue Calibration Procedure

Solutions of metformin HCl were prepared dissolving samples from 1.0 to 1500 mg in 100 mL demineralized water. A volume of 10 mL of each solution was volumetrically transferred to a volumetric flask of 100 mL and filled with demineralized water. The final concentrations of metformin HCl solutions were respectively: 0.01, 0.1, 0.5, 1.0, 2.5, 5.0, 8.5, 10.0 and 15.0 mg·mL<sup>-1</sup>. The samples were filtered through filter paper and measured by the electronic tongue system.

### 7.3.15.2. Sample Preparation for Electronic Tongue Measurements

For the taste assessment of the different lipid pellet formulations, defined amounts of the pellets, corresponding to 500 mg of metformin HCl, were stirred in a glass beaker with 100 mL demineralized water at 37 °C using a magnetic stirrer for 30 and 60 s. Subsequently, the samples were filtered through a paper filter, using a vacuum pump and direct evaluated. As unpleasant taste reference, an aqueous solution containing 500 mg of metformin HCl was parallel prepared and measured at the same time with the samples. A 0.5 mM quinine solution and a drug-free formulation containing only lipids were also evaluated as bitter and pleasant taste references, respectively.

### 7.3.15.3. Data Evaluation of Taste Assessment

The results were expressed as raw data in mV of the relative measurement of the sample to the reference. The sensor signal results, alone or combined by multivariate data analysis, were evaluated. For the multivariate data analysis, the raw data was pre-treated by mean centering and scaling to unit variance. Data processing and graphical illustration of the results were carried out using Excel 2013 (Microsoft, Redmond, USA) and Simca® v.13.0.3 (Umetrics, Umea, Sweden).

#### 7.3.15.4. Euclidean Distances

To determine the relative distance between the sample and the placebo (p, q) after multivariate data analysis, Euclidean distances were calculated for all the used variables (n) according to equation 7.8. The values were further normalized in percentage considering the distance of the placebo to the bitter reference (metformin HCl) as 100%.

$$d_{(p,q)} = \sqrt{\sum_{i=1}^n \sum_{j=1}^n (p_j - q_i)^2} \quad \text{Equation 7.8}$$

#### 7.3.16. Appearance and Dimensions of Tablets

The appearance of the tablets was evaluated visually by the observation of the uniformity of color and surface aspects. The thickness and diameter of 20 tablets, stored in desiccators, were measured using a caliper (CD-15CPXR, Mitutoyo Deutschland, Neuss, Germany) 24 hours after the compression.

#### 7.3.17. Mass Uniformity of Tablets

The individual weight of the tablets was held in an analytical balance (MC 210P, Sartorius, Göttingen, Germany) according to method 2.9.9 described in the Ph. Eur. (2014), measuring 20 tablets individually.

#### 7.3.18. Tensile Strength of Tablets

The crushing force of 20 tablets was determined individually, measuring the radial crush resistance in a tablet crushing strength apparatus (HT1, Sotax, Aesch, Switzerland). The dimensions (thickness and diameter) of each tablet were previously measured using a Caliper (CD-15CPXR, Mitutoyo Deutschland, Neuss, Germany). The tablets tensile strength ( $\sigma_T$ ) was calculated according to the following equation (Fell and Newton, 2006):

$$\sigma_T = \frac{2 F}{\pi D h} \quad \text{Equation 7.9}$$

where F is the force exert to crash the tablet, D the tablet diameter, and h the tablet thickness (height).

### 7.3.19. Disintegration Time of Tablets

The disintegrating time of six tablets was determined using a disintegration tester (PTZ Auto, Pharma Test Apparatebau, Hainburg, Germany) according to the Ph. Eur. (2014). The disintegration equipment consists of six tubes open at the upper end and closed by a screen at the lower. One tablet was placed in each tube and an acrylic disc with a metal ring was placed over the tablet. The tubes are placed in the medium and are automatically raised and lowered at 30 shakes per minute in the medium, in such a way that at the highest position the tubes, the screen and the tablets remains below the water surface. The assay was performed in demineralized water at 37 °C. The disintegration time is considered to be the time required for the tablet to break up into particles smaller than 2 mm and pass through the screen allowing the contact between the screen and the metal ring present in the acrylic disc generating a signal in the equipment. This contact signal is considered as the end time of the disintegration assay, and it is recorded for each tube.

### 7.3.20. Friability of Tablets

The friability of the tablets was determined using a friability tester (TAR, Erweka, Heusenstamm, Germany) according to the Ph. Eur. (2014). Samples of tablets corresponding to 6.5 g were cleaned using a soft brush before the test, weighed and placed in the device where they suffer 100 drops at a rotational speed of 25 rpm. The tablets will be removed, cleaned and weighted a second time. The friability will be calculated as the percentage of weight lost.

### 7.3.21. Label Claim of Tablets

The label claim of the tablets was evaluated by HPLC using the acceptance criteria in the item 2.9.6 of the Ph. Eur. (2014). 10 tablets were separately crushed and dissolved in 250 mL purified water, sonicated for 40 min at 40 °C. Aliquots of 4 ml were taken, diluted to 100 mL in methanol-water solution (80:20: V/V) and filtered. The assay was carried out using the equipment parameters as described in section 7.3.13.

### 7.3.22. Wetting Time and Water Absorption of Tablets

The wetting time was evaluated using the simulated wetting test according to Park *et al.* (2008). A piece of folded filter paper was placed in a Petri dish of 3.6 cm in diameter and 2.0 cm height. The tablet was placed on the filter. 1.75 mL of an aqueous solution containing 1% (w/V) of brilliant blue 85 E 133 (Sicovit®, BASF,

Ludwigshafen, Germany) was added at the bottom of the Petri dish. The flat tablet face was in contact with the filter paper, and the level of the dye solution did not cover the tablet. The total wetting time was measured, defined as the time required for the blue dye solution to diffuse through the tablet and completely cover the surface. The assay was performed using ten tablets. The same procedure without the brilliant blue solution was carried out to determine the rate of water absorption. The wet tablets were weighed in a semi-analytic balance (Faust, Sartorius, Göttingen, Germany).

### 7.3.23. Dissolution Studies of Tablets

The *in vitro* drug release of the tablets was determined using the paddle method (Ph. Eur., 2014). As dissolution medium 900 mL purified water was used and its temperature was adjusted to  $37 \pm 0.5$  °C. The speed of rotation of the paddles was set to 50 rpm. The dissolution assay was held in a dissolution apparatus (AT6, Sotax, Aesch, Switzerland). Samples of 2 mL were collected at the times 1, 2, 4, 6, 8, 10, 15, 20, 40, 45 and 60 min with help of a syringe coupled to a filter. The collected samples were further analyzed using an UV transmission probe (T300-RT-UV-VIS, Ocean Optics, Ostfildern, Germany) with a path length of 10 mm, connected via an optical fiber with a deuterium light source (Mikropak® DH-2000-BAL, Ocean Optics, Ostfildern, Germany).

### 7.3.24. Dynamic Water Sorption System (SPS11)

The water sorption and desorption of samples were held at 25 °C in a dynamic water sorption system (SPS11, Projekt Masstechnik, Ulm, Germany). One cycle with a step variation of 10% relative humidity was performed, from 0 to 90% and 90 to 0% r.H. The humidity step was automatically changed if after 30 min no mass variation higher than 0.01% was observed. The samples were measured three times.

## 8. Annex

### Annex I

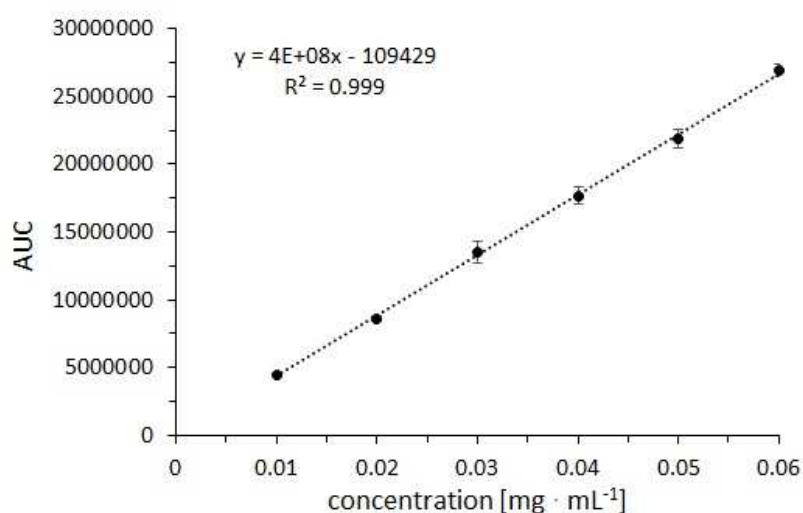


**Figure 8.1.** HPLC calibration curve of metformin HCl. Eluent: methanol-phosphate buffer (80:20; V/V; pH 4.0); flow rate: 1 mL·min<sup>-1</sup>;  $\lambda = 232$  nm (mean  $\pm$  SD, n = 3)

**Table 8.1.** AUC of the calibrations performed by HPLC

Metformin HCl concentration (mg·mL <sup>-1</sup> )	Sample	AUC (mean $\pm$ SD; n = 3)
0.01	1	4424674.67 $\pm$ 83595.50
	2	4516337.00 $\pm$ 186387.72
	3	4463016.00 $\pm$ 178864.37
0.02	1	8464911.00 $\pm$ 44098.36
	2	8764843.33 $\pm$ 343549.74
	3	8626882.67 $\pm$ 195918.40
0.03	1	12746503.30 $\pm$ 387959.735
	2	14353002.30 $\pm$ 1033781.59
	3	13583263.70 $\pm$ 392355.50
0.04	1	16929696.30 $\pm$ 62065.07
	2	18009218.00 $\pm$ 570275.07
	3	18042633.70 $\pm$ 861452.60
0.05	1	21968864.0 $\pm$ 1236782.98
	2	22532413.70 $\pm$ 827898.98
	3	21100248.00 $\pm$ 327066.67
0.06	1	26433423.70 $\pm$ 1010542.75
	2	27276952 $\pm$ 1415207.96
	3	27183743.30 $\pm$ 1997739.25

## Annex II

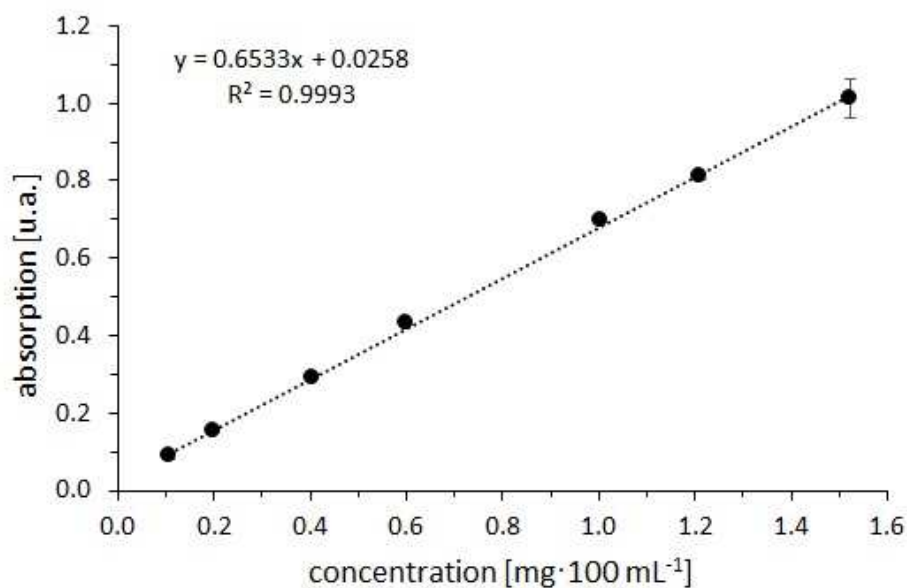


**Figure 8.2.** Calibration curve of metformin HCl on the UV/Vis probe equipment: purified water + 0.001% (w/w) polysorbate 20,  $\lambda = 232$  nm (mean  $\pm$  SD,  $n = 3$ )

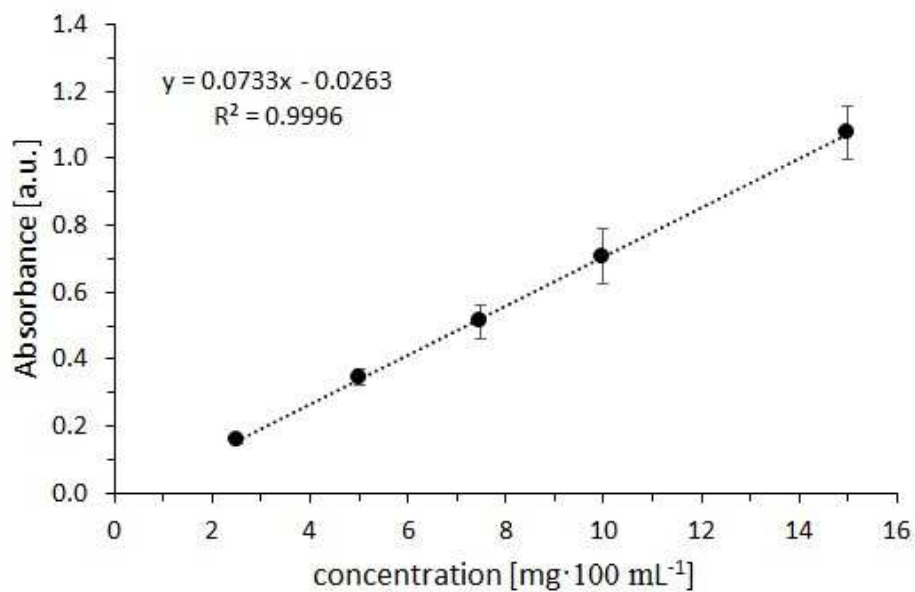


**Figure 8.3.** Calibration curve of metformin HCl in dissolution tester equipment: purified water containing 0.001% (w/w) polysorbate 20,  $\lambda = 232$  nm (mean  $\pm$  SD,  $n = 3$ )



## Annex III

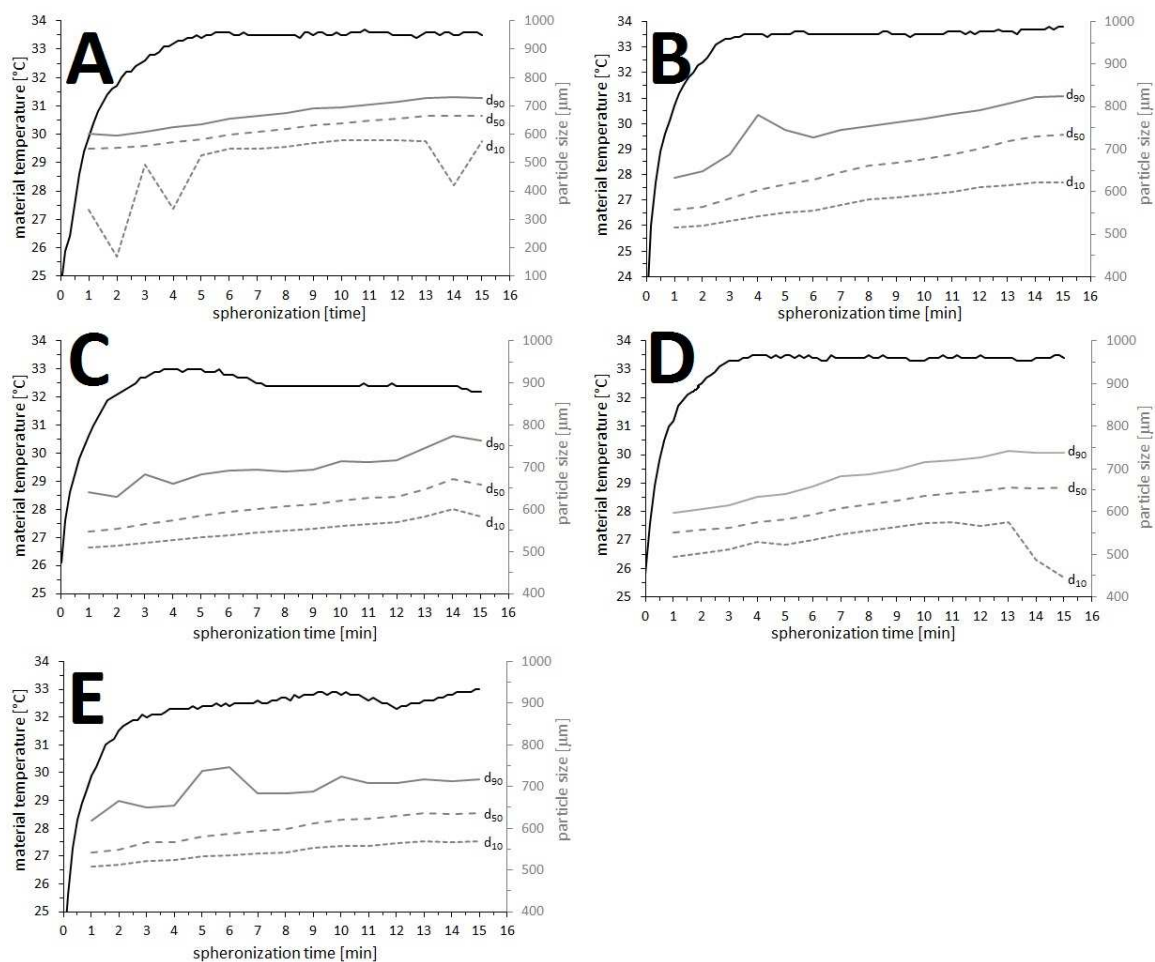


**Figure 8.4.** Comparison between the material temperature and particle size distribution during the spheronization process: (A) PMH<sub>80</sub>; (B) PMH<sub>70</sub>; (C) PMH<sub>50</sub>; (D) PMHGT<sub>80</sub>; (E) PMHGT<sub>50</sub>

## Annex IV

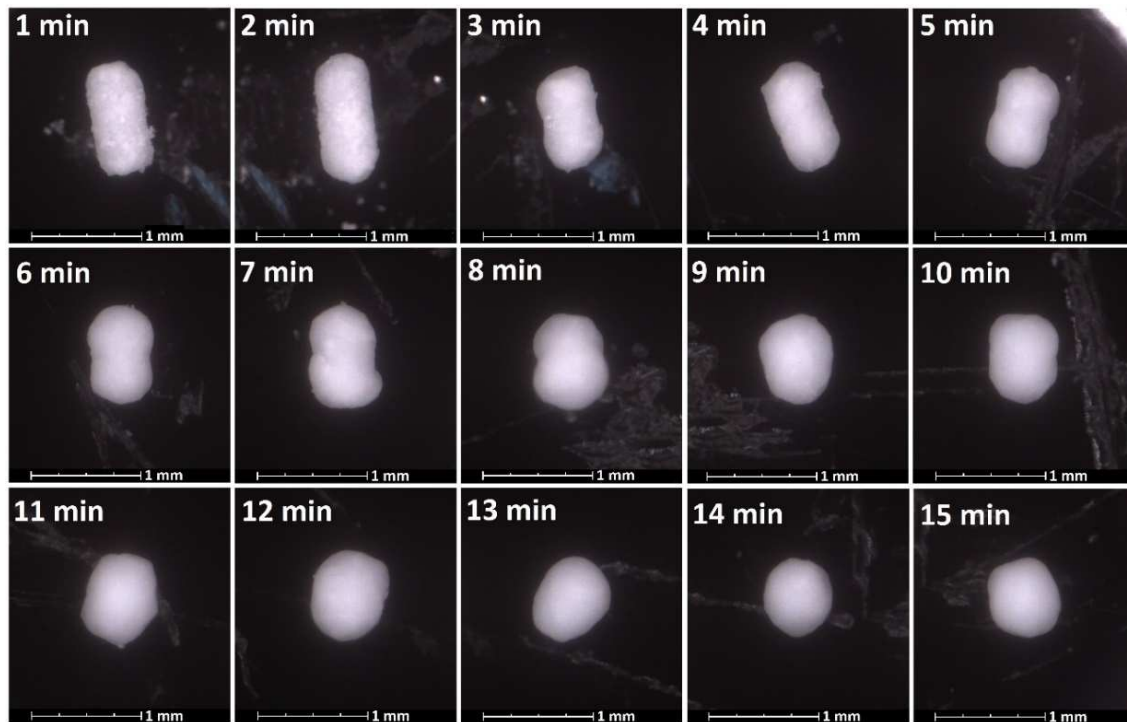


Figure 8.5. Particle form during the spheronization process taken at 120x magnification (PMH<sub>80</sub>)

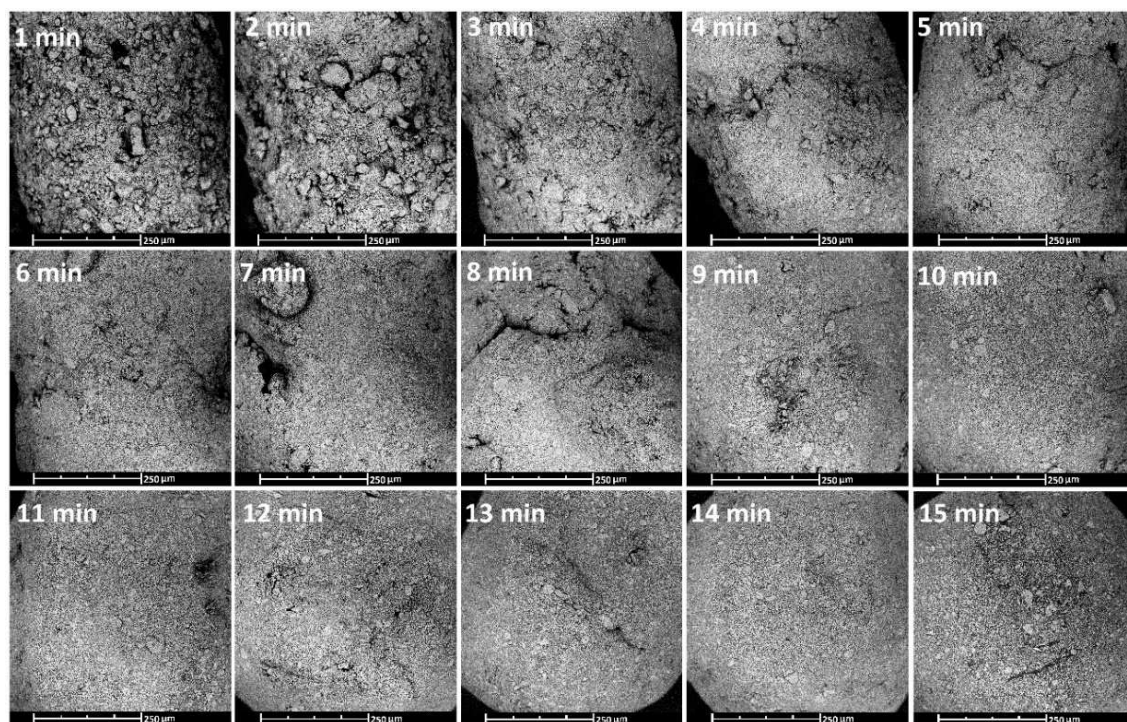


Figure 8.6. Surface modification during the spheronization process for the formulation PMH<sub>80</sub>: taken at 560x magnification



## Annex V

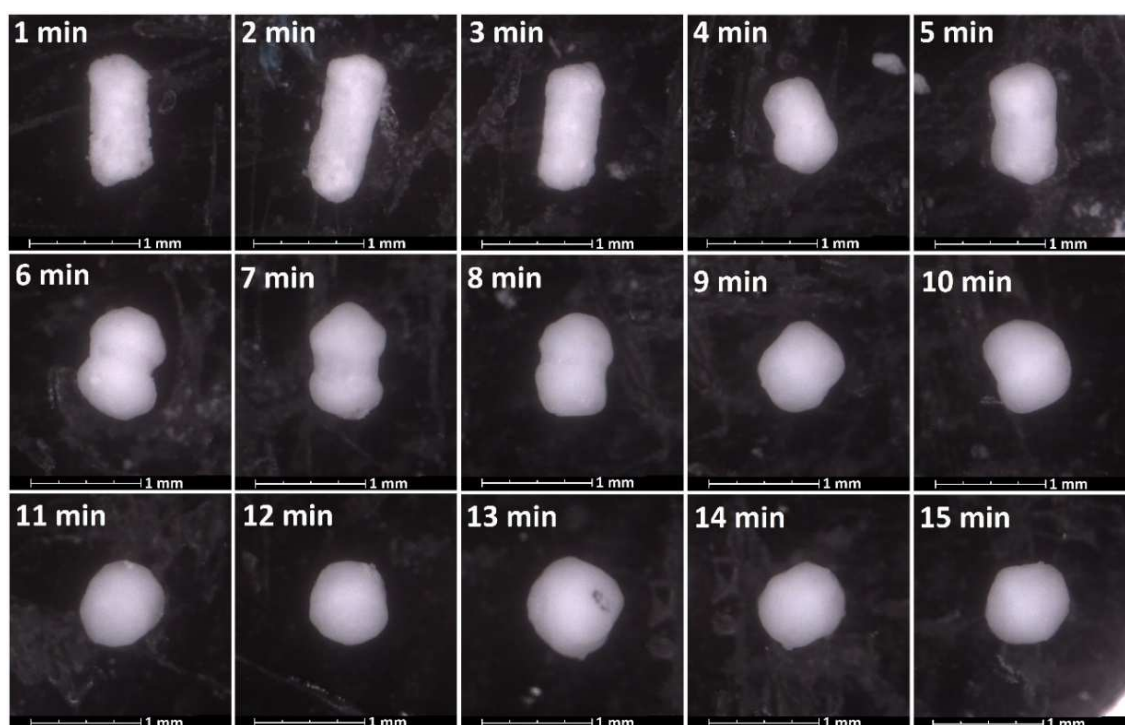


Figure 8.7. Particle form during the spheronization process taken at 120x magnification (PMH<sub>70</sub>)

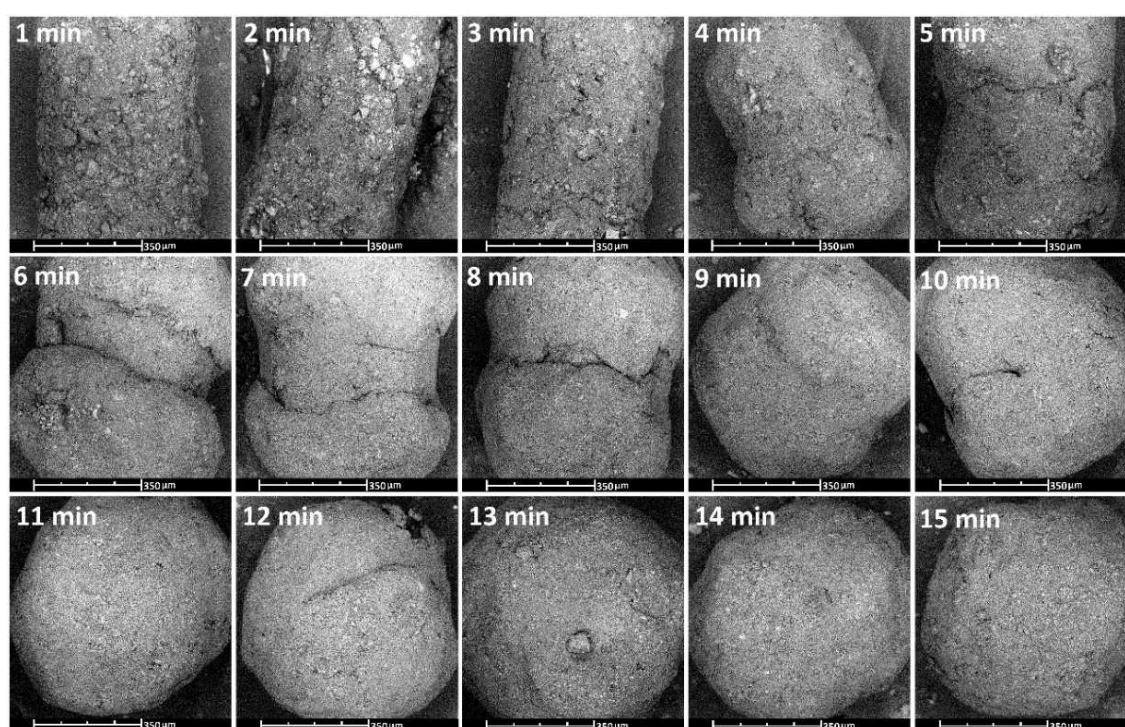


Figure 8.8. Surface modification during the spheronization process for the formulation PMH<sub>70</sub>: taken at 380x magnification



## Annex VI

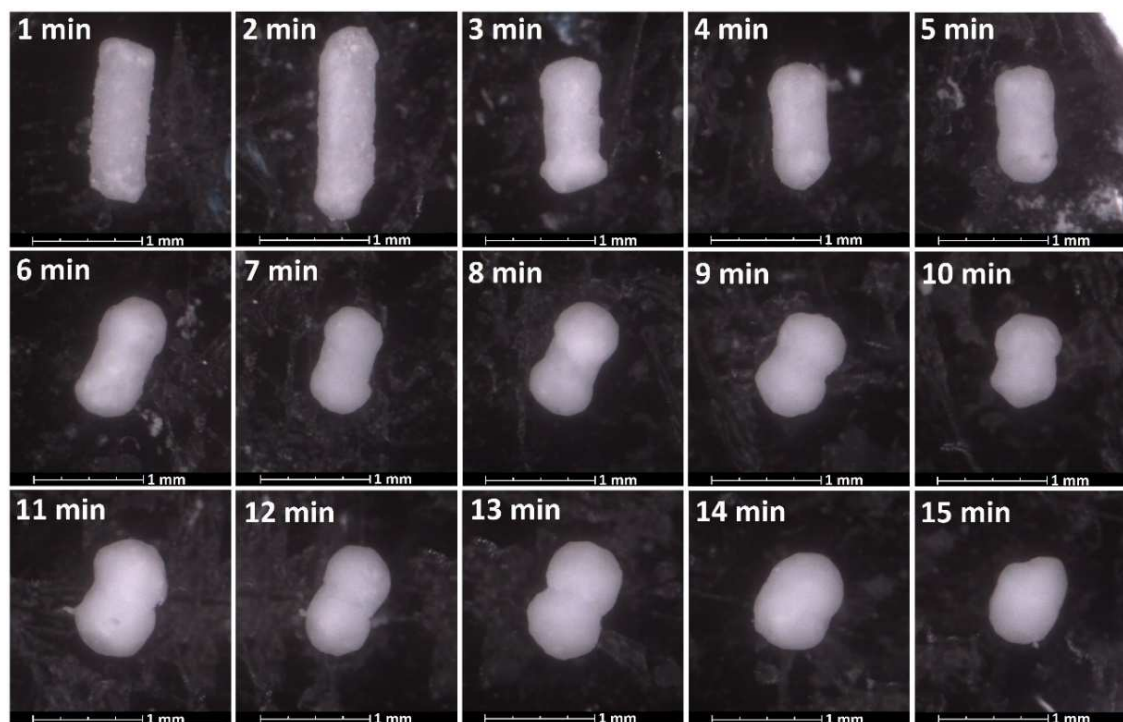


Figure 8.9. Particle form during the spheronization process taken at 120x magnification (PMH<sub>50</sub>)

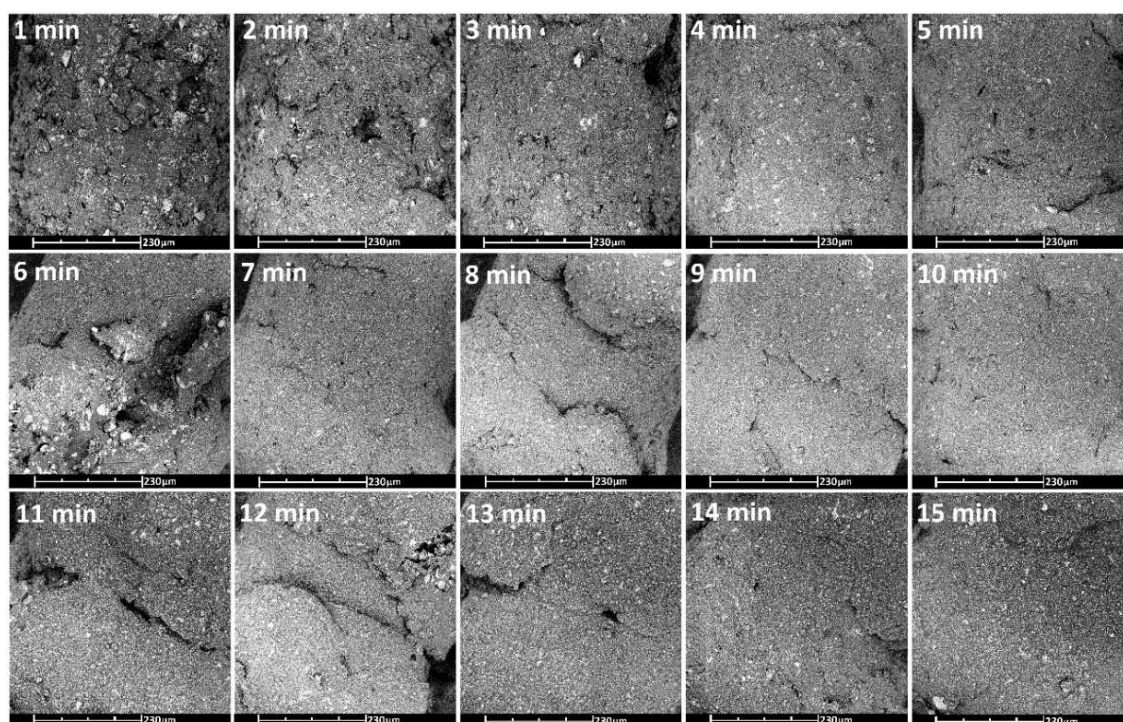


Figure 8.10. Surface modification during the spheronization process for the formulation PMH<sub>50</sub>: taken at 590x magnification



## Annex VII

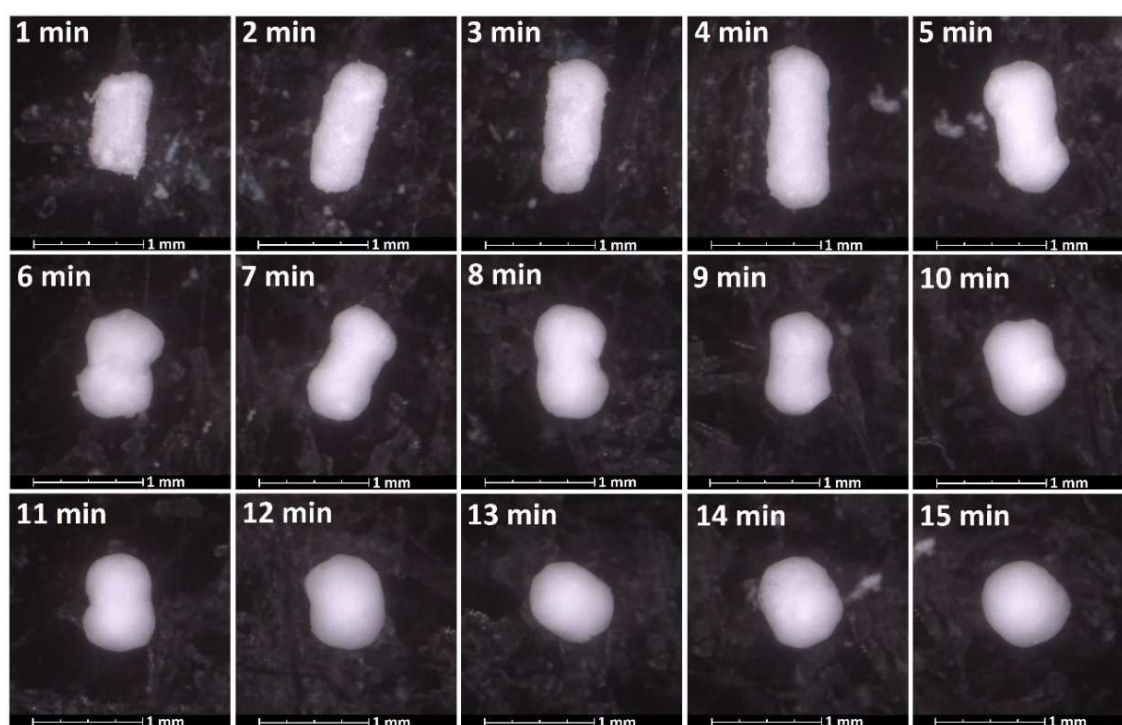


Figure 8.11. Particle form during the spheronization process taken at 120x magnification (PMHGT<sub>80</sub>)

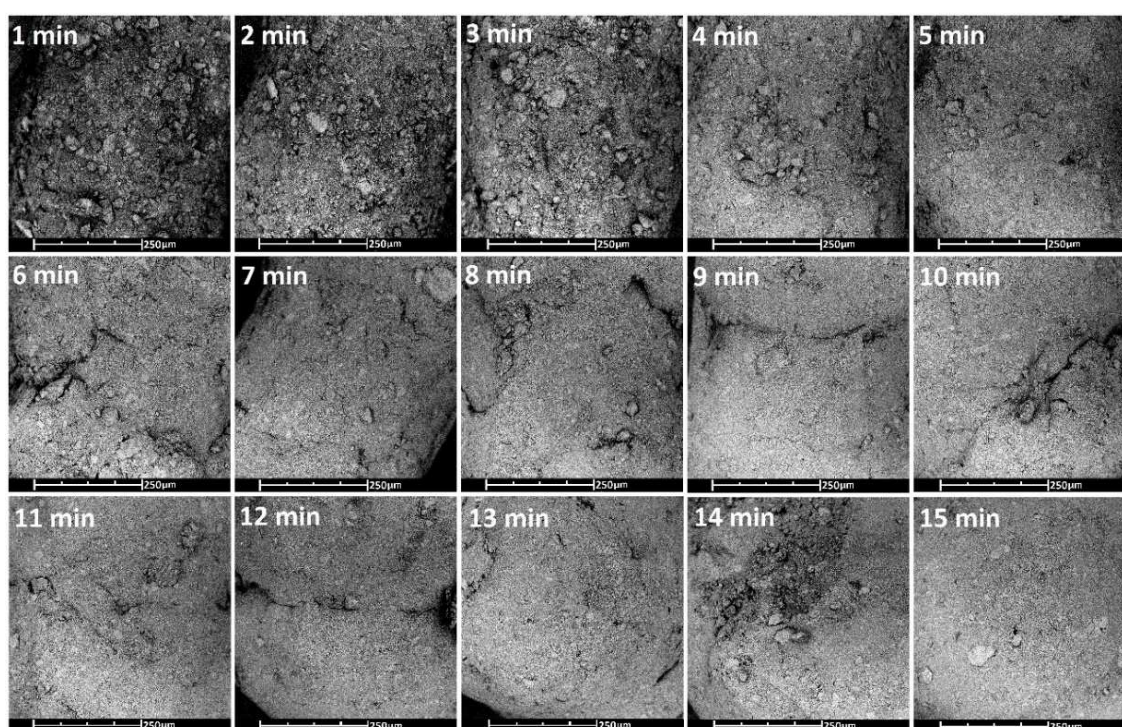


Figure 8.12. Surface modification during the spheronization process for the formulation PMHGT<sub>80</sub>: taken at 580x magnification



## Annex VIII

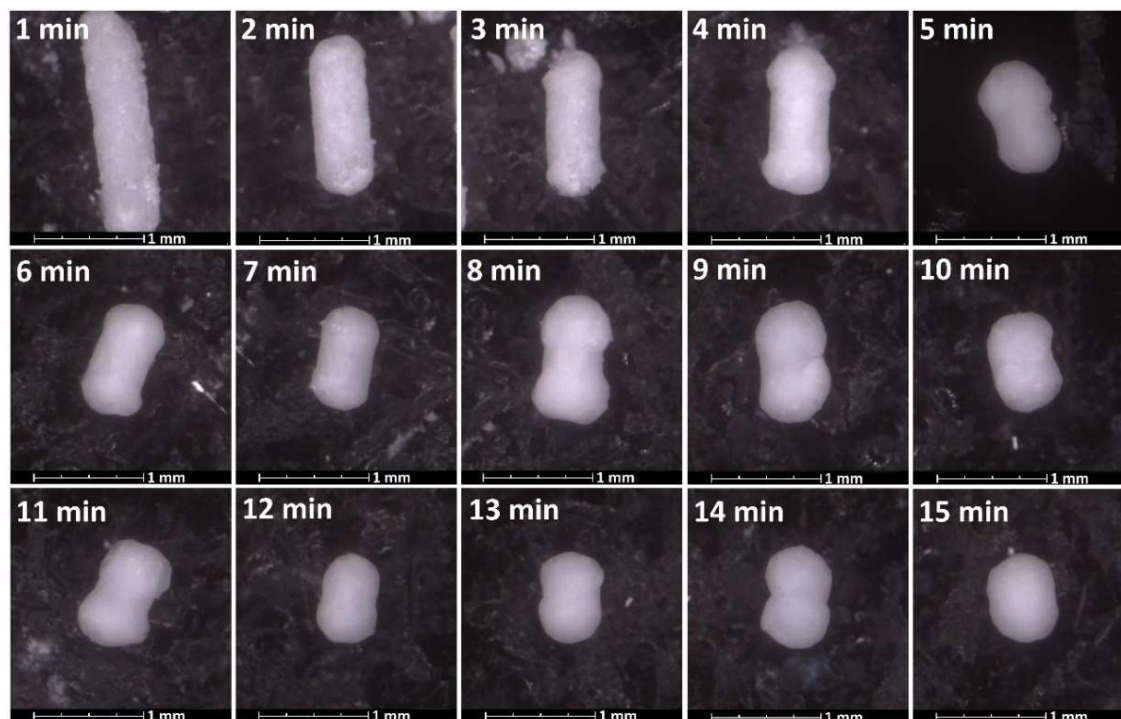


Figure 8.13. Particle form during the spheronization process taken at 120x magnification (PMHGT<sub>50</sub>)

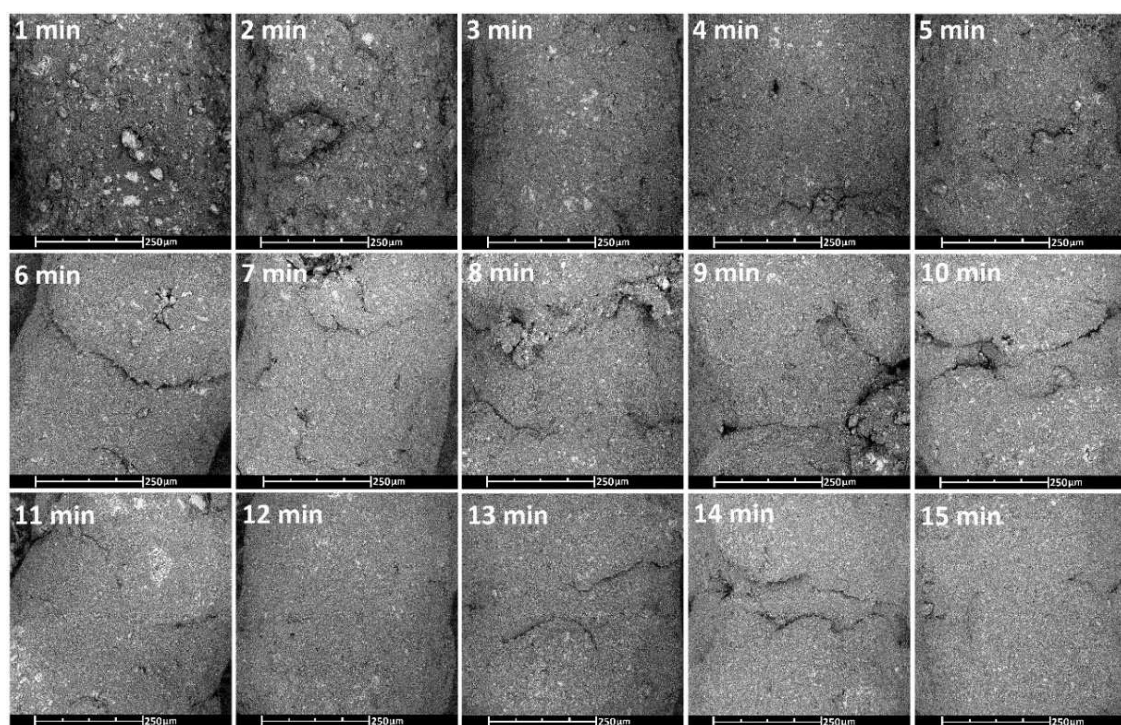


Figure 8.14. Surface modification during the spheronization process for the formulation PMHGT<sub>50</sub>: taken at 530x magnification

## Annex IX

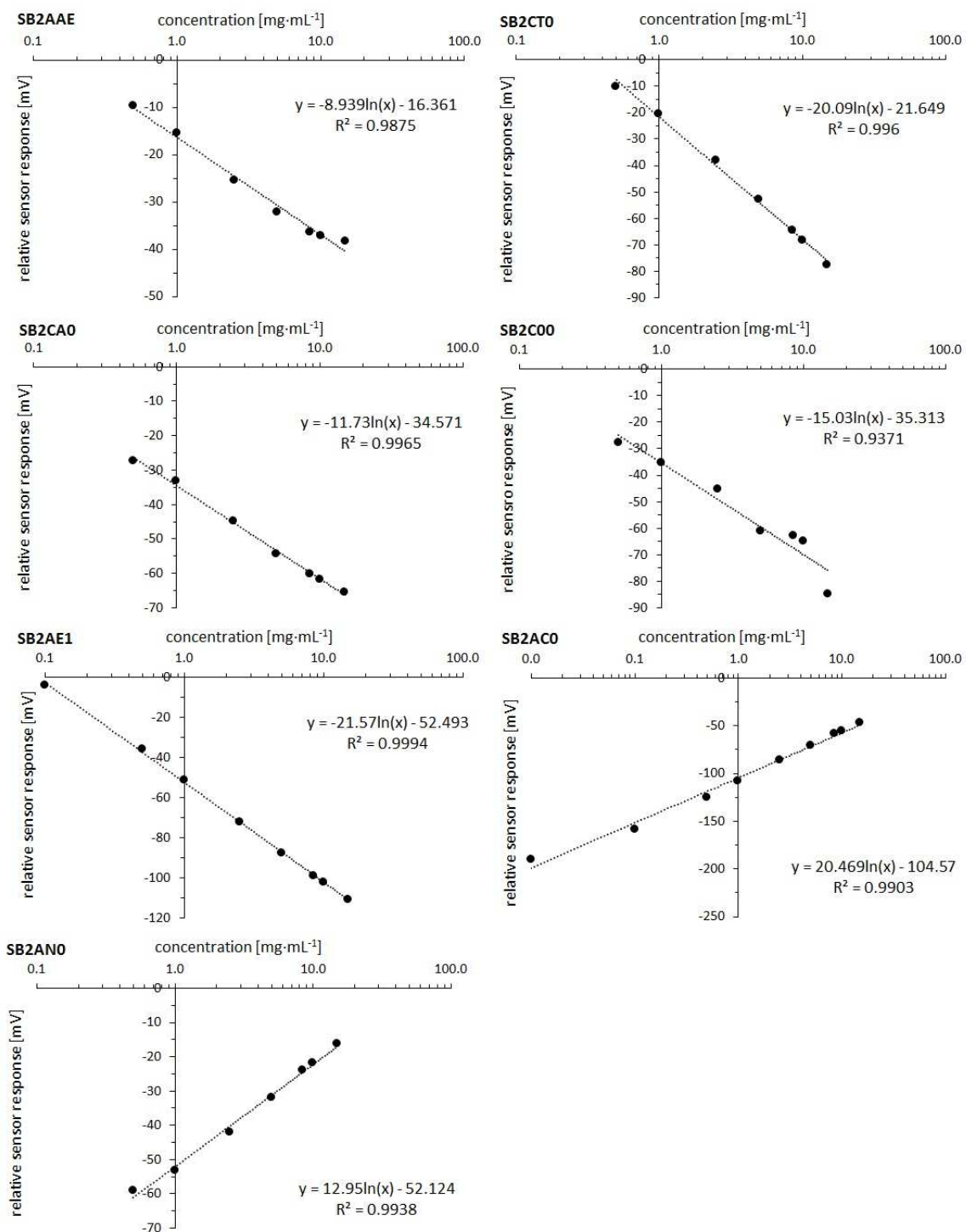


Figure 8.15. Sensors set response (at the linear range) to different concentrations of metformin HCl

## Annex X

**Table 8.2.** Lipid pellet batches shape and particle size distributions of 16 batches produced for the ODT DoE (PMHGT<sub>70</sub>)

Batch n°	d <sub>10</sub> (µm)	d <sub>50</sub> (µm)	d <sub>90</sub> (µm)	AR	Span
1	628.60	706.80	786.60	1.16	0.22
2	607.90	684.80	751.40	1.17	0.21
3	602.00	682.20	750.50	1.17	0.22
4	592.30	676.90	745.00	1.18	0.23
5	549.20	687.30	766.00	1.19	0.32
6	614.30	695.10	766.90	1.17	0.22
7	606.20	690.80	757.10	1.16	0.22
8	616.90	698.30	776.30	1.16	0.23
9	598.80	695.10	776.90	1.17	0.26
10	607.80	687.90	755.90	1.17	0.22
11	562.40	685.70	738.70	1.13	0.26
12	608.50	690.90	783.00	1.21	0.25
13	594.10	663.60	733.60	1.21	0.21
14	617.10	694.50	762.20	1.15	0.21
15	618.90	698.10	774.60	1.16	0.22
16	588.20	682.60	763.30	1.20	0.26



## 9. Scientific Publications Associated with this Thesis

The results of this thesis have been partly published in the below listed publications.

### 9.1. International Peer-Reviewed Journals

Petrovick, G.F.; Pein, M.; Thommes, M.; Breitzkreutz, J. Spheronization of solid lipid extrudates: a novel approach on controlling critical process parameters (2015). *European Journal of Pharmaceutics and Biopharmaceutics* 92: 15-21.

### 9.2. Conference Presentations

Petrovick, G.F. and Breitzkreutz, J. Development of lipid micropellets with metformin hydrochloride using solvent-free cold extrusion/spheronization, poster presentation at the *DPhG Jahrestagung*, Greifswald, Germany, 11<sup>th</sup> to 13<sup>th</sup> October 2012.

Petrovick, G.F.; Pein, M.; Breitzkreutz, J. Taste masked solid lipid pellets containing metformin hydrochloride produced by solvent-free cold extrusion/spheronization, poster presentation at the *9<sup>th</sup> World Meeting on Pharmaceutics, Biopharmaceutics and Pharmaceutical Technology*, Lisbon, Portugal, 31<sup>st</sup> March to 3<sup>rd</sup> April 2014.

Petrovick, G.F. and Breitzkreutz, J. An innovative approach on controlling critical process parameters in solid lipid spheronization, poster presentation at the *9<sup>th</sup> World Meeting on Pharmaceutics, Biopharmaceutics and Pharmaceutical Technology*, Lisbon, Portugal, 31<sup>st</sup> March to 3<sup>rd</sup> April 2014.

Petrovick, G.F. and Breitzkreutz, J. Dispersible tablets with solid lipid pellets, poster presentation at the *AAPS Annual Meeting*, San Diego, USA, 2<sup>nd</sup> to 6<sup>th</sup> November 2014.



## 10. References

- Abdul, S.; Chandewar, A.V. and Jaiswal, S.B. (2010). A flexible technology for modified-release drugs: Multiple-unit pellet system (MUPS). *Journal of Controlled Release* 147(1): 2-16.
- Abrass, I.B. (1990). The biology and physiology of aging. *The Western Journal of Medicine* 153: 641-645.
- Alberti, K.G.M.M. and Zimmet, P.Z. (1998). Definition, diagnosis and classification of diabetes mellitus and its complications. Part 1: diagnosis and classification of diabetes mellitus. Provisional report of a WHO Consultation. *Diabetic Medicine* 15(7): 539-553.
- Alderborn, G. (2013). Tablets and compaction. In: Aulton, M.E. and Taylor, K.M.G. *Aulton's Pharmaceutics: The design and manufacture of medicines*. London, UK, Churchill Livingstone - Elsevier: 505-549.
- Arias, J.L.; Gómez-Gallo, A.; Delgado, Á.V. and Ruiz, A. (2009). Kollidon® SR colloidal particles as vehicles for oral morphine delivery in pain treatment. *Colloids and Surfaces B: Biointerfaces* 70(2): 207-212.
- Augsburger, L.L. and Vuppala, M.K. (1997). Theory of granulation. In: Parikh, D.M. *The Handbook of Pharmaceutical Granulation Technology*. New York, USA, Marcel Dekker: 7-23.
- Aulton, M.E. (2013). Powder Flow. In: Aulton, M.E. and Taylor, K.M.G. *Aulton's Pharmaceutics: The Design and Manufacture of Medicines*. London, UK, Churchill Livingstone - Elsevier: 187-198.
- Baert, L.; Vermeersch, H.; Remon, J.P.; Smeyers-Verbeke, J. and Massart, D.L. (1993). Study of parameters important in the spheronisation process. *International Journal of Pharmaceutics* 96: 225-229.
- Bailey, C.J. and Turner, R.C. (1996). Metformin. *The New England Journal of Medicine* 334(9): 574-579.
- Bandari, S.; Mittapalli, R.K.; Gannu, R. and Rao, Y.M. (2008). Orodispersible tablets: An overview. *Asian Journal of Pharmaceutics* 2(1): 2-11.
- Barakat, N.S.; Elbagory, I.M. and Almurshedi, A.S. (2009). Controlled-release carbamazepine matrix granules and tablets comprising lipophilic and hydrophilic components. *Drug Delivery* 16(1): 57-65.

- Barnes, H.A. (1995). A review of the slip (wall depletion) of polymer solutions, emulsions and particle suspensions in viscosimeters: its cause, character, and cure. *Journal of Non-Newtonian Fluid Mechanics* 56: 221-251.
- Barot, B.S.; Parejiya, P.B.; Patel, T.M.; Parikh, R.K. and Gohel, M.C. (2010). Development of directly compressible metformin hydrochloride by the spray-drying technique. *Acta Pharmaceutica* 60(2): 165-175.
- Bauer, H. (2000). *Herstellung und Charakterisierung von Kombinationen aus Mannit und Sorbit durch Sprühtrocknung und Co-granulation*. PhD Dissertation, Universität Tübingen. Tübingen, Deutschland.
- Bauer, H.; Herkert, T.; Bartels, M.; Kovak, K.A.; Schwarz, E. and Schmidt, P.C. (2000). Investigations on polymorphism of mannitol/sorbitol mixtures after spray drying using differential scanning calorimetry, X-ray diffraction and near infrared spectroscopy. *Pharmazeutische Industrie* 62(3): 231-235.
- Bhojar, P.K.; Bhanarkar, A.B.; Nagulwar, D.B.; Y.M., A.; Tripathi, A.K.; Bhandarkar, S. and Muraleedharan, R. (2011). Taste masked sustained release tablet of metformin hydrochloride. *International Journal of Pharmaceutical Sciences* 2(2): 110-117.
- Bhojar, P.K. and Biyani, D.M. (2010). Formulation and in vitro evaluation of sustained release dosage form with taste masking of metformin hydrochloride. *Indian Journal of Pharmaceutical Sciences* 72(2): 184-190.
- Bornhöft, M.; Thommes, M. and Kleinebudde, P. (2005). Preliminary assessment of carrageenan as excipient for extrusion/spheronisation. *European Journal of Pharmaceutical Sciences* 59(1): 127-131.
- Breitkreutz, J. and Boos, J. (2007). Pediatric and geriatric drug delivery. *Expert Opinion on Drug Delivery* 4(1): 37-45.
- Breitkreutz, J.; El-Saleh, F.; Kiera, C.; Kleinebudde, P. and Wiedey, W. (2003). Pediatric drug formulations of sodium benzoate: II. Coated granules with a lipophilic binder. *European Journal of Pharmaceutics and Biopharmaceutics* 56(2): 255-260.
- Bretnall, A.E. and Clarke, G.S. (1998). Metformin hydrochloride. In: Harry, G.B. *Analytical Profiles of Drug Substances and Excipients*. Moreton, UK, Academic Press. Volume 25: 243-293.
- Buckton, G. (2013). Solid-state properties. In: Aulton, M.E. and Taylor, K.M.G. *Aulton's Pharmaceutics: The design and manufacture of medicines*. Edinburgh, Churchill Livingstone - Elsevier: 126-137.
- Campbell, I.W. (1991). Management of type 2 diabetes mellitus with special reference to metformin therapy. *Diabetes & Metabolism* 17(1): 191-196.

- Carey, M.C.; Small, D.M. and Bliss, C.M. (1983). Lipid digestion and absorption. *Annual Reviews of Physiology* 45: 651-677.
- Carnaby-Mann, G. and Crary, M. (2005). Pill swallowing by adults with dysphagia. *Archives of Otolaryngology - Head and Neck Surger* 131(11): 970-975.
- Carr, R. (1965). Evaluation flow properties of solids. *Chemical Engineering Journal* 72(2): 163-168.
- Chatchawalsaisin, J.; Podczec, F. and Newton, J.M. (2005). The preparation by extrusion/spheronization and the properties of pellets containing drugs, microcrystalline cellulose and glyceryl monostearate. *European Journal of Pharmaceutical Sciences* 24(1): 35-48.
- Chaudhary, S.A.; Chaudharya, A.B. and Mehtab, T.A. (2010). Excipients updates for orally disintegrating dosage forms. *International Journal of Pharmaceutical Sciences* 1(2): 103-107.
- Choy, Y.W.; Khan, N. and Yuen, K.H. (2005). Significance of lipid matrix aging on in vitro release and in vivo bioavailability. *International Journal of Pharmaceutics* 299: 55-64.
- Cowart, B.J.; Yokomukai, Y. and Beauchamp, G.K. (1994). Bitter taste in aging: Compound-specific decline in sensitivity. *Physiology & Behavior* 56(6): 1237-1241.
- Cox, J.P. (1991). *Lipid pelletization methods, apparatus and products*. United States Patent. USA, United States Application, 5,221,980.
- Cullen, E.; Liao, J.; Lukacs, P.; Niecestro, R. and Friedhoff, L. (2004). Pharmacokinetics and dose proportionality of extended-release metformin following administration of 1000, 1500, 2000 and 2500 mg in healthy volunteers. *Biopharmaceutics & Drug Disposition* 25(6): 261-263.
- Dailey, G.; Kim, M.S. and Lian, J.F. (2001). Patient compliance and persistence with antihyperglycemic drug regimens: evaluation of a medicaid patient population with type 2 diabetes mellitus. *Clinical Therapeutics* 23(8): 1311-1320.
- Daoust, R.G. and Lynch, M.J. (1963). Mannitol in chewable tablets. *Drug and cosmetic industry* 93(1): 26-28.
- Davidson, M.B. and Peters, A.L. (1997). An overview of metformin in the treatment of type 2 diabetes mellitus. *The American Journal of Medicine* 102(1): 99-110.
- Day, C. (1999). The elderly: Pharmacy's best repeat customer. *Drug Store News*.
- DeFronzo, R.A. (1999). Pharmacologic therapy for type 2 diabetes mellitus. *Annals of Internal Medicine* 131(4): 281-303.

Di Cianni, G.; Benzi, L.; Giannarelli, R.; Orsini, P.; Villani, G.; Ciccarone, A.M.; Cecchetti, P.; Fedele, O. and Navalesi, R. (1994). A prevalence study of known diabetes mellitus in Tuscany assessed from pharmaceutical prescriptions and other independent sources. *Acta Diabetologica* 31(2): 87-90.

Dukić-Ott, A.; Thommes, M.; Remon, J.P.; Kleinebudde, P. and Vervaet, C. (2009). Production of pellets via extrusion–spherionisation without the incorporation of microcrystalline cellulose: A critical review. *European Journal of Pharmaceutical Sciences* 71(1): 38-46.

Eckert, C.; Pein, M. and Breitzkreutz, J. (2014). Lean production of taste improved lipidic sodium benzoate formulations. *European Journal of Pharmaceutics and Biopharmaceutics* 88(2): 455-461.

Eriksson, L.; Johansson, E.; Kettaneh-Wold, N.; Wikström, C. and Wold, S. (2008). *Design of experiments: Principles and applications*. Umea, Sweden, Umetrics Academy.

Erkoboni, D.F. (1997). Extrusion-spherionization as a granulation technique. In: Parikh, D. *The Handbook of Pharmaceutical Granulation Technology*. New York, Marcel Dekker: 333-368.

Faham, A.; Prinderre, n.; Farah, n.; Eichelner, K.D.; Kalantzis, G. and Joachim, J. (2000). Hot-melt coating technology. I. Influence of Compritol 888 ATO and granule size on theophylline release. *Drug Development and Industrial Pharmacy* 26(2): 167-176.

FDA, F.a.D.A. (2000). Guidance for Industry, Waiver of In Vivo Bioavailability and Bioequivalence Studies for Immediate Release Solid Oral Dosage Forms based on a Biopharmaceutics Classification System. Services, U.S.D.o.H.a.H. Rockville, Center for Drug Evaluation and Research (CDER).

FDA, F.a.D.A. (2007). Guidance for industry - Orally disintegrating tablets. USA, U.S. Department of Health and Human Services.

Fell, J.T. and Newton, J.M. Determination of tablet strength by the diametral-compression test. *Journal of Pharmaceutical Sciences* 59(5): 688-691.

Franceschinis, E.; Voinovich, D.; Grassi, M.; Perissutti, B.; Filipovic-Grcic, J.; Martinac, A. and Meriani-Merlo, F. (2005). Self-emulsifying pellets prepared by wet granulation in high-shear mixer: influence of formulation variables and preliminary study on the in vitro absorption. *International Journal of Pharmaceutics* 291: 87-97.

Fu, Y.; Yang, S.; Jeong, S.H.; Kimura, S. and Park, K. (2004). Orally fast disintegrating tablets: developments, technologies, taste-masking and clinical studies. *Critical Reviews in Therapeutic Drug Carrier Systems* 21(6): 433-476.

- Führer, C. (1995). Interparticulate attraction mechanisms. In: Alderborn, G. and Nyström, C. *Pharmaceutical Powder Compaction Technology*. New York, USA, Marcel-Dekker. 71.
- Fujioka, K.; Pans, M. and Joyal, S. (2003). Glycemic control in patients with type 2 diabetes mellitus switched from twice-daily immediate-release metformin to a once-daily extended-release formulation. *Clinical Therapeutics* 25(2): 515-529.
- Gaisford, S. (2013). Pharmaceutical preformulation. In: Aulton, M.E. and Taylor, K.M.G. *Aulton's Pharmaceutics: The Design and Manufacture of Medicines*. London, UK, Churchill Livingstone - Elsevier: 367-394.
- Gandhi, P.P.; Vaidya, K.A.; Shelake, G.T.; Yadav, J.D. and Kulkarni, P.R. (2010). Formulation and evaluation of metformin hydrochloride fast disintegrating tablets by using polacrillin potassium NF from different sources as superdisintegrants. *International Journal of Pharmacy and Pharmaceutical Sciences* 2(2): 55-57.
- Ghebre-Sellassie, I. and Knoch, A. (2006). Pelletization Techniques. In: Swarbrick, J. and Boylan, J.C. *Encyclopedia of Pharmaceutical Technology*. New York, USA, Marcel Dekker: 2651-2663.
- Giannella-Neto, D. and Gomes, M.B. (2009). Diabetology & Metabolic Syndrome: providing an open access future for diabetes research. *Diabetology & Metabolic Syndrome* 1(1): 1-3.
- Gittings, S.; Turnbull, N.; Roberts, C.J. and Gershkovich, P. (2014). Dissolution methodology for taste masked oral dosage forms. *Journal of Controlled Release* 173(0): 32-42.
- Graham, G.G.; Punt, J.; Arora, M.; Day, R.O.; Doogue, M.P.; Duong, J.K.; Furlong, T.J.; Greenfield, J.R.; Greenup, L.C.; Kirkpatrick, C.M.; Ray, J.E.; Timmins, P. and Williams, K.M. (2011). Clinical pharmacokinetics of metformin. *Clinical Pharmacokinetics* 50(2): 81-98.
- Gregorio, F.; Manfrini, S.; Testa, I. and Filipponi, P. (1996). Metformin treatment in elderly type II diabetic patients. *Archives of Gerontology and Geriatrics* 22(1): 261-270.
- Güres, S. and Kleinebudde, P. (2011). Dissolution from solid lipid extrudates containing release modifiers. *International Journal of Pharmaceutics* 412: 77-84.
- Güres, S.; Siepmann, F.; Siepmann, J. and Kleinebudde, P. (2011). Drug release from extruded solid lipid matrices: Theoretical predictions and independent experiments. *European Journal of Pharmaceutical Sciences* 80(1): 122-129.
- Hall, C. (2002). Special considerations for the geriatric population. *Critical Care Nursing Clinics of North America* 14(4): 427-434.

- Hamdani, J.; Moës, A.J. and Amighi, K. (2003). Physical and thermal characterisation of Precirol® and Compritol® as lipophilic glycerides used for the preparation of controlled-release matrix pellets. *International Journal of Pharmaceutics* 260(1): 47-57.
- Harris, M.I. (1998). Diabetes in America: Epidemiology and scope of the problem *Diabetes Care* 21(3): C11-C14.
- Hausner, H.H. (1967). Friction conditions in a mass of metal powder. *International Journal of Powder Metallurgy* 3(4): 7-13.
- Heng, P.W.S. (2005). Pelletization and pellet coating. *15th International Symposium on Microencapsulation*.
- Heng, P.W.S.; Chan, L.W.; Easterbrook, M.G. and Li, X. (2001). Investigation of the influence of mean HPMC particle size and number of polymer particles on the release of aspirin from swellable hydrophilic matrix tablets. *Journal of Controlled Release* 76: 39-49.
- Hu, L.; Liu, Y.; Tang, X. and Zhang, Q. (2006). Preparation and in vitro/in vivo evaluation of sustained-release metformin hydrochloride pellets. *European Journal of Pharmaceutical Sciences* 64(2): 185-192.
- Hundal, R.S. and Inzucchi, S.E. (2003). Metformin: New understandings, new uses. *Drugs* 63(18): 1879-1894.
- IDF, International Diabetes Federation. (2006). Global guideline for type 2 diabetes: recommendations for standard, comprehensive, and minimal care. *Diabetes & Metabolism* 23(6): 579-593.
- IDF, International Diabetes Federation. (2013). *IDF Diabetes Atlas*, IDF, International Diabetes Federation.
- Jain, H.; Panchal, R.; Pradhan, P.; Patel, H. and Pasha, T.Y. (2010). Electronic Tongue: A new taste sensor. *International Journal of Pharmaceutical Sciences Review and Research* 5(2): 91-96.
- Jannin, V.; Musakhanian, J. and Marchaud, D. (2008). Approaches for the development of solid and semi-solid lipid-based formulations. *Advanced Drug Delivery Reviews* 60(6): 734-746.
- Jenike, A.W. (1964). Storage and flow of solids, Bull. No. 123. *Bulletin of the University of Utah*. Salt Lake City, University of Utah. Volume 53: 198.
- Jeong, S.H.; Takaishi, Y.; Fu, Y. and Park, K. (2008). Material properties for making fast dissolving tablets by a compression method. *Journal of Materials Chemistry* 18(30): 3527-3535.



- Khan, N. and Craig, D.Q.M. (2004). Role of blooming in determining the storage stability of lipid-based dosage forms. *Journal of Pharmaceutical Sciences* 93(12): 2962-2971.
- Khan, S.; Kataria, P.; Nakhat, P. and Yeole, P. (2007). Taste masking of ondansetron hydrochloride by polymer carrier system and formulation of rapid-disintegrating tablets. *AAPS PharmSciTech* 8(2): E1-E7.
- Kharb, V.; Saharan, V.A.; Kharb, V.; Jadhav, H. and Purohit, S. (2014). Formulation and evaluation of lipid based taste masked granules of ondansetron HCl. *European Journal of Pharmaceutical Sciences* 62: 180-188.
- King, P.; Peacock, I. and Donnelly, R. (1999). The UK Prospective Diabetes Study (UKPDS): clinical and therapeutic implications for type 2 diabetes. *British Journal of Clinical Pharmacology* 48(5): 643-648.
- Kinsella, K. and He, W. (2009). An Aging World: 2008 - International Population Reports, U.S. Department of Health and Human Services.
- Kirpichnikov, D.; McFarlane, S.I. and Sowers, J.R. (2002). Metformin: An update. *Annals of Internal Medicine* 137(1): 25-33.
- Klancke, J. (2003). Dissolution testing of orally dissolution testing of orally disintegrating tablets. *Dissolution Technologies*, 6-8.
- Kleinebudde, P. (1994). Shrinking and swelling properties of pellets containing microcrystalline cellulose and low substituted hydroxypropylcellulose: II. Swelling properties. *International Journal of Pharmaceutics* 109(3): 221-227.
- Kleinebudde, P. (1995). Use of a power-consumption-controlled extruder in the development of pellet formulations. *Journal of Pharmacy Research* 84(10): 1259-1264.
- Kleinebudde, P. (1997). *Pharmazeutische Pellets durch Extrudieren/Sphäronisieren: Herstellung, Eigenschaften, Modifizierung*. Habilitationsschrift, Christian-Albrechts-Universität. Kiel.
- Kleinebudde, P. (2013). Solid lipid extrusion. In: Repka, M.A.; Langley, N. and DiNunzio, J. *Melt Extrusion: Materials, Technology and Drug Production Design*. New York, Springer: 299-328.
- Koennings, S.; Berié, A.; Tessmar, J.; Blunk, T. and Goepferich, A. (2007). Influence of wettability and surface activity on release behavior of hydrophilic substances from lipid matrices. *Journal of Controlled Release* 119(2): 173-181.
- Koester, M. and Thommes, M. (2010). New insights into the pelletization mechanism by extrusion/spheronization. *AAPS PharmSciTech* 11(4): 1549-1551.

Kolter, K.; Karl, M. and Gryczke, A. (2012). *Hot-Melt Extrusion with BASF Pharma Polymers: Extrusion Compendium*. Ludwigshafen, Germany, BASF <<se.

Krause, J. (2008). *Novel paediatric formulations for the drug sodium benzoate*. Doctorate Thesis, Heinrich-Heine-Universität Düsseldorf. Düsseldorf.

Krause, J.; Thommes, M. and Breitzkreutz, J. (2009). Immediate release pellets with lipid binders obtained by solvent-free cold extrusion. *European Journal of Pharmaceutics and Biopharmaceutics* 71(1): 138-144.

Krueger, C.; Thommes, M. and Kleinebudde, P. (2013). Spheronisation mechanism of MCC II-based pellets. *Powder Technology* 238: 176-187.

Kundu, S. and Sahoo, P.K. (2008). Recent trends in the developments of orally disintegrating tablet technology. *Pharma Times* 40(4): 11-20.

Laine, E.; Auramo, P. and Kahela, P. (1988). On the structural behaviour of triglycerides with time. *International Journal of Pharmaceutics* 43(3): 241-247.

Lantz, R.J. (1989). Size reduction. In: Lieberman, H.A.; Lachman, I. and Schwartz, J. *Pharmaceutical Dosage Forms: Tablets*. New York, USA, Marcel Dekker. Volume 2: 107-199.

Larsson, K. (1966). Classification of glyceride crystal forms. *Acta chemica Scandinavica* 20(8): 2255-2260.

Lindenberg, M.; Kopp, S. and Dressman, J.B. (2004). Classification of orally administered drugs on the World Health Organization Model list of Essential Medicines according to the biopharmaceutics classification system. *European Journal of Pharmaceutics and Biopharmaceutics* 58(2): 265-278.

Lindgren, S. and Janzon, L. (1991). Prevalence of swallowing complaints and clinical findings among 50–79-year-old men and women in an urban population. *Dysphagia* 6(4): 187-192.

Liu, F.; Ranmal, S.; Batchelor, H.; Orlu-Gul, M.; Ernest, T.; Thomas, I.; Flanagan, T. and Tuleu, C. (2014). Patient-centred pharmaceutical design to improve acceptability of medicines: similarities and differences in paediatric and geriatric populations. *Drugs*: 1-19.

Maniyar, R.; Ranch, M.; Koli, R.; Vyas, A.; Parikh, R.K.; Modi, J.G. and Vyas, R.B. (2010). Formulation and optimization of fast disintegrating tablet of metformin using disintegrant blends for improved efficacy. *International Journal of Pharmaceutical Sciences* 1, 295-305.

- Michalk, A.; Kanikanti, V.; Hamann, H. and Kleinebudde, P. (2008). Controlled release of active as a consequence of the die diameter in solid lipid extrusion. *Journal of Controlled Release* 132(1): 35-41.
- Michie, H.; Podczeck, F. and Newton, J.M. (2012). The influence of plate design on the properties of pellets produced by extrusion and spheronization. *International Journal of Pharmaceutics* 434(1-2): 175-182.
- Miller, T.A. and York, P. (1988). Pharmaceutical tablet lubrication. *International Journal of Pharmaceutics* 41: 1-19.
- Mizumoto, T.; Masuda, Y.; Yamamoto, T.; Yonemochi, E. and Terada, K. (2005). Formulation design of a novel fast-disintegrating tablet. *International Journal of Pharmaceutics* 306: 83-90.
- Mohamed, H.M.A. and Larsson, K. (1992). Effects on phase transitions in tripalmitin due to the presence of dipalmitin, sorbitan-monopalmitate or sorbitan-tripalmitate. *Fat Science Technology* 9: 338-341.
- Mohapatra, A.; Parikh, R. and Gohel, M. (2008a). Formulation, development and evaluation of patient friendly dosage forms of metformin, Part-I: Orally disintegrating tablets. *Asian Journal of Pharmaceutics* 2(3): 167-171.
- Mohapatra, A.; Parikh, R. and Gohel, M. (2008b). Formulation, development and evaluation of patient friendly dosage forms of metformin, Part-II: Oral soft gel. *Asian Journal of Pharmaceutics* 2(3): 172-176.
- Mohapatra, A.; Parikh, R. and Gohel, M. (2008c). Formulation, development and evaluation of patient friendly dosage forms of metformin, Part-III: Soluble effervescent tablets. *Asian Journal of Pharmaceutics* 2(3): 177-181.
- Mollan, M. (2003). Historical overview. In: Ghebre-Sellassie, I. and Martin, C. *Pharmaceutical Extrusion Technology*. New York, USA, CRC Press: 1-18.
- Mostafavi, S.A.; Varshosaz, J. and Arabian, S. (2014). Formulation development and evaluation of metformin chewing gum with bitter taste masking. *Advanced Biomedical Research* 3(92): 2277-9175.
- Murray, O.J.; Dang, W. and Bergstrom, D. (2004). Using an Electronic tongue to optimize taste-masking in a lyophilized orally disintegrating tablet formulation. *Pharmaceutical Technology Outsourcing Resources*, 42-52.
- Nakahara, N. (1966). *Method and apparatus for making spherical granules*. United States Patent. USA, United States Patent, US 3,277,520A.
- Nathan, D.M.; Buse, J.B.; Davidson, M.B.; Heine, R.J.; Holman, R.R.; Sherwin, R. and Zinman, B. (2006). Management of hyperglycemia in type 2 diabetes: A consensus

algorithm for the initiation and adjustment of therapy. *Diabetes Care* 29(8): 1963-1972.

Navarro, V. (2010). Improving medication compliance in patients with depression: Use of orodispersible tablets. *Advances in Therapy* 27(11): 785-795.

Netz, P.A. and Ortega, G.G. (2002). *Fundamentos de físico-química: Uma abordagem conceitual para as ciencias farmaceuticas*. Porto Alegre, Artmed.

Nilsson, H.; Ekberg, O.; Olsson, R. and Hindfelt, B. (1996a). Quantitative aspects of swallowing in an elderly nondysphagic population. *Dysphagia* 11(3): 180-184.

Nilsson, H.; Ekberg, O.; Olsson, R.; Kjellin, O. and Hindfelt, B. (1996b). Quantitative assessment of swallowing in healthy adults. *Dysphagia* 11(2): 110-116.

Nyström, C. and Karehill, P.-G. (1995). The importance of intermolecular bonding forces and the concept of bonding surface area. In: Alderborn, G. and Nyström, C. *Pharmaceutical Powder Compaction Technology*. New York, USA, Marcel Dekker.

Okuda, Y.; Irisawa, Y.; Okimoto, K.; Osawa, T. and Yamashita, S. (2009). A new formulation for orally disintegrating tablets using a suspension spray-coating method. *International Journal of Pharmaceutics* 382: 80-87.

Pandey, S.; Kumar, S.; Prajapati, S.K. and Madhav, N.V.S. (2010). An overview on taste physiology and masking of bitter drugs. *International Journal of Pharma and Bio Sciences* 1(3): 1-11.

Park, J.H.; Holman, K.M.; Bish, G.A.; Krieger, D., G.; Ramlose, D.S.; Herman, C.j. and Wu, S.H. (2008). An alternative to the USP disintegration test for orally disintegrating tablets. *Pharmaceutical Technology* 32: 54-58.

Parkin, J. (2007). Micropellet technology comes of age. *Plastics, Additives and Compounding* 9(5): 44-45.

Passerini, N.; Qi, S.; Albertini, B.; Grassi, M.; Rodriguez, L. and Craig, D.Q.M. (2010). Solid lipid microparticles produced by spray congealing: Influence of the atomizer on microparticle characteristics and mathematical modeling of the drug release. *Journal of Pharmaceutical Sciences* 99(2): 916-931.

Pein, M.; Preis, M.; Eckert, C. and Kiene, F.E. (2014). Taste-masking assessment of solid oral dosage forms—A critical review. *International Journal of Pharmaceutics* 465: 239-254.

Pentikainen, P.J. (1986). Bioavailability of metformin. Comparison of solution, rapidly dissolving tablet, and three sustained release products. *International Journal of Clinical Pharmacology, Therapy, and Toxicology* 24(4): 213-220.

- Pentikäinen, P.J.; Neuvonen, P.J. and Penttilä, A. (1979). Pharmacokinetics of metformin after intravenous and oral administration to man. *European Journal of Clinical Pharmacology* 16(3): 195-202.
- Ph. Eur., E.P. (2014). *European Pharmacopoeia*. Strasbourg, France, Council of Europe.
- Pickup, J.C. and Crook, M.A. (1998). Is type II diabetes mellitus a disease of the innate immune system? *Diabetologia* 41(10): 1241-1248.
- Pinto, J.F. and Silverio, N.P. (2001). Assessment of the extrudability of three different mixtures of saturated polyglycolysed glycerides by determination of the "specific work of extrusion" and by capillary rheometry. *Pharmaceutical Development and Technology* 6(1): 117-128.
- Pouton, C.W. and Porter, C.J.H. (2008). Formulation of lipid-based delivery systems for oral administration: Materials, methods and strategies. *Advanced Drug Delivery Reviews* 60(6): 625-637.
- Prabhu, S.; Ortega, M. and Ma, C. (2005). Novel lipid-based formulations enhancing the in vitro dissolution and permeability characteristics of a poorly water-soluble model drug, piroxicam. *International Journal of Pharmaceutics* 301: 209-216.
- Rabell-Santacana, V.; Pastor-Ramon, E.; Pujol-Ribó, J.; Solà-Genovés, J.; Díaz-Egea, M.; Layola-Brias, M. and Fernández-Campi, M.D. (2008). Inhaled drug use in elderly patients and limitations in association with geriatric assessment scores. *Archivos de Bronconeumología* 44(10): 519-524.
- Rahman, A.; Ahuja, A.; Baboota, S.; Bhavna; Bali, V.; Saigal, N. and Ali, J. (2009). Recent advances in pelletization technique for oral drug delivery: A review. *Current Drug Delivery* 6(1): 122-129.
- Reimerds, D. (1993). The near future of tablet excipients. *Manufacturing Chemistry* 64(7): 14-15.
- Reitz, C. and Kleinebudde, P. (2007a). Influence of thermal and thermo-mechanical treatment: Comparison of two lipids with respect to their suitability for solid lipid extrusion. *Journal of Thermal Analysis and Calorimetry* 89(3): 669-673.
- Reitz, C. and Kleinebudde, P. (2007b). Solid lipid extrusion of sustained release dosage forms. *European Journal of Pharmaceutical Sciences* 67(2): 440-448.
- Reitz, C. and Kleinebudde, P. (2009). Spheronization of solid lipid extrudates. *Powder Technology* 189(2): 238-244.

- Reitz, C.; Strachan, C. and Kleinebudde, P. (2008). Solid lipid extrudates as sustained-release matrices: The effect of surface structure on drug release properties. *European Journal of Pharmaceutical Sciences* 35(4): 335-343.
- Reynolds, A.D. (1970). A new technique for the production of spherical particles. *Manufacturing Chemistry and Aerosol News* 41(6): 40-43.
- Rosenberg, J. and Breitenbach, J. (2002). *Use of lipids as adjuvants in the production of solid medicinal forms by the melt extrusion process*, BASF, US 6,387,401 B2.
- Rosiaux, Y.; Jannin, V.; Hughes, S. and Marchaud, D. (2014). Solid lipid excipients — Matrix agents for sustained drug delivery. *Journal of Controlled Release* 188: 18-30.
- Rote Liste, R.L. (2014). *Rote Liste: Arzneimittelverzeichnis für Deutschland* Frankfurt, Germany, Rote Liste Service GmbH.
- Rowe, R.C. (1985). Spheronization: a novel pill-making process. *Pharmaceutical International* 6: 119-123.
- Rowe, R.C.; Sheskey, P.J.; Cook, W.G. and Fenton, M.E. (2012). *Handbook of Pharmaceutical Excipients*. London, UK, APhA/Pharmaceutical Press.
- Saha, S. and Shahiwala, A.F. (2009). Multifunctional coprocessed excipients for improved tableting performance. *Expert Opinion on Drug Delivery* 6(2): 197-208.
- Sajal, J.K.; Raj Uday, S. and Surendra, V. (2008). Taste masking in pharmaceuticals: an update. *Journal of Pharmacy Research* 1(2): 126-130.
- Sambol, N.C.; Brookes, L.G.; Chiang, J.; Goodman, A.M.; Lin, E.T.; Liu, C.Y. and Benet, L.Z. (1996). Food intake and dosage level, but not tablet vs solution dosage form, affect the absorption of metformin HCl in man. *British Journal of Clinical Pharmacology* 42(4): 510-512.
- Saraiya, D. and Bolton, S. (1990). The use of Precirol to prepare sustained release tablets of theophylline and quinidine gluconate. *Drug Development and Industrial Pharmacy* 16(13): 1963-1969.
- Sastry, S.V.; Nyshadham, J.R. and Fix, J.A. (2000). Recent technological advances in oral drug delivery - a review. *Pharmaceutical Science & Technology Today* 3(4): 138-145.
- Sato, K. (2001). Crystallization behaviour of fats and lipids — A review. *Chemical Engineering Science* 56(7): 2255-2265.
- Scheen, A.J. (1996). Clinical pharmacokinetics of metformin. *Clinical Pharmacokinetics* 30(5): 359-371.

- Schiermeier, S. and Schmidt, P.C. (2002). Fast dispersible ibuprofen tablets. *European Journal of Pharmaceutical Sciences* 15(3): 295-305.
- Schiffman, S.S.; Gatlin, L.A.; Sattely-Miller, E.A.; Graham, B.G.; Heiman, S.A.; Stagner, W.C. and Erickson, R.P. (1994). The effect of sweeteners on bitter taste in young and elderly subjects. *Brain Research Bulletin* 35(3): 189-204.
- Schmidt, C. and Kleinebudde, P. (1998). Comparison between a twin-screw extruder and a rotary ring die press. Part II: influence of process variables. *European Journal of Pharmaceutical Sciences* 45(2): 173-179.
- Schröder, M. and Kleinebudde, P. (1996). The role of extrudate water content on pellet disintegration. *European Journal of Pharmaceutical Sciences* 4(1): S182.
- Sicras-Mainar, A.; de Cambra-Florensa, S. and Navarro-Artieda, R. (2009). Consumo de analgésicos de formulación oral y adecuación de las formas galénicas en pacientes mayores: estudio de base poblacional. *Farmacia Hospitalaria* 33(3): 161-171.
- Siepmann, J. and Peppas, N.A. (2011). Higuchi equation: Derivation, applications, use and misuse. *International Journal of Pharmaceutics* 418(1): 6-12.
- Siepmann, J. and Siepmann, F. (2011). Mathematical modeling of drug release from lipid dosage forms. *International Journal of Pharmaceutics* 418(1): 42-53.
- Siewert, M.; Dressman, J.; Brown, C.; Shah, V.; Aiache, J.-M.; Aoyagi, N.; Bashaw, D.; Brown, C.; Brown, W.; Burgess, D.; Crison, J.; DeLuca, P.; Djerki, R.; Dressman, J.; Foster, T.; Gjellan, K.; Gray, V.; Hussain, A.; Ingallinera, T.; Klancke, J.; Kraemer, J.; Kristensen, H.; Kumi, K.; Leuner, C.; Limberg, J.; Loos, P.; Margulis, L.; Marroum, P.; Moeller, H.; Mueller, B.; Mueller-Zsigmondy, M.; Okafo, N.; Ouderkirk, L.; Parsi, S.; Qureshi, S.; Robinson, J.; Shah, V.; Siewert, M.; Uppoor, R. and Williams, R. (2003). FIP/AAPS guidelines to dissolution/in vitro release testing of novel/special dosage forms. *AAPS PharmSciTech* 4(1): 43-52.
- Singh, I.; Kumar, P.; Rani, N. and Rana, V. (2009). Investigation of different lipid based materials as matrices designed to control the release of a hydrophobic drug. *International Journal of Pharmaceutical Sciences and Drug Research* 1(3): 158-163.
- Sohi, H.; Sultana, Y. and Khar, R.K. (2004). Taste masking technologies in oral pharmaceuticals: Recent developments and approaches. *Drug Development and Industrial Pharmacy* 30(5): 429-448.
- Soto, A.; Iglesias, M.J.; Buño, M. and Bellido, D. (2008). Metformina. *Endocrinología y Nutrición* 55(2): 39-52.
- Staniforth, J. and Taylor, K.M.G. (2013). Particle size analysis. In: Aulton, M.E. and Taylor, K.M.G. *Aulton's Pharmaceutics: The Design and Manufacture of Medicines*. London, UK, Churchill Livingstone - Elsevier: 138-155.

Stegemann, S.; Gosch, M. and Breitzkreutz, J. (2012). Swallowing dysfunction and dysphagia is an unrecognized challenge for oral drug therapy. *International Journal of Pharmaceutics* 430: 197-206.

Sutananta, W.; Craig, D.Q.M. and Newton, J.M. (1994). The effects of ageing on the thermal behaviour and mechanical properties of pharmaceutical glycerides. *International Journal of Pharmaceutics* 111(1): 51-62.

Suzuki, H.; Onishi, H.; Hisamatsu, S.; Masuda, K.; Takahashi, Y.; Iwata, M. and Machida, Y. (2004). Acetaminophen-containing chewable tablets with suppressed bitterness and improved oral feeling. *International Journal of Pharmaceutics* 278(1): 51-61.

Suzuki, H.; Onishi, H.; Takahashi, Y.; Iwata, M. and Machida, Y. (2003). Development of oral acetaminophen chewable tablets with inhibited bitter taste. *International Journal of Pharmaceutics* 251: 123-132.

Sweetman, S.C. (2006). *Martindale: The Complete Drug Reference*. London, UK, Pharmaceutical Press.

Thiele, W. (2003). Twin-screw extrusion and screw design. In: Ghebre-Sellassie, I. and Martin, C. *Pharmaceutical Extrusion Technology*. New York, Marcel Dekker.

Thomas, C. and Pourcelot, Y. (1991). Preformulation of five commercial celluloses in drug development: Rheological and mechanical behavior. *Drug Development and Industrial Pharmacy* 19(15): 1951-1964.

Tibaldi, J.M. (2014). Evolution of Insulin: From human to analog. *The American Journal of Medicine* 127: S25-S38.

Tucker, G.T.; Casey, C.; Phillips, P.J.; Connor, H.; Ward, J.D. and Woods, H.F. (1981). Metformin kinetics in healthy subjects and in patients with diabetes mellitus. *British Journal of Clinical Pharmacology* 12(2): 235-246.

Turkoski, B.B. (1998). Medication timing for the elderly: The impact of biorhythms on effectiveness. *Geriatric Nursing* 19(3): 146-152.

Twitchell, A.M. (2012). Mixing. In: Aulton, M.E. and Taylor, K.M.G. *Aulton's Pharmaceutics: The Design and Manufacture of Medicines*. London, UK, Churchill Livingstone - Elsevier: 170-186.

Uko-Ekpenyong, G. (2006). Improving medication adherence with orally disintegrating tablets. *Nursing* 36(9): 20-21.

USP 34, T.U.S.P. (2011). *USP 34: the United States pharmacopeia*. Rockville, USA, United States Pharmacopeial Convention.



- Vaassen, J.; Bartscher, K. and Breitskreutz, J. (2012). Taste masked lipid pellets with enhanced release of hydrophobic active ingredient. *International Journal of Pharmaceutics* 429: 99-103.
- van Langevelde, A.; Peschar, R. and Schenk, H. (2001). Structure of [beta]-trimyristin and [beta]-tristearin from high-resolution X-ray powder diffraction data. *Acta Crystallographica Section B* 57(3): 372-377.
- Vervaet, C. and Remon, J.P. (2005). Continuous granulation in the pharmaceutical industry. *Chemical Engineering Science* 60(14): 3949-3957.
- Virally, M.; Blicklé, J.F.; Girard, J.; Halimi, S.; Simon, D. and Guillausseau, P.J. (2007). Type 2 diabetes mellitus: epidemiology, pathophysiology, unmet needs and therapeutical perspectives. *Diabetes & Metabolism* 33(4): 231-244.
- Wagh, V.D. and Ghadlinge, S.V. (2009). Taste masking methods and techniques in oral pharmaceuticals: current perspectives. *Journal of Pharmacy Research* 2(6): 1049-1054.
- Wallace, J.I. (1999). Management of Diabetes in the Elderly. *Clinical Diabetes* 17(1).
- Walsh, J.; Cram, A.; Woertz, K.; Breitskreutz, J.; Winzenburg, G.; Turner, R. and Tuleu, C. (2014). Playing hide and seek with poorly tasting paediatric medicines: Do not forget the excipients. *Advanced Drug Delivery Reviews* 73: 14-33.
- Watanabe, A.; Hanawa, T.; Sugihara, M. and Yamamoto, K. (1995). Development and pharmaceutical properties of a new oral dosage form of theophylline using sodium caseinate for the possible use in elderly patients. *International Journal of Pharmaceutics* 117(1): 23-30.
- Wells, J.I. (1988). *Pharmaceutical preformulation: The physicochemical properties of drug substances*. Chichester, UK, Ellis Horwood.
- WHO, W.H.O. (1994). Prevention of diabetes mellitus: report of a WHO study group. Organization, W.H. Geneva, World Health Organization.
- Windbergs, M.; Strachan, C.J. and Kleinebudde, P. (2009a). Influence of structural variations on drug release from lipid/polyethylene glycol matrices. *European Journal of Pharmaceutical Sciences* 37(5): 555-562.
- Windbergs, M.; Strachan, C.J. and Kleinebudde, P. (2009b). Influence of the composition of glycerides on the solid-state behaviour and the dissolution profiles of solid lipid extrudates. *International Journal of Pharmaceutics* 381(2): 184-191.
- Windbergs, M.; Strachan, C.J. and Kleinebudde, P. (2009c). Understanding the solid-state behaviour of triglyceride solid lipid extrudates and its influence on dissolution. *European Journal of Pharmaceutical Sciences* 71(1): 80-87.

Witzleb, R.; Kanikanti, V.-R.; Hamann, H.-J. and Kleinebudde, P. (2011a). Influence of needle-shaped drug particles on the solid lipid extrusion process. *Powder Technology* 207: 407-413.

Witzleb, R.; Kanikanti, V.R.; Hamann, H.J. and Kleinebudde, P. (2011b). Solid lipid extrusion with small die diameters – Electrostatic charging, taste masking and continuous production. *European Journal of Pharmaceutics and Biopharmaceutics* 77(1): 170-177.

Witzleb, R.; Müllertz, A.; Kanikanti, V.R.; Hamann, H.J. and Kleinebudde, P. (2012). Dissolution of solid lipid extrudates in biorelevant media. *International Journal of Pharmaceutics* 422(1-2): 116-124.

Woertz, K.; Tissen, C.; Kleinebudde, P. and Breitzkreutz, J. (2010). Performance qualification of an electronic tongue based on ICH guideline Q2. *Journal of Pharmaceutical and Biomedical Analysis* 51(3): 497-506.

Yan, X.; He, H.; Meng, J.; Zhang, C.; Hong, M. and Tang, X. (2012). Preparation of lipid aspirin sustained-release pellets by solvent-free extrusion/spheronization and an investigation of their stability. *Drug Development and Industrial Pharmacy* 38(10): 1221-1229.

Yeh, S.; Lovitt, S. and Schuster, M.W. (2007). Pharmacological treatment of geriatric cachexia: Evidence and safety in perspective. *Journal of the American Medical Directors Association* 8(6): 363-377.

York, P. and Pilpel, N. (1973). The tensile strength and compression behaviour of lactose, four fatty acids, and their mixtures in relation to tableting. *Journal of Pharmacy and Pharmacology* 25: Suppl:1P-11P.

Zheng, J.Y. and Keeney, M.P. (2006). Taste masking analysis in pharmaceutical formulation development using an electronic tongue. *International Journal of Pharmaceutics* 310: 118-124.

Zimmet, P.Z.; McCarty, D. and de Courten, M.P. (1997). The global epidemiology of non-insulin-dependent diabetes mellitus and the metabolic syndrome. *Journal of Diabetes and Its Complications* 11: 60-68.

## 11. Danksagung

Meinem Doktorvater, Herrn Prof. Dr. Jörg Breitreutz, danke ich für die mir gegebene Gelegenheit nach Deutschland zu kommen und in seinem Arbeitskreis am Institute für Pharmazeutische Technologie und Biopharmazie zu promovieren zu dürfen. Ich möchte mich auch für die damit verbundene hervorragende Betreuung und dem besonderen akademischen Beispiel bedanken. Er hatte immer ein offenes Ohr und war stets diskussionsbereit. Außerdem ermögliche er mir die Teilnahme an zahlreichen Kongressen und Konferenzen, die für mich beruflich als auch privat spannende und lehrreiche Erfahrung darstellten. Herzlichen Dank.

Herrn Prof. Dr. Dr. h.c. Peter Kleinebudde, dem Korreferenten dieser Arbeit, danke ich dem professionellen Beispiel und für die viele unterhaltsamen, Konstruktiven und Motivierenden Diskussionen über die Leidenschaft für die Pharmazeutische Technologie.

Meinen Kollegen und Kolleginnen am Institut danke ich für die besonderen und unvergesslichen 4 Jahren, ins besonderen Frau Carmen Stomberg, Herrn Dr. Christian Mühlenfeld, Herrn Dr. Florian Keine, Frau Isabell Immohr, Herrn Dr. Julian Quodbach und Frau Dr. Miriam Pein, die mir unglaubliche Kraft gegeben haben, in den Momenten, die ich überhaupt keine Kraft mehr hatte. Ich erlaube mich sie als „wahre Freunde“ zu nennen und werde sie in meinem Herz für immer halten.

Herrn Stefan Stich danke ich für die Hilfe mit den „big“ Extruder Reparaturen und für die Herstellung des IR Lampe Prototyps.

Frau Karin Matthée danke ich für diverse DSC-Messungen.

Der Deutscher Akademische Austauschdienst (DAAD) danke ich für das 4 Jahre Stipendium und Unterstützung.

Meinem Vater, Lehrer und Freund Prof. Dr. Pedro Petrovick danke ich für die tiefe Ermutigung und die bedingungslose Unterstützung in den kritische Momente meines gesamten wissenschaftlichen „Reises“.

Meiner Brasilianischen Familie Petrovick ins besonders meiner Mutter Sonia, meinem Bruder André und meiner Schwester Débora danke ich von ganzem Herzen für die fortwährende und liebevolle Unterstützung und Ermutigung während meiner Doktorarbeit in Deutschland. Ohne sie hätte ich diesem Ziel nicht verwirklichen.

Meiner Deutschen Familie Nordmann ins besonders meinem Vater Franjo, meiner Mutter Doris und meinen Geschwistern Jörg, Doris, Markus und Inna danke ich für die liebevolle und bedingungslose Unterstützung an jeder Momenten meines Lebens

in Deutschland. „Unser Haus ist wo unserem Herz ist“ und jetzt ein Teil meines Herzes bleibt in Vechta, Osnabrück und Pforzheim.

## **Eidesstattliche Versicherung und Selbstständigkeitserklärung**

Ich versichere an Eides statt, dass ich die vorliegende Dissertation eigenständig und ohne unerlaubte Hilfe unter Beachtung der Grundsätze zur Sicherung guter wissenschaftlicher Praxis an der Heinrich-Heine-Universität Düsseldorf angefertigt habe. Die Dissertation habe ich bisher keine erfolglosen Promotionsversuche unternommen.

---

Ort, Datum

---

Gustavo Freire Petrovick